ISSN: 2764-5886
e-ISSN: 2764-622X

Volume 9· N° 7 · July 2026

Journal of Bioengineering, Technologies and Health

An Official Publication of
SENAI CIMATEC

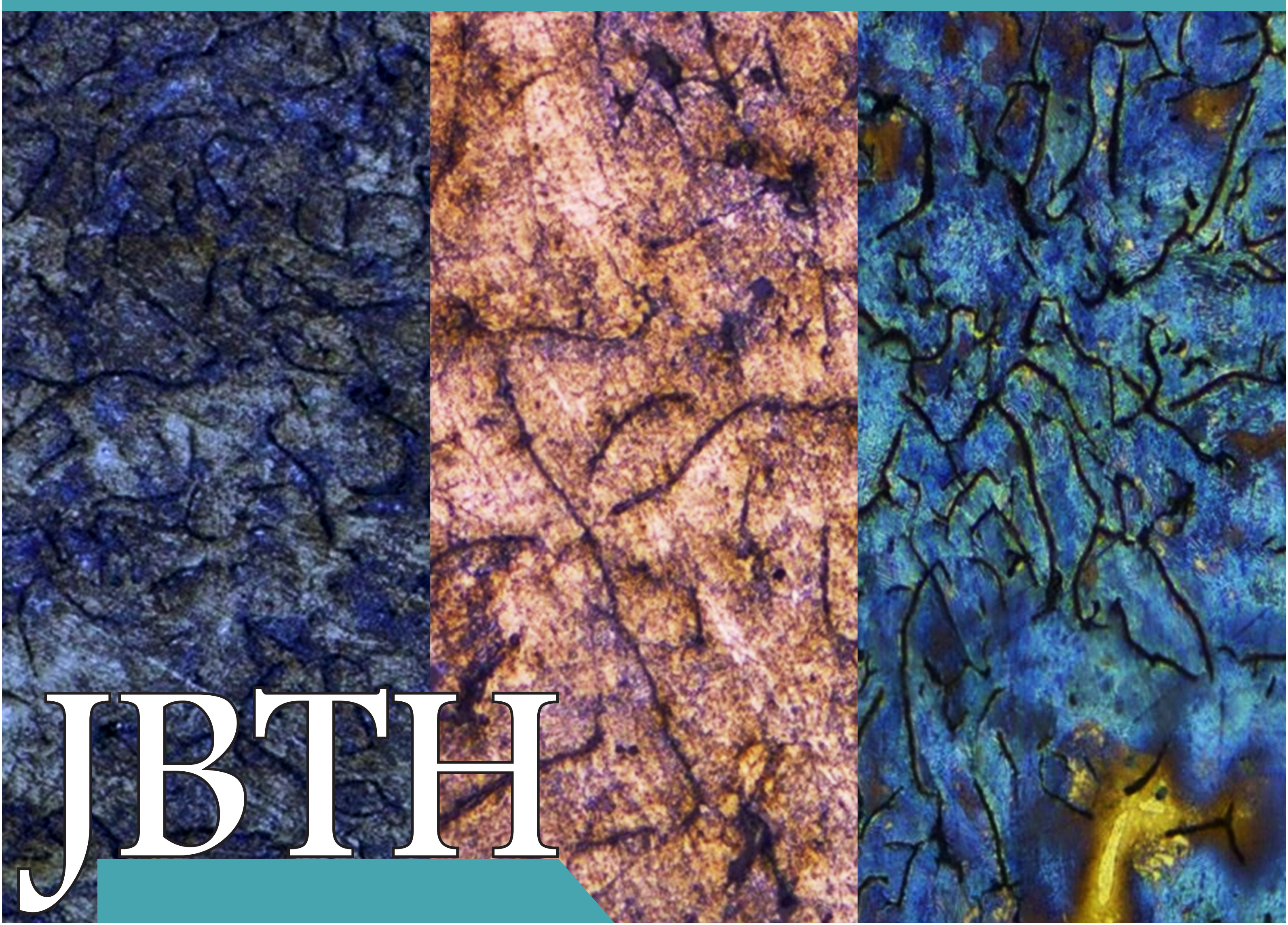

ISSN: 2764-5886 / e-ISSN 2764-622X

Volume 9 • Number 7 • July 2026

JOURNAL OF BIOENGINEERING TECHNOLOGIES AND HEALTH

An Official Publication of SENAI CIMATEC

EDITOR-IN-CHIEF
Leone Peter Andrade

PUBLISHED BY SENAI CIMATEC

July 2026
Printed in Brazil

JOURNAL OF BIOENGINEERING TECHNOLOGIES AND HEALTH

An Official Publication of SENAI CIMATEC

JOURNAL OF BIOENGINEERING TECHNOLOGIES AND HEALTH

Volume 9 • Number 7 **SUMMARY** *July 2026*

Original Articles

The Journal of Bioengineering, Technologies and Health (JBTH) is an official publication of the SENAI CIMATEC University (Serviço Nacional de Aprendizagem Industrial - Universidade Centro Integrado de Manufatura e Tecnologia). It is published montly (January to December) in English by SENAI CIMATEC University – Avenida Orlando Gomes, 1845, Piatã, Zip Code: 41650-010, Salvador-Bahia-Brazil; phone: (55 71) 3879-5501. The editorial offices are at SENAI CIMATEC University.

Editorial Office

Correspondence concerning subscriptions, advertisements, claims for missing issues, changes of address, and communications to the editors should be addressed to the Deputy Editor, Dr. Roberto Badaró, SENAI CIMATEC University (Journal of Bioengineering, Technologies and Health – JBTH) – Avenida Orlando Gomes, 1845, Piatã, Zip code: 41650-010, Salvador-Bahia-Brazil; phone: (55 71) 3879-5501; or sent by e-mail: jbth@fieb.org.br / jbth.cimatec@gmail.com.

Permissions

Postmaster

Send address changes to JBTH, Avenida Orlando Gomes, 1845, Piatã, Zip Code: 41650-010, Salvador-Bahia-Brazil.

Information by JBTH-SENAI CIMATEC University
Address: Avenida Orlando Gomes, 1845, Piatã, Zip Code: 41650-010, Salvador-Bahia-Brazil
Home-page: www.jbth.com.br
E-mail: jbth@fieb.org.br / jbth.cimatec@gmail.com
Phone: (55 71) 3879-5501 / 3879-5500 / 3879-9500

DOI:10.34178

ISSN: 2764-5886 / e-ISSN 2764-622X

COVER: Figure 5, 6 and 7. Effects of Inoculation in Gray Cast Iron with the Addition of Niobium from Scrap by Henrique Silva et al. J Bioeng. Tech. Health 2026;9(7):670.

Analysis of Environmental and Social Factors in the Dynamics of Arboviruses in Bahia: A Methodological Proposal

Elias Reis da Silva[1,2]*, Filipe Cardoso Brito[2,3], Toni Alex Reis Borges[2,4], Aloísio Santos Nascimento Filho[2,3], Hugo Saba[1,2]
[1]State University of Bahia (UNEB), Department of Exact and Earth Sciences; [2]Center for Applied Research and Innovation – NPAI; [3] SENAI CIMATEC University, Stricto Sensu Department, Salvador, Bahia; [4]Federal Institute of Bahia – IFBA, Department of Computer Science; Feira de Santana, Bahia, Brazil

Arboviruses represent a significant challenge to public health, requiring a careful analysis of the environmental factors that impact their propagation. This research project mapped the relationships between epidemiological, climatic, and environmental data for the development of more effective public policies. The methodology adopted was based on experimental research and followed an iterative and incremental path, divided into stages ranging from data collection to the analysis and interpretation of the results found. The results include the development of a model of the relationships between variables and the analysis of the patterns found.
Keywords: Arboviruses. Environmental Health. Data Analysis. Methodological Model. PDCA.

The spread of arboviruses like Dengue, Zika, and Chikungunya represents a persistent public health problem in Brazil. The complexity of their dynamics in urban and rural centers demands an investigative approach that transcends purely epidemiological analysis, integrating multiple factors influencing their dissemination, whose recent impact can be observed in the expressive increase of cases across the country.

The state of Bahia, due to its climatic and social characteristics, presents a complex epidemiological scenario, with recurrent outbreaks that impact the population and overload health services. Understanding the mechanisms of diffusion of these diseases in the Bahian territory is, therefore, a fundamental step, with previous studies already highlighting the non-local dispersion of dengue [1] and the relevance of transportation networks in the distribution of cases [2].

This work's general objective is to map and analyze the relationships between epidemiological data of arboviruses and environmental, climatic, and social factors in the state of Bahia. From this analysis, the aim is to generate subsidies that can assist public managers in formulating more targeted and efficient surveillance and control policies.

Received on 12 March 2026; revised 26 May 2026.
Address for correspondence: Lucas Câncio de Jesus Cunha. Av. Orlando Gomes, 1845 - Piatã, Salvador – BA – Brazil, Zipcode: 41650-010. E-mail: eliasreis1704@gmail.com.

J Bioeng. Tech. Health 2026;9(7):638-642

Literature Review

Scientific literature consistently indicates the multifactorial nature of arbovirus dynamics. Climatic factors like temperature and precipitation directly influence the life cycle of the *Aedes aegypti* mosquito, the main vector in Brazil. Studies, such as Oliveira and colleagues [3], examine the paradox between sanitation and rainfall in dengue cases, highlighting that infrastructure alone is insufficient without proper management during high rainfall periods.

Beyond climatic factors, human mobility has been identified as a key driver of the spatial spread of epidemics. Research focusing on Bahia, like that by Saba and colleagues [2], has shown the importance of transportation networks for the correlation and distribution of dengue cases, suggesting that municipalities with stronger road connections tend to experience synchronized outbreaks [4-7]. This view is supported by Araújo and colleagues [1], who investigated the nonlocal dispersion of dengue in the state, and by Santos and colleagues [8], who employed complex network analysis to compare the dynamics of various arboviruses within the same geographical area [8-10].

Time series analysis of cases also provides valuable insights, as demonstrated by Azevedo and colleagues [11], who identified self-affinity properties in dengue series, indicating memory and complexity in occurrence patterns [11-16]. Consequently, this study's approach aims to integrate these diverse dimensions—climatic, spatial, and social—to construct a more comprehensive model of territorial vulnerability to arboviruses.

Materials and Methods

The methodological strategy was designed for iterative and incremental execution, organized according to the four phases of the PDCA (Plan-Do-Check-Act) cycle, as proposed by Gil [17].

Plan

In this phase, the research foundations were defined:

1. **Problem Identification and Objectives:** The central problem was defined as the need to understand the relationships between environmental/social factors and the incidence of arboviruses in Bahia. The objectives were established as: (i) collecting and integrating data from different sources; (ii) analyzing the relationships between variables; and (iii) discussing the implications of the findings for public health.
2. **Database Survey:** Public and reliable data sources were selected. For epidemiological data, the Notifiable Diseases Information System (SINAN) [18], was used. For climatic data, the National Institute of Meteorology (INMET) [19], was consulted. Socioeconomic and mobility data were obtained from the Brazilian Institute of Geography and Statistics (IBGE) [20], and the State Agency for Regulation of Public Energy, Transport, and Communications Services of Bahia (AGERBA, [21]).
3. **Study of Applicable Models:** A review of analytical techniques was carried out, including, but not limited to, Correlation Analysis, Time Series Analysis, and Spatial Analysis.

Do

This phase corresponded to the technical execution of the plan:

1. **Data Pre-processing and Integration:** The raw data underwent a cleaning process, treatment of missing values, and aggregation into common temporal (monthly) and spatial (municipal) units.
2. **Elaboration of Relationship Mapping:** The analytical techniques were applied to generate correlation matrices, models, and thematic maps.

Check

In this phase, the results were critically evaluated:

1. **Analysis and Interpretation:** Quantitative results were interpreted in light of epidemiological knowledge and the reviewed literature.

Act

Based on the analysis, this phase focused on consolidation and dissemination:

1. **Consolidation of Findings and Scientific Writing:** The results and discussions were consolidated in this article.

Results and Discussion

The exploration of the dataset revealed significant association patterns.

Relationship between Precipitation and Dengue Cases

The historical series of the dengue incidence coefficient in Brazil demonstrates clear and recurrent seasonality (Figure 1). It is observed that, for all geographical regions, including the Northeast, case peaks consistently concentrate in the first half of each year, a period that typically coincides with higher rainfall volumes and higher temperatures in much of the country. The year 2024, in particular, shows an outbreak of exceptional magnitude compared to previous years [4].

Figure 1. Incidence coefficient (cases per 100,000 inhabitants) of dengue by geographical region according to the epidemiological week of symptom onset – Brazil, 2022-2024.

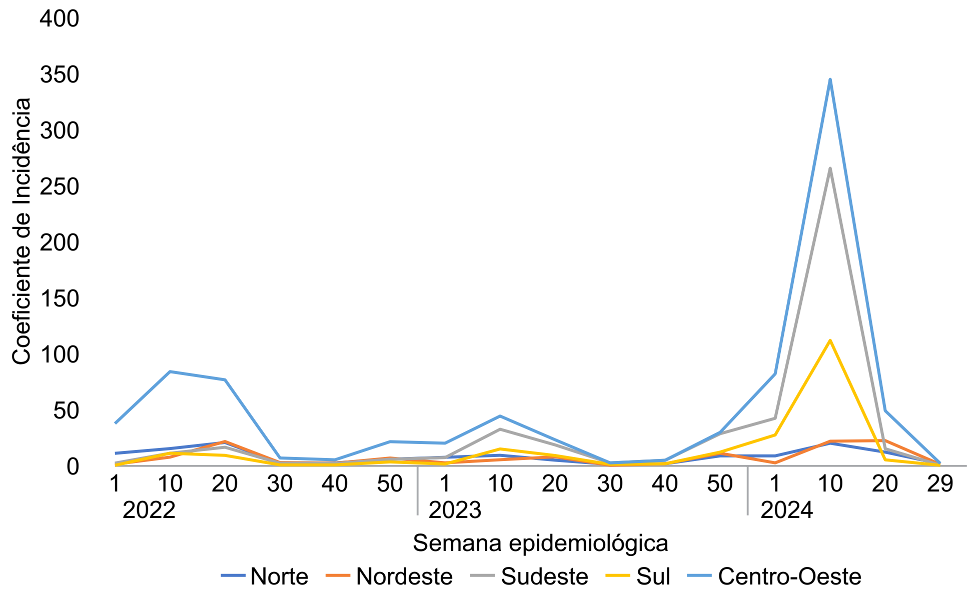

Source: Brazil. Ministry of Health (2024) [4].

The seasonal pattern visualized in Figure 1 is the starting point for investigating the environmental factors that modulate it. The central hypothesis is that climatic variations, especially precipitation, are the main triggers for the increase in the vector mosquito population. The correlation analysis performed in this study sought to quantify this relationship for the state of Bahia, revealing a positive association with a temporal lag between peaks in rainfall and peaks in dengue cases. This finding, aligned with the literature [3], suggests that increased rainfall expands the availability of breeding sites for *Aedes aegypti*, and the time lag (approximately 1-2 months) corresponds to the mosquito's life cycle and the virus's incubation period.

Analysis of the Spatial Distribution of Arboviruses in Bahia

In addition to temporal patterns, the spatial distribution of arboviruses in the Bahian territory shows significant heterogeneity. According to data from the State Operative Plan for Arbovirus Control (SESAB) [5], up to Epidemiological Week 11 of 2023, the state recorded 11,001 probable cases of dengue, 4,348 of Chikungunya, and 391 of Zika. The density maps in Figure 2 illustrate the concentration of these cases, revealing the formation of "hotspots" with a higher risk of illness.

The overlapping risk areas for the three arboviruses, especially in the Southwest region, suggest the existence of common environmental and social factors that persistently favor vector proliferation and viral transmission. Identifying these critical areas is fundamental for directing resources and intensifying actions in surveillance, vector control, and healthcare, as recommended by the state plan (SESAB)[5]. Analyzing these hotspots allows for more strategic planning, focusing efforts where the public health impact is most pronounced.

Study Limitations

Firstly, underreporting of arbovirus cases is a chronic problem in Brazil, which can impact the accuracy of epidemiological data. Secondly, this study is based on data aggregated by municipality, which can lead to the "ecological fallacy"—the

Figure 2. Density maps (hotspots) of Dengue, Chikungunya, and Zika cases in the state of Bahia.

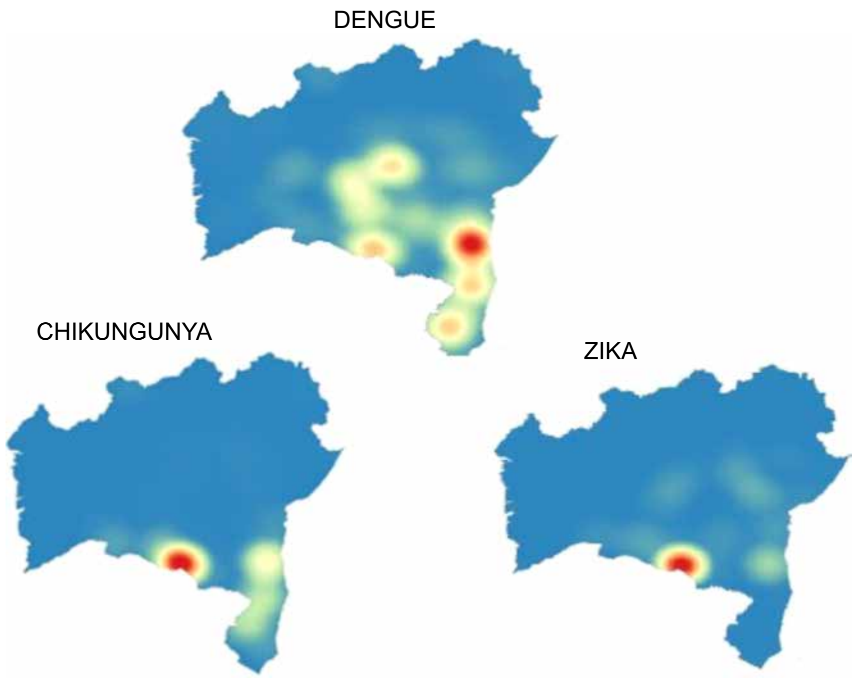

Source: Bahia State Health Secretariat (2023) [5].

assumption that relationships observed at the aggregated level are valid at the individual level. Finally, as emphasized, the statistical associations found here do not establish a causal relationship but rather generate hypotheses that require validation through other types of studies.

Conclusion

This work analyzed the relationship between environmental, climatic, and social factors and the incidence of arboviruses in the state of Bahia. The data investigation allowed for the identification of relevant association patterns, such as the temporal lag between rainfall and dengue outbreaks and the heterogeneous spatial distribution of cases. The main contribution of the study was the characterization of a vulnerability model that integrates these multiple factors. It is concluded that the research findings provide subsidies for the optimization of surveillance and control strategies, allowing for the development of more targeted and proactive actions by health managers.

References

1. Araujo MLV, et al. Nonlocal dispersal of dengue in the state of Bahia. Sci Total Environ. 2018;631-632:40-6.
2. Saba H, et al. Relevance of transportation to correlations among criticality, physical means of propagation, and distribution of dengue fever cases in the state of Bahia. Sci Total Environ. 2018.
3. Oliveira JB, et al. Paradox between adequate sanitation and rainfall in dengue fever cases. Sci Total Environ. 2023;860:160491.
4. Brasil. Ministério da Saúde. Secretaria de Vigilância em Saúde e Ambiente. Monitoramento das arboviroses urbanas transmitidas pelo *Aedes aegypti* (dengue, chikungunya e zika), Semanas Epidemiológicas 1 a 24, 2024. Boletim Epidemiológico [Internet]. 2024;55(11). Available from: https://www.gov.br/saude/pt-br/centrais-de-conteudo/publicacoes/boletins/epidemiologicos/edicoes/2024/boletim-epidemiologico-volume-55-no-11.pdf
5. Bahia. Secretaria da Saúde do Estado da Bahia (SESAB). Plano Operativo Estadual de Enfrentamento das Arboviroses Urbanas na Bahia – 2023 [Internet]. Salvador: SESAB; 2023. Available from: https://www.saude.ba.gov.br/wp-content/uploads/2023/03/Plano-Operativo-das-Arboviroses-2023.pdf
6. Miranda JGV, et al. Scaling effect in COVID-19 spreading: the role of heterogeneity in a hybrid ODE-

network model with restrictions on the inter-cities flow. Physica D. 2021;415:132792.
7. Saba H, et al. Synchronized spread of COVID-19 in the cities of Bahia, Brazil. Epidemics. 2022;39:100587.
8. Santos ES, et al. Complex network analysis of arboviruses in the same geographic domain: differences and similarities. Chaos Solitons Fractals. 2023;168:113134.
9. Macedo MCF, et al. Correlation between hospitalized patients' demographics, symptoms, comorbidities, and COVID-19 pandemic in Bahia, Brazil. PLoS One. 2020;15:e0243966.
10. Rosário RS. Sincronização por motifs: uma proposta para análise de redes cerebrais variantes no tempo [dissertação]. Salvador: Universidade Federal da Bahia; 2013.
11. Azevedo SM, et al. Self-affinity in the dengue fever time series. Int J Mod Phys C. 2016;27(1):1650143. Filho ASN, et al. A spatio-temporal analysis of dengue spread in a Brazilian dry climate region. Sci Rep. 2021;11:11892.
12. Naziazeno R, et al. Explorando dinâmicas epidêmicas: estudo de um modelo compartimental e suas aplicações. Rev Bras Ensino Fis. 2024;46:e20240128.
13. SimaClim. Casos de dengue aumentam 346% em relação a 2023 [Internet]. Available from: https://simaclim.com.br/casos-de-dengue-aumentam-346-em-relacao-a-2023/
14. Saba H, Miranda JGV, Moret MA. Self-organized critical phenomenon as a q-exponential decay—avalanche epidemiology of dengue. Physica A. 2014;413:205-11.
15. Saba H, Oliveira MA, Miranda JGV. Modelo computacional para auxílio no combate a epidemias com base em redes sociais. In: Anais do WIVA 2008; 2008.
16. Saba H, et al. Spatio-temporal correlation networks of dengue in the state of Bahia. BMC Public Health. 2014;14:1085.
17. Gil AC. Como elaborar projetos de pesquisa. 4th ed. São Paulo: Atlas; 2002.
18. Brasil. Ministério da Saúde. DATASUS. Sistema de Informação de Agravos de Notificação (SINAN) [Internet]. Brasília: Ministério da Saúde. Available from: http://portalsinan.saude.gov.br/
19. Instituto Nacional de Meteorologia (INMET). Banco de Dados Meteorológicos para Ensino e Pesquisa (BDMEP) [Internet]. Brasília: INMET. Available from: https://portal.inmet.gov.br/banco-de-dados-meteorologicos
20. Instituto Brasileiro de Geografia e Estatística (IBGE). Censo Demográfico 2022 [Internet]. Rio de Janeiro: IBGE; 2022. Available from: https://www.ibge.gov.br/estatisticas/sociais/populacao/22827-censo-demografico-2022.html
21. Agência Estadual de Regulação de Serviços Públicos de Energia, Transportes e Comunicações da Bahia (AGERBA). Anuário Estatístico de Transportes [Internet]. Salvador: AGERBA; 2023. Available from: http://www.agerba.ba.gov.br/

Growth Kinetics of *Lactobacillus acidophilus*, *Lactiplantibacillus plantarum* and *Lacticaseibacillus rhamnosus* under Different Cultivation Conditions

Sabrina dos Santos Rocha[1]*, Aura Lacerda Crepaldi[1], Ingrid Lessa Leal[1], Tatiana Oliveira do Vale[1], Antônio Carlos Freitas Souza[2]

[1]SENAI CIMATEC University, Industrial Microbiology, Salvador, Bahia; [2]BACTOLAC, Research and Development; Macapá, Amapá, Brazil

Probiotics are live microorganisms that benefit the health of the host when administered in adequate amounts. Among the various microorganisms with probiotic activity, lactic acid bacteria (LAB) are commonly used for this purpose. In this perspective, we sought to evaluate the growth kinetics of strains of the species *Lactobacillus acidophilus*, *Lactiplantibacillus plantarum*, and *Lacticaseibacillus rhamnosus*, identifying suitable parameters for the cultivation process. The experiment was conducted with the addition of 1% inoculum in MRS broth. Microbial growth and specific rate (µspecific) were determined by measuring optical density (OD600) and cell viability on plates. Three treatments were tested (no agitation, 100, and 150 RPM) at a constant temperature of 37°C. The results obtained demonstrate that *L. plantarum* presented the highest specific growth rate (µspecific=0.34/h), followed by *L. rhamnosus* (µspecific=0.32/h) and *L. acidophilus* (0.19/h). We also demonstrated that all strains showed a decline in viability in the agitation treatments after 24 hours of cultivation. The kinetic values evaluated suggest that the three strains can be cultivated under static conditions for a period of 24 hours without compromising the productivity of the bioprocess in terms of cell viability.

Keywords: Probiotics. Lactic Acid Bacteria. Bioprocess.

Probiotics are live microorganisms that, when consumed in adequate amounts, provide health benefits to the host [1]. They primarily act in the gastrointestinal tract, where their main mechanisms include inhibiting pathogenic microbes, restoring the gut microbiota, strengthening the intestinal barrier, modulating the immune system, and influencing both the endocrine and nervous systems [2].

Lactic Acid Bacteria (LAB) are commonly used as commercial probiotics due to their classification as Generally Recognized As Safe (GRAS) [3]. The commercial production of probiotics involves complex processes that demand strict quality control to ensure efficacy.

Key requirements include a minimum concentration of viable microorganisms (10^6 CFU/g), along with stability, reproducibility, and cost-effectiveness [4].

Received on 15 March 2026; revised 28 May 2026.
Address for correspondence: Sabrina dos Santos Rocha.com. Av. Orlando Gomes, 1845 - Piatã, Salvador – BA – Brazil, Zipcode: 41650-010. E-mail: saabrinarocha07@gmail.

J Bioeng. Tech. Health 2026;9(7):643-647

This study aimed to evaluate the microbial growth kinetics of three LAB strains used as probiotics and to assess the impact of agitation on biomass production.

Materials and Methods

The specific growth rate (µspecific) of the strains was determined using a high-throughput experimental design approach, which allows for the collection of a larger number of data points in less time and with minimal material usage [5]. This was accomplished through optical density (OD) measurements via spectrophotometry and viability assessments based on colony-forming unit (CFU) counts.

Activation of Bacterial Strains

To activate the strains, the lyophilized samples were thawed and resuspended in sterile MRS broth, then incubated at 37 °C for 24 hours. An aliquot equivalent to 1% (v/v) of the medium volume was subsequently transferred to a fresh tube containing MRS broth and incubated again at 37 °C for approximately 12 hours (overnight) to allow for bacterial adaptation to the culture medium.

Static Condition

Following activation of the lyophilized strain, an aliquot corresponding to 1% (v/v) of the cultured cells was inoculated into test tubes containing 5 mL of MRS broth. The tubes were incubated at 37 °C in a microbiological incubator to allow for the growth of new cultures. Microbial growth was monitored by measuring optical density at 600 nm (OD600) using a UV/VIS spectrophotometer at time intervals of 2, 4, 6, 8, 12, 24, 36, and 48 hours.

Cell viability was assessed at 0, 6, 12, 24, and 48 hours using the Drop Plate method [6], with samples plated on MRS agar and incubated at 37 °C for 48 hours in an anaerobic jar.

Agitation Condition at 100 and 150 RPM

For this assay, Erlenmeyer flasks containing 20 mL of MRS broth were inoculated with 1% (v/v) of the activated strains and incubated at 37 °C in an orbital shaker at 100 and 150 rpm. Microbial growth was monitored following the same protocol as the static assay, with evaluations conducted at 2, 6, 12, 24, and 48 hours of cultivation.

Data Collection

The experiment was performed in triplicate using sacrifice samples. Results, expressed as Absorbance Units (AU) and CFU/mL, were plotted over time (t) to generate growth curves. The specific growth rate (µspecific) was determined by fitting a straight line to the logarithmic phase of growth and applying the following equation:

$$\mu = \frac{(\ln X2 - \ln X1)}{(t2 - t1)} \quad (1)$$

X_1 = OD600 at time t_1
X_2 = OD600 at time t_2
ln = natural logarithm

Results and Discussion

Under the tested conditions, all three strains reached maximum growth after 24 hours of cultivation. The highest cell concentration was observed for *L. plantarum* (2.15×10^9 CFU/mL), followed by *L. rhamnosus* (1.8×10^9 CFU/mL) and *L. acidophilus* (9.7×10^7 CFU/mL) (Figures 3, 4, and 5). *L. plantarum* also exhibited the highest specific growth rate (μ= 0.34 h^{-1}), followed by *L. rhamnosus* (μ = 0.32 h^{-1}) and *L. acidophilus* (μ = 0.19 h^{-1}) (Table 1).

Table 1. Specific growth rates (µ) and residual standard deviations calculated by linear regression during the exponential growth phase (4–10 hours) for various LAB strains.

Microorganism	µspecifics(h^{-1})	Standard Deviation
L. acidophilus	0.3434	0.174
L. plantarum	0.3434	0.3634
L. rhamnosus	0.3214	0,2828

Exposure of the strains to agitation at 100 rpm resulted in a marked decrease in cell viability, with counts falling to 1.40×10^4 CFU/mL after 48 hours (Figure 1). A comparable growth pattern followed by a decline was also observed under agitation at 150 rpm (Figures 2 and 3)

L. rhamnosus showed the best performance in terms of cell viability under agitation at 150 rpm, reaching 1.8×10^9 CFU/mL after 24 hours of cultivation. However, as also observed for L. plantarum, a significant reduction in viability occurred after this period (Figures 4, 5 and 6).

The highest viability of *L. acidophilus* (9.7×10^7 CFU/mL) was recorded under static conditions after 24 hours of cultivation, in agreement with previous reports [7] under similar conditions. A decline in cell viability over time was also observed in the agitated treatments (Figures 7, 8, and 9).

Figure 1. Cell growth of *L. plantarum* over time under static cultivation.

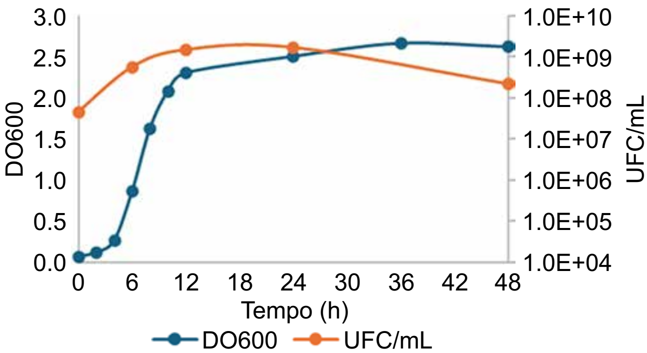

Figure 2. Cell growth of *L. plantarum* over time under cultivation with agitation at 100 rpm.

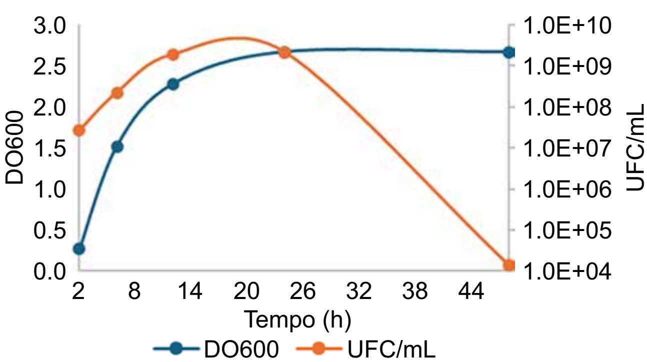

Figure 3. Cell growth of *L. plantarum* over time under cultivation with agitation at 150 rpm.

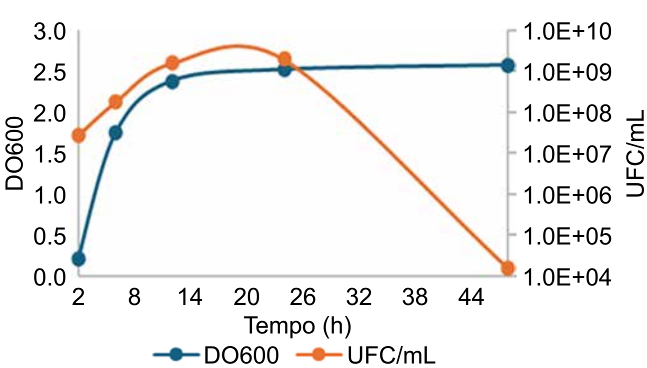

Figure 4. Cell growth of *L. rhamnosus* over time under static cultivation.

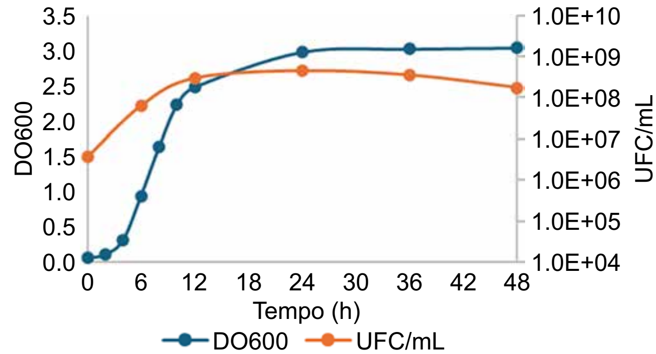

Figure 5. Cell growth of *L. rhamnosus* over time under cultivation with agitation at 100 rpm.

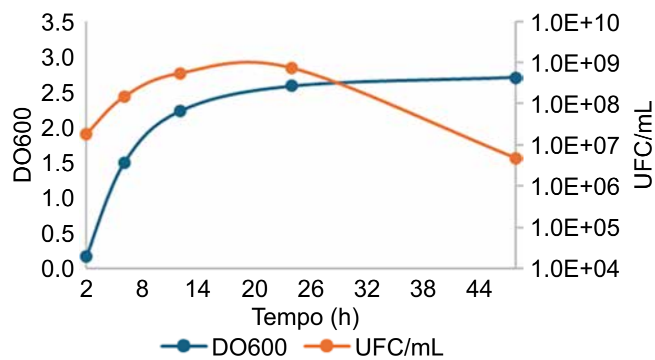

Figure 6. Cell growth of *L. rhamnosus* over time under cultivation with agitation at 150 rpm.

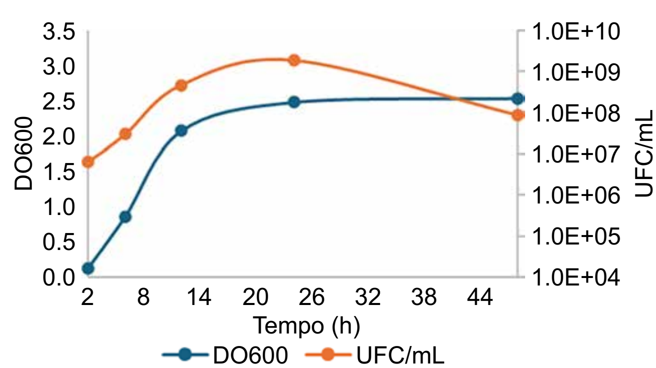

Figure 7. Cell growth of *L. acidophilus* over time under static cultivation.

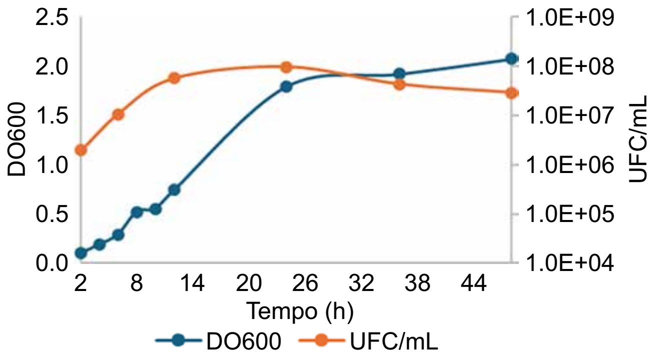

Figure 8. Cell growth of *L. acidophilus* over time under cultivation with agitation at 100 rpm.

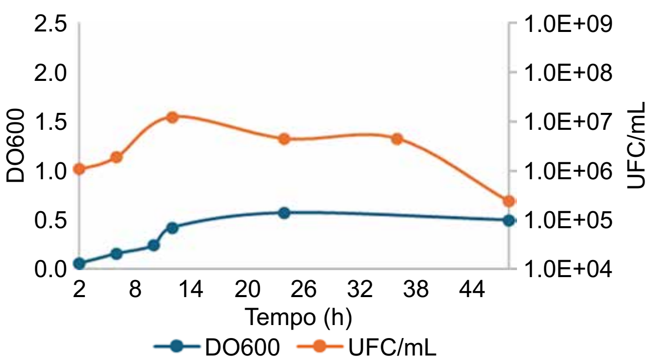

Figure 9. Cell growth of *L. acidophilus* over time under cultivation with agitation at 150 rpm.

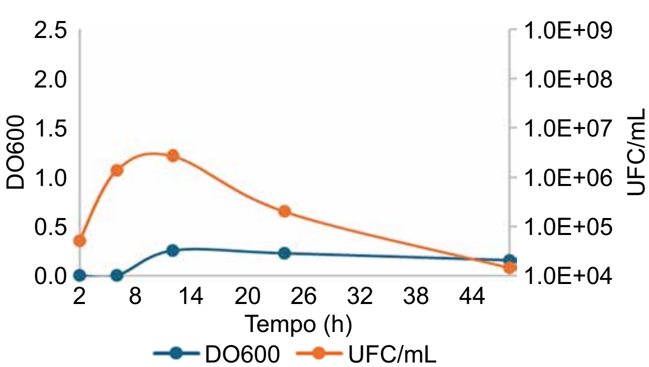

Based on the data obtained in the conducted assays, it is recommended to use inocula cultivated under static conditions at 37 °C for a period of 8 to 16 hours for *L. plantarum* and *L. rhamnosus*, and 12 to 20 hours for *L. acidophilus*. This recommendation is based on the absence of significant differences in viability values and on the fact that the ideal phase for inoculum addition in bioprocesses is the logarithmic phase, which is characterized by high metabolic activity, greater viability, cellular vitality, and better adaptation to the new culture medium [8].

Other relevant aspect is the morphological and physiological similarity between the strains *L. plantarum* and *L. rhamnosus*. In contrast, the *L. acidophilus* strain showed greater sensitivity to variations in culture conditions in the present study, as also demonstrated in a previous study [9].

Other relevant aspect is the morphological and physiological similarity (Figure 1, 2 e 3) between the strains *L. plantarum* and *L. rhamnosus*, which has also been demonstrated previously [9]. In their study, when evaluating different pH levels, NaCl, and sucrose concentrations, these strains showed similar specific growth rates. In contrast, the *L. acidophilus* strain exhibited a lower growth rate and greater sensitivity to variations in cultivation conditions, as observed in the present study.

Conclusion

Based on the results obtained under laboratory conditions, inoculum preparation under static conditions proved to be the most effective. The growth kinetics also revealed distinct differences between *Lactiplantibacillus plantarum* and *Lacticaseibacillus rhamnosus* in comparison to *Lactobacillus acidophilus*, underscoring the need for specific handling practices for the latter due to its unique physiological behavior. These differences highlight the importance of tailored strategies when working with *L. acidophilus*.

Acknowledgement

We thank Bactolac for the institutional support provided for the development of this research.

References

1. Agência Nacional de Vigilância Sanitária (ANVISA). Resolução da Diretoria Colegiada – RDC nº 323, de 10 de novembro de 2003. Diário Oficial da União. 2003 Nov 10. Available from: https://bvsms.saude.gov.br/bvs/saudelegis/anvisa/200 3/rdc0323_10_11_2003.html
2. McFarland LV. Efficacy of single-strain probiotics versus multi-strain mixtures: Systematic review of strain and disease specificity. Dig Dis Sci. 2021;66:694–704.
3. Son S, et al. Probiotic lactic acid bacteria isolated from traditional Korean fermented foods based on β-glucosidase activity. Food Sci Biotechnol. 2018;27:123–9.
4. Kieps J, Dembczynski R. Current trends in the production of probiotic formulations. Foods. 2022;11(15):2330.
5. Murray D, Wigglesworth M. HTS methods: Assay design and optimisation. In: Bittker JA, Ross NT, editors. High throughput screening methods: Evolution and refinement. Cambridge: Royal Society of Chemistry; 2016. p. 1–15.
6. Silva N, et al. Manual de métodos de análise microbiológica de alimentos e água. 5th ed. São Paulo: Blucher; 2017.
7. Akdemir SC, Toupal S, Aslan O. Growth kinetics and survival of Lactobacillus acidophilus in black rice milk. Gida. 2021;6:1440–9.
8. Granato D, Branco GF, Nazzaro F, Cruz AG, Faria JAF. Functional foods and nondairy probiotic food development: Trends, concepts, and products. Compr Rev Food Sci Food Saf. 2010;9(3):292–302.
9. Bisson G, et al. Turbidimetric definition of growth limits in probiotic Lactobacillus strains from the perspective of an adaptation strategy. J Dairy Sci. 2021;104(12):12236–48.

Scientific Integrity and Innovation: A Macroprocess Model for Quality Management in Biomedical Laboratories

Saada Lima Chequer Fernandez[1]*, Renata Almeida de Souza[1], Helena Souza da Hora[2], Bruna Aparecida Souza Machado[2]
[1]Oswaldo Cruz Foundation, Rio de Janeiro, Rio de Janeiro; [2]SENAI Institute of Innovation in Advanced Health Systems - SENAI/CIMATEC; Salvador, Bahia, Brazil

Biomedical research, especially when conducted in non-regulated environments, requires a quality management system that ensures traceability, scientific integrity, regulatory compliance, and institutional accountability. The lack of an effective system can lead to serious consequences such as the loss of scientific credibility, retraction of studies, and funding difficulties. However, many laboratories face challenges in structuring and applying these requirements in an integrated, continuous, and auditable manner. This article proposes a macroprocess model that organizes, operationalizes, and monitors the requirements of the WHO's Quality Practices in Basic Biomedical Research (QPBR) Manual, adapting it to the practical/operational reality of laboratories. The model is structured into seven macroprocesses covering everything from institutional guidelines and personnel management to process digitization, data control, and results management. Each macroprocess is broken down into practical actions linked to key performance indicators and supported by a Standard Operating Procedure (SOP) that guides its step-by-step implementation. Operated in a digital environment (Miro), the model allows for both visual and collaborative tracking as well as evidence repository and continuous monitoring functions. In addition to serving as a technical guide, the model is a strategic tool for quality governance, promoting an organizational culture based on best practices, ethics, biosafety, and continuous improvement. It thus contributes to compliance with national standards and international guidelines while strengthening the credibility of scientific production in contexts of funding, publication, and international cooperation.
Keywords: Quality Management in Research. Laboratory Macroprocesses. Scientific Traceability.

Science has established itself as the main driver of human progress, and the efficiency and reliability of biomedical research are crucial to translating discoveries into tangible social benefits. However, the rapid expansion of research organizations introduces not only innovative opportunities but also threats to scientific integrity, requiring a cultural transformation that confronts entrenched biases and incorporates new evidence-based standards. As Ioannidis [1] warns, disruptive interruptions in the modus operandi of scientific investigation must be well-founded to avoid compromising its validity.

In this context, quality management emerges as a critical pillar to ensure methodological reliability, participant safety, and ethical excellence in biomedical research. Paradoxically, its implementation in university laboratories still faces resistance, being perceived as a hindrance to creativity and a source of excessive bureaucracy [2]. This tension reveals a central challenge: how to align regulatory rigor with investigative agility without compromising innovation.

The robustness of scientific results is intrinsically dependent on data management, especially in long-term trials where follow-up losses can invalidate conclusions. Friedman and colleagues [3] demonstrate that high discontinuity rates require sensitivity analyses to preserve credibility, reinforcing that international standards, such as the International Council for Harmonisation (ICH) Good Clinical Practice (GCP) guidelines [4], are not only mandatory for drug approval but also serve as shields against ethical risks [5-7].

To unify global efforts, the World Health Organization (WHO) published in 2006 the Quality Practices in Basic Biomedical Research (QPBR) Manual, translated in Brazil by Fiocruz in 2010

Received on 19 March 2026; revised 23 May 2026.
Address for correspondence: Saada Lima Chequer Fernandez. Oswaldo Cruz Foundation. Av. Brasil 4365 - Manguinhos Rio de Janeiro, Brazil. Zipcode: 21040-360. E-mail: saada.fernandez@fiocruz.br.

J Bioeng. Tech. Health 2026;9(7):648-653

[8]. This guide serves as a compass for ethical and methodological standardization, proposing reproducible guidelines that transcend borders [9]. However, its operationalization in non-regulated contexts remains fragmented, lacking adaptive models that convert principles into auditable actions. It is within this gap that our proposal is inserted: a macroprocess management model, structured based on the QPBR Manual, aimed at transforming abstract requirements into measurable operational flows. By linking WHO guidelines to performance indicators, evidence repositories, and controls, the model not only addresses historical challenges related to integrity [10], but also catalyzes a cultural shift where ethics, biosafety, and continuous improvement become the foundation for building an institutional culture focused on quality.

Materials and Methods

Step 1 - Definition of Macroprocesses

In this step, the fundamental macroprocesses of quality management were identified and organized, based on the grouping of requirements outlined in the QPBR Manual. Each macroprocess was broken down into operational actions and linked to monitoring indicators, enabling the structuring of a systemic and applicable view for continuous monitoring.

Step 2 - Use of a Digital Modeling Tool

A digital tool was incorporated to support the modeling and operationalization of the system. The collaborative platform Miro was used as a visual environment for building the model, allowing graphical representation of the macroprocesses and their breakdowns, in addition to serving as a dynamic repository of information and conformity records.

Step 3 - Presentation and Structuring of the Model

This step involved organizing the model for presentation and validation, taking into account criteria such as practical applicability, adherence to the QPBR Manual, alignment with institutional guidelines, and feasibility of implementation in real laboratory contexts.

Step 4 - Development of the Standard Operating Procedure (SOP)

A specific SOP was developed for applying the model, guiding practical implementation, evidence recording, indicator monitoring, and continuous updating.

Results

The model was developed with the aim of clearly structuring and linking the main quality management macroprocesses applicable to research laboratories, as illustrated in Figure 1.

Presentation and Structuring of the Model

The presented model integrates these issues with their respective practical applications in the laboratory context, promoting a functional and systemic visualization of the operational responsibilities linked to each area to meet quality requirements. The conceptual structure of the model was organized based on seven strategic axes, defined as Institutional Guidelines, People Management, Operational Management, Research Project Management, Data Management, Results Management, and Information Technology Management. These axes encompass three layers of breakdown: (i) organizational requirements, (ii) operational requirements, and (iii) results requirements.

Axis Institutional Guidelines represents the internal regulatory framework that guides the operation of biomedical research laboratories regarding quality and its interfaces. This structure includes institutional policies, manuals, technical standards, codes of conduct, and operational guidelines, which form the basis for quality governance. These instruments ensure coordination

Figura 1. Model for the implementation of normative quality management requirements in laboratories:

between administrative, technical, and operational aspects, allowing the laboratory to operate in compliance with ethical, regulatory, and scientific standards. This macroprocess is also responsible for integrating quality requirements into cross-sectional areas such as infrastructure, biosafety, environmental management, institutional communication, scientific integrity, and risk management. Two key indicators linked to this macroprocess are Accreditation/Recognition/Authorization and Certifications and Accreditations. The first indicates that the laboratory is formally authorized by competent regulatory bodies to perform specific activities, such as handling genetically modified organisms (GMOs) or biological risk agents, demonstrating compliance with legal requirements. The second demonstrates the laboratory's alignment with national and international quality standards, reflecting the degree of institutionalization, maturity, and reliability of the quality system. Both indicators function as seals of excellence and institutional legitimacy, contributing to the laboratory's recognition by funders, regulatory agencies, and the scientific community.

Within biomedical research laboratories, the People Management axis goes beyond human resources administration and is understood as a structuring pillar of quality. This macroprocess ensures that employees work with technical competence, institutional responsibility, and alignment with organizational objectives, in accordance with good practices required by regulated and high biological risk environments. Promoting continuous team development is central to this process. The implementation of training programs, validation of technical knowledge, and updating of training records ensure that laboratory activities are performed with accuracy, reproducibility, and scientific integrity. Simultaneously, competency and responsibility mapping, through tools such as functional matrices and codes of conduct, promote organizational clarity, action traceability, and adherence to regulatory requirements. Another critical component of People Management is structured internal communication, which goes beyond operational information exchange. Two indicators reflect the effectiveness of this macroprocess. The Number of Trainings/Events measures investment in the technical and scientific improvement of employees, indicating continuous preparation of the team in relation to quality and biosafety requirements. The Number of Bulletins/Reports/Benchmark indicates the degree of active and structured institutional communication, promoting the circulation of strategic information, visibility of actions, and encouragement of experience exchange among teams and units.

Operational Management is one of the central pillars of the quality system in biomedical research laboratories, responsible for ensuring technical accuracy, routine standardization, and documentary control of laboratory activities. This macroprocess covers everything from the implementation of internal controls for critical activities to the systematic performance of preventive maintenance and equipment calibration, which are fundamental to guaranteeing the reliability of generated data. A highlighted focus is document management, which includes both prescriptive documents, such as standard operating procedures (SOPs), work plans, and technical instructions, as well as descriptive documents that record the practical execution of these instructions. This structure guarantees traceability, reproducibility, and transparency of processes, crucial aspects for auditable and highly regulated environments. Beyond the technical axis, Operational Management also interfaces with cross-sectional regulatory and institutional support areas, such as Waste Management, through compliance with specific legislation, and Biosafety, which requires conformity with internal standards, infrastructure requirements, and official certifications. This shows that operational activities go beyond the technical plan, involving interaction with legal, environmental, and institutional security aspects. Two indicators are directly associated with this macroprocess: the Proficiency Test Approval Rate, which evaluates the laboratory's technical capacity through external comparative assays; and the Document Compliance Rate, which checks the adequacy, updating, and traceability of documents linked to laboratory routine. Both indicators form part of the monitoring system for the institution's technical and documentary quality. In summary, Operational Management is the backbone of quality execution in the laboratory, supporting the entire biomedical research cycle with safety, standardization, and technical responsibility.

The Research Management macroprocess aims primarily to ensure that scientific investigations are conducted in a structured, safe, and technically grounded manner. This macroprocess ranges from technical support for drafting and reviewing research documents, such as projects, protocols, and terms of reference, to the use of digital tools aligned with information technologies that enable efficient management of the different phases of the research cycle. An essential component of this macroprocess is risk analysis, which is introduced as a preventive practice in the planning of each study. This analysis allows for the prior identification of possible operational, methodological, or ethical failures, contributing to risk mitigation, protection of the team and environment, and robustness of scientific results. The associated indicator, Percentage of Projects with Documented Planning and Risk Analysis, measures the proportion of research projects that start with a formal plan duly recorded and accompanied by a validated risk analysis.

Results Management represents the stage in which research achieves its scientific and institutional purpose: the production of reliable, relevant, and socially applicable knowledge. This macroprocess is responsible for ensuring that data generated throughout the project are critically analyzed, technically validated, and communicated with integrity, guaranteeing scientific transparency and institutional responsibility. The model highlights four breakdowns that compose this macroprocess. The first relates to compliance with good research practices, ensuring that studies have been conducted according to ethical standards, validated technical protocols, and standardized operational criteria. The second axis concerns the execution of periodic critical analyses and evaluations based on results, which guide strategic decisions and allow methodological corrections throughout the research cycle. The third axis involves formal study closure procedures, which ensure the existence of complete final reports, describing conduct, methodology, changes, results, critical discussion, and conclusions, promoting traceability and final documentation of the research. Finally, the macroprocess includes institutional support for scientific publication, ensuring clear policies on authorship, peer review, respect for data integrity, and encouragement of the dissemination of negative results, in line with open science principles. The associated indicator, Percentage of Projects in Compliance with Good Practices, measures the proportion of research fully complying with the ethical, technical, and documentary requirements defined institutionally. This indicator directly reflects the quality and credibility of produced results, being fundamental for audits, scientific publications, accountability to funders, and strengthening the institutional reputation of the research unit.

In the context of biomedical research laboratories, Data Management represents one of the pillars of scientific credibility and regulatory compliance. This macroprocess ensures that data generated throughout research is preserved, accessible, traceable, and protected against loss or unauthorized alteration. Its structure is anchored in three central and complementary components. The first component refers to data preservation, which involves the existence of adequate and secure infrastructure for storing raw data, technical forms, and critical records. This preservation covers both physical means (such as dedicated cabinets and archives) and digital environments (internal servers, institutional repositories, and secure clouds), ensuring record maintenance according to traceability and audit requirements. The second component is information integrity and recovery, translated into the implementation of reliable backup and restoration procedures. These measures ensure the full recovery of data in case of technical failures, accidents, or cyberattacks, protecting accumulated scientific knowledge and maintaining continuity of laboratory activities. The third component is the chronological recording of experimental data, which requires sequential, continuous, and dated documentation of all observations, measurements, and procedures performed. The associated indicator, Percentage of Data with Traceability and Backup, measures the proportion of data sets that have complete, chronologically organized records stored with secure recovery mechanisms.

Information Technology Management is configured as an essential macroprocess in contemporary biomedical research laboratories, providing the necessary digital infrastructure to ensure security, traceability, integration, and efficiency of scientific, administrative, and operational processes. This component goes beyond the traditional technical support role, positioning itself as a strategic axis supporting quality. Its actions include implementing and using reliable, validated, and authorized computerized systems for secure management of data, processes, and laboratory workflows. Compliance with information security standards is ensured through validation of critical software, access management based on responsibility profiles, and adoption of good digital protection practices, which guarantee data integrity and change control. The role of IT in supporting the systematization and visualization of operational flows stands out, through tools such as process mapping systems that facilitate planning, transparency, and data-driven decision-making. Furthermore, IT drives the digital culture in the laboratory environment, promoting adoption of advanced technologies such as artificial intelligence (AI), applied to analysis of large data volumes, protocol optimization, and automation of critical routines.

The central indicator of the proposed model is the Internal Quality Audits, conceived as a systematic and structured mechanism for monitoring compliance and effectiveness of all macroprocesses comprising a quality system in biomedical research laboratories. Due to its transversal nature, this indicator allows an integrated evaluation of the implemented practices, from people and project management to data preservation and communication of scientific results, aligning with the requirements of the PQPB Manual, institutional standards, and good laboratory practices.

Its systematic application enables the identification of deviations, promotion of corrective actions, and proposal of continuous improvements, strengthening not only regulatory compliance but also the organizational and scientific maturity of processes. By integrating all macroprocesses under a single verification criterion, the indicator helps reduce operational risks, increase data reliability, and reinforce the scientific integrity of activities developed in the laboratory environment. Therefore, it is a key component for the sustainability and credibility of the quality management system in biomedical research.

Conclusion

This model overcomes the dichotomy between methodological rigor and creative agility by integrating ethical-regulatory compliance, research ethics principles, good clinical practices, robust data management, and biosafety. By enabling real-time evidence generation, it transforms quality once seen as an obstacle into a strategic foundation. This strengthens national scientific credibility with funders and international partners, fosters an institutional culture of integrity, and translates excellence into concrete impact for health research.

It is recommended that future validations include case studies across different types of institutions, as well as the systematic measurement of the model's impacts through performance indicators and internal audits. The continuous improvement of the model, along with its dissemination and adaptation, may consolidate a more integrated, auditable, and sustainable approach to quality management in biomedical research.

Acknowledgement

The authors thank SENAI CIMATEC University and its post graduate program on Industrial Management and Technology. This work was performed with the support of Escola Corporativa/ Cogepe (Fiocruz) as part of the Management Development Programme (PDG).

References

1. Ioannidis JPA. Meta-research: Why research on research matters. PLoS Biol. 2018;16(3):1–6.
2. Martínez-Perales S, Ortiz-Marcos I, Ruiz JJ. A proposal of model for a quality management system in research testing laboratories. Accred Qual Assur. 2021 Dec 8;26(6):237–48.
3. Friedman LM et al. Fundamentals of clinical trials. 2015.
4. International Conference on Harminisation (ICH). ICH harmonised tripartite guideline: guideline for good clinical practice E6(R1). Geneva: ICH; 1996.
5. Kamnoore K, et al. Regulatory requirements for conducting clinical trials in India. Res J Pharm Technol. 2020;13(3):1517.
6. Agência Nacional de Vigilância Sanitária (ANVISA). Guia de Boas Práticas Clínicas E6(R2). Brasília: ANVISA; 2019. 43 p.
7. European Medicines Agency (EMA). ICH E8: General considerations for clinical studies – scientific guideline [Internet]. London: EMA; [cited 2025 Jun 26]. Available from: https://www.ema.europa.eu/en/ich-e8-general-considerations-clinical-studies-scientific-guideline.
8. World Health Organization (WHO). Práticas da qualidade na pesquisa biomédica básica. Geneva: WHO; 2006.
9. World Health Organization (WHO). Quality practices in basic biomedical research (QPBR) training manual: trainee. Geneva: WHO; 2010.
10. Keates T. Bioethics in Italy. Lancet. 1995 Jan;345(8943):182.

Development of Eucalyptus Fiber Masterbatch for Polyethylene Additives

Ilana O. Almeida[1]*, Talyta S. Prado[2], Lucas N. Horiuchi[2], Rosana L. Fialho[2], Joyce B. Azevedo[1]
[1]Federal University of Bahia, Institute of Science, Technology and Innovation; Camaçari, Bahia; [2]Department of Industrial Engineering, Federal University of Bahia (UFBA); Salvador, Bahia, Brazil

Growing concerns about sustainability and environmental impact have driven the development of alternative materials, such as polymer composites reinforced with natural fibers. However, a gap remains between scientific advances and large-scale industrial applications of these composites. This study aimed to develop eucalyptus fiber masterbatches as an alternative to optimize the production of high-density polyethylene (HDPE) composites. To obtain the masterbatches, high fiber concentrations (30%, 40%, and 50%) were incorporated into HDPE using twin-screw extrusion. From the 50% concentrate, composites containing 10% fiber were subsequently produced. Optical microscopy analysis showed good fiber dispersion and distribution in the polymer matrix, with an estimated average length of 7.48 mm. Mechanical testing revealed that, although fiber addition reduced tensile strength, it increased the elastic modulus, indicating structural reinforcement. In terms of impact strength, no changes were observed in the composite produced from the masterbatch, confirming adequate fiber distribution and the absence of agglomerates. Overall, the results demonstrate the feasibility of using eucalyptus fiber as reinforcement in HDPE composites produced from fiber concentrates.
Keywords: Polymer Composites. Eucalyptus Fiber. Polyethylene. Additives. Masterbatch.

Growing concern for sustainability and minimizing environmental impacts has driven the development of alternative materials, such as polymer composites reinforced with natural fibers. These materials have gained prominence due to their economic, environmental, and technical advantages, such as low cost, biodegradability, good specific strength, and wide availability of raw materials [1].

In this context, eucalyptus fiber stands out as a promising option, mainly due to its abundance in Brazil, its high cellulose content, and its good mechanical properties [2–3]. However, for these fibers to be efficiently incorporated into polymer matrices, an appropriate beneficiation process is required. This process includes steps such as drying, grinding, screening, and, in some cases, physical and chemical treatments, intended to increase fiber compatibility.

One potentially efficient way to incorporate natural fibers into polymer matrices in industrial processes is through masterbatch production. This approach uses a carrier polymer to incorporate high concentrations of fibers, which can then be added directly during processing when a relatively low final concentration of additives, in this case, natural fibers, is required. Because they are pre-dispersed in the carrier polymer, they do not require an additional dispersive mixing step [4]. This technique can promote mix homogenization, improve reinforcement dispersion, and provide greater control over the properties of the final composite [5–6].

Considering this scenario, this study obtained composites with high concentrations of eucalyptus fiber in the form of masterbatch and evaluated the influence of this dispersion method on the mechanical properties of HDPE composites.

Materials and Methods

In this study,high-density polyethylene (HDPE JV060U), manufactured and supplied by Braskem, with MFI equal to 7.0 g/10 min (190°C, 2.16 kg), melting temperature of 140°C and density of 0.957 g/cm^3 was used [7]. The eucalyptus fiber was donated by the company DEXCO,containing particles in various particle sizes (range of 149 μm ≤ X ≥ 710 μm).

Received on 17 March 2026; revised 11 May 2026.
Address for correspondence: Ilana O. Almeida. Av. Orlando Gomes, 1845 - Piatã, Salvador – BA – Brazil, Zipcode: 41650-010. E-mail: ilanaoliveiraalmeida@gmail.com.

J Bioeng. Tech. Health 2026;9(7):654-658

Masterbatch Preparation

Eucalyptus fibers were initially dried in an oven at 110 °C for 4 h. The fibers and pure polymer were then processed in a co-rotating twin-screw extruder (model DR.16.AX, AX Plásticos), with a screw diameter (D) of 16 mm and a length-to-diameter ratio (L/D) of 40. The temperature profile adopted was: Z1: 150 °C, Z2: 155 °C, Z3: 160 °C, Z4: 165 °C, Z5–6: 170 °C, Z7: 175 °C, and Z8–9: 175 °C. Formulations containing 30% and 40% fiber by mass were extruded at 120 rpm, while the formulation with 50% fiber was extruded at 150 rpm, with the aim of improving fiber incorporation efficiency during this stage. The melt flow index (MFI) of the masterbatches was determined using a standardized plastometer at the Materials Development Laboratory of UFBA – Camaçari, at 190 °C with a load of 2.16 kg, in accordance with ISO 1133.

Preparation of the Composite from Masterbatches

After analyzing the melt flow index, the masterbatch containing 50% fiber was selected for compound preparation, resulting in an HDPE composite with 10% fiber (Figure 1).

The chosen masterbatch was dried at 100 °C for 5 h and subsequently processed with virgin polymer in the same extruder (model DR.16.AX, AX Plásticos), under identical conditions (D = 16 mm, L/D = 40, screw speed of 150 rpm, and the same temperature profile). For comparison, pure polymer was also extruded under the same processing conditions.

Figure 1. Masterbatch with 50% eucalyptus fiber.

Characterization of the Composite Obtained from the Masterbatch

The degree of fiber dispersion in the composite was qualitatively assessed by optical microscopy. Thin films of the material were prepared by hot pressing and subsequently analyzed using a RoHS digital microscope at the Materials Development Laboratory of UFBA – Camaçari Campus. After this step, the material for obtaining the test specimen was prepared. The composites were oven-dried at 100 °C for 5 h and then subjected to hot pressing in a heated hydraulic press (SOLAB, model SL-11). Upper and lower molds were preheated to 200 °C and filled with an average mass of 115 g. The pressing cycle consisted of 25 min of heating followed by 40 min of cooling under a pressure of 5 tons. After cooling and demolding, the specimens were laser-cut to the dimensions specified in ASTM D638, at a cutting speed of 4 mm/s. Tensile strength tests were performed at the SENAI CIMATEC Mechanical Testing Laboratory using a universal testing machine (Emic DL 2000), with data acquisition and processing performed by Tesc software, according to ISO 527, at a test speed of 5 mm/min. Impact strength was determined using an Instron CEAST 9050 impact machine, equipped with a 2.7 J hammer in Izod configuration, in accordance with ISO 180. Prior to testing, the specimens were notched at a 45° angle and 2.5 mm depth. For each formulation, five specimens were tested in both tensile and impact strength assays.

Results and Discussion

Obtaining and Characterizing Masterbatches

In the first stage, the fiber processing conditions were evaluated with HDPE in a twin-screw extruder. During the extrusion process, for the formulation containing 50% eucalyptus fiber, the screw rotation speed had to be adjusted from 120 to 150 rpm to improve the efficiency of fiber incorporation into the polymer. Figure 2 shows the melt flow index results of the concentrates.

The graph shown demonstrates a significant reduction in the flow rate as the amount of wood in the formulation increases. This behavior was expected, as incorporating a rigid phase into the polymer hinders the molecular mobility of the chains, increasing viscosity and decreasing its flowability [8]. Despite the low melt flow rate, the masterbatch with 50% fiber was selected. According to Manrich (2005) [5], the viscosity of the polymer matrix is directly linked to dispersion efficiency due to the intensity of the forces transferred during the mixing process. In situations where the mixture begins with a low melt flow rate, dispersion may occur. Subsequently, with the increase in temperature and shear during extrusion, the increase in melt flow rate resulting from these parameters contributes to good distribution and a good level of mixing.

<u>Characterization of the Composite Obtained from the Masterbatch</u>

Using optical microscopy, it was possible to observe the distribution and dispersion of wood particles in the polymer matrix after the concentrate was dispersed in the HDPE (Figure 3). The images obtained were processed and analyzed using Image J software, which enabled the segmentation and quantification of the particles present in the matrix. The analyzed sample contained a total of 108 particles, corresponding to the eucalyptus fibers incorporated into the matrix. The distribution revealed a predominance of small fibers, suggesting good dispersion of the lignocellulosic reinforcement

Figure 3. Optical microscopy of the composite with eucalyptus particles and HDPE matrix obtained from master-batch (image magnified 120x).

Figure 2. Melt flow index (MFI) of eucalyptus fiber masterbatches.

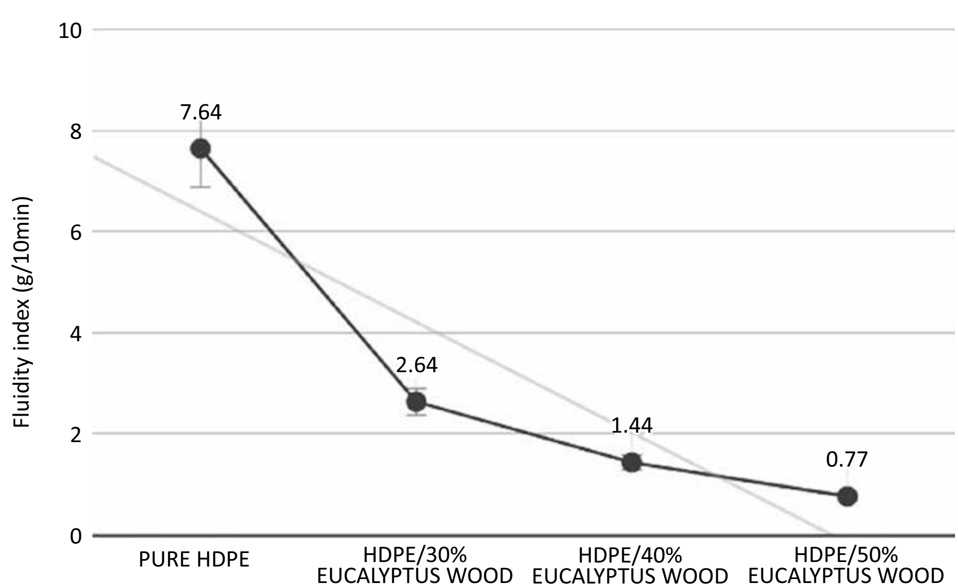

in the composite (Figure 4). Based on the fiber area analysis, an estimated average length of 7.48 mm was calculated, considering the square root of the area as an approximation of the observed fiber length.

Figure 4. Analysis of the proportion of the dispersed phase in the HDPE JV060U matrix.

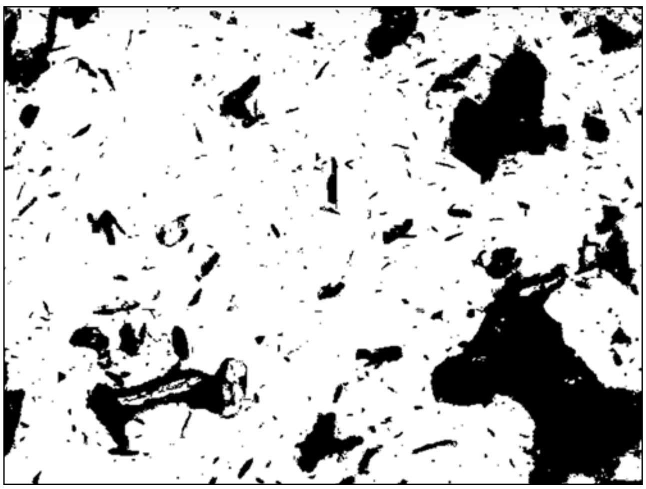

Furthermore, the volumetric proportion of the fibers in the sample was estimated based on the ratio between the sum of the particle areas and the total area of the analyzed image. The results indicated that the fibers occupied approximately 7.072% of the image area, which is close to the proportion initially intended. In terms of particle size distribution, it was observed that 90.74% of the particles had an area of less than 50 mm², while only 0.93% of the fibers exceeded 10,000 mm². This confirms a predominance of small particles, a desirable characteristic to ensure better interfacial interaction between the HDPE matrix and the eucalyptus fibers.

Table 1 presents the results of the mechanical properties under tension and impact resistance of the composite with 10% fiber.

The results indicate a reduction in the composite's tensile strength compared to the pure polymer. For a formulation with natural fiber, without the use of a compatibilizer, this decrease in strength may be associated with several factors. One of the main factors is poor interfacial adhesion between the polymer matrix and the natural fibers or the accumulation of empty balls in the specimen, since this study used press molding [9].

The modulus of elasticity represents the stiffness of a material when subjected to elastic deformation. It was observed that the presence of fiber resulted in an increase in material stiffness. A considerable increase in the modulus of elasticity when fiber was added was observed in other studies, with its maximum values also varying depending on the type of fiber used [10]. The increase in the elastic modulus can result from good fiber distribution in the matrix, as well as its orientation and interaction between phases [11].

Impact strength is a fundamental property in assessing the toughness of materials, representing their ability to absorb energy under rapid loading before fracturing. The results demonstrated that there was no significant variation in this property for the composite obtained from the masterbatch.

These results indicate that, under certain conditions, the presence of natural fiber can act as a reinforcing element, contributing to energy absorption and hindering crack propagation in the material. Another factor that influences this property is the formation of agglomerates. Agglomerates can act as stress concentrators, promoting crack formation, which reduces the energy absorbed upon impact [12]. The results obtained in this work for impact strength indicate that no agglomerates formed.

Table 1. Mechanical properties of the composite.

Material	Tensile Strength (Mpa)	Modulus of Elasticity (Mpa)	Impact Resistance (KJ/m²)
HDPE Pure	16.40 ± 1.5	1140.46 ± 134.2	5.80 ± 0.5
HDPE/10% Fiber	7.08 ± 4.7	1454.88 ± 144.3	5.64 ± 0.4

Conclusion

The study demonstrated the feasibility of producing a masterbatch with 50% eucalyptus fiber for HDPE additives. Microscopic analysis of the dispersion in the composite obtained from the concentrate revealed good fiber dispersion and a proportion close to the expected. Regarding mechanical performance, the results demonstrated the need to evaluate the interface between the fiber and the matrix to better elucidate the tensile strength results, which showed a significant reduction. The modulus of elasticity is influenced by the presence of fiber, resulting in a material with less deformation. Impact resistance was unchanged, indicating good fiber distribution in the composite, without agglomeration.

Finally, this method simplifies the composite preparation process and can bring economic benefits for large-scale production, with broad prospects for technological application.

Acknowledgement

The authors thank PIBITI-UFBA for granting the scientific initiation scholarship and DEXCO for donating the fibers.

References

1. Satyanarayana KG, Arizaga GGC, Wypych F. Biodegradable composites based on lignocellulosic fibers—An overview. Prog Polym Sci. 2009;34(9):982-1021.
2. Paiva JMF, Trindade WG, Frollini E. Compósitos de matriz termofixa fenólica reforçada com fibras vegetais. Polímeros. 1999;9:170-6.
3. Sordi JC, Schneider EE, Nachtigall SMB. Compósitos poliméricos com fibras naturais. In: Salão de Iniciação Científica da Universidade Federal do Rio Grande do Sul; 2003; Porto Alegre, Brasil. Porto Alegre: UFRGS; 2003.
4. Rabello M. Estrutura e propriedades de polímeros. São Paulo: E-Guide; 2023.
5. Manrich S. Processamento de termoplásticos: rosca única, extrusão e matrizes, injeção e moldes. São Paulo: Artliber; 2005.
6. Canedo EL. Fenômenos de transporte. Rio de Janeiro: LTC; 2000.
7. Braskem. Polietileno de alta densidade JV060U. São Paulo: Braskem; 2018.
8. Stark NM, Berger MJ. Effect of species and particle size on properties of wood-flour-filled polypropylene composites. In: Proceedings of Functional Fillers for Thermoplastics and Thermosets; 1997 Dec; p. 8-10.
9. Carvalho MS, Azevedo JB, Barbosa JDV. Effect of the melt flow index of an HDPE matrix on the properties of composites with wood particles. Polym Test. 2020;90:106678.
10. Balasuriya PW, Ye L, Mai YW. Mechanical properties of wood flake-polyethylene composites. Part I: Effects of processing methods and matrix melt flow behaviour. Compos Part A Appl Sci Manuf. 2001;32(5):619-29.
11. Karmarkar A, Chauhan SS, Modak JM, Chanda M. Mechanical properties of wood-fiber reinforced polypropylene composites: Effect of a novel compatibilizer with isocyanate functional group. Compos Part A Appl Sci Manuf. 2007;38(2):227-33.
12. Barbosa JDV, Carvalho MS, Azevedo JB, et al. Development and characterization of WPCs produced with high amount of wood residue. J Mater Res Technol. 2020;9(5):9684-90.

Enhancing Hydrophobicity in Polyester Fabrics: The Role of PDMS and Silica in Surface Treatment

Paulo Romano Correia[1]*, Débora Leal[1], Vinícius Oliveira[1], Eduardo Kerche[1], Rodrigo Polkowski[1]
[1]TRL9 Tech – Research and Development; Salvador, Bahia, Brazil

Superhydrophobic fabrics play a key role in sustainable industrial applications, including oil/water separation and self-cleaning materials. This study addresses the challenge of enhancing hydrophobicity while preserving fabric functionality by modifying its surface via dip-coating with poly(dimethylsiloxane) (PDMS) and silica nanoparticles. Water contact angle (WCA) measurements were performed by depositing droplets on the fabric surface and capturing images via optical microscopy. The angles were determined using the tangent method in the ImageJ software. Eight measurements were taken per sample to ensure reproducibility. Untreated fabric exhibited a WCA of 84°, while PDMS coatings (2 wt% and 4 wt%) increased WCAs to 129.1° and 131.7°, respectively. The incorporation of silica nanoparticles further enhanced hydrophobicity (WCA: 137°), attributed to the increased roughness on the surface observed by optical microscopy (OM). However, higher PDMS concentrations (4 wt%) reduced fabric permeability, compromising the fluid flow. These results underscore the need for PDMS's content optimization to maintain breathability while achieving robust water repellency.
Keywords: Hydrophobicity. Fabric. Filtration. Nanosilica. Coating.

Superhydrophobic behavior is observed in fabrics with a water contact angle (WCA) exceeding 150°. The surface of those fabrics integrate biomimetic principles and nanotechnological advancements to replicate hierarchical structures found in nature, such as lotus leaves (the lotus effect) and butterfly wings [1]. In addition to efficiently repelling liquids, superhydrophobic fabrics exhibit self-cleaning properties, reduced contaminant adhesion, and enhanced durability. Those characteristics are critical attributes for applications that require resistance to harsh environments, ranging from medical apparel to industrial filtration systems [2].

In a general way, the superhydrophobic effect arises from the synergy between multiscale surface roughness (micro- and nanostructures) and low-surface-energy at the liquid-solid interactions. The superhydrophobic behavior of a surface can be explained by three main theoretical models Young, Wenzel, and Cassie Baxter which describe how chemical modifications on heterogeneous surfaces affect the way water interacts with them [3].

Received on 16 March 2026; revised 20 May 2026.
Address for correspondence: Paulo Romano Correia. TRL9 Tech. R. Mundo, 121 - Trobogy. Salvador – BA – Brazil. Zipcode: 41745-715. E-mail: paulo.correia@trl9.tech.

J Bioeng. Tech. Health 2026;9(7):659-665

The increasing demand for water decontamination filters is driven by pressing global challenges, such as water scarcity and aquatic ecosystem pollution. For instance, industrial activities release an estimated two million tons of oil annually into water bodies, compromising biodiversity and public health [4]. Conventional wastewater treatment technologies, such as centrifugation and chemical precipitation, are gradually being replaced by membrane-based separation techniques, due to their higher energy efficiency and scalability [5]. However, developing membranes with tunable hydrophobicity and sufficient mechanical robustness remains a critical bottleneck, particularly for oily wastewater remediation, where selective absorption of hydrophobic contaminants is essential [5].

The engineering of superhydrophobic surfaces relies on two interrelated pillars: (1) the fabrication of hierarchical micro- and nanoscale roughness, which traps air and minimizes liquid-solid contact (Cassie-Baxter regime), and (2) chemical functionalization with low-surface-energy materials, such as fluoropolymers or silanes, to repel polar molecules [3].

Silica nanoparticles (SiO_2) and polydimethyl-siloxane (PDMS) have emerged as promising candidates in this context. While silica nanoparticles provide tunable surface topography, PDMS, a flexible and cost-effective polymer, exhibits intrinsic hydrophobicity and strong adhesion to fabrics substrates [6]. Recent studies demonstrated that combining those materials yields synergistic effects, elevating the WCA above 160° and improving resistance to abrasion and repeated washing cycles [1].

However, optimizing the ratio of silica to PDMS presents a multifaceted challenge. Excessive silica content may compromise fabric flexibility, whereas insufficient PDMS levels reduce coating cohesion, leading to delamination under mechanical stress [7]. Moreover, traditional fluoropolymer-based coatings, while highly effective, face criticism due to environmental persistence and bioaccumulation risks, urging the development of eco-friendly alternatives [8].

Although PDMS is not biodegradable, it is considered less toxic than perfluorinated compounds, making it a viable candidate for biomedical and environmental applications [8]. Deposition techniques such as dip-coating and electrospinning are widely employed to apply superhydrophobic coatings onto fabrics. However, achieving uniformity requires precise control over parameters such as solution viscosity, immersion speed, and temperature [9]. On the other hand, dip-coating, in particular, allows for adjustable coating thickness by varying particle concentration and the number of immersion cycles, yet inconsistencies in homogeneity can create hydrophilic regions, compromising overall performance [7].

Despite recent advancements, systematic studies on the impact of silica and PDMS concentrations on specific fabrics substrates, such as polyester, remain scarce. While Chen and colleagues [1] explored nature-inspired hierarchical structures, the study did not address the relationship between composition, morphology, and long-term mechanical stability, which is an essential gap for practical applications. This study addresses challenges by engineering polyester fabrics via a dip-coating process with variable PDMS and silica nanoparticle concentrations. Optical microscopy and WCA measurements were used to correlate surface morphology with wettability, respectively. Optimal formulations were identified, maximizing hydrophobicity while preserving fabric functionality. This research presents innovations for diverse sectors, including oil-water separation membranes, protective medical fabrics, and self-cleaning architectural materials, aligning with global sustainability objectives.

Materials and Methods

Figure 1 shows commercial Telesilk polyester fabric with 150 threads. Discs measuring 6 cm in diameter were pre-cleaned in a 1% nonionic detergent solution at 100°C for 1 h. The samples were then rinsed with distilled water three times and dried at 80°C for 4 h. Five formulations (Table 1) were prepared with PDMS and silica nanoparticles.

The formulations were prepared as follows: I. First, in a beaker, a solution of 2 wt.% or 4 wt.% of PDMS resin in isopropanol was prepared

Table 1. Formulations.

Codes	Samples
F0	Before washing
F1	Treatment with PDMS 2%
F2	Treatment with PDMS 2% + Silica 0.1%
F3	Treatment with PDMS 4%
F4	Treatment with PDMS 4% + Silica 0.1%

Figure 1. 150-thread polyester fabric discs before treatment.

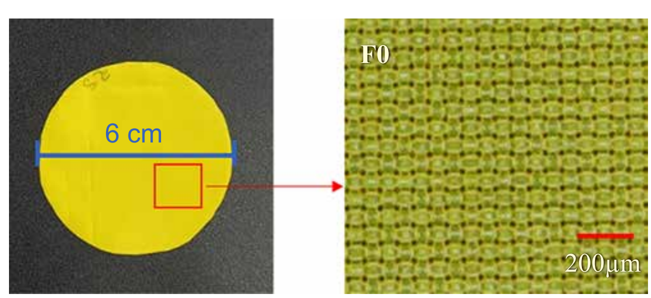

and left under agitation in an ultrasonic bath for approximately 15 minutes at 65°C; II. Then, 0.1 wt.% of nanosilica was slowly added to the isopropanol solution, and the dispersion was kept under stirring in an ultrasonic bath for homogenization; III. Finally, an equivalent amount (0.2 wt.% or 0.4 wt.%) of the PDMS-curing agent was added to the mixture, which was kept in the ultrasonic bath for another 15 minutes. For the formulations containing only PDMS, the same procedure described was followed, eliminating only step II.

After preparing the formulations, the fabrics were treated using the "dip-coating" method, chosen for its simplicity and cost-effectiveness without needing expensive machinery. Thus, the fabrics were immersed in the solution with the dispersed components and left for 30 minutes in the ultrasonic bath at 65°C. Finally, the coated fabrics were cured at 120°C for 1 hour in an oven. Optical microscopy (OM) images of the fabrics surface were carried out before and after the fabrics treatments. To evaluate the fabrics wettability after surface treatments, water contact angle (WCA) measurements were performed. For that, droplets were deposited on the fabric surface, and images of the droplets were obtained using optical microscopy. These images were analyzed using the ImageJ software, applying the tangent method to determine the contact angle value, defined between the fabric surface and the tangent line at the solid-liquid interface. Eight WCA measurements were taken in different regions of each sample to ensure data reproducibility. The average contact angle and standard deviation were calculated for statistical analysis. Filtration tests were conducted using an apparatus assembled as shown in Figure 2. A Kitasato served as a base with glassware on the top. Fabrics were positioned between the glassware and the Kitasato, and a mixture of dyed water (blue) and colorless oil was poured to evaluate separation efficiency and flux.

Results and Discussion

Figure 3 presents the water droplets on the fabrics before (F0) and after the treatments (F1, F2, F4). The results indicate a significant increase in WCA after surface treatments, demonstrating improved water repellency. This effect was more pronounced in formulations containing silica (F2 and F4), suggesting that the incorporation of nanoparticles enhances hydrophobicity.

The interaction between PDMS and nanosilica promotes the formation of hierarchical nanostructures on the fabric surface, reducing water adhesion and bringing the surface closer to a superhydrophobic state [1].

Sample F1 (2 wt% PDMS) exhibited a contact angle of 129.1° (Figure 4), which represents a significant increase compared to the untreated sample F0, which showed an WCA of 84°, indicating improved hydrophobicity. However, when PDMS concentration increased to 4% (F3) WCA improved to 131.7°, a modest gain of 1.52%. Similar findings have been reported in the literature

Figure 2. Filtration system.

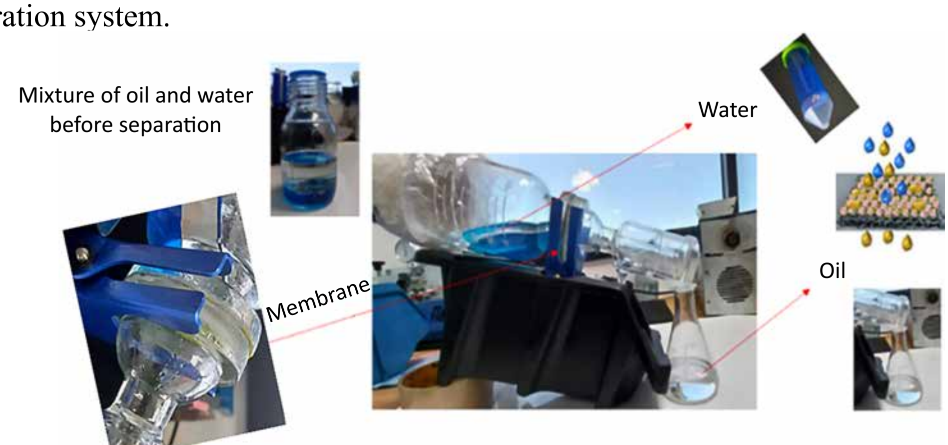

Figure 3. Water droplets on fabric's surfaces before (F0) and after PDMS (F1) and PDMS+nanosilica (F2, F4) treatments.

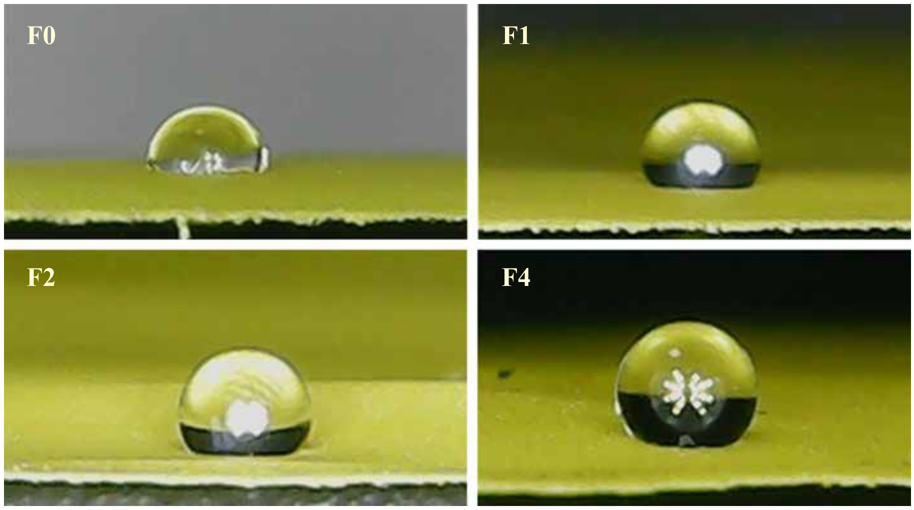

Figure 4. Water contact angle (WCA) values of the fabric's surfaces before and after surface treatments.

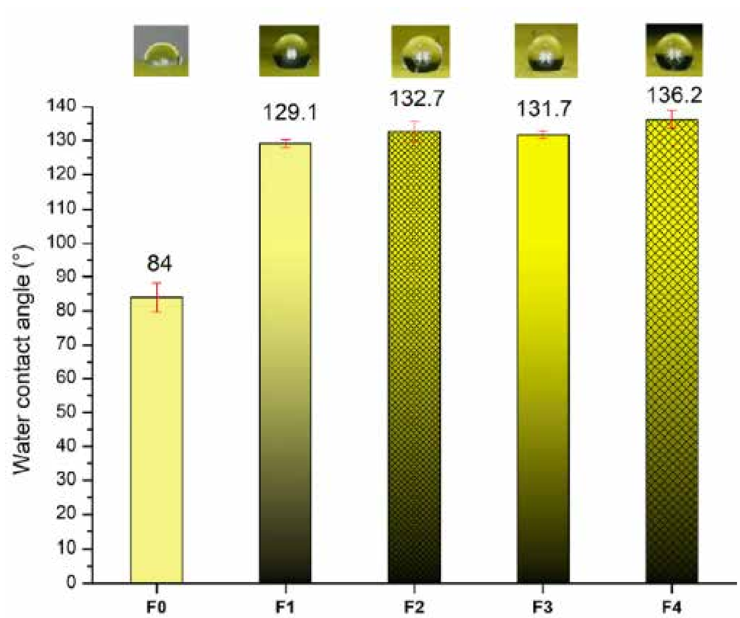

[10]. According to Öztürk and Parvate [11,12], the concentration increase of hydrophobic agent beyond a certain threshold provided diminishing returns due to the limited surface area availability for additional coating.

The incorporation of silica nanoparticles in formulations F2 and F4 demonstrated a positive effect on hydrophobicity, highlighting the role of surface roughness. While F1 and F3 (without silica) exhibited water contact angles (WCA) of 129.1° and 131.7°, respectively, F2 and F4 (with silica) achieved higher WCAs of 132.7° and 136.2°.

This corresponds to an increase of approximately 61.67% in hydrophobic performance compared to the unmodified formulations. These results suggest that the synergistic combination of PDMS and silica nanoparticles enhances hydrophobicity by generating hierarchical micro- and nanostructures that reduce the effective contact area between water droplets and the membrane surface [13]. Moreover, hierarchical structures formed by silica nanoparticles may also trap air pockets, further reducing wettability and contributing to the observed increase in WCA [11-13].

The F3 and F4 samples presented a slightly higher WCA than those of F1 and F2, indicating that PDMS concentration increase beyond a certain limit does not result in proportional benefits to hydrophobicity. This behavior suggests a saturation effect, where an excess of PDMS does not significantly contribute to water repellency but may lead to undesirable structural changes in the fabric [11].

Figure 5 presents samples' optical microscopy images. As the higher PDMS concentration, the higher is the clogging of the fabric pores, which may reduce its porosity. This phenomenon could compromise applications requiring controlled permeability, such as filtration or breathable fabrics [14].

Surface treatments significantly impacted the efficiency of oil-water separation, reflecting in the filtration flux, and in the "no filtration" condition for sample F0. Besides, F0 did not have wettability alterations, which maintained a permeable structure to both fluids (water and oil), failing to create a selective barrier. This behavior also corroborates with previous studies [1-15], stating that untreated fabrics or those with unbalanced coatings (e.g., low nanoparticle concentration) usually have insufficient surface roughness, resulting in contact angles below 130° and failure in selective separation. According to Hanosh, Unnikrishnan, and Sajan (2023) [15], the absence of a hierarchical structure (micro/nano) prevented efficient water repulsion, allowing both liquids to permeate the fabric. However, the optimization of PDMS-silica concentration is critical to avoid excessive pore blockage, a challenge not addressed in scientific formulations [16,17].

The samples treated with PDMS demonstrated distinct filtration performances, clearly highlighting the critical influence of formulation on membrane functionality. F0 sample (Table 2), this sample was unable to perform oil-water separation. The absence of surface treatment resulted in non-selective wettability, allowing both oil and water to permeate freely, and therefore failing to promote effective phase separation.

Table 2. Filtration results.

Samples	Average	Flow ($L/m^2{\cdot}h$)	Efficiency (%)
F0	Does not separate	-	-
F1	5.55 min	275.6 $L/m^2{\cdot}h$	99.9
F2	38.12 min	40.08 $L/m^2{\cdot}h$	99.9
F3	Does not filter	-	-
F4	24 h	1.061	99.9

Sample F1 exhibited a high flux of 275.6 $L/m^2{\cdot}h$, demonstrating that the introduction of PDMS coating successfully improved the membrane's hydrophobicity. This enhanced water repellency and allowed efficient oil passage while repelling water, enabling effective oil-water separation (99.9%) with minimal impact on permeability.

Sample F2 exhibited a permeate flux of 40.08 $L/m^2{\cdot}h$, representing a substantial decrease of 82.9% compared to sample F1. The increased surface roughness introduced by the nanoparticles likely added energy barriers to fluid transport, slowing the oil permeation. Nevertheless, the hierarchical roughness structure enhanced the hydrophobicity, promoting stronger water repellency and improved phase separation (99.9%).

Sample F3 did not permit any fluid passage, indicating that the excessive PDMS loading (4 wt.%) led to complete pore blockage. That is, increasing PDMS concentration negatively affected the membrane's permeability. The thick polymer coating fully obstructed the porous structure (as observed in the OM images in Figure 5), eliminating fluid passage. This observation aligns with previous

Figure 5. Optical microscopy images of F0, F2, and F3 fabrics.

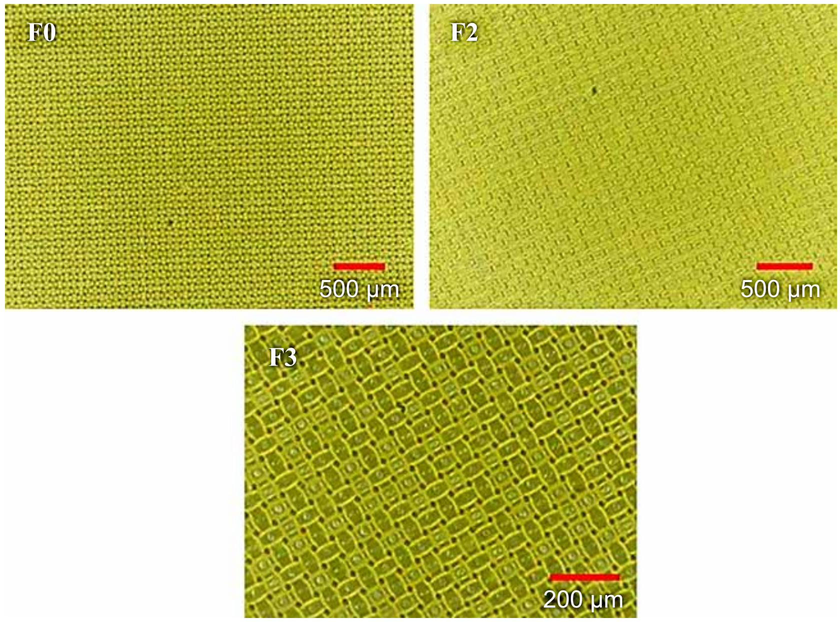

studies showing that overcoating or excess polymer deposition can fully clog membrane pores and severely compromise filtration functionality.

Sample F4 presented an extremely low flux of 1.061 L/m²·h, suggesting that while both hydrophobicity, surface roughness and separation efficiency (99.9%) increased, the combined effect of PDMS thick layers and silica nanoparticles drastically restricted permeability. The significant reduction in flux indicates that pore obstruction occurred, likely due to excessive polymer coverage, further validating the importance of maintaining an optimal balance between coating thickness and nanoparticle content.

These results are consistent with previous studies, which have shown that excessive surface modification either through high polymer loading or an overabundance of nanoparticles can lead to pore blockage. This phenomenon significantly reduces permeate flux and compromises the overall filtration efficiency of the membrane system [11,12,15].

Conclusion

The combination of PDMS and silica nanoparticles demonstrated efficacy in obtaining hydrophobicity in fabrics, with silica nanoparticles inducing surface roughness, and PDMS acting as a binding and apolar agent, ensuring coating stability and performance. However, high concentrations of PDMS (4 wt%) compromised the permeability of the fabric, reducing its flow in oil-water separation. The results also showed that optimizing the PDMS concentration is critical to balance water repellency (contact angle of up to 136.2°) and material functionality. Therefore, the findings emphasize the need for carefully optimized surface treatments to achieve a synergistic balance between hydrophobicity, surface roughness, and porosity. This balance is essential to ensure effective oil-water separation while preserving sufficient permeability.

Acknowledgement

The authors are grateful to the TRL9 TECH Company and Brazilian Research Agency (CNPq) for all the technical and financial support.

References

1. Chen J, et al. Nature-inspired hierarchical protrusion structure construction for washable and wear-resistant superhydrophobic textiles with self-cleaning ability. ACS Appl Mater Interfaces. 2021;13(15):18142-51. doi:10.1021/acsami.1c03539.

2. Li S, et al. A review on special wettability textiles: theoretical models, fabrication technologies and multifunctional applications. J Mater Chem A. 2017;5(1):31-55. doi:10.1039/C6TA07984A.
3. Huovinen E, et al. Micro-micro hierarchy replacing micro-nano hierarchy: a precisely controlled way to produce wear-resistant superhydrophobic polymer surfaces. Langmuir. 2012;28(41):14747-55. doi:10.1021/la303358h.
4. Onyena AP, Kabari S. A review of the threat of oil exploitation to mangrove ecosystem: insights from Niger Delta, Nigeria. Glob Ecol Conserv. 2020;22:e00961. doi:10.1016/j.gecco.2020.e00961.
5. Romero AS, et al. Unveiling the potential of silicon carbide as a support material and membranes for oily wastewater remediation. Sep Purif Technol. 2025;354:129044. doi:10.1016/j.seppur.2024.129044.
6. Namdari N, et al. Advanced functional surfaces through controlled damage and instabilities. Mater Horiz. 2020;7(2):366-96. doi:10.1039/C9MH01516G.
7. Laad M, Babaji G. Fabrication techniques of superhydrophobic coatings: a comprehensive review. Phys Status Solidi A. 2022;219(16):2200109. doi:10.1002/pssa.202200109.
8. Sun L, et al. Tailoring materials with specific wettability in biomedical engineering. Adv Sci (Weinh). 2021;8(19):2100126. doi:10.1002/advs.202100126.
9. Xu X, et al. Assembled one-dimensional nanowires for flexible electronic devices via printing and fuel cell. Appl Surf Sci. 2020;511:145415. doi:10.1016/j.apsusc.2020.145415.
10. Parvate S, Prakhar D, Chattopadhyay S. Superhydrophobic surfaces: insights from theory and experiment. J Phys Chem B. 2020;124(8):1323-60. doi:10.1021/acs.jpcb.9b08567.
11. Dong W, et al. Fabrication of superhydrophobic PET filter material with fluorinated SiO_2 nanoparticles via simple sol-gel process. J Sol-Gel Sci Technol. 2021;98(1):224-37. doi:10.1007/s10971-021-05483-4.
12. Stucki MT. Internal pore functionalization for applied polymer membranes [dissertation]. Zurich: ETH Zurich; 2017.
13. Hanosh S, Unnikrishnan VK, Sajan DG. Fluorine-free superhydrophobic PDMS-coated silica particles for oil-water separation and liquid marbles. J Mater Sci. 2023;58(48):18060-72. doi:10.1007/s10853-023-09171-2.
14. Kim SH, et al. Superamphiphobic PDMS/silica nanoparticle surfaces with high liquid impact resistance: effect of structural hierarchy on superamphiphobicity. Macromol Res. 2025;33(2):235-45. doi:10.1007/s13233-025-00374-x.
15. Mousa HM, et al. Membranes for oil/water separation: a review. Adv Mater Interfaces. 2022;9(27):2200557. doi:10.1002/admi.202200557.

Effects of Inoculation in Gray Cast Iron with the Addition of Niobium from Scrap

Henrique Silva[1,2]*, Orestes Alarcon[2], João Carlos Espíndola Ferreira[2]
[1]Federal Institute of Education, Science and Technology Catarinense – Fraiburgo Campus; Fraiburgo, Santa Catarina;
[2]Federal University of Santa Catarina, University Campus, Technological Center; Florianópolis, Santa Catarina, Brazil

Casting is one of the oldest and most widely used manufacturing processes in industry; however, it is known for its high consumption of natural resources and the generation of waste and pollutants. Given the growing need for sustainable practices, this work proposes the reuse of metallic materials through the casting of gray cast iron ingots, using recycled scrap with the addition of niobium from a FeSiNb alloy. The inoculation technique was applied to investigate the influence of niobium on the microstructure and mechanical properties of the cast material. Metallographic and machining tests were carried out to evaluate the quality of the recycled material. The results indicate significant potential in using recycled materials combined with alloying elements such as niobium to improve metallurgical performance and reduce the environmental impact of casting production.
Keywords: Cast Iron. Foundry. Sustainable Manufacturing. Sound Level.

Casting is recognized as one of the oldest manufacturing processes used by humankind. Despite its historical and industrial significance, the process still faces major challenges related to the excessive consumption of natural resources and the generation of waste and pollutants [1,2]. In this context, the search for sustainable solutions has become essential to mitigate the environmental impacts associated with casting. However, replacing conventional materials with more environmentally friendly alternatives faces obstacles such as limited technical knowledge, a lack of available options, and specific market demands [2]. Aiming to contribute to the sustainability of the metallurgical sector, this study proposes an investigation into the effects of varyingthe addition of recycled niobium from FeSiNb-based scrap in the casting process. The use of recyclable materials in this context represents a promising alternative to reduce environmental impact without compromising the performance of final products [3,6,7].

Cast Iron

Cast iron is a metallic alloy primarily composed of iron, carbon, and silicon, and may also contain elements such as manganese, sulfur, and phosphorus. Its classification is based on the shape of the graphite and the fracture appearance, which influence its mechanical properties [8].The chemical structure of cast iron is mainly influenced by carbon and silicon. Carbon controls graphite formation, while silicon acts as a graphitizing agent, promoting the decomposition of iron carbide. Silicon tends to push cast iron toward gray or white conditions, whereas manganese, commonly present, opposes silicon by stabilizing cementite and balancing its graphitizing effect. Manganese is also added as a desulfurizer but often stabilizes pearlite, especially in large castings. Other elements like phosphorus and sulfur play minor roles in graphitization, though phosphorus can stabilize iron carbides and phosphides, causing a white and porous appearance. Understanding cast iron metallurgy, including solidification, is essential to grasp microstructure formation and the material's mechanical properties, compromising the ability of future generations to meet their own needs [2].

Niobium and cast iron

Niobium (Nb) is a metallic element with atomic number 41, known for its unique properties such as a high melting point (2468ºC) and superconductivity at very low temperatures. Its main uses include microalloyed steel production, heat-resistant

Received on 24 March 2026; revised 27 June 2026.
Address for correspondence: Henrique Silva. Av. Orlando Gomes, 1845 - Piatã, Salvador – BA – Brazil, Zipcode: 41650-010. E-mail: heinrichguilherme@gmail.com.

J Bioeng. Tech. Health 2026;9(7):666-671

stainless steels, and superalloys. Niobium has gained growing economic importance due to rising demand.

In gray cast iron, niobium offers several benefits when added as an alloying element: it increases mechanical strength, enhances corrosion resistance, improves machinability, reduces component weight, and boosts thermal conductivity [9]. These improvements make gray cast iron more durable, cost-effective, and suitable for demanding applications like automotive parts, engines, and heat exchangers [9].Additionally, niobium contributes to sustainability by extending the lifespan of cast components and reducing maintenance needs

Determination and Solidification of Cast Iron Structure

The chemical structure of cast iron is mainly influenced by carbon and silicon. Carbon controls graphite formation, while silicon acts as a graphitizing agent, promoting the decomposition of iron carbide. Silicon tends to push cast iron toward gray or white conditions, whereas manganese, commonly present, opposes silicon by stabilizing cementite and balancing its graphitizing effect. Manganese is also added as a desulfurizer but often stabilizes pearlite, especially in large castings [4].

Other elements like phosphorus and sulfur play minor roles in graphitization, though phosphorus can stabilize iron carbides and phosphides, causing a white and porous appearance and the material's mechanical properties [10].

Materials and Methods

The development of the work is divided into two parts: obtaining the materials used in the research, including elements derived from scrap for the production of (a) cast iron, and (b) recycled niobium used. The experiments that make up this work were carried out in two foundry companies, which provided some of their laboratories for the addition of niobium to the iron alloy and the necessary material.

Material Selection

The choice of materials directly influences the quality of cast products. In this study, scrap-derived materials representative of industrial casting processes were used. In no study has gray cast iron GG-25 been used from scrap material supplied. According to DIN EN 1561 (1997), this material must have a tensile strength between 250 N/mm² and 350 N/mm² and a hardness between 180 HB and 250 HB.

Casting of test Specimens

All material used was separated and weighed on a precision scale. Therefore, the alloy of the material used was prepared in an induction furnace, with a temperature of around 1,480ºC. Following the protocol for this type of process, a small coin-shaped sample was taken for chemical analysis, in order to adjust the desired composition. Then, the oven temperature was raised to 1,505ºC for homogenization. The recycled niobium) and previously separated in the proportions of 0.2%, 0.6% and 0.8% of the 5kg volume of the sand molds was added when transferring the melt to the casting pan (Figure 1). Once you have the cast alloy and the molds, the process of pouring the pan into the molds is done manually, where a properly equipped employee pours the metallic liquid into the molds (Figure 2) made on the production line for subsequent cooling.

Metallographic Analysis

Metallography was used to examine the microstructure, which is essential for quality assurance, developing new alloys, and failure investigation. Analysis was performed using optical and electron microscopy. The metallographic test was carried out to study the influence of the addition of recycled niobium on the microstructure, which will make it possible to relate the properties to the machinability of the material. The metallographic analysis procedure was carried out in accordance

Figure 1. Cast blocks.

Figure 2. Molds with poured metal.

with standards NBR 13284:95 (2015) and NBR 6593:81 (2015).

The microstructural characterization was carried out in the central region of the samples taken from the cast specimen, which is called half radius [8].

The preparation of samples for metallographic analysis consisted of embedding the samples and sanding them using 220 and 400 mesh sandpaper, followed by polishing in a polishing machine.

To characterize the matrix, 4% Nital was used to identify pearlite and ferrite, and to count eutectic cells, the Stead reagent was applied, which highlights phosphorus and sulfur segregations and the cell contours.

Machining

Noise levels were measured using a DEC-46 sound level meter (35–130 dB, A-weighting), consistently positioned near the operator's ear during equipment operation (Figure 3) [11].

Figure 3. Sound level.

Microscopic Imaging

Images obtained through optical and electron microscopy were crucial for quality control, process optimization, and scientific research, enabling defect identification and detailed evaluation of the microstructure of cast materials.

Machinability Test

The flank wear (VB) of inserts was evaluated to estimate tool life during the machining of a cast ingot with 0.8% Nb, using VB = 0.3 mm as the end-of-life criterion. A 90° milling head with four Lamina OFMT 050405 inserts was used, with one cutting edge per insert. After 10 passes, the inserts were analyzed using a scanning electron microscope. Machining parameters were: cutting speed of 230 m/min, feed per tooth of 0.39 mm, and axial depth of cut of 3.3 mm.

Results

Results for Tool Wear

The machining parameters were: cutting speed Vc = 230 m/min; feed per tooth fo = 0.39mm; axial cutting depth Ap = 3.3 mm. In Figure 3, tool wear can be seen on each of the 4 edges of the insert used in the tests, which were visualized using a scanning electron microscope.

Flank wear on cutting tools affects machining quality. This study found an average wear of L = 0.585 mm (Figure 4), impacting precision, surface finish, and energy use. Solutions include maintenance, proper tool selection, optimized cutting parameters, and operator training. Results show good operational performance with the tested cast material.

Results for Noise Levels

For the noise level test, 10 passes of the cutting tool were performed on cast iron containing 0.8% niobium using the same conventional milling machine. Meanwhile, the sound level meter was continuously positioned near the operator's ear throughout the test. The noise level during the test remained constant, averaging 67.4 dB (NR 15, 2019), indicating good quality of the machined material. Milling noise results from the interaction between the tool and the workpiece and can impact workers' hearing health. Controlling sound pressure is essential for safety, production efficiency, and regulatory compliance, requiring innovations and safe practices in machine tool design.

Results for Metallographic Analysis

Sample 1

According to Figure 5, it is noted that sample 1 presents elongated black particles, which are called lamellar graphite, which are typical of gray cast iron. Lamellar graphite plays a fundamental role in improving the properties of gray cast iron, making it a material of choice in several

Figure 4. Images of the insert by SEM.

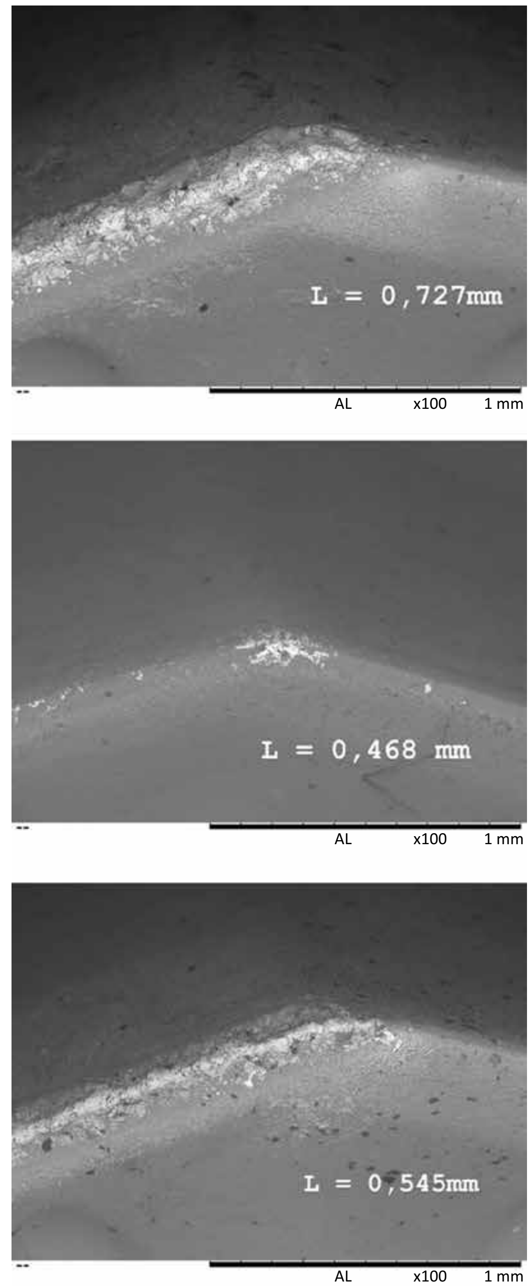

industrial applications. These benefits are mainly related to their unique microstructure and resulting mechanical characteristics.

Materials with lamellar graphite have a high vibration absorption capacity, making them ideal for components subjected to dynamic loads (e.g., engine blocks, brake drums, and gearboxes).In machining, lamellar graphite reduces cutting tool wear, making the process more efficient and cost-

Figure 5. Sample 1 (0.2% Nb).

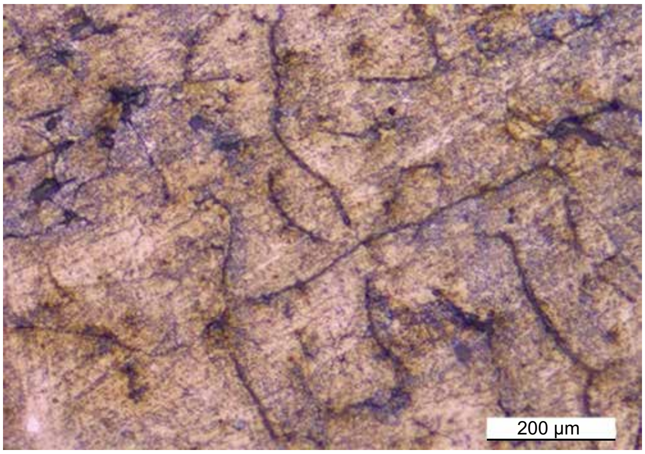

effective, especially for parts with tight tolerances [12].The material shows corrosion resistance, making it suitable for marine and industrial environments. It also improves heat dissipation and facilitates shaping into complex geometries during casting. The combination of these properties makes gray cast iron with lamellar graphite highly durable, with a prolonged service life in many applications.

Sample 2

Sample 2, shown in Figure 6, also exhibits graphite formation and, in particular, pearlite formation. The formation of pearlite in cast iron is a metallurgical process that provides a series of significant benefits for the metallurgical industry and other applications. Pearlite is a microstructure composed of alternating lamellae of ferrite and cementite (an iron–carbon compound), and its formation occurs through the controlled cooling of cast iron. Pearlite enhances the mechanical performance of cast iron by providing a balanced combination of hardness and toughness, enabling it to withstand loads, impacts, and wear moreover, pearlite formation can be controlled to meet specific requirements, ensuring wide applicability across industrial sectors [12].

Figure 6. Sample 2 (0.6% Nb).

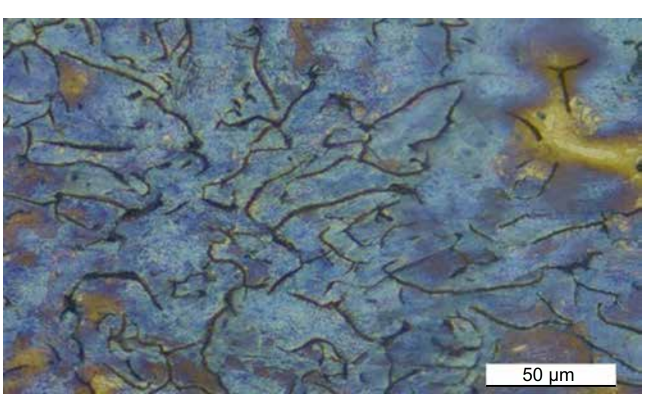

Sample 3

Sample 03 (0.8% Nb) showed ferrite formation in addition to graphite and pearlite (Figure 7). Ferrite increases malleability, making machining easier, improves corrosion resistance, enhances ductility and fatigue strength, and provides good thermal and electrical conductivity, making gray cast iron more suitable for applications requiring these properties [10].

Conclusions

This study evaluated the effects of niobium addition in cast iron alloys produced from scrap, demonstrating the technical and environmental viability of this approach for the metallurgical

Figure 7. Sample 3 (0.8% Nb).

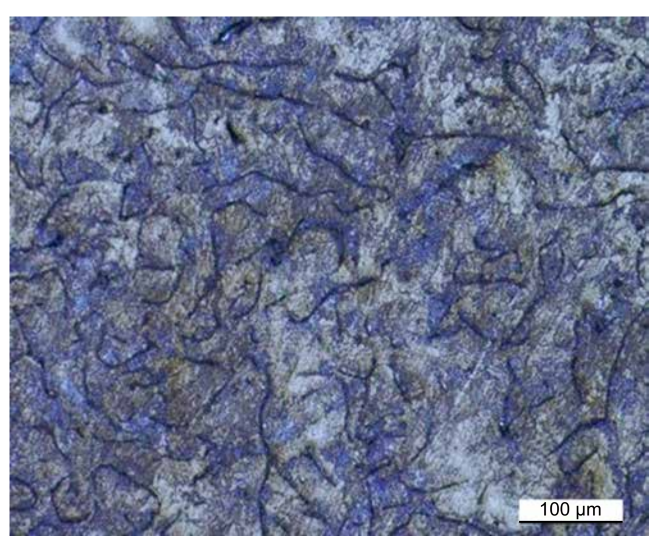

industry. Microstructural analysis revealed the presence of lamellar graphite, pearlite, and ferrite (0.8%), indicating that the composition and mechanical properties remain consistent with those obtained from virgin materials. Pearlite provided increased toughness and improved machinability, while ferrite contributed to enhanced ductility and corrosion resistance. Machinability tests showed results consistent with the literature, highlighting good surface finish quality and process efficiency. Additionally, acoustic monitoring during machining indicated noise levels below 85 dB, complying with occupational safety standards. Further studies on tool wear under varying cutting conditions are recommended to optimize the process.

References

1. Silva HG. Benchmarking da produção mais limpa em empresa de fundição em moldes de areia [dissertação]. Florianópolis: Universidade Federal de Santa Catarina, Programa de Pós-Graduação em Engenharia Mecânica; 2019.
2. Silva HG. Estudo comparativo na utilização de dois inoculantes alternativos e suas influências na rugosidade e tração do ferro fundido cinzento. Pato Branco: Universidade Tecnológica Federal do Paraná, Departamento de Engenharia Mecânica; 2015.
3. Silva HG, Ferreira JCE, Kumar V, Garzas-Reyes JA. Benchmarking of cleaner production in sand mould casting companies. Manag Environ Qual. 2020.
4. Gong X, Xiao X, Li Q, Zhao J, Zitiano V. Rapid recycling of waste salt core materials in foundry industry using fractional crystallization. 2023.
5. Lorenzetti DH, Cruz RM, Ricili S. Estratégia empresarial e sustentabilidade: um modelo integrador. Rev Pós-Grad Adm. 2008;2(3):33-57.
6. Bastas A. Sustainable manufacturing technologies: a systematic review of latest trends and themes. 2021.
7. Kazakova E, Lee J. Sustainable manufacturing for a circular economy. Sustainability. 2022.
8. Chiaverini V. Aços e ferros fundidos. 6th ed. São Paulo: ABM; 1988.
9. Guvik E, Kopycinski A, Ziolko A, Szczesny A. The method of inoculation of high-quality grey cast iron intended for massive castings for bottom and distance plates as well as counterweights manufactured as vertical castings. Arch Metall Mater. 2023.
10. Avdusinovic A, Gekic AG, Cubela D. Influence of inoculation methods and the amount of an added inoculant on the mechanical properties of ductile iron. 2015.
11. Brasil. Ministério do Trabalho e Emprego. Norma Regulamentadora nº 15: atividades e operações insalubres. Portaria SIT nº 339, de 31 de outubro de 2012. Brasília: MTE; 2012.
12. Franzen D, Weiss K, Gundlach J, Buhrig-Polaczek A. Application of surface layer inoculation processes to solid solution-strengthened ductile cast iron. Int J Metalcast. 2020;14:1041-51.

G.R.O.W Project: Development of a Technical Manual for Sustainable and Educational Cultivation in Governador Mangabeira

Alessandra Cardim[1]*, Gabriela Lopes[1], Mauro Reis[1], Nathalya Barros[1], Sara do Vale[1], Clariane Teixeira Pessoa Mamona[1], Pietro Carlos Gonçalves Conceição[1]
[1]*SENAI CIMATEC University, Department of Biotechnology; Salvador, Bahia, Brazil*

This study presents the G.R.O.W Project, an educational and technological initiative designed to strengthen sustainable agricultural practices in school and family gardens within the municipality of Governador Mangabeira, Bahia, Brazil. Addressing a socio-environmental context marked by land fragmentation, soil degradation, and limited access to agroecological knowledge, the project integrates the disciplines of geography, chemistry, and mathematics to develop low-cost, replicable solutions for food production and environmental education. Methodologically, the study employed an ethnoscientific approach, combining participatory observation, informal interviews, and bibliographic research to document local agricultural practices and integrate traditional knowledge into technical recommendations. The resulting manual details strategies for soil preparation, crop layout optimization, automated drip irrigation using Arduino-based moisture sensors, rainwater drainage systems, and ecological pest control through botanical extracts and biological competition. Experimental implementation demonstrated the technical and economic feasibility of these systems, with an estimated total cost of R$ 338.34, significantly lower than conventional alternatives, while ensuring water efficiency and crop productivity. The proposed solutions directly support food security, promote environmental preservation, and enhance community autonomy, positioning the school as a hub for rural innovation and socio-environmental transformation.
Keywords: Sustainable Agriculture. Low-Cost Technologies. Technical Manual. Community Gardens. Environmental Education.

Family farming constitutes the foundation of rural social and productive organization in the municipality of Governador Mangabeira, located in the Recôncavo Baiano region, where more than 90% of properties have less than 30 hectares. This fragmented land structure reveals an agrarian landscape deeply marked by small-scale production, scarcity of resources, and a continuous search for survival strategies. In this context, tobacco monoculture, carried out through integration contracts with large companies, represents the main source of income for farming families. However, this integrated production tends to intensively exploit family labor, imposes high production costs, and compromises food security, as it prioritizes the cultivation of a single crop destined for export [1].

Received on 22 March 2026; revised 10 June 2026.
Address for correspondence: Alessandra Cardim. Av. Orlando Gomes, 1845 - Piatã, Salvador – BA – Brazil, Zipcode: 41650-010. E-mail: ale.acardim@gmail.com.

J Bioeng. Tech. Health 2026;9(7):672-678

As a consequence, farmers face numerous difficulties in reproducing socially within their own agrarian space, being forced to seek off-farm employment, especially in the services sector and public service positions, as a way to supplement their income [2]. Production for self-consumption, including vegetables, roots, and small animal husbandry, has been a recurring and strategic practice to mitigate food insecurity and ensure a minimal diet for families, even in a context of precariousness [3].

In view of this scenario of structural vulnerability and limited qualifications for family farming production in Governador Mangabeira, the G.R.O.W Project, developed by technical students from Universidade SENAI Cimatec, in partnership with Educandário Construir, emerges as an educational initiative aimed at strengthening sustainable cultivation practices in school and family gardens in the municipality. The project is set within a territory marked by soil degradation, excessive use of chemical inputs in conventional agriculture, and a growing detachment of youth from rural life and agricultural work [4,5].

In orderto help reverse this situation, the project integrates knowledge from geography, chemistry, and mathematics to create low-cost solutions that optimize food production, preserve the environment, and promote critical environmental education [6].

Among the proposed solutions, the following stand out: the implementation of an automated irrigation system based on Arduino boards, the use of rainwater, and the production of natural extracts for pest and disease control in crops. These measures directly align with the principles of agroecology, which prioritize productive autonomy, the rational use of natural resources, and the appreciation of traditional knowledge [5].

Furthermore, the project acknowledges the transformative role of schools in strengthening the connection between youth and rural spaces, encouraging student protagonism and the production of knowledge applicable to the local reality. The choice of Educandário Construir as the pilot site is justified by its commitment to an interdisciplinary pedagogical approach and its presence in a community historically linked to family farming [6].

This work aims to develop a technical manual with practical instructions and guidelines for improving and optimizing the stages of cultivation and harvesting in the school garden, following the QSMS&RS management system (Quality, Safety, Environment, Health, and Social Responsibility), and for specific objectives: develop accessible technologies to optimize soil preparation, irrigation, drainage, and crop protection processes, ensuring proper management of the agricultural space; promote effective agroecological practices for pest control, integrated soil management, and sustainable reuse of water resources; encourage educational actions within the school community that reinforce the importance of safety protocols in agricultural management; systematize the knowledge produced in a technical manual to support sustainable and safe agricultural practices, facilitating its application by rural families.These objectives provide a comprehensive foundation for understanding the problems and recommending practical actions that contribute to environmental preservation and the subsistence of the populations that depend on this garden in Governador Mangabeira.

G.R.O.W Project offers a concrete response to a context of exclusion and invisibility of family farming in the Recôncavo Baiano, reinforcing the role of schools as spaces for social and environmental transformation.

Materials and Methods

Study Area

The research was conducted in the municipality of Governador Mangabeira, located in the state of Bahia, Brazil (12°36′07″S, 39°02′34″W). The study area encompasses the surroundings of the Educandário Construir School, situated in a region characterized by the predominance of small rural properties, with agricultural practices based on family farming. The municipality is part of the Recôncavo Baiano identity territory and stands out for its historical, cultural, and productive relevance in the regional agricultural context.

The Educandário Construir School, where the actions of the G.R.O.W Project are concentrated, is embedded in a socio-environmental context of vulnerability, in which access to sustainable cultivation practices and environmental education is still limited. The institution serves as a training hub and a space for experimenting with agroecological techniques aimed at strengthening food security and fostering ecological awareness among students.

The area around the school (Figure 1) consists of soils typical of the Atlantic Forest biome, with secondary vegetation and the presence of small productive backyards traditionally used for growing vegetables, roots, and fruits intended for self-consumption.

Ethnoscience

The reality of the Educandário Construir garden (Figure 2) was analyzed through an approach grounded in ethnoscience, using photographic

Figure 1. Area surrounding the Educandário Construir School.

Source: Retrieved and adapted from Google Earth: http://earth.google.com/2025.

Figure 2. Garden of the Educandário Construir School.

Source: Retrieved and adapted from Google Earth: http://earth.google.com/2025.

records, videos, oral accounts, and exchanges of experiences with the management team, staff, and students of the institution. To this end, informal interviews and participatory observations were carried out to understand local practices related to soil preparation, organization of the productive space, agricultural planning, pest and disease control, as well as safety measures adopted during handling. This active and sensitive listening allowed the project's actions to reflect the knowledge and habits rooted in the local agricultural culture. In this way, the aim was to value the traditional knowledge of the residents of Governador Mangabeira, strengthening the connection between science, community, and territory.

<u>Scientific Axes</u>

Geography

The content of the manual within the geography axis was structured around soil preparation, organization of the agricultural space, crop selection, and sustainable management practices.

Soil preparation was described considering the sandy-clay composition of the terrain and its slightly acidic pH, typical of the Atlantic Forest biome in which the region is located. Guidelines were also included on organic fertilization, enrichment with natural compounds, and practices for conserving soil fertility after understanding soil layers, in order to support agronomic decision-making (Figure 3).

The garden layout was designed (Figure 4) to optimize space use, suggesting the division of beds by crop type (roots, vegetables, and fruits) and

Figure 3. Development of soil profile layers.

detailing the spacing, depth, and average harvest time of each plant.

Species selection prioritized foods with high nutritional value, good acceptance among children, and cultivation cycles adapted to local climatic conditions.

Figure 4. Mapping and layout of the Educandário Construir School garden.

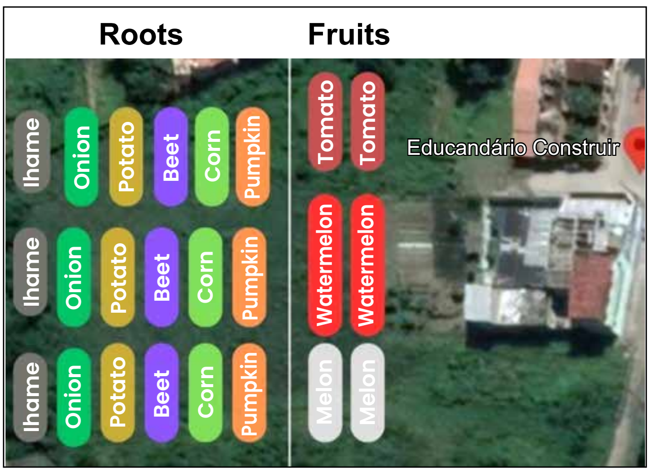

Mathematics

Regarding automated irrigation, a proposal was developed based on the use of the Arduino Uno R3, an open-source electronic prototyping platform widely used in educational projects (Figure 5). The functioning of the system was described step-by-step, beginning with soil moisture readings taken by an analog sensor connected to the A0 pin of the Arduino, followed by the activation of a water pump via a 1-channel relay when the soil moisture level falls below a pre-programmed threshold value (300). The system was designed to take measurements every 12 hours, using intervals defined in C++ code, and ensuring irrigation only when necessary, thus promoting water resource conservation.

The manual also provides detailed guidance on installing a drip irrigation system built with PVC hoses, connectors, and regular perforations. The main hose is placed along the beds and connected to a perforated secondary hose, with holes positioned near plant roots, respecting variable spacings

Figure 5. Representation of the Arduino board for system construction.

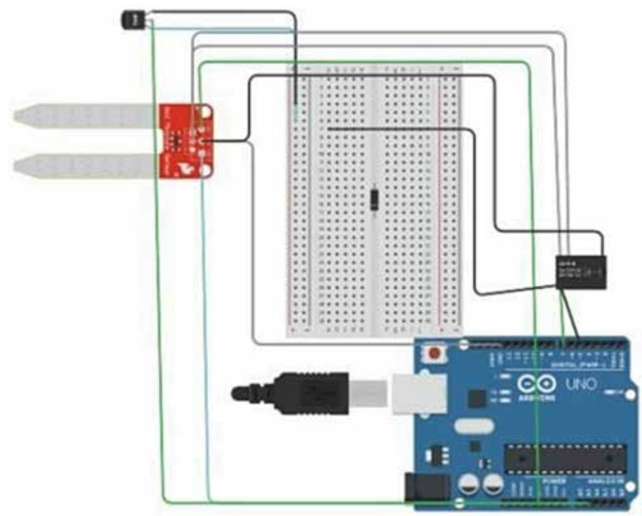

according to the water needs of each crop. The system layout was designed to ensure uniform coverage and optimize water absorption by plants (Figure 6).

For rainwater drainage (Figure 7), the assembly of an underground system was described, consisting of a PVC pipe 100 mm in diameter and approximately two meters in length, installed at a depth of about two hand spans in the soil. The pipe is perforated every 50 centimeters and covered with non-woven fabric (TNT) glued over the holes to prevent the entry of solid particles. The system is designed with a slope between 15° and 20°, facilitating water flow to an external area outside the school grounds, reducing the risk of waterlogging, and promoting greater water stability in the soil.

Chemistry

Based on literature reviews and interviews with school management members, a theoretical mapping was carried out of the main pest species affecting school crops, such as the leaf-cutting ant (*Atta sexdens rubropilosa*) [7], the cabbage looper (*Ascia monuste orseis*) [8], and the gamba grass (*Andropogon gayanus*) [3,5,9].

For each identified pest, natural compounds and their preparation methods were described.

Figure 6. Visual representation of the hose irrigation system in Tinkercad software.

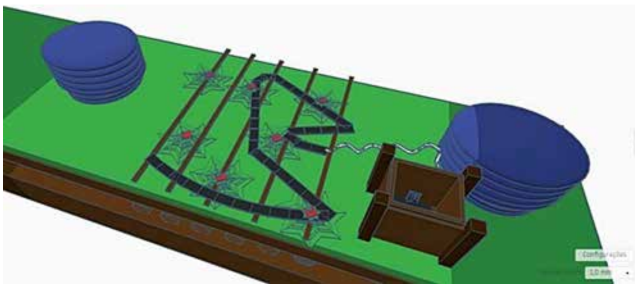

Figure 7. Illustration of the garden drainage system.

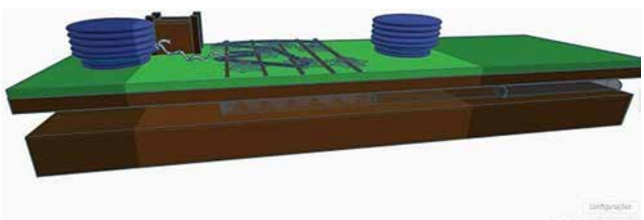

The control of leaf-cutting ants, for example, was addressed through the use of black sesame seeds, whose toxicity to the colony's symbiotic fungus (Leucoagaricus) represents an effective biological control method. In the case of the cabbage looper, extracts based on combinations such as lemongrass and mint, chestnut husks with Plantago leaves, chrysanthemum with marigold, and garlic extract were proposed. For controlling gamba grass (Figure 8), biological competition techniques with native plant species were recommended, as well as the use of pathogenic fungi and insects.

The guidelines included details on the methods of extraction, formulation, and application of natural extracts. Essential oils were obtained from plants cultivated in the rural zone itself, such as citronella and lemongrass. Extraction followed simple processes, using alcohol as a solvent, fresh or dried leaves as raw material, and maceration periods ranging from four to eight weeks, with storage in dark bottles to preserve efficacy. Application methods were described in a standardized way, prioritizing safety and phytosanitary effectiveness. The manual also included procedures for verifying the quality of natural extracts, based on visual observations, efficacy tests, and odor control, as well as guidance on monitoring biological traps installed in the cultivated area. The recording of practices carried out and the documentation of results were also recommended for continuous evaluation and improvement of the techniques described.

Figure 8. Diagram of strategies against gamba grass.

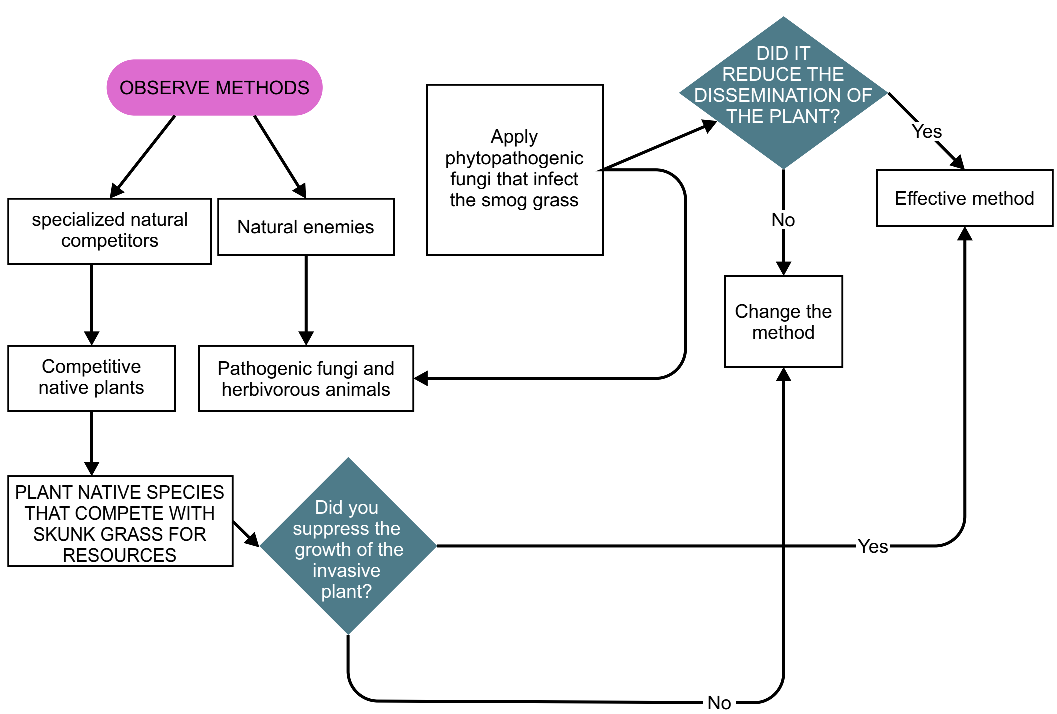

Results and Discussion

The data gathered during the preparation of the technical manual demonstrate the feasibility of implementing sustainable and low-cost systems for school-based agricultural cultivation in Governador Mangabeira. As shown in Table 1, the total estimated budget amounted to R$ 338.34, evidencing the cost-effectiveness of the proposed automated irrigation system with soil moisture sensors when compared to conventional market systems.

Table 1. List of materials and estimated budget for assembling the automated irrigation system.

Materials	Price (R$)
Irrigation hose	64.00
PVC elbow (50 cm)	15.00
PVC elbow (20 cm)	13.70
Pressure pump	84.60
Main hose	32.00
TNT fabric (nonwoven fabric)	5.90
Arduino	45.00
Acrylic box	28.14
100 mm pipe	50.00
Total	**338.34**

It was observed that the black hose used in the proposal (Figure 9) is suitable for adapted drip irrigation systems, allowing efficient water distribution after manual perforation, with reduced cost and high availability in the local market. The combination of a main white hose with branches of perforated black hose demonstrated theoretical hydraulic efficiency for small school gardens, with potential to optimize soil moisture and reduce water waste.

Regarding pest control, the research and organization of natural alternatives highlighted the potential of extracts such as garlic, mint, citronella, and infusions of native plants for the ecological management of invasive species [1,5,9,10], with emphasis on controlling the leaf-cutting ant (*Atta sexdens rubropilosa*) through the use of black sesame seeds [7] and the cabbage looper (*Ascia monuste orseis*) through botanical compounds [8]. Finally, based on the mapping of the garden, it was concluded that the best crops are root vegetables (yam, potato, onion, beet, corn, and pumpkin) and fruits (tomato, watermelon, melon, and strawberry), which, in addition to being nutrient-rich, have favorable harvest times, as shown in Table 2.

Figure 9. Black irrigation hose installed in the garden bed, manually perforated for water release.

Table 2. Agricultural crops and their harvest periods.

Fruits	Harvest Time
Tomato	60 to 90 days after planting
Watermelon	80 to 100 days after planting
Melon	55 to 75 days after planting
Strawberry	60 to 90 days after planting
Roots	**Harvest Time**
Yam	6 to 12 months
Potato	4 months
Onion	100 to 180 days after planting
Corn	60 days
Beet	60 to 70 days after planting
Squash	90 to 100 days after planting

References

1. Santos AJ, et al. O espaço agrário do município de Governador Mangabeira-BA: uma breve abordagem a partir da produção e reprodução social da agricultura familiar. Rev Territorium. 2024;1(1):1-15.
2. Corrêa da Silva HB, Cartes Patrício C, editors. Fortalecimento da agricultura familiar e desenvolvimento sustentável: cooperativismo, ATER e pesquisa agropecuária, ATER digital pós-COVID-19. Brasília: FAO; SEAB/PR; IAPAR-EMATER; 2022. Available from: https://www.fao.org/documents/card/en/c/cb9932pt/
3. Brasil. Ministério da Agricultura, Pecuária e Abastecimento. Secretaria de Desenvolvimento Agropecuário e Cooperativismo. Hortaliças não-convencionais (tradicionais). Brasília: MAPA; 2010. 52 p. Available from: https://www.gov.br/agricultura/pt-br/assuntos/sustentabilidade/tecnologias-sustentaveis/hortalicas-nao-convencionais
4. Silva MC, et al. A escola do campo e a juventude rural: desafios para a permanência no campo e o fortalecimento da agroecologia. Rev Educ Ruralidades. 2023;5(2):89-107.
5. Caporal FR, Costabeber JA. Agroecologia: enfoques teóricos e estratégias de ação. Brasília: Ministério do Meio Ambiente; 2004.
6. Brasil. Ministério da Agricultura, Pecuária e Abastecimento. Secretaria de Inovação, Desenvolvimento Sustentável e Irrigação. Boas práticas agrícolas para a produção de alimentos seguros: café, feijão, tomate, morango e hortaliças folhosas. Brasília: MAPA; 2022. 308 p. Available from: https://www.gov.br/agricultura/pt-br/assuntos/inspecao/produtos-vegetal/boas-praticas-agricolas
7. Peres Filho O, Dorval A. Efeito de formulações granuladas de diferentes produtos químicos e à base de folhas e de sementes de gergelim (*Sesamum indicum*) no controle de formigueiros de Atta sexdens rubropilosa Forel, 1908 (Hymenoptera: Formicidae). Cienc Florest. 2003;13(2):67-70.
8. Medeiros CAM, Boiça Júnior AL. Efeito da aplicação de extratos aquosos em couve na alimentação de lagartas de Ascia monuste orseis. Bragantia. 2005;64(4):633-41.
9. Gliessman SR. Agroecologia: processos ecológicos em agricultura sustentável. 2nd ed. Porto Alegre: UFRGS; 2009.
10. Lorenzi H, Matos FJA. Plantas medicinais no Brasil: nativas e exóticas. 2nd ed. Nova Odessa: Instituto Plantarum; 2008.

Assessment of Two Environmental Indicators in *Agave sisalana* Seedling Production

Ana Nadja Lopes Lucas[1]*, Lorena Rodrigues Cunha[1], Matheus Martins Teixeira Cota[1], Edna dos Santos Almeida[1]
[1]*SENAI CIMATEC University, Environmental Area; Salvador, Bahia, Brazil*

Sisal (*Agave sisalana*) is a renewable and versatile natural fiber widely used in ropes, rugs, bags, and composite materials for the automotive and construction industries. Beyond its industrial applications, sisal plays an important socioeconomic role, particularly in semi-arid regions such as northeastern Brazil, where it represents a major source of income for local communities. Maintaining this production chain, however, relies on continuous crop renewal, which depends directly on the availability of healthy and sustainable seedlings. In this context, nursery practices become essential for ensuring productivity and controlling phytosanitary problems, such as red rot, which has significantly affected sisal fields since the 1970s. This study evaluates key environmental indicators associated with the production of *Agave sisalana* seedlings, focusing on Global Warming Potential (GWP) and Cumulative Energy Demand (CED) of fossil origins. A gate-to-gate life cycle assessment was conducted to quantify the contributions of inputs such as fertilizers, polyethylene, electricity, and transportation. Fertilizer use was identified as the largest contributor to GWP (61.8%), while electricity (56.5%) and polyethylene (27.20%) were the largest contributors to cumulative energy demand. These results highlight significant opportunities for sustainability improvements through renewable energy adoption, input optimization, and enhanced operational efficiency. The integrated assessment provides a basis for advancing sustainable nursery practices and reducing the environmental footprint of *Agave sisalana* seedling production. Nevertheless, a more comprehensive assessment including additional environmental indicators is required to capture the full range of impacts and to guide more robust sustainability strategies.
Keywords: Nursery. Energy Demand. Greenhouse Gas Emission. Global Warming Potential. Life Cycle Assessement.

Sisal fiber has a bunch of uses, from making twine, rope, rugs, and bags to being used in the auto and construction industries through composites. It is also a big source of income for a lot of communities. Sisal is becoming increasingly important in the world looking for affordable alternatives because it is versatile and sustainable [1,2].

Extracted from the leaves of the *Agave sisalana* plant, sisal fibers are renewable and relatively inexpensive natural resources. Grown mainly in northeastern Brazil and other semi-arid regions, these robust and drought-tolerant plants have been cultivated for centuries due to their high resistance and durability [1-3].

Addition to their economic and social relevance, sisal crops have an environmental dimension, as they can contribute to carbon sequestration in semi-arid ecosystems and represent a low-impact alternative to synthetic fibers [2,4,5].

However, maintaining this production chain depends directly on crop renewal, which reinforces the importance of efficient and sustainable practices for seedling production.

The production of *Agave sisalana* seedlings from bulbils in nurseries is an important strategy for the renewal of productive areas, especially in the face of phytosanitary problems such as red rot, which since the 1970s has severely affected sisal in the Northeast, particularly in Bahia, reducing productivity and leading to the premature death of plants [6]. Factors such as nutritional deficiencies, water stress, and low physiological resistance increase susceptibility to pathogens [7,8].

To contain the spread of the disease, it is essential to use healthy seedlings obtained through techniques such as tissue culture or propagation via selected bulbils [9].

These bulbils, originating from the inflorescence of adult plants (8–10 years old), should be chosen based on the vigor, size, and health of the mother

Received on 15 March 2026; revised 21 June 2026.
Address for correspondence: Ana Nadja Lopes Lucas. Av. Orlando Gomes, 1845 - Piatã, Salvador – BA – Brazil, Zipcode: 41650-010. E-mail: ana.lucas@fbter.org.br.

J Bioeng. Tech. Health 2026;9(7):679-685

plant, in addition to being larger than 10 cm and undergoing preventive treatments [10,11].

Proper cultivation in a nursery ensures the adequate development of seedlings, which, after growing, can be transplanted to the field, contributing to the sustainability and productivity of the crop [12].

Despite its importance, there are still few studies that quantify the environmental impacts of sisal seedling production. As this stage represents the foundation of the entire value chain, it is essential to understand its contributions to key environmental parameters.

Considering the relevance of this initial stage for the entire sisal production chain, this study aims to evaluate two critical environmental the indicators carbon footprint fossil and cumulative energy demand, to support more sustainable and efficient practices in seedling production. The selection of these parameters is justified, since greenhouse gas emissions and energy use are among the main drivers of climate change and resource depletion, making them fundamental for the environmental performance of agricultural systems.

Materials and Methods

This study was conducted in accordance with the Life Cycle Assessment (LCA) methodology, as outlined in ABNT NBR ISO 14040 and ABNT NBR ISO 14044 (2009; 2014) [13,14], with the objective of assessing the global warming potential associated with the production of Agave sisalana seedlings.

The product system boundaries were defined as gate-to-gate, as illustrated in Figure 1, which depicts the processes evaluated in this study for the nursery.

The system was modeled using OpenLCA version 2.5, coupled with the Ecoinvent v3.10 database. The environmental impacts assessed included both the Global Warming Potential (GWP) over a 100-year time horizon, which quantifies the contribution of greenhouse gas emissions in terms of carbon dioxide equivalents (CO_2 eq), and the Cumulative Energy Demand (CED), representing

Figure 1. Product system of *Agave sisalana* seedling.

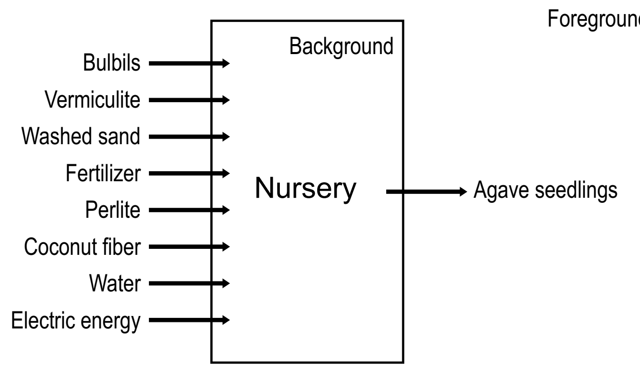

the total amount of energy required throughout the life cycle of seedling production. Biogenic carbon absorbed by sisal seed was not evaluated in this preliminary study.

Table 1 presents the inputs and output flows required to produce 2000 *Agave sisalana* seedlings.

The data used in the modeling were obtained from primary data collected directly in the field,

Table 1. Input and output flows to produce 2000 *Agave sisalana* seedlings.

Materials	Unity	Value
Inputs		
Agave bulbils	Item(s)	2000
Expanded vermiculite substrate	Kg	12
Expanded perlite substrate	Kg	6,666
Coconut husk	Kg	4.8
Water	mL³	13,608
Fertilizer	Kg	75
Electricity (water pumps)	Kwh	87.48
Transport, lorry	t.km	16.49
Plastic (trays)	Kg	5,617
Polyethylene (screens)	Kg	3,301
Output		
Agave sisalana seedlings	Item(s)	2000

as they were difficult to find in the literature and to ensure greater accuracy and representativeness. The metal infrastructure of the nursery was already installed and is highly durable; for this reason, its contribution as input to the study was not considered. For cultivation, *Agave bulbils* were selected as propagative material, although propagation by other techniques is also feasible for this species.

Regarding the inputs used in the preparation of the substrate, washed sand, vermiculite, perlite, and coconut fibers were used to improve the soil structure and promote the healthy development of the seedlings. Irrigation was carried out with water from the local public network, using electric pumps, whose energy consumption was estimated based on the nominal power of the pumps and the operating time.

The inputs used in the nursery in Conceição do Coité, Bahia (Brazil) were mainly transported by truck. For those coming from Salvador, Bahia (Brazil), an average distance of 220 km was considered, while inputs such as sand were obtained from local suppliers, thus reducing the logistical impact. The calculation of the environmental impact of this stage was based on the total weight of each input transported and the respective distances, allowing for an accurate estimate of vehicle fuel consumption (diesel) and associated atmospheric emissions, according to standard emission factors.

In addition to the supplies used to grow Agave seedlings, we also considered the rigid plastic trays where the bulbs are cultivated and nourished until they reach the desired size. These trays have an average useful life of five years. The nursery cultivation process lasts approximately six months, which means that the trays are used twice a year over the course of those five years. Therefore, the total weight of the plastic tray was distributed proportionally to its useful life.

The same methodology was applied to the black monofilament screens, made of polyethylene, used to cover the nursery. These screens have an average useful life of ten years, a value considered for modeling based on their time of use. These materials are essential for the efficient operation of the nursery.

Results and Discussion

In Figure 2, the contributions to the carbon footprint of the *Agave sisalana* seedling nursery are presented, allowing the identification of the share of each input, process, and stage in the Global Warming Potential (GWP), expressed in kilograms of carbon dioxide equivalent (kg CO_2eq),

Figure 2. Impact of GHG emissions from the production of 2000 *Agave sisalana* seedlings.

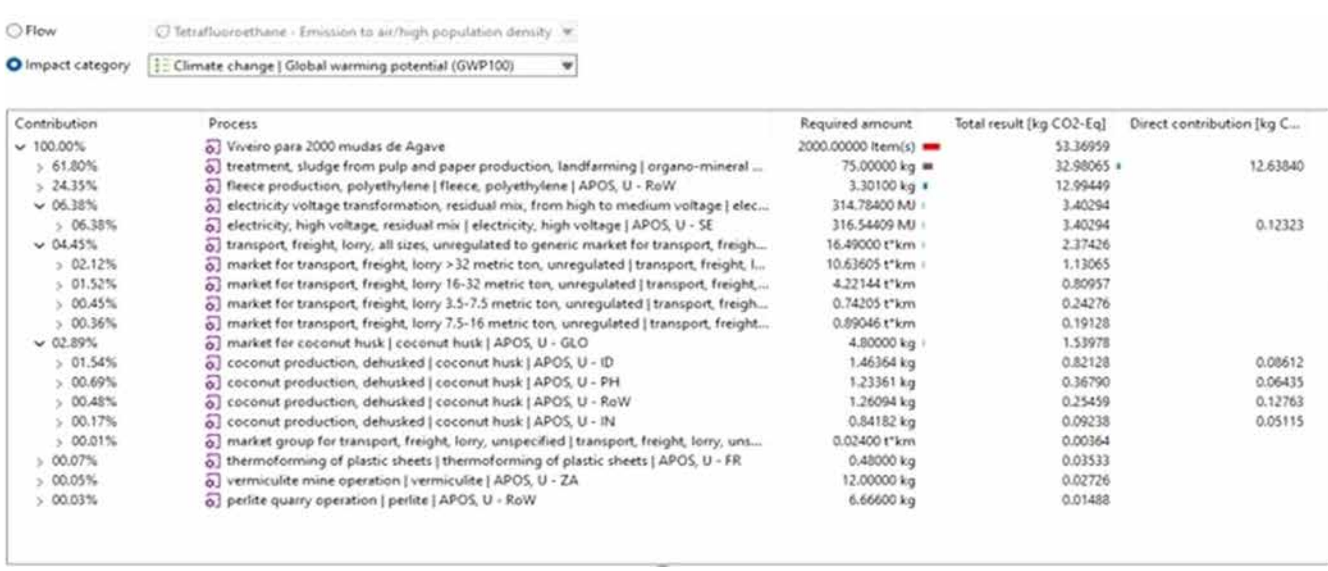
Flow: Tetrafluoroethane - Emission to air/high population density

Impact category: Climate change | Global warming potential (GWP100)

Contribution	Process	Required amount	Total result [kg CO2-Eq]	Direct contribution [kg C...
100.00%	Viveiro para 2000 mudas de Agave	2000.00000 Item(s)	53.36959	
61.80%	treatment, sludge from pulp and paper production, landfarming | organo-mineral ...	75.00000 kg	32.98065	12.63840
24.35%	fleece production, polyethylene | fleece, polyethylene | APOS, U - RoW	3.30100 kg	12.99449	
06.38%	electricity voltage transformation, residual mix, from high to medium voltage | elec...	314.78400 MJ	3.40294	
06.38%	electricity, high voltage, residual mix | electricity, high voltage | APOS, U - SE	316.54409 MJ	3.40294	0.12323
04.45%	transport, freight, lorry, all sizes, unregulated to generic market for transport, freigh...	16.49000 t*km	2.37426	
02.12%	market for transport, freight, lorry >32 metric ton, unregulated | transport, freight, l...	10.63605 t*km	1.13065	
01.52%	market for transport, freight, lorry 16-32 metric ton, unregulated | transport, freight,...	4.22144 t*km	0.80957	
00.45%	market for transport, freight, lorry 3.5-7.5 metric ton, unregulated | transport, freigh...	0.74205 t*km	0.24276	
00.36%	market for transport, freight, lorry 7.5-16 metric ton, unregulated | transport, freight...	0.89046 t*km	0.19128	
02.89%	market for coconut husk | coconut husk | APOS, U - GLO	4.80000 kg	1.53978	
01.54%	coconut production, dehusked | coconut husk | APOS, U - ID	1.46364 kg	0.82128	0.08612
00.69%	coconut production, dehusked | coconut husk | APOS, U - PH	1.23361 kg	0.36790	0.06435
00.48%	coconut production, dehusked | coconut husk | APOS, U - RoW	1.26094 kg	0.25459	0.12763
00.17%	coconut production, dehusked | coconut husk | APOS, U - IN	0.84182 kg	0.09238	0.05115
00.01%	market group for transport, freight, lorry, unspecified | transport, freight, lorry, uns...	0.02400 t*km	0.00364	
00.07%	thermoforming of plastic sheets | thermoforming of plastic sheets | APOS, U - FR	0.48000 kg	0.03533	
00.05%	vermiculite mine operation | vermiculite | APOS, U - ZA	12.00000 kg	0.02726	
00.03%	perlite quarry operation | perlite | APOS, U - RoW	6.66600 kg	0.01488	

throughout seedling production. These results are preliminary and serve to provide an initial insight into the relative importance of each component in the overall carbon footprint, pending further detailed analysis and data refinement.

Global warming refers to the gradual increase in the Earth's average temperature, caused by the accumulation of greenhouse gases (GHGs) in the atmosphere, such as chlorofluorocarbons (CFCs), carbon dioxide (CO_2), and other pollutants predominantly generated by human activities [15]. The increasing concentration of these gases intensifies the greenhouse effect, raising the temperature of the lower atmosphere and triggering large-scale climate change [16].

The analyzed production process resulted in a total GWP of 53.37 kg CO_2eq for 2,000 seedlings, equivalent to 0.026685 kg CO_2eq per individual seedling. This value is comparable to that reported in the literature for forest nursery seedlings (0.02945 kg CO_2eq) [16].

The analysis shows that the largest share of emissions is associated with fertilizer use, accounting for 32.98 kg CO_2eq (61.80% of the total), as illustrated in Figure 3. This impact includes both indirect N_2O emissions from soils and emissions associated with fertilizer manufacturing processes [17].

Polyethylene was the second most significant contributor, with 12.99 kg CO_2eq (24.35%), primarily linked to emissions generated along its production chain. Electricity used to operate water pumping systems for irrigation contributed 3.40 kg CO_2eq (6.38%), while road transportation by truck, even over relatively short distances within the same state, accounted for 2.37 kg CO_2eq, reflecting the impact of fossil fuel use.

It is important to note that this gate-to-gate analysis does not include the benefits of carbon sequestration by seedlings during growth, nor the impacts associated with the end-use phase. From a process sustainability perspective, the results indicate that targeted interventions to reduce fertilizer use, adopt lower-carbon alternatives (such as organic or renewable-based fertilizers), and replace plastic inputs with recycled or biodegradable materials could substantially decrease the total GWP. Furthermore, optimizing energy consumption—either by integrating renewable sources for water pumping or improving irrigation system efficiency—represents a concrete opportunity for emission mitigation. When combined with more efficient logistics planning, these measures can contribute to aligning seedling production processes with the principles of the circular economy and global carbon neutrality targets.

Figure 3. Contributions GHG emission of produce 2000 *Agave sisalana* seedlings.

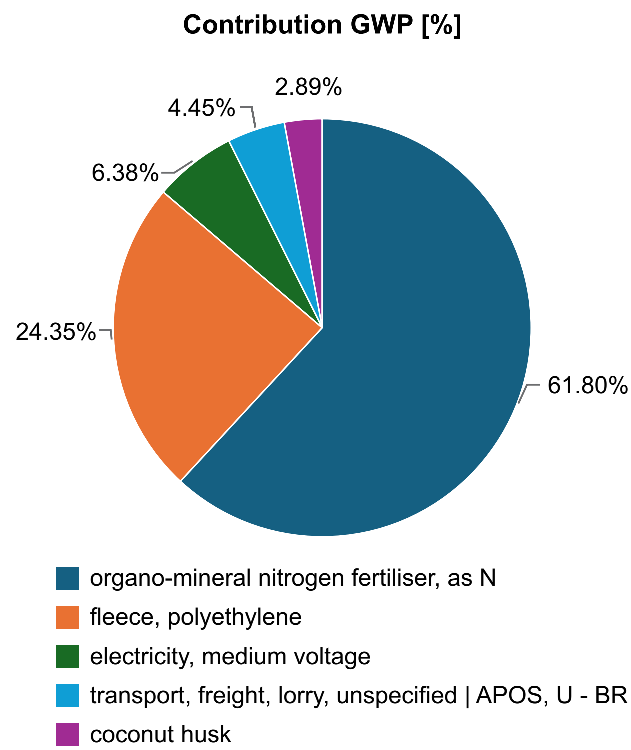

Complementary to GWP, Cumulative Energy Demand (CED) is another important life cycle indicator, defined as the total amount of energy required throughout the entire life cycle of a product, encompassing its production, use, and end-of-life stages [15]. This metric serves as a methodological approach to assess, analyze, and determine the sustainability of a product based on its overall energy consumption.

In the production process analyzed, the total CED was 12.734 MJ for 2,000 seedlings, including electricity, polyethylene, and fertilizers (Figure 4). Electricity accounted for the largest share, with 7,193 MJ (56.5% of the total), followed by polyethylene with 3.465 MJ (27.2%), while fertilizers contributed the remaining portion. These findings are preliminary and provide an initial overview of energy consumption distribution among the main inputs, These findings are consistent with previous studies highlighting the significant role of electricity and plastics—particularly seedling trays, greenhouse structures, and irrigation systems—in the total CED of nursery operations [19,20].

The CED assessment also indicates clear opportunities for impact reduction, including replacing fossil-based electricity with renewable sources (e.g., photovoltaic systems), optimizing plastic use, and selecting inputs with lower cumulative energy requirements. As emphasized in the literature, improving energy efficiency can provide not only environmental benefits but also economic advantages, given that energy is among the main operational costs in nursery production [21].

Together, the assessments of Global Warming Potential (GWP) and Cumulative Energy Demand (CED) provide a comprehensive understanding of the environmental impacts associated with the production of *Agave sisalana* seedlings. This dual approach is essential for advancing sustainable nursery practices that align with broader environmental and economic goals.

Figure 4. Contributions CED emission of produce 2000 *Agave sisalana* seedlings.

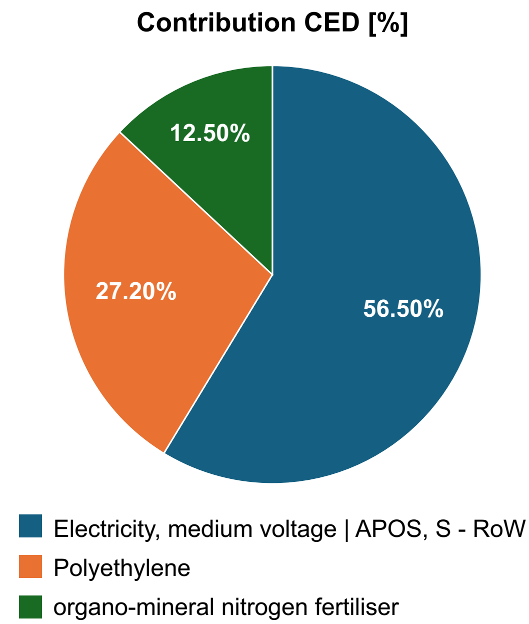

Conclusion

This study provided a preliminary assessment of the environmental impacts associated with *Agave sisalana* seedling production, employing a gate-to-gate system, and highlighting the main contributors to the Carbon Footprint (Global Warming Potential, GWP) and Cumulative Energy Demand (CED). Aligned with the initial objective of supporting more sustainable and efficient nursery practices, the results identified fertilizer use as the largest contributor to GWP, accounting for 61.8% of greenhouse gas emissions, while electricity consumption and plastic inputs predominated in driving CED, together representing over 80% of the total energy demand. These findings reveal clear opportunities for interventions aimed at improving the sustainability of the production process, such as the adoption of renewable energy sources (e.g., photovoltaic systems to supply nursery electricity), the development of strategies to optimize and reduce fertilizer application, and the replacement or recycling of plastic materials with alternatives of lower environmental impact. Additionally, enhancements in irrigation system efficiency, combined with more sustainable logistical practices, may further amplify reductions in overall environmental impacts.

The scarcity of specific studies for comparison, together with the limitations of the available data, represents a significant constraint to this analysis. As next steps, sensitivity analyses focusing on critical parameters are recommended to further understand result variability and to refine mitigation strategies. Moreover, the incorporation of more detailed regional data could increase the robustness and accuracy of future environmental assessments.

Finally, expanding the analysis to cradle-to-grave approaches is essential to capture the environmental benefits associated with seedling growth and final use, as well as potential offsets resulting from carbon sequestration by the plants. A relevant gap in this study refers to the non-consideration of biogenic carbon fluxes, which could affect the carbon balance of the nursery system. Including this accounting in future evaluations is fundamental to provide a more comprehensive understanding of the net greenhouse gas emissions associated with *Agave sisalana* seedling production.

Acknowledgement

The authors gratefully acknowledge Senai Cimatec and Embrapii for supporting this work through the doctoral scholarship.

References

1. Molina A, Kothari A, Odundo A, Prakash M. *Agave sisalana*: toward distributed manufacturing of absorbent media for menstrual pads in semi-arid regions. Commun Eng. 2023;2(1):81. doi:10.1038/s44172-023-00130-y.
2. Broeren ML, Dellaert SN, Cok B, Patel MK, Worrell E, Shen L. Life cycle assessment of sisal fibre: exploring how local practices can influence environmental performance. J Clean Prod. 2017;149:818-827. doi:10.1016/j.jclepro.2017.02.073.
3. Santos AFJ, Moreira ZPM, Souza JT, Oliveira LM, Barbosa HR, Silva ES, et al. Culturable diazotrophic bacterial community associated with *Agave sisalana* Perrine plants from semi-arid regions in Brazil. Rev Bras Ciênc Agrár. 2019;14(3):1-10. doi:10.5039/agraria.v14i3a5666.
4. Matsuura MDS, Silva O, Novaes R, Picoli J, Picoli JF. Life cycle assessment of sisal produced in semiarid regions in Brazil. In: Proceedings of the International Conference on Natural Fibres; 2019; Guimarães, Portugal. Guimarães: University of Minho; 2019. p. 416-417.
5. Pinheiro Junior CR, Ferreira TO, Oliveira Filho JDS, Queiroz H, Canisares LP, Greschuk LT, et al. Drivers of soil carbon accumulation and Agave expansion potential in Brazilian drylands [preprint]. SSRN; 2024. doi:10.2139/ssrn.4740996.
6. Alves MO, Santiago ES, Lima ARM. Diagnóstico socioeconômico da região nordestina produtora de sisal. Fortaleza: Banco do Nordeste do Brasil; 2004. (Série Documentos do ETENE; no. 4).
7. Salgado ALDB, Azzini A, Feitosa CT, Hiroce R. Efeito da omissão de macronutrientes em sisal. Bragantia. 1982;41:125-134. doi:10.1590/S0006-87051982000100013.
8. Abreu KCLM. Epidemiologia da podridão vermelha do sisal no Estado da Bahia [thesis]. Cruz das Almas (BA): Universidade Federal do Recôncavo da Bahia; 2010.
9. Silva ORF, Coutinho WM, Cartaxo WV, Filho JLS, Carvalho SO, Costa LB. Cultivo do sisal no Nordeste. Campina Grande: Embrapa Algodão; 2008. (Circular Técnica; 123).
10. Suinaga FA, Silva ORF, Coutinho WM. A história do sisal no Brasil. In: Andrade W, editor. O sisal do Brasil. Salvador: SINDIFIBRAS/APEX; 2008. p. 16-21.
11. Embrapa. Sisal: plantio [Internet]. Campina Grande: Embrapa Algodão; 2021. Available from: https://www.embrapa.br/agencia-de-informacao-tecnologica/cultivos/sisal/producao/plantio
12. Oumahmoud M, Alouani M, Elame F, Tahiri A, Bouharroud R, Qessaoui R, et al. Nursery production, acclimatization, and orchard transplantation of *Argania spinosa*: evaluating the impact of costs and plant age. Sci Hortic. 2024;338:113742. doi:10.1016/j.scienta.2024.113742.
13. Associação Brasileira de Normas Técnicas. NBR ISO 14044: gestão ambiental: avaliação do ciclo de vida: requisitos e orientações. Rio de Janeiro: ABNT; 2009.
14. Associação Brasileira de Normas Técnicas. ABNT ISO/TS 14067: gases de efeito estufa: pegada de carbono de produtos: requisitos e orientações sobre quantificação e comunicação. Rio de Janeiro: ABNT; 2014.
15. Iritani R, Takeuchi N, Kawakatsu H. Intricate heterogeneous structures of the top 300 km of the Earth's inner core inferred from global array data: I. Regional 1D attenuation and velocity profiles. Phys Earth Planet Inter. 2014;230:15-27. doi:10.1016/j.pepi.2014.02.002.
16. Yousaf A, Hussain M, Ahmad S, Riaz A, Shaukat S, Shah SWA, et al. Environmental sustainability assessment of softwood and hardwood seedlings production in forest nurseries: a case study from Pakistan. Braz J Biol. 2022;84:e260615. doi:10.1590/1519-6984.260615.
17. Li L, Awada T, Shi Y, Jin VL, Kaiser M. Global greenhouse gas emissions from agriculture: pathways to sustainable reductions. Glob Change Biol. 2025;31(1):e70015. doi:10.1111/gcb.70015.
18. Finnveden G, Hauschild MZ, Ekvall T, Guinée JB, Heijungs R, Hellweg S, et al. Recent developments in life cycle assessment. J Environ Manag. 2009;91(1):1-21. doi:10.1016/j.jenvman.2009.06.018.
19. Jareborg I. Determining the primary energy demand and greenhouse gas emission of carrots: comparing organic and conventional small-scale carrot production and supply in Sweden [dissertation]. Uppsala:Swedish University of Agricultural Sciences; 2019.

20. Wu Y. Determining the cumulative energy demand and greenhouse gas emission of Swedish wheat flour [master's thesis]. Uppsala: Swedish University of Agricultural Sciences; 2021.

21. Matos C, Junkes VH, Lermen FH, Magalhães RFD, Matias GDS, Ribeiro JLD, et al. Life cycle sustainability assessment of the agri-food chain: empirical review and bibliometrics. Production. 2024;34:e20230043. doi:10.1590/0103-6513.20230043.

Biogas Generation Potential from Swine Manure in the Microregion of Feira de Santana, Brazil

Tiago Silva e Silva[1]*, Luiz Henrique Santos Silva[1], Fillipe Valente Braz[1], Maylane Neres Costa Santos[1], Daniel do Carmo Silva Ribeiro[2], Henrique Nunes Teixeira[2]
[1]Federal University of Recôncavo da Bahia, CETENS; Feira de Santana, Bahia; [2]Federal University of Bahia, DEEC; Salvador, Bahia, Brazil

This study assesses the potential for biogas generation from swine manure in the microregion of Feira de Santana, Bahia, Brazil, an area with significant pig farming activity. The improper disposal of swine manure poses significant environmental risks, including water and soil pollution and the emission of greenhouse gases. This research aims to quantify the energy potential of these residues by applying anaerobic digestion technology. The methodology involved collecting data on the swine population from official sources such as IBGE and ADAB for the year 2018. Theoretical models and stoichiometric equations were used to estimate the daily and annual production of manure, the potential for biogas generation, and its corresponding energy value. The results indicate a significant potential for biogas production, estimated at approximately 16,083 m3/day, with a methane (CH4) content of about 9,650 m3/day. This volume could be converted into approximately 36.67 MWh of electricity daily, assuming a 35% conversion efficiency. The conclusion highlights the technical feasibility and environmental benefits of implementing biodigesters in the region, transforming an environmental liability into a valuable renewable energy asset, contributing to the local energy matrix and promoting sustainable development. The most viable application identified is the use of biogas as a substitute for cooking gas (LPG), offering a rapid financial return for farmers.
Keywords: Biogas. Biodigester. Swine Farming. Renewable Energy. Feira de Santana.

Climate change and the search for sustainable energy sources are central themes in the global scientific and political agenda. The high dependence on fossil fuels, which accounted for about 81% of the global energy matrix in 2019 [1], makes the current energy model unsustainable. In this context, renewable sources like biomass gain prominence. Brazil has significant potential for biomass-derived energy due to favorable climatic conditions and a strong agribusiness sector.

Among the various sources of biomass, livestock residues, especially from pig farming, stand out. Pig farming is a rapidly growing economic activity in Brazil, but it generates a large volume of waste with high polluting potential. These wastes can contaminate soil, water resources, and the atmosphere through the emission of gases such as methane (CH_4) and nitrous oxide (N_2O) [2]. Anaerobic digestion technology, using biodigesters, presents itself as a promising solution to treat this waste, transforming an environmental liability into two valuable products: biogas, a renewable fuel, and biofertilizer, a nutrientrich organic fertilizer.

This study aims to quantify the potential for biogas generation from swine manure in the microregion of Feira de Santana, Bahia, a region with a representative share of the state's pig production. The goal is to provide a quantitative basis to encourage the adoption of this technology, reducing environmental impacts and creating a new source of income for local farmers.

Materials and Methods

This study was conducted through an exploratory research approach, based on data collection and bibliographic review to estimate the biogas potential from confined swine herds in the microregion of Feira de Santana. The methodological framework was designed to provide a robust estimation of biogas generation, considering the specific characteristics of swine manure and the regional context.

Received on 13 March 2026; revised 17 May 2026.
Address for correspondence: Tiago Silva e Silva. Rua Godofredo Rebello de Figueiredo Filho, nº 697, SIM, Feira de Santana, Bahia, Brazil. Zipcode: 44085-132. E-mail: tiagofsa8@gmail.com.

J Bioeng. Tech. Health 2026;9(7):686-692

Data Collection and Characterization of the Study Area

The microregion of Feira de Santana, located in the state of Bahia, Brazil, was selected due to its significant pig farming activity. Data regarding the swine population in confinement for the year 2018 were meticulously collected from official and reputable sources, primarily the Brazilian Institute of Geography and Statistics (IBGE) and the State Agency for Agricultural Defense of Bahia (ADAB). These institutions are recognized for their comprehensive and reliable agricultural statistics, ensuring the accuracy of the baseline data. According to the collected data, the microregion of Feira de Santana housed a total of 74,147 confined pigs in 2018. This figure represents a substantial portion, specifically 6.65%, of the total swine herd in the state of Bahia, highlighting the region's importance in the state's pig farming sector and the potential environmental impact of its waste if not properly managed.

Estimation of Manure Production

The initial step in quantifying the biogas generation potential involved estimating the daily production of swine manure. This estimation is crucial as the volume and characteristics of the raw material directly influence the amount of biogas that can be produced. The daily production of swine manure (PDDS) was calculated using Equation 1, which considers the total number of animals and their specific manure production rate. This approach allows for a precise estimation tailored to the size of the swine herd in the study area.

Where:

$$\mathrm{PDDS} = \sum(\mathrm{N^o} \cdot \mathrm{PE}) \qquad (1)$$

PDDS is the daily production of swine manure, expressed in cubic meters of manure per day (m^3_manure/day).

Nº denotes the number of heads within a specific animal category (e.g., confined pigs).

PE signifies the specific manure production per head, measured in cubic meters of manure per head per day (m^3_manure/head/day). This value is typically derived from empirical studies and varies depending on factors such as animal age, diet, and housing conditions. For this study, average values from established literature were utilized to ensure consistency and comparability with similar research.

Methane Emission Factor and Biogas Production Estimation

To understand the environmental implications and the energy potential, the methane emission factor was considered. The methane emission factor (CH_4_emissions) was calculated based on the Intergovernmental Panel on Climate Change (IPCC) methodology from 2006 [3], which provides standardized guidelines for estimating greenhouse gas emissions from various sources, including livestock. Equation 2 illustrates this calculation:

$$\mathrm{CH_4\_emissions} = (\mathrm{M_i} \cdot 365 \cdot \mathrm{EF_i}) \cdot 10^{-3} \qquad (1)$$

Where:

M_i is the average daily mass of organic matter produced per pig, measured in kilograms (kg).

EF_i is the anaerobic emission factor, with a value of 1.5 kg CH_4/kg, as specified by IPCC (2006). This factor accounts for the amount of methane produced per unit of organic matter under anaerobic conditions.

Following the estimation of manure production and considering the methane emission factors, the daily biogas production (P_B) was estimated. This calculation is fundamental to determining the energy recovery potential from the swine manure. Equation 3, derived from established principles of anaerobic digestion, was employed for this purpose:

$$P\_B = B_0 \cdot \mathrm{SV} \cdot \mathrm{Q} \qquad (1)$$

Where:

P_B represents the daily biogas production, expressed in cubic meters per day (m^3/day).

B_0 is the maximum theoretical biogas production capacity, which, according to IPCC (2006), is 0.45 m^3/kg_SV. This value represents the maximum volume of biogas that can be generated per kilogram of volatile solids under ideal conditions.

SV denotes the volatile solids content, a critical parameter that indicates the biodegradable organic matter present in the manure. For this study, a value of 53.1 g_SV/L was adopted, also in accordance with IPCC (2006) guidelines. Volatile solids are the primary substrate for anaerobic digestion, and their concentration directly impacts biogas yield.

Q is the total volume of manure produced per day, expressed in cubic meters per day (m^3/day), as calculated in the previous step (Section II.B).

Energy Potential Calculation and Conversion Efficiency

Once the daily biogas production was estimated, the next crucial step was to determine its energy potential. This involved converting the volume of biogas into electrical energy, providing a tangible measure of its value as a renewable energy source. The conversion process considers the methane content within the biogas and the efficiency of the energy conversion system. It is widely accepted that the methane content in biogas typically ranges from 50% to 80%, with an average of approximately 60% for swine manure [4]. Methane is the primary combustible component of biogas, responsible for its energy content.

The energy conversion efficiency of a generator set, which transforms the chemical energy of biogas into electrical energy, was assumed to be 35%. This value is a realistic representation for typical small to medium-scale biogas-to-electricity systems. According to Oliveira (2009) [5], a commonly cited equivalence in the field, 1 m3 of biogas is equivalent to approximately 6.5 kWh. This conversion factor was used to translate the estimated biogas volume into its equivalent electrical energy output. The calculation for the daily electrical energy generation was performed using the following relationship:
Electrical Energy (kWh/day) = P_B (m^3/day) ×Energy Equivalence (kWh/m^3)×Conversion Efficiency (%).

This comprehensive methodological approach ensures that the estimations of biogas potential and energy generation are robust, relying on established scientific principles and data from credible sources. The detailed breakdown of each step allows for transparency and reproducibility of the results, contributing to the reliability of the study's findings.

Detailed Parameters and Justifications for Calculations

To ensure the robustness and accuracy of the biogas potential estimation, specific parameters and assumptions were adopted based on established scientific literature and guidelines from reputable organizations. These parameters are critical for the reliability of the calculations presented in this study.

Specific Manure Production (PE)

The value of 0.0091 m^3/head/day for specific manure production per pig was derived from a synthesis of various studies on swine waste management. This average accounts for different growth stages and feeding regimes commonly found in confined pig farming operations. It is important to note that actual manure production can vary based on factors such as animal weight, feed intake, water consumption, and housing system. However, for a regional-scale assessment, an average value provides a practical and sufficiently accurate basis for estimation. This value typically includes both solid and liquid fractions of the manure, which are relevant for anaerobic digestion processes.

Maximum Theoretical Biogas Production Capacity (B_0)

The IPCC (2006) [3] provides a default value of 0.45 m^3/kg_SV for the maximum theoretical biogas production capacity. This parameter represents the stoichiometric potential of volatile solids to be converted into biogas under ideal anaerobic conditions. It is a theoretical maximum, as real-world biodigesters may not achieve 100% conversion efficiency due to various operational factors such as temperature, pH, retention time, and the presence of inhibitory substances. Nevertheless, using this theoretical value allows for a consistent and comparable estimation across different studies and regions.

Volatile Solids Content (SV)

The volatile solids content of swine manure is a crucial indicator of its organic matter concentration and, consequently, its biogas potential. A value of 53.1 g_SV/L (or 53.1 kg_SV/m^3) was adopted, also in accordance with IPCC (2006) guidelines [3]. Volatile solids are the fraction of total solids that are combustible and represent the organic material available for microbial degradation during anaerobic digestion. Variations in diet, animal age, and manure handling practices can influence the SV content. However, the chosen value is representative of typical swine manure characteristics and provides a reliable basis for calculation.

Methane Content in Biogas

While biogas composition can vary, a methane (CH_4) content of approximately 60% was assumed for the energy potential calculations. This is a commonly observed concentration for biogas derived from swine manure, with ranges typically falling between 50% and 80% [4]. The higher the methane content, the greater the calorific value of the biogas. This assumption directly impacts the estimated electrical energy output, as methane is the primary energy-carrying component of biogas.

Energy Equivalence of Biogas

The conversion factor of 6.5 kWh per cubic meter of biogas is a widely accepted empirical value in the field of bioenergy [5]. This factor simplifies the translation of biogas volume into its equivalent electrical energy potential, facilitating comparisons with other energy sources. It is important to note that this equivalence assumes a certain calorific value for methane and a standard efficiency for its conversion into electricity.

Energy Conversion Efficiency of Generator Set

An efficiency of 35% for the generator set was used to calculate the final electrical energy output. This percentage reflects the typical efficiency of internal combustion engines used in small to medium-scale biogas power generation systems. Factors such as engine type, maintenance, and load can influence actual efficiency. However, 35% provides a reasonable and conservative estimate for planning purposes.

These detailed parameters and their justifications underpin the quantitative analysis presented in this study, ensuring that the estimations are grounded in scientific principles and reflect realistic conditions for biogas production from swine manure. The transparency in parameter selection allows for a clear understanding of the assumptions made and the potential for future refinements based on more specific local data or advanced research findings.

Results and Discussion

The comprehensive analysis of swine population data and the application of established methodological frameworks yielded significant insights into the biogas generation potential from swine manure in the microregion of Feira de Santana. This section presents the quantified results, discusses their implications, and provides comparative analyses to contextualize the findings within broader energy and environmental landscapes.

<u>Quantification of Swine Population and Manure Production</u>

Based on the most recent available data from ADAB (Agência Estadual de Defesa Agropecuária da Bahia) for the year 2018, the microregion of Feira de Santana is home to a substantial swine population, totaling 74,147 confined pigs. This figure underscores the regions´ prominence in the states´ pig farming industry and, consequently, the considerable volume of organic waste generated. To accurately estimate the daily manure production, an average manure production rate of 0.0091 m^3/head/day was adopted from existing literature and empirical studies, as referenced in Table 7 of the original TCC [7]. This value represents a conservative yet realistic estimate for confined swine operations.

Applying this specific production rate to the total swine population, the total daily manure production (Q) for the microregion of Feira de Santana was calculated as follows: Q = 74,147 heads ×0.0091m^3/head/day≈674.7m^3/day.

This daily volume of approximately 674.7 cubic meters of swine manure represents a significant environmental challenge if not properly managed. However, it also signifies a substantial untapped resource for renewable energy generation. The consistent and large-scale availability of this feedstock is a critical factor in the economic viability and sustainability of biogas production facilities.

Biogas and Methane Generation Potential

With the daily manure production quantified, the next step involved estimating the potential for biogas generation. Utilizing Equation 3 from the methodology section, which incorporates the maximum theoretical biogas production capacity (B0 = 0.45 m^3/kg_SV) and the volatile solids content (SV = 53.1 kg_SV/m^3), the daily biogas production (P_B) was calculated: P_B = 0.45 m^3/kg_SV × 53.1kg_SV/m^3 × 674.7m3/day ≈ 16, 083.49m^3/day.

This calculation reveals a remarkable potential for biogas production, exceeding 16,000 cubic meters per day. Biogas is a mixture of gases, primarily methane (CH_4) and carbon dioxide (CO_2), along with trace amounts of other gases. The methane content is the most critical component for energy utilization due to its high calorific value. For swine manure biogas, the methane concentration typically ranges from 50% to 80%, with a conservative average of 60% methane content assumed, which is consistent with typical values observed in anaerobic digestion of swine waste [4].

Based on this assumption, the daily methane production (P_M) was estimated: P_M = 16,083.49 m^3/day ×0.60 ≈ 9, 650.09m^3/day.

The production of nearly 9,650 cubic meters of methane per day is particularly significant. Methane is a potent greenhouse gas, approximately 25 times more effective at trapping heat in the atmosphere than carbon dioxide over a 100-year period [3]. Capturing and utilizing this methane through anaerobic digestion not only provides a renewable energy source but also substantially mitigates greenhouse gas emissions that would otherwise be released into the atmosphere from the decomposition of raw manure. This dual benefit underscores the environmental imperative and economic opportunity presented by biogas technology.

There is typical composition of biogas, highlighting the variability in methane content. The values used in this study (60% CH_4) fall well within the expected range, reinforcing the reliability of the energy potential estimations.

Energy Potential and Economic Comparison

The conversion of the generated biogas into usable energy, particularly electrical energy, represents the ultimate goal of this assessment. Considering the established equivalence of 6.5 kWh per cubic meter of biogas [5] and assuming a realistic energy conversion efficiency of 35% for a typical generator set, the daily electrical energy generation potential was calculated: Energy = 16,083.49 m^3/day ×6.5kWh/m^3 × 0.35 ≈ 36, 667MWh/day.

This figure, approximately 36.67 MWh per day, signifies a substantial contribution to the local energy matrix. To put this into perspective, the TCC highlights that this daily generation corresponds to approximately 2.5% of the installed capacity of the Sobradinho Hydroelectric Plant in Bahia [6]. While this percentage might seem small in the context of a large hydroelectric plant, it is crucial to recognize that biogas offers a decentralized, distributed energy source, which can enhance energy security and reduce transmission losses.

Furthermore, it represents a consistent, baseload power source, unlike intermittent renewable sources such as solar or wind, making it a valuable addition to the energy mix.

Beyond electricity generation, the energy content of the biogas can be compared to conventional fossil fuels to better appreciate its value. The TCC provides a compelling comparison: the daily biogas production is equivalent to approximately 3,537 liters of gasoline. This volume of gasoline is sufficient to fuel about 70 Hyundai HB20 cars daily, assuming average fuel consumption. This analogy vividly illustrates the high energy value contained within the swine manure, transforming what is often considered a waste product into a valuable energy commodity. Such comparisons are vital for policymakers and farmers to grasp the economic incentives associated with adopting biogas technology.

Environmental and Socio-Economic Implications

The findings of this study extend beyond mere energy quantification, touching upon significant environmental and socio-economic implications. From an environmental perspective, the anaerobic digestion of swine manure offers a robust solution to several pressing issues. It significantly reduces the emission of methane and nitrous oxide, both potent greenhouse gases, thereby contributing to climate change mitigation efforts. Furthermore, the process effectively treats the manure, reducing its biochemical oxygen demand (BOD) and chemical oxygen demand (COD), which are key indicators of water pollution potential. The resulting digestate, or biofertilizer, is a nutrient-rich effluent that can replace synthetic fertilizers, reducing chemical runoff and improving soil health. This closed-loop system embodies the principles of a circular economy, transforming waste into valuable resources.

Socio-economically, the adoption of biodigester technology can bring substantial benefits to the rural communities in the Feira de Santana microregion. For individual farmers, it offers energy independence, reducing reliance on expensive and volatile fossil fuels like LPG for cooking and potentially electricity from the grid. This can lead to significant cost savings and improved household budgets. Moreover, the production of biofertilizer can enhance agricultural productivity and reduce input costs, further boosting farmersíncomes. At a broader regional level, the development of a biogas industry can create new employment opportunities in the construction, operation, and maintenance of biodigesters, as well as in the distribution of biogas and biofertilizer. This contributes to local economic development and diversification.

However, it is important to acknowledge the challenges associated with the widespread adoption of this technology. The initial capital investment for biodigester construction can be substantial, particularly for small-scale farmers. This highlights the need for supportive government policies, financial incentives, and accessible credit lines to facilitate adoption. Additionally, technical knowledge and training are required for the proper operation and maintenance of biodigester systems. Despite these challenges, the overwhelming environmental and economic benefits strongly advocate for the promotion and implementation of biogas technology in regions with high concentrations of livestock farming.

In summary, the results demonstrate that swine manure in the Feira de Santana microregion is not merely a waste product but a valuable resource capable of generating significant amounts of renewable energy. The detailed quantification of biogas and methane potential, coupled with the energy conversion analysis, provides a compelling case for investing in anaerobic digestion technology. The environmental benefits of greenhouse gas reduction and pollution control, combined with the socio-economic advantages of energy independence and income generation, position biogas as a key component of a sustainable future for the region.

Conclusion

The comprehensive study on the potential for biogas generation from swine manure in the microregion of Feira de Santana, Bahia, unequivocally demonstrates the significant technical and environmental viability of this renewable energy source. The meticulous quantification of manure production and subsequent estimation of biogas yield reveal a substantial untapped resource. Specifically, the estimated daily production of 16,083 m3 of biogas, with a high methane content, underscores its capacity to contribute meaningfully to the local energy matrix.

The conversion of this biogas into electrical energy, with a potential generation of approximately 36.67 MWh daily, highlights its transformative power. This not only addresses the pressing issue of waste management in pig farming but also offers a sustainable alternative to conventional energy sources. The environmental benefits are manifold, including the reduction of greenhouse gas emissions, mitigation of water and soil pollution, and the production of nutrient-rich biofertilizer, which promotes sustainable agricultural practices

While the prospect of converting biogas to electricity is highly attractive from an energy security and environmental standpoint, it often entails considerable initial capital investment, which can be a barrier for small and medium-sized producers. Therefore, the study identifies the direct use of biogas as a substitute for liquefied petroleum gas (LPG) for cooking as the most immediate and economically viable solution for these farmers. This application offers a quicker financial return, enhances energy autonomy for rural families, and significantly reduces their operational costs.

To fully realize this potential, it is imperative that robust public policies and accessible credit lines are established and promoted. These measures would incentivize the adoption and implementation of biodigester technology across the region. Such initiatives would not only mitigate the adverse environmental impacts associated with intensive pig farming but also foster a circular economy model. This model transforms agricultural waste into valuable resources, generates new income streams for farmers, and contributes to the diversification and long-term sustainability of the regional energy matrix. The findings of this research provide a strong foundation for advocating for the widespread adoption of biogas technology, paving the way for a more sustainable and energy-independent future for the microregion of Feira de Santana.

References

1. International Energy Agency. World energy outlook 2019. Paris: International Energy Agency; 2019.
2. Fernandes F. Impactos ambientais da suinocultura. Rev Bras Eng Agríc Ambient. 2012;16(5):543-550.
3. Intergovernmental Panel on Climate Change. 2006 IPCC guidelines for national greenhouse gas inventories. Volume 5: Waste. Hayama (JP): Institute for Global Environmental Strategies; 2006.
4. Deublein D, Steinhauser A. Biogas from waste and renewable resources: an introduction. Weinheim: Wiley-VCH; 2008.
5. Oliveira PAV. Geração de energia elétrica a partir de biogás. In: Anais do Simpósio sobre Manejo e Nutrição de Aves e Suínos; 2009; Campinas, SP, Brasil. Campinas: [publisher unknown]; 2009. p. 211-225.
6. Agência Nacional de Energia Elétrica. Atlas de energia elétrica do Brasil. 3rd ed. Brasília: ANEEL; 2008.
7. Ribeiro DCS. Estudo de geração de biogás dos dejetos suínos da microrregião de Feira de Santana [undergraduate thesis]. Feira de Santana (BA): Centro de Ciência e Tecnologia em Energia e Sustentabilidade, Universidade Federal do Recôncavo da Bahia; 2022.

Operational Modeling of Green Hydrogen Production in Sugarcane Biorefineries Considering Electricity Price Variability

Julia Bahia Hufnagel Cavalcante[1]*, Fernando Luiz Pellegrini Pessoa[2]
[1]SENAI CIMATEC University, Postgraduate Program in Computational Modeling and Industrial Technology; [2]SENAI CIMATEC University, Chemical Department; Salvador, Bahia, Brazil

This study evaluates green hydrogen production from surplus electricity in sugarcane biorefineries, considering partial electrolyzer operation as a function of electricity price. A techno-economic model was developed to estimate the Levelized Cost of Hydrogen (LCOH) under different electricity price scenarios. The results indicate that electricity cost is the main driver of LCOH, accounting for approximately 45% of total annual cost under low-price conditions and reaching values close to 80% in high-price scenarios. Distinct operational regimes were identified, with full electrolyzer utilization at low electricity prices (0.04–0.06 R$/kWh), resulting in LCOH between 10.7 and 11.8 R$/kg, and reduced operation at higher prices, leading to a sharp increase in costs. A critical electricity price range between 0.10 and 0.16 R$/kWh was identified, above which the economic viability of green hydrogen deteriorates significantly. Although competitive with values reported in the literature for green hydrogen, the results indicate limited competitiveness compared to grey hydrogen and closer proximity to blue hydrogen costs under favorable conditions. Overall, the findings highlight the potential of the Brazilian sugarcane sector for decentralized green hydrogen production under low-cost electricity conditions.
Keywords: Green Hydrogen. Electrolysis. Sugar Cane. Cogeneration. PEM.

The growing concern about climate change and the need to reduce greenhouse gas emissions have driven the search for energy sources that are both economically viable and environmentally sustainable. In this context, green hydrogen (GH_2) has emerged as a strategic energy carrier for the decarbonization of sectors such as heavy industry and transportation [1]. According to the International Energy Agency (IEA), low-emission hydrogen production grew by 10% in 2024, but still accounts for less than 1% of total global production, being limited by high capital costs, regulatory uncertainties, and infrastructure challenges [2].

In Brazil, the scenario may be more favorable for green hydrogen production due to the high share of renewable sources in the electricity mix, which exceeds 88% of total generation. This expansion of renewable sources may lead to the occurrence of surplus electricity, creating opportunities for its use in hydrogen production via electrolysis and contributing to lower electricity costs [3,4]. Brazilian sugarcane biorefineries emerge as a promising opportunity in this context. In addition to producing sugar and ethanol, these facilities use bagasse and straw to generate energy through cogeneration, often producing significant electricity surpluses per production unit. In 2025, sugarcane biomass accounted for approximately 12,697 MW of installed cogeneration capacity, representing about 71.9% of the total biomass-based capacity in Brazil [5,6]. However, most studies in the literature consider electrolyzer operation coupled with wind or solar energy, which can be modeled based on hourly electricity prices. This approach does not adequately represent the operational reality of industrial cogeneration systems based on renewable energy, such as sugarcane biorefineries. In this sense, the integration of these facilities with electrolysis systems emerges as a promising alternative for green hydrogen production [7].

In this context, this study aims to propose a model to evaluate green hydrogen production from surplus energy in sugarcane biorefineries, considering electrolyzer operation as a function of electricity prices.

Received on 8 April 2026; revised 3 June 2026.
Address for correspondence: Julia Bahia Hufnagel Cavalcante. Av. Orlando Gomes, 1845 - Piatã, Salvador – BA – Brazil, Zipcode: 41650-010. E-mail: julia.cavalcante@aln.senaicimatec.edu.br.

J Bioeng. Tech. Health 2026;9(7):693-697

Materials and Methods

This study adopts a techno-economic modeling approach to evaluate green hydrogen (GH_2) production from surplus electricity in sugarcane biorefineries, considering the operation of the electrolyzer as a function of electricity prices in the Brazilian short-term (spot) market.

A high-efficiency sugarcane biorefinery was considered as a case study, with an annual electricity surplus of 377 GWh. The electrolyzer capacity was sized based on the available energy, assuming an average annual operation of 5,500 hours during the harvest season in Brazil, resulting in an installed capacity of 68.5 MW [8,9].

Proton Exchange Membrane (PEM) electrolysis was selected as the hydrogen production technology due to its balance between technological maturity, operational flexibility, and the high purity of the hydrogen produced. The specific energy consumption of the electrolyzer was assumed to be 53 kWh/kg, based on values reported in the literature [10–13].

Although the electricity used in the electrolysis process is derived from the surplus generated by the biorefinery itself, an opportunity cost was assigned to this energy, since it could alternatively be sold in the spot electricity market. Therefore, by allocating surplus electricity to hydrogen production, the plant foregoes potential revenue from electricity sales.

The operation of the electrolyzer was modeled as a function of electricity price (Equation 1), representing the economic decision regarding the use of surplus energy (0–100%). At low electricity prices, the entire surplus generated by the plant is directed to hydrogen production rather than being sold in the spot market. Conversely, at higher electricity prices, the electrolyzer operates at a minimum level, ensuring that capital investment is not underutilized while prioritizing electricity sales.

$$f(P) = \begin{cases} 1, & P \le P_{low} \\ f_{min} + (1 - f_{min}) \cdot \frac{P_{high} - P}{P_{high} - P_{low}}, & P_{low} < P < P_{high} \\ f_{min}, & P \ge P_{high} \end{cases} \quad (1)$$

Where P is the electricity price in the spot market, f_{min} is the minimum fraction of surplus energy used for hydrogen production (20%), P_{low} = 0.06 R$/kWh and P_{high} = 0.58 R$/kWh, corresponding to real values observed between 2021 and 2026 in the Central-West/Southeast region of Brazil [14].

The specific cost of the electrolyzer was assumed to be 1100 $/kW, a value consistent with commercial PEM electrolysis systems, converted to Brazilian reais (exchange rate of 5.25 R$/US$ as of March 12, 2026) [12,13,15].

Costs related to water consumption, hydrogen compression, and storage were treated in a simplified manner as auxiliary system costs. According to the literature, these components represent a relatively small share of the total production cost and were incorporated as additional percentages in the model.

The OPEX for compression and storage was assumed to be 2% of the total CAPEX for each component. Based on literature data, the general operation and maintenance costs (OPEX) of the electrolysis system were assumed to be approximately 2% of the total CAPEX per year. Considering the additional OPEX associated with compression and storage, the total operational expenditure in the model corresponds to approximately 6% of the CAPEX on an annual basis [16].

The capital expenditure (CAPEX) was annualized using the capital recovery factor (CRF), considering a discount rate of 7% and a project lifetime of 20 years. The electricity cost was calculated based on the energy consumption and electricity prices ranging from 0.04 to 0.9 R$/kWh, in order to evaluate the model behavior [5].

The total annual cost was defined as the sum of the annualized CAPEX, OPEX, and electricity cost. The Levelized Cost of Hydrogen (LCOH) was then calculated as the ratio between the total annual cost and the annual hydrogen production.

Results and Discussions

The electricity price assumptions, as well as the corresponding LCOH results, are presented in Table 1.

Table 1. Model results.

Case	Price (R$/kWh)	f(P)	Energy used (GWh/year)	H_2 (t/year)	Electricity Cost (MR$/year)	Total Cost (MR$/year)	LCOH (R$/kg)
1	0.04	100%	377.7	7,127	15,110	76,350	10.71
2	0.06	100%	377.7	7,127	22,666	83,905	11.77
3	0.10	94%	354.5	6,689	35,451	96,691	14.46
4	0.16	85%	319.6	6,031	51,143	112,382	18.63
5	0.30	63%	238.3	4,495	71,484	132,723	29.52
6	0.40	48%	180.2	3,399	72,064	133,305	39.22
7	0.50	32%	122.1	2,303	61,023	122,262	53.09
8	0.58	20%	75.5	1,425	43,820	105,059	73.70
9	0.90	20%	75.5	1,425	67,997	129,236	90.66

The results indicate that electricity cost exerts a strong influence on the LCOH, accounting for approximately 45% of the total annual cost under low electricity price scenarios and reaching values close to 80% in high-price scenarios. More importantly, the results reveal the existence of distinct operational regimes directly linked to electricity price.

For low electricity prices (0.04–0.06 R$/kWh), the system operates at full capacity ($f \approx 1$), resulting in LCOH values between 10.7 and 11.8 R$/kg. In this regime, the high utilization of the electrolyzer allows for better dilution of capital costs, leading to more competitive hydrogen production. When compared to values reported in the literature for green hydrogen (R$ 15.1–18.7/kg), the results indicate that surplus-based systems can achieve competitive cost levels under favorable electricity conditions [17].

However, when compared to conventional hydrogen production routes, the competitiveness remains limited. Even under low electricity price scenarios, the LCOH remains above the cost range of grey hydrogen (R$ 2.6–8.9/kg), mainly due to the high capital cost of electrolyzers. On the other hand, the results show closer proximity to blue hydrogen costs (R$ 5.3–10.5/kg), particularly under low-cost electricity scenarios [13].

As electricity prices increase, the system enters a transition regime (0.10–0.16 R$/kWh), in which the utilization factor decreases (f between 0.94 and 0.85). In this range, the reduction in electrolyzer operation is not sufficient to offset the increase in electricity cost, resulting in a significant rise in LCOH (14.5–18.6 R$/kg). In this regime, green hydrogen becomes less competitive even when compared to other low-carbon alternatives.

For higher electricity prices (>0.30 R$/kWh), the electrolyzer operates at low capacity ($f \leq 0.63$), with a substantial reduction in hydrogen production and a sharp increase in LCOH, reaching values above 90 R$/kg. In this regime, electricity cost dominates the economic performance, making hydrogen production economically unattractive across all considered production pathways.

These results highlight that the economic viability of green hydrogen production in integrated systems is highly dependent on access to low-cost electricity, reinforcing the importance of operational flexibility in response to market conditions.

Conclusion

This study proposed a techno-economic model to evaluate green hydrogen production from surplus electricity in sugarcane biorefineries, integrating both the opportunity cost of electricity and the partial operation of the electrolyzer as a function of electricity price. Unlike conventional approaches, the proposed model provides a more realistic representation of operational decision-making by considering electricity not only as an input, but also as an economic alternative.

The results demonstrated that electricity cost exerts a strong influence on the LCOH, accounting for approximately 45% of the total annual cost under low-price scenarios and reaching values close to 80% under higher electricity price conditions. The identification of distinct operational regimes, as well as a critical electricity price range, highlights the model's consistency in capturing the economic behavior of the system under varying market conditions.

Furthermore, the model structure, based on technical and economic parameters widely reported in the literature, ensures robustness and allows its application across different scenarios and plant scales. This approach makes the model a useful tool for both academic analysis and decision-making support in real-world projects.

From an applied perspective, the results reinforce the potential of the Brazilian sugarcane sector as a platform for green hydrogen production, particularly due to the availability of surplus electricity and the well-established cogeneration infrastructure. The integration of electrolyzers into these facilities represents a concrete opportunity for revenue diversification, improved energy utilization, and reduced exposure to electricity market volatility.

Future work may further develop the model through sensitivity analysis to identify additional parameters that significantly influence the LCOH, alongside electricity price.

Acknowledgement

The authors acknowledge the financial support provided by the National Council for Scientific and Technological Development (CNPq).

References

1. Glenk G, Reichelstein S. Economics of converting renewable power to hydrogen. Nat Energy. 2019.
2. International Energy Agency. Global hydrogen review 2025 [Internet]. Paris: IEA; 2025. Available from: https://www.iea.org/reports/global-hydrogen-review-2025
3. Brasil. Ministério de Minas e Energia. Brasil gera 88% da sua energia elétrica a partir de fontes renováveis [Internet]. Brasília: Ministério de Minas e Energia; 2025. Available from: https://www.gov.br/mme/pt-br/assuntos/noticias/brasil-gera-88-da-sua-energia-eletrica-a-partir-de-fontes-renovaveis
4. Giocoli A, et al. Techno-economic viability of renewable electricity surplus to green hydrogen and biomethane for a future sustainable energy system: hints from Southern Italy. Renew Sustain Energy Transit. 2023.
5. Fukai R. Estudo do potencial de geração de eletricidade excedente produzida no setor sucroalcooleiro visando a produção de hidrogênio verde [master's thesis]. Guaratinguetá (SP): Universidade Estadual Paulista; 2024.
6. União da Indústria de Cana-de-Açúcar e Bioenergia. Bioeletricidade gerada com bagaço e palha cresce 14% em 2023 [Internet]. São Paulo: UNICA; 2024. Available from: https://unica.com.br/noticias/bioeletricidade-gerada-com-bagaco-e-palha-cresce-14-em-2023/
7. Zhu P, Mae M, Matsuhashi R. Techno-economic analysis of grid-connected hydrogen production via water electrolysis. Energies. 2024;17:1653.
8. NovaCana. Ranking cogeração: Cerradão exportou 377,76 GWh de energia em 2024 [Internet]. Ribeirão Preto: NovaCana; 2025. Available from: https://www.novacana.com/noticias/ranking-cogeracao-cerradao-exportou-377-76-gwh-energia-2024-050625
9. Oliveira M. Potencial de produção de energia elétrica em 10 usinas no setor sucroalcooleiro no estado do Paraná na safra 2012/2013 [master's thesis]. Curitiba (PR): Universidade Federal do Paraná; 2013.
10. Carmo M, Fritz DL, Mercier JS, Stolten D. A comprehensive review on PEM water electrolysis. Int J Hydrogen Energy. 2013.
11. Kumar SS, Himabindu V. Hydrogen production by PEM water electrolysis: a review. Mater Sci Energy Technol. 2019;2(3):442-454.
12. International Renewable Energy Agency. Green hydrogen cost reduction: scaling up electrolysers to meet the 1.5°C climate goal [Internet]. Abu Dhabi: IRENA; 2020. Available from: https://www.irena.org/publications/2020/Dec/Green-hydrogen-cost-reduction
13. International Energy Agency. The future of hydrogen: seizing today's opportunities [Internet]. Paris: IEA; 2019. Available from: https://www.iea.org/reports/the-future-of-hydrogen

14. Electra Energy. Histórico do preço de liquidação das diferenças (PLD) [Internet]. São Paulo: Electra Energy; 2025. Available from: https://electraenergy.com.br/historico-do-preco-de-liquidacao-das-diferencas-pld
15. Open Jack. Electrolyser [Internet]. 2026. Available from: https://www.openjack-energy.com/electrolyser?id=1 Berrada A, Sanjari MJ, El Mrabet R. Techno-economic assessment of hydrogen production: comparative analysis of electrolyser technologies in a hybrid PV/wind system. Int J Hydrogen Energy. 2025;141:193-211. doi:10.1016/j.ijhydene.2025.05.384.
16. Centro de Estudos em Energia e Infraestrutura. LCOH: custo nivelado de hidrogênio verde no Brasil [Internet]. São Paulo: CELA; 2024. Available from: https://cela.com.br/estudos/lcoh-custo-nivelado-de-hidrogenio-verde-no-brasil-cela/

Climate Vulnerability in Solar Microgeneration: Analysis of the Impacts of Urban Flooding on Photovoltaic Systems

Diogo Antonio Queiroz Gomes[1,3,5]*, Filipe Cardoso Brito[2,5], Aloísio Santos Nascimento Filho[2,5], Eduardo Manuel de Freitas Jorge[3,5], Márcio Luis Valença Araújo[4,5], Natalia Silva Coimbra de Sá[3,5], Hugo Saba[2,3,5]
[1]Federal Institute of Bahia – IFBAIANO; Campus Uruçuca, Bahia; [2]SENAI CIMATEC University, Stricto Sensu Department; [3]State University of Bahia – UNEB, Campus I; Salvador, Bahia; [4]Federal Institute of Bahia – IFBA, Campus Lauro de Freitas; Lauro de Freitas, Bahia; [5]Applied Research and Innovation Center—NPAI; Salvador, Bahia, Brazil

The increased frequency of extreme weather events, especially floods, has exposed the vulnerability of photovoltaic microgeneration systems in urban areas. This theoretical, descriptive study analyzed the physical and operational impacts associated with flooding, focusing on three recurring categories in the literature: inverter damage, photovoltaic module failure, and electric shock risk. In addition to financial losses, structural damage was identified, which impacts the safety and resilience of these systems. The results highlighted the importance of preventive measures, such as elevating sensitive components, adopting moisture-resistant materials, and adopting safe shutdown protocols. The conclusion is that, although solar microgeneration is strategic for the energy transition, it directly depends on the adoption of adaptive solutions to mitigate vulnerabilities during extreme hydrometeorological episodes.
Keywords: Photovoltaic Microgeneration. Urban Flooding. Climate Vulnerability. Structural Impacts. Energy Security.

Investing in renewable and alternative energy sources has been considered an important low-impact strategy to reduce greenhouse gas emissions and generate energy efficiency through clean energy, both at the national level and for locations in more remote areas [1-3]. Stimulating investment in distributed generation of photovoltaic solar energy has been considered a priority action to stimulate decarbonization through the diversification of the energy matrix [4]. It was estimated that this would contribute 9% of electricity consumption in Brazil by 2034, generating greater autonomy and minimizing the impact of interruptions in the network [4,5], however, ANEEL data from 2024 already shows that this contribution in 2024 was 10.68%, exceeding the EPE estimate [6].

In this context, microgeneration of photovoltaic energy contributes positively to climate change by enabling the replacement of fossil fuels and the consequent reduction in pollutant gas emissions, especially in urban centers [7]. Improving the efficiency and stability of these systems, particularly through the integration of climate data, aligns technology with global sustainability and energy transition policies [5]. n a scenario where extreme events affect energy generation, transmission, and consumption, renewable sources, however, are considered quite vulnerable [4]. Therefore, the expansion of photovoltaic installations has also been affected by extreme weather events [7].

The feasibility of implementing these structures must consider the risk of flooding, which can result in damage and structural failures [8]. Floods cause multidimensional effects, and the electricity supply is often affected, generating a cascading effect. Power outages and damage to the electrical grid are reported in the literature as a direct consequence of urban flooding, requiring continuous improvement in the electrical grid infrastructure [9-11].

As discussed, the literature highlights solar photovoltaic energy as a strategic solution in the context of the energy transition, yet it is vulnerable to the effects of the climate crisis. Especially in residential and commercial settings, it requires continuous monitoring of its resilience, safety, and operational stability. Faced with the intensifying

Received on 17 April 2026; revised 28 June 2026.
Address for correspondence: Kevin Luís dos Santos. Av. Orlando Gomes, 1845 - Piatã, Salvador – BA – Brazil, Zipcode: 41650-010. E-mail: professor.diogo@yahoo.com.br.

J Bioeng. Tech. Health 2026;9(7):698-704

climate emergency, these technologies will need to adapt to scenarios marked by increasingly frequent extreme events, such as heavy rainfall, flooding, and urban inundation [12,13].

This approach sought to characterize the impacts of floods and severe storms on photovoltaic microgeneration systems through an analytical survey. To guide the analyses, the research question is presented as follows: How can extreme weather events, such as floods and storms, impact the operation and safety of photovoltaic systems installed in urban areas?

Materials and Methods

This study is theoretical in nature and descriptive in approach, focused on analyzing and systematizing information related to the impacts of urban flooding on photovoltaic systems. A comprehensive approach was adopted to address technical, safety, and economic aspects associated with the operation and vulnerability of these systems in the context of extreme hydrometeorological events.

The first step in the study consisted of a literature review to map the scientific literature relevant to the topic. Articles indexed in the Scopus and Web of Science databases were selected, addressing the interfaces between climate change, energy infrastructure, and risks associated with distributed microgeneration. In addition to the academic literature, a documentary analysis of institutional sources was conducted, highlighting technical reports from the Energy Research Company (EPE), which support national electricity sector planning and provide relevant data on the expansion of solar energy in Brazil.

To broaden understanding of the topic, based on applied technical information, digital channels of institutions specializing in electricity sector services and industry associations were consulted. This methodological combination allowed us to construct a well-founded and up-to-date overview of the adverse effects that affect photovoltaic systems during flooding. The methodological choice for this approach highlighted the three most common types of impacts in the literature for detailed analysis: inverter damage, photovoltaic module damage, and electric shock hazard.

Results

This section discusses the main findings of this study. Figure 1 presents a systematic overview of the three most frequently mentioned types of impacts in the analyzed publications, and Table 1 lists the publications addressing the topic.

Figure 1. Approach to flood impacts on photovoltaic systems in the analyzed publications. Prepared by the authors.

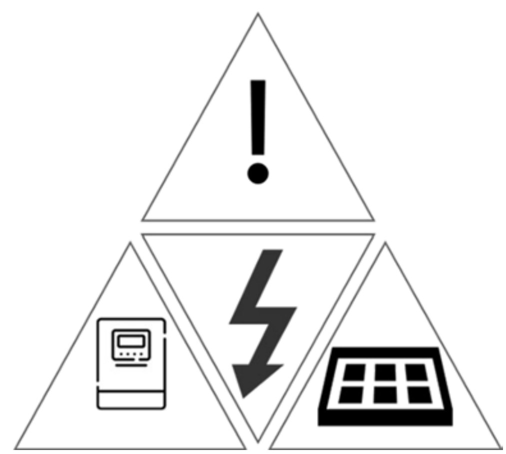

Table 1. Main impacts mentioned in the publications.

Impact	Publications
Damage to inverters	[14, 15, 16, 17, 18]
Damage to photovoltaic modules	[12, 14, 16, 18]
Electric shock hazard	[15, 16, 17, 18]

<u>Damage to Inverters</u>

During urban flooding events, photovoltaic inverters were highlighted as the most vulnerable and frequently damaged components in solar microgeneration systems [14]. These devices are responsible for converting the direct current generated by solar panels into usable alternating current at 127 or 220 volts [15]. When installed in lower areas of buildings to facilitate access, they become more susceptible to flooding. Although they have an IP65 protection rating, this level was not sufficient to withstand total or even partial submersion [16]. Figure 2 illustrates the condition of an inverter after flooding.

Figure 2. Inverter damaged by flooding.

Contact with water and mud can irreversibly compromise the inverter's internal circuits, generating the risk of immediate short circuits or progressive failures in the medium and long term [16]. Even when flooding occurs partially, preventive replacement of the equipment is recommended, given the impossibility of guaranteeing its integrity and safety after the event [17]. Restarting the system without a thorough inspection and before it has completely dried out not only poses a risk to the electrical safety of the installation, but can also cause overloads in distribution panels and compromise the stability of other system components [18].

The loss of inverters has implications that go beyond simply halting power generation. In many cases, entire systems become inoperable, requiring insurance claims and resulting in significant losses, especially for small businesses that rely on solar energy as a primary or backup power source [16]. Sludge contamination, accelerated corrosion, and the complexity of replacing damaged equipment exacerbate the vulnerability scenario, highlighting the need for more resilient installation strategies in flood-prone areas, as well as safe shutdown and restart protocols based on thorough technical inspections.

<u>Damage to Photovoltaic Modules</u>

Photovoltaic modules, essential components of solar energy systems, are designed to withstand adverse weather conditions, including heavy rainfall and prolonged exposure to the outdoors. High-quality solar panels typically feature a robust structure consisting of an aluminum frame, tempered glass, and a vacuum-sealed backing, which gives them significant resistance to water penetration [18]. Therefore, even after extreme precipitation events, the modules may be able to remain structurally intact and continue to operate. However, their physical integrity alone does not guarantee full system operation, as damage to electrical wiring, inverters, or the support structure can compromise the entire array [18].

During urban flooding, particularly those with strong currents, modules can be torn from their mounting structures, especially when installed in lower elevations or on ground supports [12,14]. In these situations, there is a risk of the panels being swept away by floodwaters, suffering mechanical damage, or causing accidents by colliding with other objects [14]. Panels mounted at ground level, while also waterproof, are more vulnerable to displacement during floods. In these cases, it is recommended that they be installed in elevated locations and with reinforced anchoring systems to mitigate these risks, as illustrated in Figure 3 [16].

It is worth noting that, even in cases where the modules appear to have suffered no visible damage, a specialized technical assessment must be conducted before any attempt to reconnect the system. Compatibility between the durability of the panels and the resistance limits of the supporting electrical infrastructure, such as cables, connectors, inverters, and metal structures, contributes to

Figure 3. Panels after floods.

Figure 4. Properties flooded by flooding.

ensuring the safety and operational continuity of the photovoltaic system [16,18].

Electric Shock Hazard

During urban flooding events, photovoltaic systems installed in homes or commercial buildings can pose serious risks to the physical safety of occupants and rescue teams. Although solar energy is a clean and promising source, in flooding situations it can be life-threatening due to the possibility of electric shock [17].

The continuous generation of energy by solar panels, even when the grid is disconnected, can be considered an aggravating factor. As long as sunlight is present, the photovoltaic modules will continue to produce voltage, energizing cables, electrical panels, and inverters [17]. Therefore, submerged buildings equipped with solar systems significantly increase the risk of electrocution, especially when in contact with contaminated water or when attempting to access roofs and elevated structures for shelter or rescue, as illustrated in Figure 4 [15].

Given this reality, it is recommended that, upon identifying an imminent risk of flooding, residents turn off the home's main circuit breaker before the water reaches the property [17]. It is also advisable to cover solar panels with opaque tarps to reduce energy generation and the potential for electric shock [18]. However, these actions should be taken in advance and with caution. Once flooding begins, do not attempt to disconnect photovoltaic equipment, especially if it is wet or submerged, as it remains energized even when the power grid is disconnected [17]. Another important point is to maintain a safe distance from panels, inverters, circuit breakers, and cables, considering that any malfunction can energize the water and result in fatalities [15].

Specialized technical teams are required for both post-event inspections and preventive guidance for the public [18]. These professionals must wear appropriate personal protective equipment (PPE), since even the direct current generated by photovoltaic systems can cause electric shocks [16]. Rescue procedures in flooded areas should also provide for complete isolation of electricity, avoiding operations on roofs equipped with solar panels, where there is a risk of slipping combined with electrical hazards [17]. In all cases, safe conduct seeks to prioritize moving away from the affected areas and awaiting technical evaluation before re-entering flooded buildings that use solar energy.

Discussion

Although solar modules are structurally designed to withstand high winds and continuous exposure to the elements, components such as inverters, charge controllers, and batteries remain highly susceptible to damage from flooding, especially when installed in low-lying areas or areas lacking adequate protection against water ingress [17]. Exposing these devices to moisture, mud, or submersion can seriously compromise their operation, cause short circuits, and result in irreversible damage to the system.

Structural and electrical damage to photovoltaic systems can vary depending on the type of architecture adopted. In general, systems fall into three categories: those with string inverters, microinverters, or batteries. All of these models, even the most advanced, can suffer operational interruptions or permanent damage in flooding situations [17]. In particular, hybrid systems that integrate solar panels and storage batteries are vulnerable to loss of functionality when critical electronic components are exposed to water or mud, with additional risks of short circuits and contamination from solid waste [17]. If the neighborhood power grid is damaged by flooding, users with battery systems and inverters with islanding capabilities can still rely on their own generation, as long as the equipment is preserved [18].

Rooftop installations offer a relative advantage, as they elevate the photovoltaic modules above the water level in flood scenarios. However, this does not guarantee the integrity of the system as a whole. Falling trees, strong winds, and structural collapses can affect the panels even in elevated locations. Furthermore, the connection between the solar system and the utility meter, typically located on ground level, remains at risk of flooding and accidental energization [18].

In emergency situations, it is necessary to reinforce safety guidelines. After the partial or total submersion of buildings equipped with solar systems, residents and rescue teams should not, under any circumstances, attempt to disconnect or tamper with electrical connections, inverters, panels, or panels, as there is a high risk of electric shock even with the grid deactivated [17]. The appropriate response involves isolating the area, awaiting specialized inspection, and, when necessary, replacing damaged components to ensure safety and the reliable restoration of solar energy generation.

More broadly, this situation has repercussions, especially in the scale of the financial impacts resulting from flooding on photovoltaic systems.

A survey revealed that between May and July 2024, approximately 52% (n=92/176) of claims compensated by an insurer specializing in the sector, these losses were directly linked to flooding and inundation, totaling over one million reais in compensation payments. That year, the state of Rio Grande do Sul was the most impacted by extreme weather events, accounting for approximately 32% of registered claims and 22% of the total compensation paid [13].

Despite the state's high installed capacity—approximately 2.7 gigawatts, corresponding to 9.6% of the country's self-generation—with over 302,000 connections distributed across its 497 municipalities. Only 30% of the facilities affected by the floods had some type of insurance, and only 10% of these policies specifically covered flood damage [13, 14]. This scenario exposes the financial vulnerability of thousands of users, particularly small businesses and households that invested in solar systems without considering the risks associated with extreme weather events.

Conclusion

The increased recurrence of urban flooding associated with extreme weather conditions requires the implementation of preventive guidelines and appropriate technical procedures for the installation and management of photovoltaic systems in flood-prone urban areas.

Mitigation of structural and electrical impacts begins at the planning stage, with the identification of risk zones and the selection of elevated locations for the installation of inverters and sensitive components, significantly reducing vulnerability.

Based on the sources consulted, preference is given to equipment with an IP65 protection rating or higher, along with the use of watertight connections, anti-corrosive materials, and technical seals suitable for moisture. Reinforced anchoring of support structures and photovoltaic modules is another suggested measure, especially in areas subject to strong currents or winds. For ground-based installations, adopting robust drainage solutions, technical elevation of inverters, and monitoring systems increases the resilience of systems to flooding. The use of sealed batteries and their positioning above historical flood levels were also reported as desirable interventions.

In terms of electrical safety, the installation of residual current circuit breakers and automatic reconnection systems is recommended, in addition to periodic maintenance with preventive inspection of equipment performance. In situations of meteorological alert or imminent risk, safe and preventive shutdown of the system must be carried out in advance. After a flood event, technical cleaning and thorough inspection are essential before any reconnection. Ensuring qualified technical support is available for emergencies contributes to the safe and efficient resumption of system operations.

From an economic perspective, the importance of purchasing insurance with specific coverage for extreme weather events was highlighted, as well as a detailed review of contractual conditions with suppliers and installers. Because this represents an emerging topic, the prospect of more in-depth approaches is anticipated, through research applied to specific territorial realities, encompassing socio-environmental and climate aspects. Public policies and adaptation measures, especially in the context of the state of Bahia, represent promising avenues for future research seeking solutions capable of improving the stability and operational safety of photovoltaic systems in extreme weather scenarios.

References

1. Schipper CA, Dekker GGJ, de Visser B, Bolman B, Lodder Q. Characterization of SDGs toward coastal management: sustainability performance and crosslinking consequences. Sustainability. 2021;13:1560. doi:10.3390/su13031560.
2. Hamin EM, et al. Pathways to coastal resiliency: the adaptive gradients framework. Sustainability. 2018;10(8):2629. doi:10.3390/su10082629.
3. Ajani A, van der Geest K. Climate change in rural Pakistan: evidence and experiences from a people-centered perspective. Sustain Sci. 2021;16:1999-2011. doi:10.1007/s11625-021-01036-4.
4. Empresa de Pesquisa Energética. Estruturação e modelagem de base de dados de indicadores e estatísticas socioambientais de riscos climáticos, mitigação e adaptação às mudanças climáticas no setor de energia [Internet]. Rio de Janeiro: EPE; 2022. Available from: https://www.epe.gov.br/sites-pt/acesso-a-informacao/participacao-social/Documents/BMC-D-60-600.0002A-RE-R0-Com%20anexo.pdf
5. Empresa de Pesquisa Energética. Plano Decenal de Expansão de Energia 2034 [Internet]. Rio de Janeiro: EPE; 2024. Available from: https://www.gov.br/mme/pt-br/assuntos/secretarias/sntep/publicacoes/plano-decenal-de-expansao-de-energia/pde-2034
6. Agência Nacional de Energia Elétrica. Relatório dos dados de receita, mercado de energia e número de unidades consumidoras [Internet]. Brasília: ANEEL; 2025. Available from: https://portalrelatorios.aneel.gov.br/luznatarifa/cativo
7. Yilmaz K, Dinçer AE, Ayhan EN. Exploring flood and erosion risk indices for optimal solar PV site selection and assessing the influence of topographic resolution. Renew Energy. 2023;216:119056. doi:10.1016/j.renene.2023.119056.
8. Chan FKS, et al. Build in prevention and preparedness to improve climate resilience in coastal cities: lessons from China's Greater Bay Area. One Earth. 2021. doi:10.1016/j.oneear.2021.09.016.
9. Peiris MTOV. Assessment of urban resilience to floods: a spatial planning framework for cities. Sustainability. 2024;16:9117. doi:10.3390/su16209117.
10. Kesavan H, Choudhary S, Khan S, et al. AI-based urban resilience planning: opportunities and challenges. J Environ Earth Sci. 2024;6(2):200-214. doi:10.30564/jees.v6i2.6681.
11. Pamplona N. Eventos climáticos extremos são desafios para energias renováveis [Internet]. Folha de S.Paulo. 2024. Available from: https://www1.folha.uol.com.br/mercado/2024/08/eventos-climaticos-extremos-sao-desafio-para-energias-renovaveis-diz-empresa-norueguesa.shtml
12. Associação Brasileira de Energia Solar Fotovoltaica. Providências em sistemas solares fotovoltaicos frente aos alagamentos no Rio Grande do Sul [Internet]. São Paulo: ABSOLAR; 2024. Available from: https://www.absolar.org.br/noticias-externas/os-impactos-do-desastre-climatico-no-rio-grande-do-sul-sobre-sistemas-fotovoltaicos-e-a-mobilizacao-do-setor-para-ajudar-as-vitimas/

13. Elétron Seguros. Alagamentos e seus impactos nos sistemas fotovoltaicos após a tragédia no RS [Internet]. 2024 [cited 2026 Jul 21]. Available from: https://blog.eletronseguros.com.br/alagamentos-e-seus-impactos-nos-sistemas-fotovoltaicos-apos-a-tragedia-no-rs/
14. TSEN. Com enchente, painéis de energia solar em prédios e casas podem causar choque elétrico [Internet]. 2024. Available from: https://gauchazh.clicrbs.com.br/geral/noticia/2024/05/com-enchente-paineis-de-energia-solar-em-predios-e-casas-podem-causar-choque-eletrico-clvvfrpqw0073011h0cfmiw23.html
15. Duarte DM. Sistema de energia solar após enchente [Internet]. 2024. Available from: https://periciaeletrica.com.br/sistema-de-energia-solar-apos-enchente-medidas-de-seguranca-necessarias/
16. Passos F. Procedimentos de segurança para o sistema solar fotovoltaico em caso de enchente [Internet]. 2024. Available from: https://microgeracaofv.wordpress.com/2024/05/10/quais-os-procedimentos-de-seguranca-para-seu-sistema-solar-fotovoltaico-em-caso-de-enchente-antes-e-depois/
17. RedePress. Sistemas de energia solar em áreas inundadas podem gerar riscos à população [Internet]. 2024. Available from: https://www.redepress.com.br/noticias/2024/05/sistemas-de-energia-solar-em-areas-inundadas-podem-gerar-riscos-a-populacao/
18. Rar Energia. Painéis solares, chuva e inundações: seus painéis são feitos para durar? [Internet]. 2024. Available from: https://rarenergia.com.br/paineis-solares-chuva-e-inundacoes-seus-paineis-sao-feitos-para-durar/

Gamified Strategies for Teaching Construction Planning

Regina Maria Cunha Leite[1,2]*, Lynn Rosalina Alves Gama[3,4] , Larissa da Silva Paes Cardoso[4], Matina Leite Vieira Lima[2], Hugo Meijon Morêda Neto[2]

[1]Department of Civil Construction, Federal Institute of Bahia; [2]GCIS Research Group—Federal Institute of Bahia; [3]Institute of Humanities, Federal University of Bahia; [4]SENAI CIMATEC University Center; Salvador, Bahia, Brazil

This study examines a gamified interface that can be accessed over the Web and aims to develop social and cognitive skills in students enrolled in undergraduate civil engineering and technical building courses who will ultimately work in construction companies. The methodological approach chosen is Design Science. This study is aligned with the generalization phase of a gamified solution for construction workers. To support the activities developed in the classroom, considering aspects of context, educational objectives, required skills, desired behaviors, and interactions, the gamified system was evaluated by 7 teachers and students, who focused on the functionalities, usability of the system (System Usability Scale - SUS) and promotability (Net Promoter Score - NPS). It also helps future technicians and engineers learn the importance of meeting deadlines, planning, and organizing the dynamics of the work that needs to be done, negotiating, and making decisions as a group, and reading the instructions to perform the tasks that need to be done in planning and budgeting for construction sites. The approach that the model takes to teach construction planning and budgeting is new and can captivate students, as well as encourage leadership and teamwork among the participants.
Keywords: Gamification. Education. Teaching. Collaboration. IHC. Construction Planning.

Gamification has grown across a variety of socioeconomic areas, including business, health, tourism, and education. These areas are seeking strategies to mediate the teaching-learning process or to boost customer loyalty to a particular brand or organization. This approach has been questioned for a variety of reasons, including the effect of neoliberal policies on behaviorist inspiration, which builds tactics on the paradigm of points, medals, and ranking, demanding a closer look.

To go beyond environments that prioritize competition and prizes, it is necessary to examine behaviors that have emerged in academic and educational settings. The purpose of this article is to examine the theoretical foundations that contributed to the development of a gamified interface that is accessible via the Web and mediates the dynamics of attitude development among construction planning students in technical or higher education courses that are critical to their preparation to become future technicians and engineers working for construction companies.

The article is divided into four sections, with a final thought in mind. The first section's brief introduction serves to establish the article's organizational framework. The second part, named "Gamification," describes the core notions that define and describe this category, as well as the components that should influence recommendations for gamified strategies, which may differ from behaviors mediated by digital and/or analog games. This section also covers a list of projects launched in the educational sector.

The project's strategy, which contributed to the outcomes stated in this article, is detailed in the third part. The empirical data gathered with the aid of the research participants and comments made it possible to suggest alternative applications for the gamified system in other disciplines, notably education. The fourth component proposes a gamified technique to guide building site planning.

This section describes the backdrop that led to the development of a Web interface that may be used on construction sites to facilitate and transparently communicate the tasks with workers in this setting. In this section, we will also go

Received on 12 April 2026; revised 21 June 2026.
Address for correspondence: Regina Maria Cunha Leite. R. Emídio dos Santos, s/n - Barbalho, Salvador – BA – Brazil, Zipcode: 40301-015. E-mail: regina.leite@ifba.edu.br

J Bioeng. Tech. Health 2026;9(7):705-717

over the gamified interface structure and how it is used. To achieve the goal of conceptual learning, preliminary discoveries and interface constraints were highlighted in the final discussions.

The idea is to encourage more critical readings and actions around these approaches by broadening the debate around gamification, particularly in learning environments.

Gamification

Gamified tactics have been solidifying in several industries over the last few years, ranging from airline loyalty programs to health applications that try to guide and encourage users to adopt better habits. In the sphere of education, there has been an increase in both study and creation of gamified apps, particularly during the Covid-19 epidemic, when we witnessed student instructors interacting with Kahoot, an application that incorporates game logic. However, many people do not comprehend what gamification is.

Gamification is the application of game-based mechanics, dynamics, and thinking in a real-world context to improve skills, motivate actions, promote learning, and solve problems [1-6].

Such a strategy seeks to engage a target audience through challenges, missions, storylines, performance-based feedback and rewards to attain predetermined goals. The initial definition by Deterding and colleagues [1] inspired authors such as Leite and colleagues [7-11] to investigate gamification in construction, Sailer and colleagues [12] to study its application in industrial settings, and Moura Junior [13] to create an app using gamified strategies to motivate wheelchair users to avoid injuries, among many others, who conducted research in domains such as teaching, health, work, business, and so on.

The adoption of gamified applications has been growing in the field of education, such as Alves et al [14] who evaluated the interactive environment COMnPLAYer to foster scientific and digital literacy of teachers and students, exploring non-formal learning in science, instigating curiosity, and Alécio and Schweikart [15]who propose for the teaching of English language with the aid of technological resources, in this specific case, the digital platform Duolingo, for children.

However, gamification is not without controversy. Authors such as Mcgonigal [16] regard the method as a pleasant way to engage and encourage others. Thus, surroundings become more intrinsically motivating, promoting total value creation, such as when marketing a product [17] or engaging students in the teaching and learning process, among other options. On the other side, gamification has faced criticism and uncertainty, with some doubting its usefulness and the length of its long-term impact [18]. Bogost [19] suggested the word "exploitationware," which may be translated as 'exploitation form', as a synonym for gamification, whilst Escribano [20] described gamification as a "ludic dictatorship."

Kim and Werbach [21] investigated gamification as a source of exploitation and manipulation, confirming the violation of values such as autonomy, responsiveness to reason, and justice, which can result in harm and humiliation, considering aspects such as dignity, self-esteem, and physical or psychological harm to the participant. Thorpe [22] examined the ethics of gamification in the marketing environment and emphasized the need to make the rules transparent to all stakeholders to fulfill the standards of honesty, truthfulness, and social accountability. Finally, the author proposed that an ethical review be undertaken at each level of creation and implementation process.

According to Chou [23], two elements are necessary to deem a gamified system ethical: full openness about what it is meant for, and the user's agreement to participate in gamification. According to Deterding [24], selecting a gamification architecture refines the practices of the environment to be gamified. As a result, in terms of ethics, it is critical to thoroughly examine how the process functions without gamification. Furthermore, data protection must comply with the General Law on Personal Data Protection [25].

According to Positive Psychology, humans are social, emotional, meaning makers, and growth-oriented [24, p.133]. Positive Psychology began as a research movement dedicated to studying what is healthy in humans, whereas psychology was previously primarily concerned with their disorders. According to Balancho [26], Positive Psychology originated with the purpose of improving public health, balance, and well-being in response to the scientific void created by its initial focus on illness research.

Positive Psychology is the study of positive feelings, emotions, institutions, and behaviors with the goal of human happiness [27] assuming that all people are immersed in a social context, in structures that transcend the individual (family, communities, education, and economic safety nets). Snyder and Lopez [28] define this approach as a scientific focus on the discovery and use of human traits, as well as the development of good functioning.

According to Deterding [24], the application of gamified tactics in the workplace, educational, and corporate environments, among other things, aims to improve practical outcomes. This is because the usage of game design and gamification is based on the well-being requirements of all parties involved, as well as positive psychology, resulting in rewarding experiences for goal completion.

Alves and colleagues [29] presented some criteria that can be considered for the construction of a gamification process: having a well-defined mission; an efficient scoring system so that rewards and feedbacks are fair, gaining the participant's trust; having well-defined narratives and strategies facilitating adherence to the tasks performed; having clear, evident, and organized missions, with a difficulty level appropriate to the target audience, and allowing the participation. Given the perspectives presented above, it is necessary to propose transparent gamified environments that respect their users' sensitive data, while also acknowledging that gamification extends beyond interaction with a playable and ludic environment, as well as stimulus-response mechanics or simple quizzes.

Gamification in Education

Gamified practices have always existed in education, whether through a quantitative assessment system that assigns grades based on performance, the attribution of stars, feedback and collaboration among students for the completion of activities, or more recently through the mediation of applications such as Kahoot (mentioned above) or the development of strategies that motivate students to overcome a specific individual or group challenge.

To Fardo [30], such tactics advocate the development of an educational aesthetic that is more like games in form and language, as it is more recognizable to students, while also delivering entertaining activities. Interactive surroundings and gamified tactics are more likely to excite pupils because they are more closely related to the language of digital games and have a higher level of engagement and connectedness.

Netflix is developing an interesting example with its interactive narratives, such as Stretch Armstrong: The Escape, which presents a gamified structure that can be explored in school settings with children through discussion of the narrative and the implicit and explicit concepts related to curriculum issues [31].

In terms of teaching, with a focus on building technician courses and higher education in civil engineering, gamified strategies can help to increase interaction and collaboration by engaging students in assigning meaning to concepts and actions inherent in their future profession. Thus, incorporating gamification into technical education is one option for improving the teaching and learning process, while constantly keeping an eye on how students react when game design is introduced into the planned activities. According to Deterding [24] the "Gamer Generation" wants non-gaming surroundings to resemble gaming environments, with clear objectives and rules, graphics and game language, and positive feedback. As a result, tactics such as gamification can help students engage, collaborate, and build leadership skills.

Materials and Methods

The research discussed in this article is part of a gamification experiment on construction sites, which resulted in a gamified system for increasing communication with construction workers. This work takes the Design Science methodological approach, which is utilized in research to design, develop, and explore novel solutions [32]. This is an exploratory, empirical, and qualitative study.

The gamification initiative at construction sites was divided into four phases: understanding/ comprehension, development, analysis and assessment, and reflection (Table 1).

Learning objectives include comprehension, development, evaluation, and reflection. Identify and comprehend problems, develop and test solutions, collect and analyze data, and identify theoretical and practical contributions. The process includes selecting a construction site, observing the field, developing a gamified system, testing its usability, and proposing a final model and generalizing it.

The first phase involved recognizing and analyzing the problem to establish criteria for the creation of a solution to improve communication between managers and construction workers. Following the requirements analysis, the second phase specified the gamification methods and implementations required for the solution to perform properly. This phase culminated in the creation of the gamified system. As a result, after listening to the workers and conducting observations on the building site, it was feasible to create a solution, develop and test the gamified system, and incorporate improvements from early testing and assessments.

The final step included reviews with managers, employees, and testers. Among other tools, Brooke [33] developed the System Usability Scale (SUS), which consists of ten statements scored on a Likert scale, with odd-numbered questions having a positive meaning and even-numbered ones having a negative connotation. To account for the outcome, values ranging from 0 to 4 are assigned to the responses; for odd ones, 1 is removed from the value informed; and for even ones, the result is reduced by 5, combining all the results and multiplied by 2.5 to achieve a percentile value [13]. The acceptability categorization uses the following criteria: not acceptable [0 - 49], average [50 - 70], and acceptable [70 - 100].

For the testers, the Promotion Index (NPS) was also used, which, although having only one question, has the primary goal of determining if the user would indicate the product [13]. This index was used to determine if the subject trusted the model enough to recommend it to a friend. In this scenario, a scale of 0 to 10 was employed, with answers divided into three categories: [0-6] - critics, [7- 8] passives, and [9-10] promoters. Finally, the NPS is determined, which is equal to the proportion of promoters minus the percentage of detractors, and classified as follows: Excellence Zone [76 - 100], Quality Zone [51 - 75], and Improvement Zone [0 - 50].

The fourth step, which is the subject of this research, consists of views on generalizing the

Table 1. Research outline.

DSR Driving Stages and Outputs			
Comprehension	**Development**	**Evaluation**	**Reflection**
Problem identification and understanding	Solution development and testing	Data collection and analysis	Identification of theoretical and practical contributions
Construction site selection and field observation	Gamified System Development	Usability test of the Gamified System	Final proposal of Gamified Model and generalization

Source: Adapted from Leite [11].

usage of the gamified system to aid student task planning. The goal of this research is to discover how gamification tactics might promote student engagement by fostering cooperation among team members and boosting natural leader creation. Three professors and four students from technical and higher education courses evaluated the system. The pupils ranged in age from 18 to 25, and two of the professors were between the ages of 26 and 35, with one older than 56.

The gamified system is comprised of a dashboard that can be accessed via the web and is designed to provide feedback to the teams on the progress of the championship. Consequently, it was a straightforward process to generalize the system by simply modifying the objectives and missions that must be completed during the match.

The results and discussion section refers to the analysis of the data from the questionnaires answered by teachers and students for the context of the work and the presentation of a proposal for using this tool in the classroom using new rules but maintaining the soccer championship narrative.

Results and Discussion

The findings were systematized following interaction with the system, considering the data collected in the SUS questionnaire, which was completed by instructors and students of the technical and higher education courses. Thus, using this instrument, the average of the values obtained (Table 2) was calculated, yielding a score of 68.1, indicating the level of tolerance of the aforesaid group to the gamification system. The method was rated average/correct (50-70) points by the assessing public, indicating that there is room for improvement.

To determine the level of trust in the system, students and instructors were asked if they would recommend the system to a friend on a scale of 0 to 10. Three of them scored eight, two scored nine, and two scored ten. So, because three of the raters were passive, the system is in the Quality Zone [51–75]. Because the findings show that the system is correct and in the quality zone, a proposal for employing it with this target audience was created.

A Proposed Gamified System to Guide Construction Planning

Work planning is the translation of a project into executive and financial terms, making it one of the most important stages of management [34]. It is a necessary and crucial stage in developing a project's execution plan. When planning, the manager prepares crucial instruments to direct his efforts, create priorities, monitor service progress, and control through the referential research completed at this stage, allowing him to take appropriate action if these findings alter [34].

To improve production efficiency on the construction site, eliminate waste, promote transparency at all stages, and meet deadlines, the construction industry has adopted the "Lean Construction" method, which is based on the Japanese philosophy of production and seeks to eliminate production losses, i.e., everything that does not add value to the product but consumes time and resources [35]. As a result, while planning is crucial, efforts must also be made to manage buying, budgeting, production, personnel management, communications, and other areas.

The adoption of Lean Construction concepts, along with civil construction work planning [36], has improved the process, allowing enterprises to establish themselves in the market with competitive advantages in the current context. As a result, future construction technicians and engineers must be oriented to give meaning to and absorb lean principles so that they may implement them in their everyday lives as professionals in the field.

Given this context and the profile of students enrolled in building and civil engineering courses who have interacted with interactive environments such as digital games since childhood, a gamified system for the web was developed with the goal of guiding planning practices on construction sites.

The narrative's topic was chosen in accordance with the profile of civil construction workers, as

Table 2. System usability scale (SUS).

Teacher / Student Buildings	How old are you?	I think I would like to use this system often	I think the system is unnecessarily complex	I found the system easy to use	I think I would need support from a technical person to be able to use this system	The various functions in this system have been well integrated	I think there is a lot of inconsistency in this system	I would imagine that most people would learn to use this system very quickly	I found the system very complicated to use	I felt very confident using the system	I needed to learn a lot about context before using this system	Results
Student	Between 18 to 25	4	0	4	0	4	2	4	0	3	0	71.5
Teacher	> 56	4	3	4	0	4	0	4	0	4	0	70.0
Teacher	From 26 to 35	4	0	4	0	4	0	2	0	3	0	74.5
Student	Between 18 to 25	2	0	0	4	2	2	4	0	0	0	50.5
Student	From 26 to 35	3	1	4	3	2	1	3	1	3	3	50.0
Student	From 26 to 35	4	0	4	0	4	0	4	0	4	1	75.0
Teacher	From 26 to 35	4	1	4	2	3	1	4	0	3	0	65.5
Student	Between 18 to 25	4	0	4	0	3	0	2	0	4	2	69.5
												68.1

determined by a semi-structured questionnaire administered in person and designed to learn significant information about this group, such as age, degree of education, time of service, hobbies, and so on.

The group's hobby was the soccer championship, which subsidized the system's gamified strategy by including a simulation of this activity in its narrative, which is a sport that has a high level of engagement not only for construction workers but also for students.

This environment, which can be accessible immediately on the web via an Internet connection, is linked to a gamified proposal for the subject construction planning and budgeting, which is available to fourth-year students in the technical building course and the Civil Engineering course.

The concept sought to encourage timeliness in activity delivery, reading content prior to courses, and team collaboration to complete and present the work on time. In this way, the proposed system aimed to create real-life situations for the budget and construction planning teams, allowing students to interact with decision-making activities such as bidding, meetings with top management to discuss projects and deadlines, and so on. Thus, this plan was created in accordance with the web environment and will be presented in this paper, highlighting the educational opportunities and limitations.

The gamified environment can expose students to circumstances that teach them the value of meeting deadlines, planning and arranging the dynamics of the work to be done, negotiating and making group choices, reading assignment rules, and so on. These elements are essential to the practice of construction management and planning.

The gamified learning environment replicates the dynamics of building planning operations through weekly tasks and missions, with a set of rules, feedback, and incentives. The missions are week-long assignments connected to building planning, such as logistics and material control, construction cost spreadsheets, and so on, with a teacher-set deadline. The challenge, on the other hand, is a surprise element introduced by the instructor into the classroom and will have a deadline for the teams to complete before the conclusion of the meeting.

A challenge might be a question concerning the class's topic, a brief activity, or a puzzle to solve with instructions from the teacher (live clue) or a video made accessible by him (online clue). The task and challenge do not have to take place at every meeting.

The team performance screen will display feedback to the teams using the system's symbols. The award is up to the instructor; it might be a point at the conclusion of the course for the winning team, a digital certificate for the winner of the "Best Construction Planning Team" championship, or anything else to stimulate the students. However, learning is the most valuable reward.

The planned tournament is inspired on the 'Brasileirão', an annual competition between soccer clubs. During the season, clubs earn three points for victories and one for draws. In the 'Brasileirão', no points are granted for defeats. This score in the gamified system is adaptable and configurable since it was designed to foster more collaborative practices and teamwork while diminishing the focus on competition.

In each round, the players' motions determine the score. What motivates the players are the activities created by students in class, such as providing exercises, publishing engaging information on the course website, attending meetings, and meeting deadlines. These examples might teach students, in a humorous way, circumstances that lead to better time management and teamwork.

To demonstrate the dynamics described above, the following scores were used: ball in the net - 5 points; ball against goal - 3 points; ball out - 1 point; and free kicks and penalties: ball in the net - 10 points; ball against goal - 6 points; ball out - 3 points. As a result, even if the team fails to score a goal, they can still receive points.

To earn the highest score, teams must have the cooperation of at least two-thirds of their members. As a result, if just one-third of the group members participate in the activities, the team 'balls out'. If half of the group participates, 'ball in the goalpost'; if more than two-thirds participate, 'ball in the net'. This is a method of increasing engagement, which translates into a desire to participate in the team, and cooperation, which is demonstrated by an interest in planning the week's assignments.

The free kick represents the team's progress toward fulfilling the challenge given by the instructor in class, while the penalty shootout represents the completion of the objective defined over the week. At this stage, the teacher assesses how successfully the team met its goal and notifies the system.

Similarly to the Brazilian Championship, clubs are classed in each round based on total points scored, however the season's champion team is determined solely by goal differential. The goal difference is calculated by the number of times a team has attained 'ball in the net' status, and the team with the biggest goal difference wins the title at the conclusion of the season. In the event of a tie in each round, everyone is awarded a trophy, which will be gathered over the season.

The gamified system has no grade; it consists only of attitudinal norms such as time management and timeliness in delivery; cognitive rules such as decision making under time constraints; and collaboration with other team members.

Missions and challenges are components that contribute to team empowerment, which is vital when collaboration and cooperation are needed [37]. While collaboration necessitates learning to work with others, cooperation entails conducting mental processes with others in interaction spaces [37]. Missions are long-term tasks that need elaborate planning, whereas challenges are one-time events.

According to Schell [38], competition satisfies the player's deep internal desire to identify their skill level in comparison to another person in their social group, allowing them to employ more complicated strategies and behavioral choices. Collaboration, on the other hand, according to the author, is the "other way" of interacting with the other, allowing you to participate in actions and employ game strategies that would be impossible with just one person, as well as providing a deep sense of satisfaction from solving group problems and being a part of a team that wins the game.

Collaborative games are modeled after team sports, allowing for both the pleasures of collaboration and competitiveness [38].

Burke and colleagues [39] argue that for gamification to be effective, both competition and cooperation must be mixed. Competition can elicit sentiments of belonging to a group [40], whereas collaboration might foster the desire to collaborate toward a shared objective [12,21].

In collaborative knowledge creation, live hints are gathered through interaction with people who possess the information required to produce a certain project or challenge. These cues might be supplied by the teacher or anybody he designates. Online Clues, on the other hand, are digital features that give some signal for the development of the mission or challenge; these elements can include QRCodes or any other form of access to material essential to the task's completion [38].

To engage in the gamified system, students should create teams of four to six individuals and identify their team (see team shield in Figure 2), using the 'Brasileirão' as a metaphor for storytelling (as previously stated).

Given the positive potential of collaboration and cooperation, the system developed does not emphasize competitive activities, while we feel that competition in a regulated and contextualized setting can be a motivating factor in mobilizing individuals in pursuit of their goals.

System Interface

The gamified system consists of two screens: one with the weekly goals and one with the team performance.

Figure 1 depicts the weekly goals screen, which includes a table with the teams playing, the assignment description, and the weekly objective. The system refers to each week as a 'round' to relate it to the soccer championship. The example provided is for the sixth round, which corresponds to the building budget. While the work is in progress, the information 'Shots on goal' will show in red. After delivery, it will turn green to indicate that the assignment has been completed.

On the right side of the screen, a picture of the project on which the teams are working is displayed; this might be a blueprint or even a 3D graphic that clearly shows the week's aim. This page also shows you what happened in prior rounds.

The Detail capability displays a screen that permits video watching, where the teacher can submit a video including some task-related information. The Overview capability allows you to display a 3D image of the entire project (parts, facade, etc.) with the goal of describing the job to be completed.

Figure 2 depicts the teams' performance screenswhich begin on the day of class 6 and terminate the day before class 7, corresponding to the sixth round. The screen displays the championship teams, the players' actions during the tournament, and whether a mission or a challenge exists in each round.

To get points for the players' motions, the team must complete the following activities: (1) Mov. Defense: hand in summaries before class (promote teamwork and individual time management); (2) Mov. Attack - be present in class (to encourage individual time management); (3) Move. Midfield - share intriguing stuff on the discipline page (to encourage cooperation); and (4) Move. Goalkeeper - complete activities on time (stimulate team time management).

The 'Free Kicks' and 'Penalty Kicks' require task division, decision-making, and everyone's teamwork to produce on time.

The values of the week (round) are totaled in points scored to decide which team leads the round and is most likely to win the weekly trophy. Throughout the competition, the number of times the team has a 'ball in the net' is recorded in the goal balance.

The rules governing the gamified environment are:

Figure 1. Weekly goals

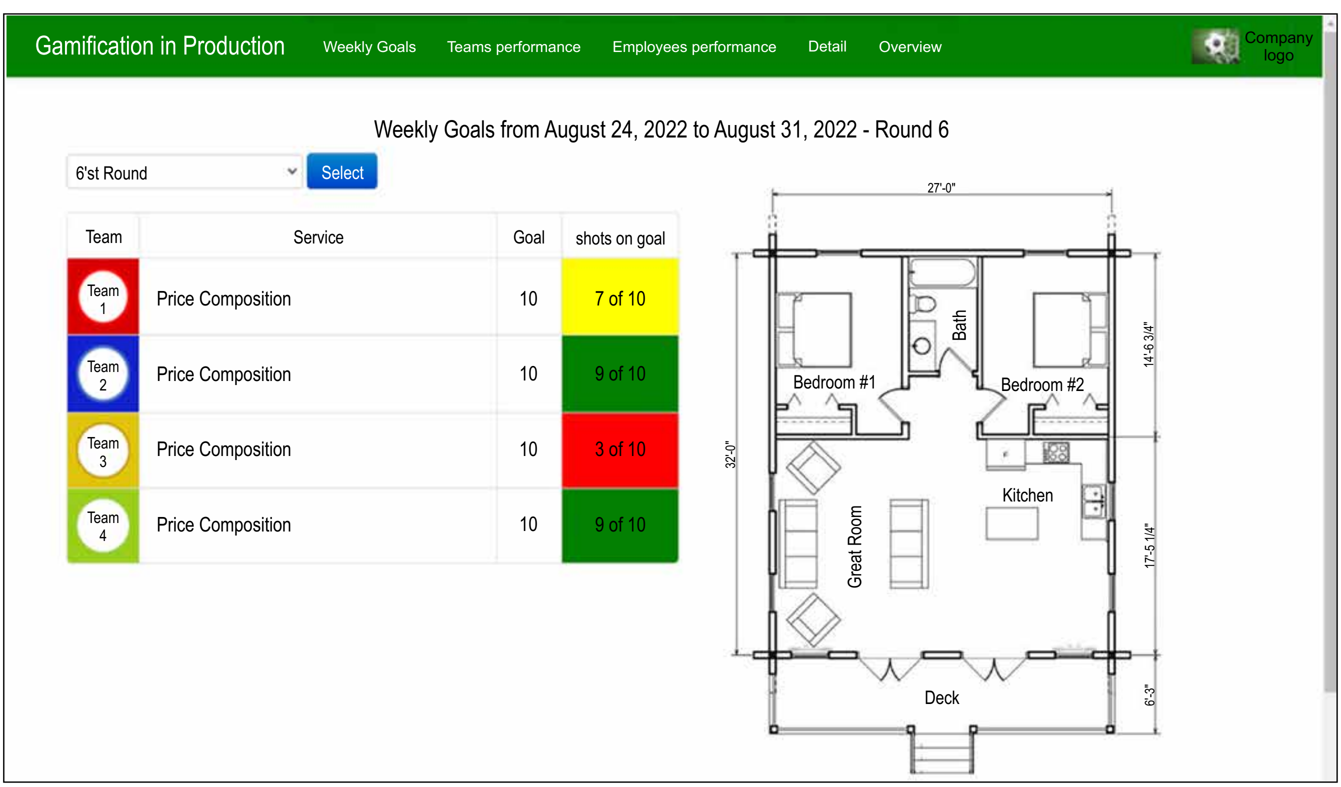

Figure 2. Performance of the teams after class 6.

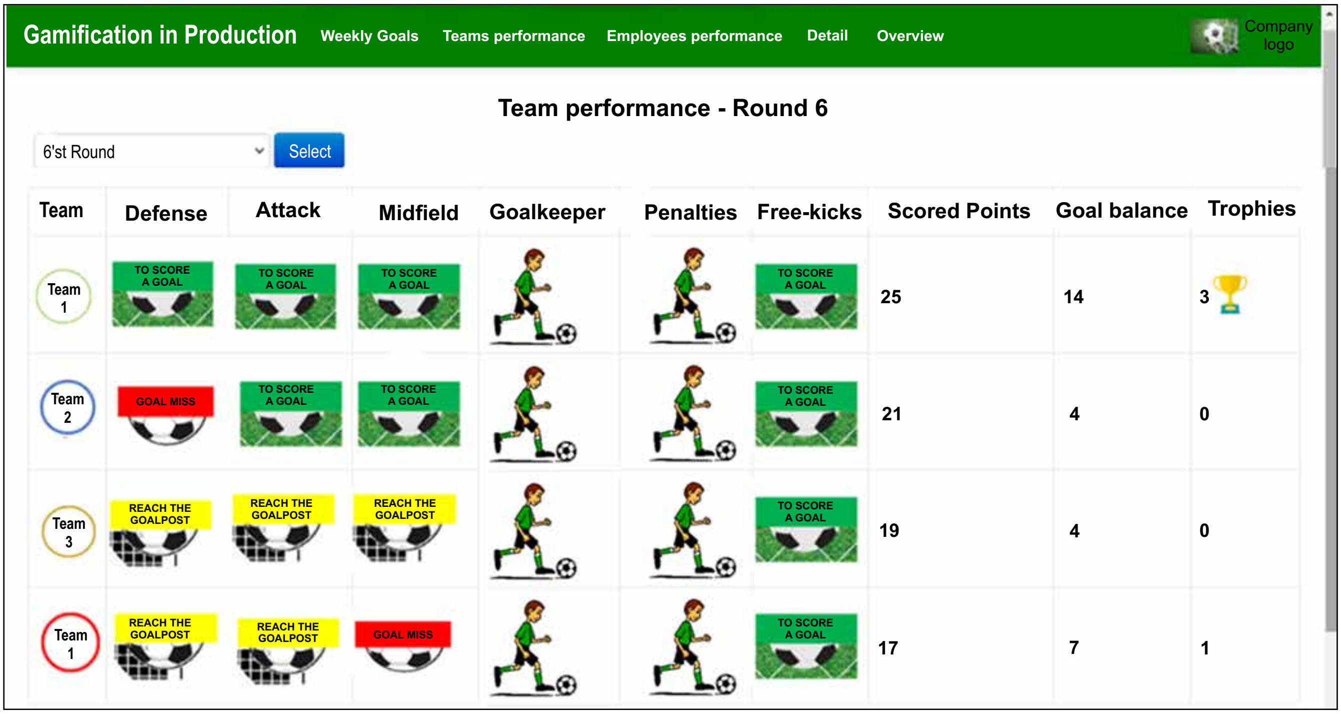

- Student involvement is voluntary and limited to teams.
- The student may quit the team at any moment but cannot join another.
- Any team that does not engage in activities for four consecutive meetings will be eliminated from the tournament.
- Abstracts must be submitted using the online platform (Google Classroom) up to 15 minutes before the start of class.
- Missions (out-of-class assignments) must be submitted using the online platform (AVA) by the deadline.

In the 'Brasileirão', the seasons and rounds correspond to nine months and one week. These deadlines are changeable in the system; thus, they may be set by the system administrator, who may also be the teacher.

The volunteer team leaders will get all the participants' names and forward them to the administrator so that they may be entered into the system. The system is divided into two modes: administrator, where data is entered, and viewer, where users may view and track weekly objectives and team performance via mobile device or monitor (Figure 3).

Only the administrator profile may insert data. The system was written in Python, and the database is hosted on the Heroku cloud platform (Figure 4), which employs data protection measures in accordance with the General Data Protection Regulation [25].

<u>Simulating a Pedagogical Practice in the Gamified Environment</u>

The example below was intended to help students comprehend the dynamics of the classroom setting. Analyzing the example shown in Figure 2, which corresponds to the status of the teams at the end of the practical home budget work class that appears in the image, on the right side of the screen in Figure 1, the first team is an example of cooperation and good individual time management, with three trophies accumulated from previous classes. All the components planned for the class were there, and the course page had engaging information. The

Figure 3. Sketch of the gamified environment.

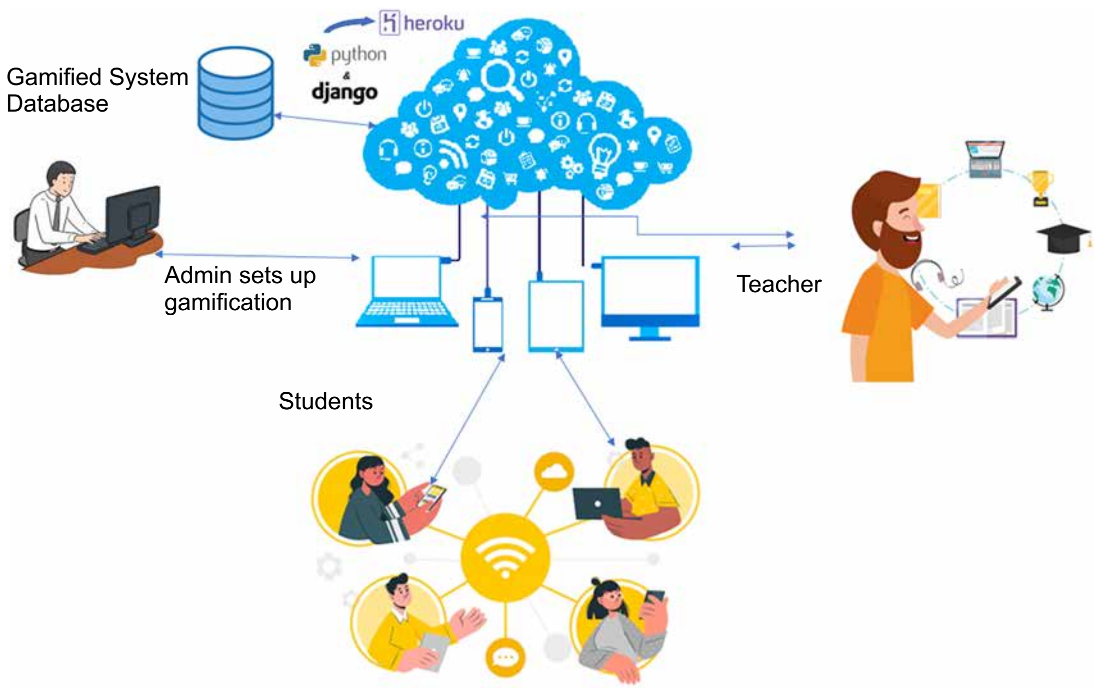

second, although being there and earning points for submitting material, did not add to the summary.

Observing the third team, not all members were present in class; some presented summaries and shared interesting stuff. The fourth team, whether none or just one, offered noteworthy stuff. This demonstrates that the squad was not particularly involved this week, despite having previously won a trophy in the previous class, and this attitude may alter before the end of the season. The week's objectives have yet to emerge; nevertheless, once the deadline is met, the result of the sixth round displayed in this sample should alter.

Conclusion

Gamification in the classroom aims to motivate and engage students in carrying out the discipline's activities, as well as to assist them in reviewing their practices, evaluating their attitudes, achievements, and difficulties in the face of learning new concepts and practices, so that they feel more confident in acting in the planning of works.

In terms of system implementation, the plan fits the ethical standards for voluntary involvement, rule openness, and scoring mechanisms. The system tracks the teacher's efforts in parallel, and even though it is a competition, it never reveals a specific student's status because grades are not disclosed in this discipline. The rivalry between teams, as envisioned in the system, is an incentive for the team to be among the best scorers, and compliance with the defined regulations is sufficient to achieve the suggested goals.

For the student, the gamified environment proposes to motivate him through team rivalry, with the idea that this form of stimulation stimulates teamwork, whether in classroom participation or in the preparation of extra class activities. As a result, gamification can help to improve understanding by motivating students to access the discipline's contents in advance, either by summarizing the available material or searching to post on the discipline page, allowing the class to be transformed into a more interactive space with questions and discussions on the issues.

Furthermore, students are driven to do extra class duties as a result of team collaboration and competitiveness. The gamified system can also increase communication between teachers and work teams by revealing what is expected of them on the system's first screen, making duties more engaging and relaxed.

One restriction of the approach is that the system must be tailored to the setting in which the gamification is intended before it can be implemented. In the future, other elements that allow users to participate more in the gamified environment can be investigated. Furthermore, it is aimed to investigate methods of integrating data with the platforms utilized in the disciplines.

References

1. Deterding S, Sicart M, Nacke L, O'Hara K, Dixon D. Gamification: using game-design elements in non-gaming contexts. In: CHI '11 Extended Abstracts on Human Factors in Computing Systems. New York: ACM; 2011. p. 2425-2428.
2. Zichermann G, Cunningham C. Gamification by design: implementing game mechanics in web and mobile apps. Sebastopol: O'Reilly Media; 2011.
3. Kapp KM. The gamification of learning and instruction: game-based methods and strategies for training and education. Hoboken: John Wiley & Sons; 2012.
4. Alves LRG, Minho MRS, Diniz MVC. Gamificação: diálogos com a educação. São Paulo: Editora Pimenta; 2014. Available from: http://repositoriosenaiba.fieb.org.br/handle/fieb/667
5. Huotari K, Hamari J. Defining gamification: a service marketing perspective. In: Proceedings of the 16th International Academic MindTrek Conference. New York: ACM; 2012. p. 17-22.
6. Huotari K, Hamari J. A definition for gamification: anchoring gamification in the service marketing literature. Electron Mark. 2017;27(1):21-31.
7. Leite RMC, Bastos Costa D, Meijon Morêda Neto H, Araújo Durão F. Gamification technique for supporting transparency on construction sites: a case study. Eng Constr Archit Manag. 2016;23(6):801-822.
8. Leite R, Alves L. A gamified model for the building site: a solution to motivate construction workers in pandemic time. J Bioeng Technol Health. 2020;3(4):319-327.
9. Leite RMC, Alves LRG. Estratégias de gamificação: um sistema web para disseminar as informações de produção para os trabalhadores da construção civil. Res Soc Dev. 2021;10(12):e241101220293.
10. Leite RMC, Winkler I, Alves LRG. Visual management and gamification: an innovation for disseminating information about production to construction professionals. Appl Sci. 2022;12(11):5682. doi:10.3390/app12115682.
11. Leite RMC. Estratégias de gamificação e gerenciamento visual: um modelo para disseminação de informações de produção e feedback aos trabalhadores da construção civil [doctoral thesis]. Salvador: Centro Universitário SENAI CIMATEC; 2022.
12. Sailer M, Hense JU, Mayr SK, Mandl H. How gamification motivates: an experimental study of the effects of specific game design elements on psychological need satisfaction. Comput Hum Behav. 2017;69:371-380.
13. Moura Júnior RMF. Práticas colaborativas gamificadas para prevenir lesões por pressão [doctoral thesis]. Salvador: Universidade Federal da Bahia; 2020.
14. Alves LRG, Almeida BO, Oliveira MP. COMnPLAYer: ambiente interativo e lúdico para aprender ciência. Rev EducaOnline. 2021;15(2):151-166.
15. Alécio PF, Schweikart JF. Proposta de uso da plataforma Duolingo no ensino e aprendizagem de línguas estrangeiras para crianças. Leitura. 2020;(67):421-432. Available from: https://www.seer.ufal.br/index.php/revistaleitura/article/view/11082
16. McGonigal J. Reality is broken: why games make us better and how they can change the world. New York: Penguin; 2011.
17. Vesa M, Hamari J, Harviainen JT, Warmelink H. Computer games and organization studies. Organ Stud. 2017;38(2):273-284.
18. Koivisto J, Hamari J. Demographic differences in perceived benefits from gamification. Comput Hum Behav. 2014;35:179-188.
19. Bogost I. Exploitationware. In: Rhetoric/composition/play through video games: reshaping theory and practice of writing. Pittsburgh: Carnegie Mellon University Press; 2013. p.139-147.
20. Escribano F. Gamificación versus ludictadura. Obra Digit. 2013;(5):58-72.
21. Kim TW, Werbach K. More than just a game: ethical issues in gamification. Ethics Inf Technol. 2016;18(2):157-173.
22. Thorpe AS, Roper S. The ethics of gamification in a marketing context. J Bus Ethics. 2019;155:597-609.
23. Chou YK. Octalysis: complete gamification framework. Fremont: Octalysis Media; 2015.
24. Deterding, S. Gamification in management: Between choice architecture and humanistic design. Journal of Management Inquiry. 2019; 28(2):131-136. 25. Brasil. Lei nº 13.709, de 14 de agosto de 2018. Lei Geral de Proteção de Dados Pessoais (LGPD) [Internet]. Brasília: Presidência da República; 2018. Available from: https://www.gov.br/cidadania/pt-br/acesso-a-informacao/lgpd
26. Balancho LS. Felicidade na pobreza. Curitiba: Juruá; 2013.
27. Seligman MEP, Csikszentmihalyi M. Positive psychology: an introduction. Am Psychol. 2000;55(1):5-14.

28. Snyder CR, Lopez SJ, Costa RC. Psicologia positiva: uma abordagem científica e prática das qualidades humanas. Porto Alegre: Artmed; 2009.
29. Alves LRG et al.. Gamificação: diálogos com a educação. 2014.
30. Fardo ML. A gamificação aplicada em ambientes de aprendizagem. Renote. 2013;11(1).
31. Lopes D, Santos WDS, Alves L. Uma análise do processo de gamificação em narrativas interativas da Netflix na prática de ensino. Temática. 2021;17:153-170.
32. Dresch, A, Lacerda D, Júnior J. Design science research: método de pesquisa para avanço da ciência e tecnologia. Porto Alegre: Bookman, 2015.
33. Brooke J. SUS: a retrospective. Journal of usability studies, 2013, 8(2).
34. Mattos AD. Planejamento e Controle de Obras. São Paulo: PINI, 2010.
35. Koskela L. Application of the new production philosophy to construction. Stanford: Stanford University; 1992.
36. Ballard HG. The last planner system of production control [doctoral dissertation]. Birmingham: University of Birmingham; 2000.
37. Schlemmer E. Projetos de aprendizagem gamificados: uma metodologia inventiva para a educação na cultura híbrida e multimodal. Momento Diál Educ. 2018;27(1):42-69.
38. Schell J. The art of game design: a book of lenses. Boca Raton: CRC Press; 2008.
39. Burke B. Gamify: how gamification motivates people to do extraordinary things. New York: Routledge; 2016.
40. Van Roy R, Zaman B. Need-supporting gamification in education: an assessment of motivational effects over time. Comput Educ. 2018;127:283-297.

Numerical and Experimental Analysis of Radial Compression in Umbilical Cables Using the Finite Alement Method

Bruno da Cunha Diniz[1]*, Maria Vitória dos Santos Alcântara e Figueiredo[1], Rui Felipe Cardoso Queiroz[1] Sarah Beatriz Ferreira Ramos de Cerqueira[1]
[1]*Federal University of Bahia, Polytechnic School; Salvador, Bahia, Brazil*

This study evaluates the performance of a two-dimensional numerical radial compression model applied to umbilical cables, comparing its results with experimental data. These cables are multifunctional structures essential to the oil and gas industry, responsible for interconnecting platforms and subsea systems, enabling control, monitoring, and fluid injection. Their internal configuration may include hydraulic hoses, electrical cables, optical fibers, steel tubes, filler elements, and armor layers. Installation is carried out by Pipe Laying Support Vessels (PLSVs), operating in vertical or horizontal lay modes. During installation, tensioners apply radial compression and axial tension, and, secondarily, cause radial crushing of the armor layers onto the core due to their helical arrangement. The numerical model was developed using the Finite Element Method in HyperWorks, with OptiStruct as the solver, adopting two-dimensional elements under the plane stress assumption. Loading was divided into three stages, simulating internal pressurization, shoe compression, and crushing pressure from axial tension. Layer interactions were assessed with Helica software. The results showed good agreement for residual and compressed diameters, with absolute errors <1.5 mm and relative errors <1% in most measurements. However, larger discrepancies were observed in residual ovalization, particularly for low-magnitude values, where the relative error was amplified. Thus, the use of absolute error is recommended as the criterion for evaluating sensitive quantities, such as ovalization and deformation.
Keywords: Umbilical Cables. Radial Compression. Finite Element Method. Numerical Modeling and Experimental Validation.

The objective is to analyze the performance of the numerical radial compression model applied to the umbilical, comparing its results with experimentally obtained data.

Umbilical cables are multifunctional structures of high complexity and versatility, widely employed in the oil and gas industry. They play a critical role in the interconnection between the production platform and the set of subsea valves installed at the wellhead. Their primary function is to enable the control and monitoring of subsea operations, as well as to allow the injection of chemical fluids aimed at optimizing flow. The configuration of the components within an umbilical cable varies according to its specific function and intended application, and may include hydraulic and injection hoses, electrical cables, optical fibers, and steel tubes. As described by Marzo (2010) [1], the arrangement of these internal elements is designed to ensure flexibility, reduce stresses, and provide mechanical strength. The components can exhibit two main motion patterns: local rotation, which occurs when only a single internal element undergoes rotational movement, and global rotation, characterized by the simultaneous rotational movement of all internal components around a common reference axis, generally coinciding with the umbilical's center.

Received on 6 March 2026; revised 27 May 2026.
Address for correspondence: Bruno da Cunha Diniz. Escola Politécnica da UFBA; Rua Prof. Aristides Novis, 2 - Federação, Salvador – BA – Brazil, Zipcode: 40210-630. E-mail: bruno.diniz@ufba.br.

J Bioeng. Tech. Health 2026;9(7):718-723

Umbilical Components

The hydraulic hose consists of a central tube responsible for maintaining hydraulic fluid containment, an aramid layer designed to withstand internal pressure, and an outer sheath whose function is to protect and bundle the internal elements. According to Alves (2022)[2], the electrical cables used in umbilicals can be classified into two types: signal cables and power cables. Depending on the application, these cables may include armor layers to enhance mechanical strength.

The rods are polymeric filaments used to fill voids in the umbilical's cross section, thereby reducing the likelihood of slippage and crushing between internal components. The armor is composed of wires arranged helically in opposite directions, whose primary function is to protect the umbilical core against axial tensile loads and external pressure, in addition to providing torsional stiffness (SUÑÉ, 2008,[3]). Finally, the inner sheath protects the umbilical core during the manufacturing process, while the outer sheath serves to protect the armor during installation and operation (Figure 1).

Umbilical Installation

Umbilicals are installed using vessels known as Pipe Laying Support Vessels (PLSVs), which can operate in either vertical or horizontal lay configurations. In vertical lay operations, the tensioners are arranged in an upright position, pulling the umbilical in this direction and guiding it toward the sea through a sheave located at the top of the tower. In horizontal lay operations, the tensioners are positioned horizontally, directing the umbilical toward a sheave located at the vessel's stern.

According to Mendonça (2016) [4], the tensioners function to control the umbilical's descent speed and to support the weight of the installed section, relying on the friction generated by the contact between the track shoes and the umbilical's outer sheath. The umbilical cross section passing through the tensioners is primarily subjected to two types of loading: radial compression, resulting from contact with the track shoes, and axial tension, caused by the weight of the already deployed line. In addition to these loads, Mendonça (2016)[4] also reports a secondary effect of radial crushing of the armor layers onto the umbilical core, induced by axial tension due to the helical arrangement of these layers.

Materials and Methods

Numerical modeling, particularly through the Finite Element Method (FEM), has assumed an increasingly significant role in engineering. According to Alves Filho (2000)[5], FEM, based on the discretization of the continuum, offers broad applicability regardless of geometry or loading conditions, providing approximate solutions that must meet the accuracy criteria established for the

Figure 1. Umbilical cables.

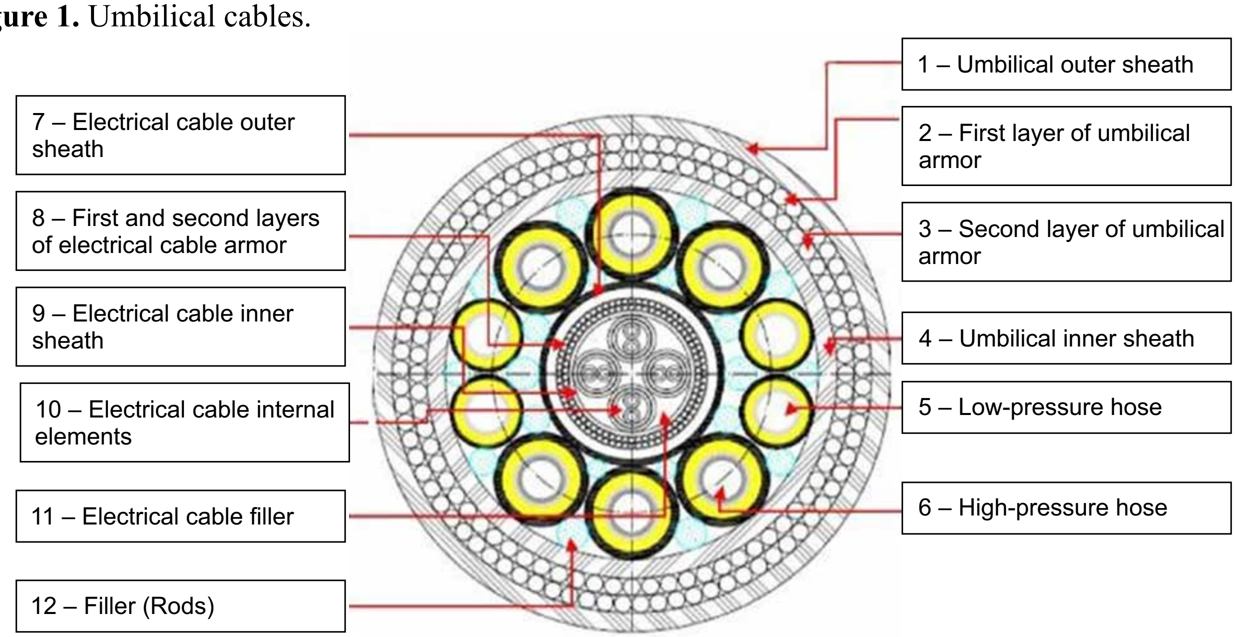

Source: MFX do Brasil (2015) [10].

problem under analysis. In this context, Guttner (2015) [6] validated a two-dimensional numerical model for the analysis of crushing in umbilical cables, based on the methodology developed by Pesce and colleagues (2015) [7]. This approach incorporates three-dimensional effects into a two-dimensional model by considering the radial loads induced by helical elements as a result of the choking effect. According to the author, this integration enables the consideration of conditions not accounted for in purely two-dimensional analyses, thereby making the numerical representation of the problem more faithful to the actual behavior.

For the development of the two-dimensional numerical model, the HyperWorks software was used for pre- and post-processing [8], while OptiStruct was employed as the solver due to its efficiency in structural, dynamic, and optimization analyses, including nonlinear and high-complexity problems.

The model was constructed under the plane stress assumption, using first-order two-dimensional elements: quadrilateral CQPSTN elements, with four nodes, and triangular CTPSTN elements, with three nodes. Inspired by the experimental radial compression test of the umbilical, the loading was applied sequentially to accurately reproduce the observed conditions. Initially, the umbilical hoses were internally pressurized to 3,000 psi. Subsequently, a compressive force of 39.20 tf/m was applied through two equally spaced shoes, while a third shoe had all its degrees of freedom fully constrained, ensuring that the reaction force matched the experimental load of 39.20 tf/m. After applying the internal pressure and the shoe compression, the umbilical sample was longitudinally tensioned to 113.74 tf, with a loading rate of 30.59 tf/min. Using the proprietary software Helica, developed by DNV-GL, the interaction between the layers in the umbilical cross section was analyzed. The tensile load was converted into 4.21 MPa of crushing pressure between the intermediate sheath and the internal elements, following a loading rate of 1.30 MPa/min.

The loading procedure was divided into three load cases. In the first, covering 0 to 120 seconds, the internal hose pressure was gradually applied until reaching 3,000 psi, accompanied by an initial compression force of 8.62 tf (22% of the total experimental load) to stabilize the model. The second load case, lasting from 120 to 1120 seconds, began by maintaining the internal pressure at its maximum value and progressively increasing the compression force to 100% of the total load within the first 360 seconds. Between 360 and 600 seconds, the crushing pressure was applied, and together with the other loads, held at maximum for the following 520 seconds to stabilize the model and minimize potential hysteresis effects. The third load case, from 1120 to 1800 seconds, involved the gradual release of loads: initially, the shoe compression force was reduced to 22% of the total load, followed by the removal of the crushing pressure. Finally, the internal hose pressure and the remaining compression were gradually released.

<u>Processing</u>

The solver is responsible for generating the local stiffness matrices of each element, taking into account its geometry and material properties, and subsequently assembling the global stiffness matrix [K]. With this matrix established, and knowing the applied loads represented by the force vector {F}, it is possible to determine the nodal displacements, described by the vector {U}, by solving Equation (1). From these nodal displacements, the corresponding strain and stress vectors are then calculated.

$$\{F\} = [K]\{U\} \tag{1}$$

<u>Post- Processing</u>

In a numerical radial compression model, it is essential that the macroscopic behavior of the umbilical be represented accurately. At the same time, the internal elements, which act as sacrificial components under this type of loading, must be modeled precisely to ensure the reliability of the simulation. To complete the correlation study, it is necessary to calculate the absolute and relative errors between the numerical and experimental results, using Equations (2) and (3), respectively. These calculations make it possible to assess the degree of agreement between the datasets and to determine the representativeness of the numerical results in relation to the experimentally obtained values.

$$E_a = |x_{medido} - x_{verdadeiro}| \quad (2)$$

$$E_r = \frac{|x_{medido} - x_{verdadeiro}|}{x_{verdadeiro}} \quad (3)$$

Results and Discussion

The horizontal and vertical displacements, in millimeters, at the end of the first load case, when the internal pressure in the hoses reaches its maximum value and the compression applied by the shoe corresponds to 22% of the total load, are presented in Figure 2.

Figure 3 illustrates the maximum horizontal and vertical displacements, in millimeters, at the end of the second load case, when all three loadings, internal hose pressure, shoe compression, and crushing pressure on the inner sheath resulting from the axial tension of the sample, reach their maximum values.

Figure 4 presents the residual horizontal and vertical displacements, in millimeters, after the complete removal of all applied loads.

Figure 2. Horizontal and vertical displacement, first load case, in millimeters.

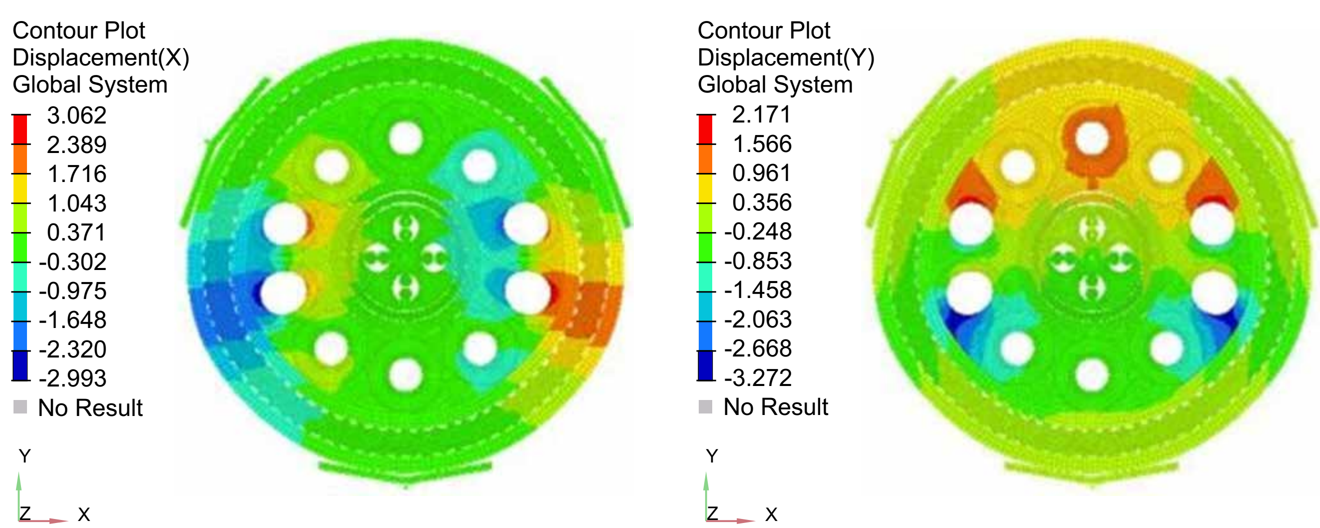

Figure 3. Horizontal and vertical displacement, second load case, in millimeters.

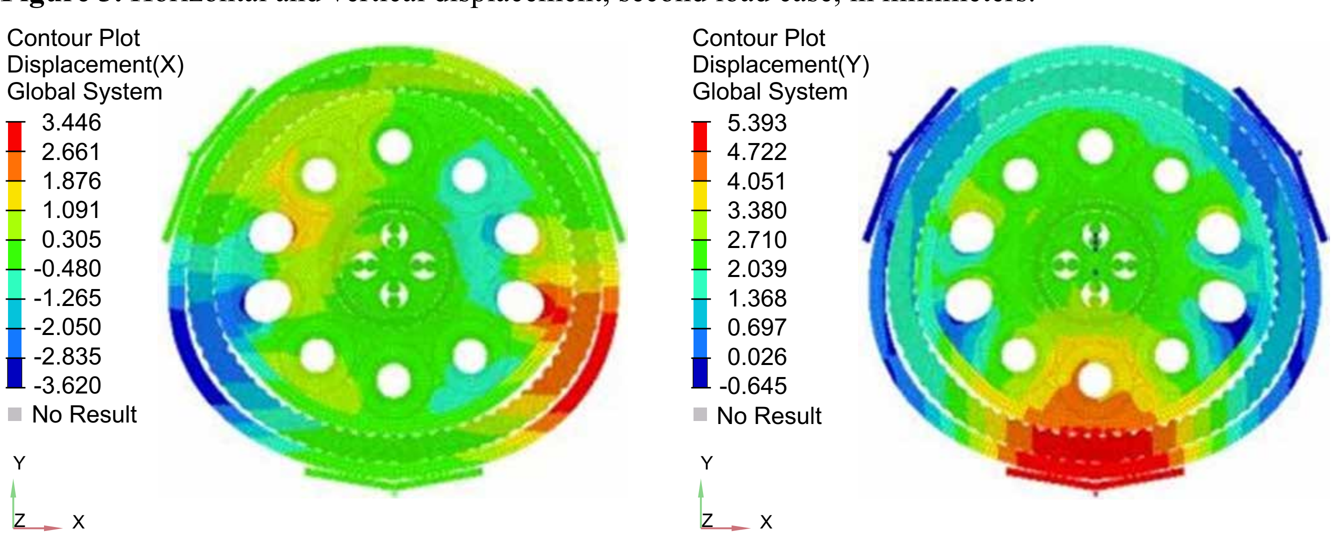

Figure 4. Horizontal and vertical displacement, third load case, in millimeters.

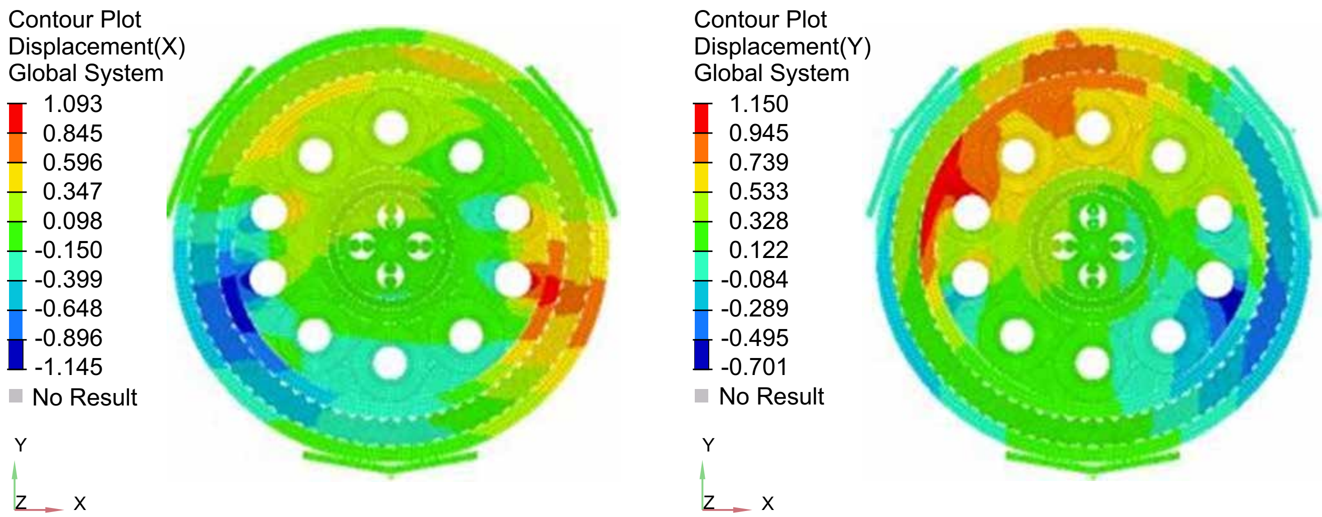

Source: MFX do Brasil (2015) [9].

Small asymmetries can be observed in the distributions, even when considering the symmetry of both the umbilical cross section and the applied loading. These asymmetries can be attributed to the high sensitivity of the model, stemming from its pronounced nonlinearity. Factors contributing to these nonlinearities include the use of frictional contact between elements and layers, as well as the adoption of materials with nonlinear stress–strain curves. This asymmetric behavior was also verified in the experimental tests conducted by MFX do Brazil in 2015 [9]. As illustrated in Figure 5, it is possible to identify the compression-induced deformation and the pronounced asymmetry of the cross section, which is more significant than that observed in the numerical results. This difference is explained by the fact that, in the experimental test, the compression reached 80 tf/m, whereas in the numerical model it was limited to 39.20 tf/m.

The vertical and horizontal diameters under compression (DVc and DHc), as well as the residual diameters (DVr and DHr) of the umbilical's outer sheath obtained through the numerical simulations, are presented in Table 1, alongside the corresponding experimental values. The macroscopic behavior of the cross section is characterized by the dimensions under compression and by the residual deformation of the outer sheath. The results indicate that the numerical model adequately represents the diameters, with a relative error of less than 1.00% in all four measurements. However, in the case of ovalization, although the absolute error remains below 1.50%, the relative error exceeds 50.00%. Despite the high relative error values for ovalization, the low absolute error suggests that the numerical model provides a good overall approximation in relation to the experimental results.

Figure 5. Umbilical cross section compressed in the experimental crushing test at 80 tf/m per shoe.

Table 1. Comparison between numerical and experimental values of diameters and ovalizations for the umbilical outer sheath, with associated absolute and relative errors.

Measurement	Numerical	Experimental	Absolute Error	Relative Error
DVc	161.61 mm	162.53 mm	0.92 mm	0.57%
DHc	168.49 mm	167.00 mm	1.49 mm	0.89%
OVc	4.17%	2.71%	1.46%	53.87%
DVr	165.45 mm	165.15 mm	0.30 mm	0.18%
DHr	165.66 mm	164.75 mm	0.91 mm	0.55%
OVr	0.13%	0.24%	0.11%	45.83%

Conclusion

The results indicate that the numerical model showed good agreement for the residual and compressed diameters of the umbilical's outer sheath, with absolute errors below 1.5 mm and relative errors under 1% in most measurements. However, significant discrepancies were observed in the residual ovalization values, particularly in low-magnitude quantities, such as the residual ovalizations of the high- and low-pressure hoses. In these cases, the relative errors were amplified, although the absolute errors remained small, highlighting the need for improvements to the model. Accordingly, this study proposes the adoption of absolute error as a more reliable criterion for assessing the correlation of sensitive quantities, such as ovalization and deformation.

References

1. Marzo GRD. Aplicação do método dos elementos finitos na análise de tensões induzidas em cabos umbilicais [master's dissertation]. São Paulo: Universidade de São Paulo; 2010.
2. Alves FFCL. Processo de qualificação de umbilicais para a indústria de óleo e gás [undergraduate thesis]. Niterói: Escola de Engenharia, Universidade Federal Fluminense; 2022.
3. Suñé Cordovés DLC. Análise de confiabilidade estrutural de cabos umbilicais [master's dissertation]. São Paulo: Universidade de São Paulo; 2008.
4. Mendonça HG. Análise paramétrica do efeito de cargas de esmagamento e estrangulamento sobre um tubo flexível na operação de lançamento [dissertation]. 2016.
5. Alves Filho A. Elementos finitos: a base da tecnologia CAE. 6th ed. São Paulo: Editora Érica; 2000.
6. Guttner WC. Modelo tridimensional em elementos finitos para a análise de cabo umbilical STU submetido ao carregamento de crushing [master's dissertation]. São Paulo: Escola Politécnica, Universidade de São Paulo; 2015.
7. Pesce CP, Santos CCP, Franzini GR, Salles R, Tanaka R. A finite element model for umbilical cable crushing analysis. In: Proceedings of the 34th International Conference on Ocean, Offshore and Arctic Engineering (OMAE2015); 2015 Jun 6–12; St. John's, Newfoundland, Canada. New York: ASME; 2015.
8. Altair. Practical aspects of finite element simulation: a study guide. 5th ed. Available from: https://altairuniversity.com/free-ebooks/free-ebook-practical-aspects-of-finite-element-simulation-a-study-guide/
9. MFX do Brasil. Ovalização Mangueira HCR – Máquina Crimp. Salvador: MFX do Brasil; 2015. Internal report.
10. MFX do Brasil. Datasheet No. 0672 Rev. 2. Salvador: MFX do Brasil; 2018. Internal report.

Development of the Goodman Diagram for DD5 Composite Using a Modular ANN

Bruno da Cunha Diniz[1]*, Maria Vitória dos Santos Alcântara Figueiredo[1], Rui Felipe Cardoso Queiroz[1], Sarah Beatriz Ferreira Ramos de Cerqueira[1]
[1]Federal University of Bahia, Polytechnic School; Salvador, Bahia, Brazil

This work presents an analysis of how the learning rate in a modular Artificial Neural Network (ANN) influences the development of the Goodman Diagram for the DD5 composite material. Experimental data involving multiple S-N curves were collected, and a mathematical approach based on the Generalized Power Law was employed to determine the stress amplitude and the average number of cycles to failure. The Goodman Diagram was constructed by calculating the mean stress from the stress amplitude and fatigue ratio. Data normalization was applied to prevent neuron saturation and enhance the generalization capability of the ANN. For training, three fatigue ratio values (R = 0.1, 2, and 10) were chosen, while an additional value (R = 0.5) was reserved for validation purposes. The hidden layer neuron count varied from 5 to 25, with learning rates tested at 0.05, 0.1, and 0.5 over 3000 training epochs. Analysis of the mean squared error (MSE) demonstrated that learning rates of 0.05 and 0.1 yielded errors on the order of 10^{-4}, whereas the 0.5 rate produced higher errors around 10^{-3}. The best performance was achieved with the 0.1 learning rate, as its Goodman Diagram curves closely matched the experimental data, reflecting superior learning ability and robustness of the model. This methodology illustrates that modular ANNs provide an efficient, fast, and cost-effective alternative for fatigue life analysis of composite materials, supporting improvements in structural design with enhanced safety and reliability.
Keywords: Fatigue Analysis. Goodman Diagram. Artificial Neural Network (ANN). Composite Materials and Learning Rate.

The objective of this work is to analyze how the learning rate of a modular architecture Artificial Neural Network influences the results of the development of the Goodman diagram for the DD5 composite.

Each material has a tensile strength limit. However, when subjected to time-varying stresses, materials may fail at stress levels lower than this limit, characterizing fatigue failure [1,2]. Since machine elements are subjected to cyclic loads, their design must take into account the material's service life (Sutherland, 1999). An important relation for the study of fatigue is the fatigue ratio (R) (Equation 1) [1,3,4].

$$R = \frac{\sigma_{\min}}{\sigma_{\max}} \quad (1)$$

Received on 17 April 2026; revised 25 May 2026.
Address for correspondence: Bruno da Cunha Diniz. Escola Politécnica da UFBA; Rua Prof. Aristides Novis, 2 - Federação, Salvador – BA – Brazil, Zipcode: 40210-630. E-mail: bruno.diniz@ufba.br.

J Bioeng. Tech. Health 2026;9(7):724-729

<u>Composite</u>

The data used for training and validating the ANN refer to the DD5 material and were extracted from the work of Mandell and Samborsky (1997) [5]. The DD5 is a glass fiber structural composite widely used in applications requiring good mechanical performance under static and cyclic loading, such as wind turbine blades, nautical components, and automotive structures. Its performance strongly depends on the reinforcement layer configuration, fiber volume fraction, and polymer matrix characteristics. The DD5 consists of a laminate with a [0/±45/0] layer configuration, indicating that most fibers are oriented in the longitudinal direction (0°), while some are inclined at ±45° relative to the main loading direction. This hybrid architecture aims to provide strength both in tension and shear. The fiber distribution in the laminate comprises approximately 70% of fibers in the 0° direction, favoring uniaxial tensile strength, and 30% in the ±45° layers, which contribute to shear stiffness and material performance under complex loading conditions.

Goodman Diagram

In the prevention of fatigue failures in composites, the Goodman Diagram has proven to be an effective tool, although it requires the development of a specific diagram for each type of composite analyzed. Obtaining the curve requires representative data of the material's behavior, which can be achieved by keeping the fatigue ratio constant and subjecting each specimen to a specific maximum stress value during testing. To determine the number of cycles to failure for different R values, new tests must be conducted, and specific S–N curves must be constructed for each condition [3,6]. According to Bond (1999) [7], the construction of the Goodman Diagram requires, at a minimum, a mathematical model representing the S–N curve, obtained from experimental data from alternating stress tests, in addition to the tensile and compressive strength limits of the material. With this data, the diagram is developed using the mathematical model to determine the values of stress amplitude (σ_a) and mean stress (σ_{me}d) for 10^3, 10^4, 10^5, 10^6, and 10^7 cycles. For composites, the main function of the Goodman Diagram is to define the safe regions of cyclic loading, indicating the number of cycles the material can withstand before failure. This is because, in most cases, these materials do not present a fatigue strength limit; that is, regardless of the applied stress, failure will occur after a finite number of cycles.

Mathematical Equations

The specialized literature, such as Subramanian and colleagues (1995) [8], Mandell and colleagues (1997) [5], (Sutherland 1999) [9]) presents several equations aimed at modeling the fatigue behavior of composites. However, none of these mathematical expressions proves to be sufficiently comprehensive to satisfactorily represent the fatigue phenomenon in all types of composites. For a mathematical function to adequately represent fatigue behavior, it must consider at least three essential variables: the number of cycles to failure (N), the stress value (σ), and the fatigue ratio (R). Following this approach, Equation 2 expresses the stress amplitude (σ_a) as a function of the mean stress (σ_{med}) and the number of cycles, without compromising the representation of the material's behavior:

$$\sigma_a = f(\sigma_{med}, N) \tag{2}$$

However, the previous equation does not satisfactorily represent the material's behavior, requiring a generalization. In this sense, Equation (3), proposed by Subramanian and colleagues (1995) [9], can be used to more adequately describe the relationship between maximum stress and the average number of cycles to failure ($\overline{N}$):

$$\sigma_{max} = A - B[\log(N)]^c \tag{3}$$

The addition of parameters A and C in Equation 3 aims to provide a better fit of the curve to the analyzed experimental results, allowing a representation closer to the fatigue behavior of composites. Another way to represent the S-N curve data is by using the Power Law (Equation 4). The main advantage of this equation is to provide smoothing of the curve for high numbers of cycles. However, it assumes that the material exhibits linear behavior on a log–log scale, which is not always experimentally observed. In such cases, it is possible to apply a generalization, presented in Equation 5 [10,11].

$$\sigma_{max} = a\overline{N}^{-B} \tag{4}$$

$$\log(\sigma_{max}) = A - B[\log(\overline{N})]^c \tag{5}$$

The parameters a, A, B, and C must be determined during the curve fitting process. With these values, it is possible to define the equation necessary for the development of the normalized Goodman Diagram.

$$\frac{\sigma_a}{UTS} = f\left(1 - \frac{\sigma_{med}}{UTS}\right)^u \left(\frac{UCS}{UTS} + \frac{\sigma_{med}}{UTS}\right)^v \tag{6}$$

In Equation 6, UTS and UCS represent, respectively, the tensile and compressive strength limits. The variables f, u, and v are parameters that vary as a function of the number of cycles to failure (N). According to Freire Jr. and Aquino (2009)[12], the main limitation of Equation 5 is the need for a large number of S-N curves to obtain satisfactory results. Another factor that disadvantages the model is the possible lack of correspondence between constant-life curves, which usually occurs when the number of available S-N curves is insufficient, compromising the faithful representation of the material's fatigue behavior. In their studies, Vassilopoulos and colleagues (2010) [13] proposed the development of a model capable of determining the fatigue behavior of a composite from a relatively reduced number of S-N curves. To this end, they mathematically demonstrated the existence of a relationship between mean stress (σ_{med}), fatigue ratio (R), and stress amplitude (σ_a), expressed in Equation 7. This model allows describing the material behavior using only two parameters, since the third can be obtained from the equation itself.

$$\sigma_a = \frac{1-R}{1+R}\sigma_{med} \tag{7}$$

Based on this proposal, equations were developed to represent each of the fatigue ratio regions, whose boundary conditions were defined from the experimental data of the S-N curves. The corresponding equations, as well as details about the construction of the constant-life Goodman Diagram, can be found in Vassilopoulos and colleagues (2010) [13].

<u>Artificial Neural Network</u>

An artificial neural network (ANN) is a massively parallel processor composed of simple processing units, with a natural capacity to store experimentally obtained knowledge and make it available for use. Several characteristics make the field of ANNs attractive for solving complex problems. Among them, the ability to learn from examples and generalize information stands out; that is, the network can provide consistent responses for unknown situations or inputs even with a reduced amount of data. Therefore, it is essential to have a well-designed training set that is representative of real behavior, combined with an appropriate network architecture and an efficient training algorithm.

The activation function defines the neuron's output in terms of its internal activation level. Various types of activation functions can be applied, such as threshold function, piecewise threshold, ReLU, hyperbolic tangent (TanH), and sigmoid [14-16]. Among these, the last is highlighted and was used in this work. The sigmoid function is considered the most common form of activation function in multilayer artificial neural networks trained by the back-propagation algorithm, as pointed out by Iyoda (2000) [14] and Silva (2009) [17]. It is defined as a strictly increasing function that offers an appropriate balance between linear and nonlinear behavior [15]. Equations 8 and 9 mathematically express the sigmoid function and its respective derivative.

$$\varphi(v) = \frac{1}{1+e^{-a_i v}} \tag{8}$$

$$\varphi'(v) = \frac{-(-a_i e^{-a_i v})}{(1+e^{-a_i v})^2} = a_i\varphi(v)[1-\varphi(v)] \tag{9}$$

The main characteristic of the perceptron network is the use of neurons with nonlinear activation functions and a feedforward layered architecture. Generally, this type of network consists of a set of sensory units (input layer), one or more hidden layers of computational neurons, and an output layer. Its training is performed in a supervised manner through the error backpropagation algorithm.

Modular Networks are neural networks composed of two or more independent modules (subsystems), without direct connections between them. The outputs of these modules are mediated by a routing network, which does not provide feedback. This routing network combines the outputs of the modules to form the system's final output, as well as determines how input patterns are distributed among the modules[15]. According to Ishikawa (1995) [18], learning in modular networks occurs in two stages: the first involves training the synaptic weights in each expert module, and the second corresponds to adjusting the synaptic weights that connect the different modules.

The ability to learn through interaction with the environment or the information source is one of the main characteristics of neural networks. The fundamental concept of training a neural network consists of gradually modifying the synaptic weights, following a learning rule that determines how these weights will be adjusted [15].

Supervised training is the most commonly used method for training ANNs. It is based on a predefined set of input and output data that guides the network's learning. Thus, the network is expected to respond approximately to the presented data. Furthermore, it is desirable that the network has the ability to generalize, i.e., provide consistent responses for both known and previously unseen data. According to Iyoda (2000) [14], a common way to implement supervised learning in neural networks is through iterative error correction procedures. Using a training algorithm structured to minimize error, combined with an adequate training set and a sufficient number of iterations, results in a neural network capable of performing tasks such as pattern classification and function approximation [14,15].

The backpropagation algorithm is the most used method for training multilayer perceptron artificial neural networks (ANNs), based on the error correction rule. Its computational structure basically consists of two stages: feedforward processing, in which an input is applied to the network and its effect is propagated layer by layer, with weights kept fixed, until the output layer generates a set of actual network responses; and backward processing, in which an error signal is propagated in the opposite direction, layer by layer. At the end of this process, the network weights are adjusted according to the error correction rule [14,15,19,20]. Thus, the function of backpropagation training is based on minimizing the mean squared error as in Equation 10.

$$EMQ = \frac{1}{2Q}\sum_{1}^{Q}\sum_{k=1}^{K}(d_k - z_k)^2 \qquad (10)$$

Where EMQ is the mean squared error, Q is the total number of data points, K is the number of neurons in the output layer, and dk and zk are the desired response and the actual response of the k-th output neuron, respectively.

Materials and Methods

The study development begins with the collection of experimental data, involving at least three S-N curves of the material under analysis. With these data, a mathematical approach based on the Generalized Power Law (Equation 5) was adopted, from which the values of stress amplitude (σ_a) and average number of cycles ($\overline{N}$) were determined. Finally, using the stress amplitude and the fatigue ratio, the mean stress (σ_{med}) was calculated according to Equation 7.

Normalization is a data preprocessing step aimed at preventing neuron saturation in the network, thus avoiding inadequate training. This method consists of restricting the input values of the S-N curves to a range between 0 and 1 for the stress amplitude, as shown in Equation 11.

$$\overline{N}_{nor} = \frac{\log(\overline{N})}{\log(N_{max})} \qquad (11)$$

Normalization of the other parameters also aids in the generalization of the ANN architecture usage. After normalizing the dataset during the preprocessing stage, the choice of network architecture constitutes the next step, being equally fundamental for successful training.

For network training, three fatigue ratio values were selected: R = 0.1, R = 2, and R = 10. To validate the synaptic weights obtained by the ANN, a dataset including all data plus an additional fatigue ratio, R = 0.5, was used. It is worth noting that the DD5 material employed has ultimate tensile strength (UTS) values of 1397 MPa and ultimate compressive strength (UCS) of -722 MPa.

The number of neurons in the hidden layer ranged from 5 to 25 in each module. For training, 3000 epochs were used, with learning rates varying between 0.05, 0.1, and 0.5.

The selection of synaptic weights for the representation of the Goodman Diagram considered the parameter set that showed the lowest mean squared error when evaluating all data.

The analysis of the dispersion of the Mean Squared Error (EMQ) values allows assessing two main characteristics of an artificial neural network (ANN): its generalization capability and the robustness (repeatability) of the trained algorithm. The errors obtained were on the order of 10^{-4} for learning rates 0.05 and 0.1, and on the order of 10^{-3} for the learning rate 0.5.

Results and Discussion

The construction of the Goodman Diagram results from the combination of the experimental data used in training with the curves generated by the ANN. As illustrated in Figure 1 to Figure 3, the points on the lines, which represent each value of R, correspond to the experimental data used in training, except for R = 0.5, which was used only for network validation. The curves represent the set of points of stress amplitude *versus* mean stress for a given number of cycles. Figure 1, Figure 2, and Figure 3 present the Goodman Diagrams obtained through the applied methodology, considering learning rates of 0.05, 0.1, and 0.5, respectively.

The curves located below the points presented in the graph indicate that the model's behavior remains within safe limits, ensuring structural integrity and the reliability of the obtained results. This relationship demonstrates that the model meets the established performance criteria, providing confidence for its practical application.

Conclusion

In the evaluation of the Mean Squared Error, which attests to the robustness (repeatability during training) of the trained algorithm, it is concluded that the adoption of only three S–N curves is sufficient to ensure consistent and representative results. This number of curves proves capable of adequately capturing the material's fatigue behavior, providing reliable information for both service life prediction and structural integrity assessment. Such an approach streamlines the modeling process, reducing experimental complexity without

Figure 1. Goodman diagram for learning rates 0.05.

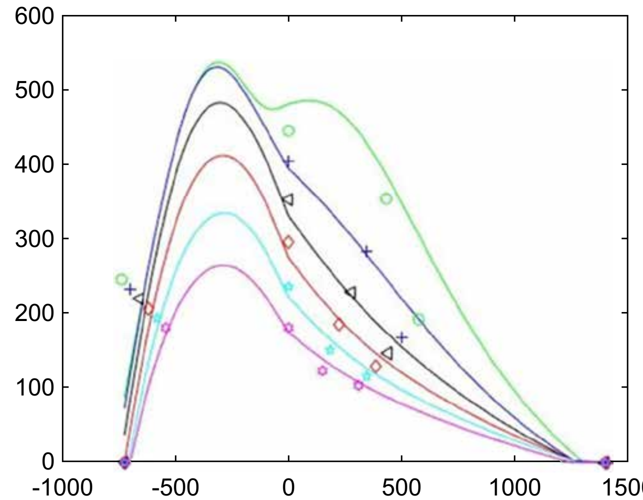

Figure 2. Goodman diagram for learning rates 0.1.

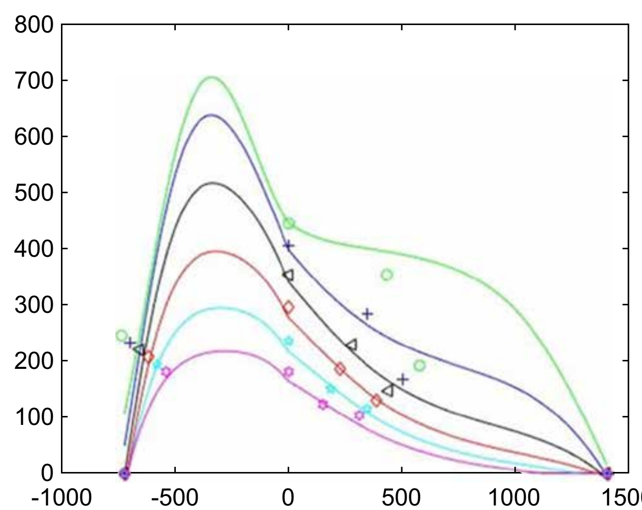

Figure 3. Goodman diagram for learning rates 0.5.

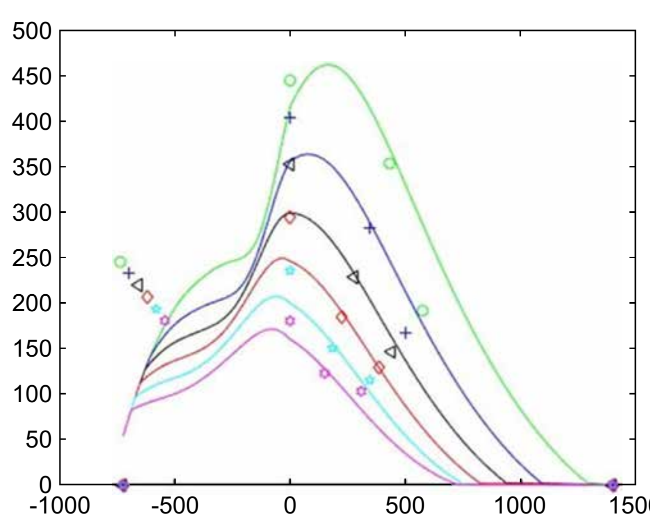

compromising estimation accuracy, thus enabling faster and more cost-effective fatigue life analyses By analyzing the generated Goodman Diagrams, it is observed that the ANN trained with a learning rate of 0.1 delivered the best results, as the curves of this diagram were closer to the experimental data. Therefore, even compared to higher learning rates, the learning capability of the network with a 0.1 rate proved to be superior. This result indicates that increasing the processing rate, as well as extending the time allocated to performing the analyses, does not necessarily lead to an improvement in the quality or accuracy of the results obtained. In other words, even with greater computational capacity or longer processing time, the model's performance may remain unchanged, highlighting that efficiency is not solely associated with intensive resource usage, but rather with the adequacy of the parameters and methods employed.

References

1. Souza SA. Ensaios mecânicos de materiais metálicos: fundamentos teóricos e práticos. 5th ed. São Paulo: Edgard Blücher; 1982.
2. Budynas RG, Nisbett JK. Elementos de máquinas de Shigley. 10th ed. Porto Alegre: AMGH; 2016.
3. Freire Júnior RCS. Fadiga de alto ciclo em compósitos de PRFV: modelagem por RNAs e prevenção de falha [doctoral thesis]. Natal: Universidade Federal do Rio Grande do Norte; 2005.
4. Mott RL. Elementos de máquinas em projetos mecânicos. 5th ed. Rio de Janeiro: LTC; 2015.
5. Mandell JF, Samborsky DD. DOE/MSU composite material fatigue database: test methods, materials and analysis. Albuquerque (NM): Sandia National Laboratories; 1997. Report No.: SAND97-3002.
6. Diniz BDC. Desenvolvimento de diagramas de vida constante probabilísticos de compósitos utilizando RNA modular [doctoral thesis]. Natal: Universidade Federal do Rio Grande do Norte; 2017.
7. Bond IP. Fatigue life prediction for GRP subjected to variable amplitude loading. Compos Part A. 1999;30:961-970.
8. Subramanian S, Reifsnider KL, Stinchcomb W. A cumulative damage model to predict the fatigue life of composite laminates including the effect of a fibre-matrix interphase. Int J Fatigue. 1995;17(5):343-351.
9. Sutherland HJ. On the fatigue analysis of wind turbines. Albuquerque (NM): Sandia National Laboratories; 1999. Report No.: SAND99-0089.
10. Philippidis TP, Vassilopoulos AP. Complex stress state effect on fatigue life of GFRP laminates. Part I. Experimental. Int J Fatigue. 2002;24(8):813-823.
11. Wahl N, Samborsky D, Mandell J, Cairns D. Effects of modeling assumptions on the accuracy of spectrum fatigue lifetime predictions for a fiberglass laminate. Wind Energy. 2002;5:19-26.
12. Freire Júnior RCS, Aquino EMF. Comparative study between ANN models and conventional equations in the analysis of fatigue failure of GFRP. Int J Fatigue. 2009;31:831-839.
13. Vassilopoulos AP, Manshadi BD, Keller T. Influence of the constant life diagram formulation on the fatigue life prediction of composite materials. Int J Fatigue. 2010;32:659-669.
14. Iyoda EM. Inteligência computacional no projeto automático de redes neurais híbridas e redes neurofuzzy heterogêneas [doctoral thesis]. Campinas: Universidade Estadual de Campinas; 2000.
15. Haykin S. Redes neurais: princípios e prática. 2nd ed. Porto Alegre: Bookman; 2001.
16. Glorot X, Bordes A, Bengio Y. Deep sparse rectifier neural networks. In: Proceedings of the Fourteenth International Conference on Artificial Intelligence and Statistics (AISTATS); 2011. p. 315-323.
17. Silva ALF. Obtenção da distribuição de pressão em asas usando redes neurais [master's dissertation]. São Paulo: Universidade de São Paulo; 2009.
18. Ishikawa M. Learning of modular structured networks. Artif Intell. 1995;75:51-72.
19. Braga AP, Ludermir TB, Carvalho ACF. Redes neurais artificiais: teoria e aplicações. Rio de Janeiro: LTC; 2000.
20. Nied A. Treinamento de redes neurais artificiais baseado em sistemas de estrutura variável com taxa de aprendizado adaptativa [doctoral thesis]. Belo Horizonte: Universidade Federal de Minas Gerais; 2007.

Grover's Algorithm Using IBM's Fake Providers

Frank Acasiete[1]*, Anderson Buarque[1]
[1]QuIIN, SENAI CIMATEC University; Salvador, Bahia, Brasil

In this work we will show Grover's algorithm using Fake Providers which are images of real quantum computers to give us an idea of their behavior in the implementation in Qiskit and we will show the fidelities with respect to the quantum simulator which gives us the result closest to the analytical one.
Keywords: Quantum Computing. Quantum Circuit. Quantum Algorithm.

A significant milestone in the implementation of quantum computers was established by Bennett [1], who introduced the concept of reversible computing as a model. Furthermore, Toffoli [2] made a substantial contribution by developing a universal set of gates for this model in classical computation.

Shor's Algorithm [3] has garnered considerable interest within the academic community. It has proven capable of efficiently solving challenging problems, such as the Integer Factorization Problem and the Discrete Logarithm Problem, when executed on a quantum computer.

In a notable experiment [4], Grover's search algorithm was successfully implemented on a quantum system with four states. This represented an important step in practically demonstrating the efficiency of quantum algorithms compared to their classical counterparts.

Preliminaries

In this section, we'll discuss Grover's Algorithm and Fake Providers. These are the essential tools we'll use to achieve the results presented in this work.

Grover's Algorithm

Grover's algorithm can find the marked element with high probability using only $O(\sqrt{N})$ function evaluations, compared to classical search which evaluations [5]. Grover's algorithm is a powerful tool in quantum computing, especially in search and optimization problems where efficiency is crucial.

Received on 21 March 2026; revised 26 May 2026.
Address for correspondence: Frank Acasiete. Av. Orlando Gomes, 1845 - Piatã, Salvador – BA – Brazil, Zipcode: 41650-010. E-mail: frank.quispe@fbter.org.br.

J Bioeng. Tech. Health 2026;9(7):730-734

The main barrier to demonstrating acceleration with Grover's algorithm is that the quadratic speedup achieved is too modest to overcome the significant overhead of near-term quantum computers.

In Grover's algorithm, we consider a function f: $\{0, 1,..., N-1\} \rightarrow \{0, 1\}$ as input. In the "unstructured database" analogy, the function's domain represents the indices of a database, and $f(x) = 1$ if and only if the data pointed to by index x satisfies the search criteria. We assume that only one index, called ω, and our goal is to identify this index.

To access the function f, we use a subroutine, also known as an oracle, in the form of a unitary operator U_ω, which acts as follows:

$$U_\omega|x\rangle = -|x\rangle \; for\ x = \omega, when, f(x) = 1,$$

$$U_\omega|x\rangle = |x\rangle \; for\ x \neq \omega, when, f(x) = 0.$$

This uses the N-dimensional state space H, which is provided by a register with $n = \lceil log_2 N \rceil$ qubits. This is often written as:

$$U_\omega|x\rangle = (-1)^{f(x)}|x\rangle. \quad (1)$$

In this algorithm, we use an N-dimensional state space H, which is provided by a register with $n = \lceil log_2 N \rceil$ qubits. In this way, the operator $U\omega$ acts on the quantum states represented by the qubits, applying a negative sign (-1) to the state $|x\rangle$ if $f(x) = 1$, and keeping the state $|x\rangle$ unchanged if $f(x) = 0$.

The oracle $U\omega$ has its behavior defined by the equation:

$$U_{\omega}: |x\rangle|a\rangle = |x\rangle|a \oplus f(x)\rangle. \quad (2)$$

where $|x\rangle \in H^N$, $|x\rangle \in H^2$, and $\oplus$ represents the XOR operation.

Grover's algorithm produces the value ω with a probability of at least 1/2 using $O(\sqrt{N})$ applications of $U\omega$. The Grover matrix, represented by G, is defined by:

$$G|x\rangle = (\tfrac{2}{N} - 1)|x\rangle + \tfrac{2}{N}\sum_{i \neq x}|i\rangle. \quad (3)$$

The Grover evolution operator, U_G, is given by:

$$U_G = GU_{\omega} \quad (4)$$

The algorithm's initial condition is:

$$|\psi_0\rangle = |G\rangle|-\rangle, \quad (5)$$

where $|-\rangle = (|0\rangle - |1\rangle)/\sqrt{N}$ and $G|x\rangle = \frac{1}{\sqrt{N}}\sum^{N-1}_{u=0} |u\rangle$. Grover's algorithm instructs us to iteratively apply U_G approximately $\lfloor \frac{\pi}{4}\sqrt{N} \rfloor$ times.

After these iterations, we measure the first register in the computational basis, and the result will be x with a probability greater than or equal to $1 - \frac{1}{N}$.

Fake Providers

The fake providers module allows developers to create realistic simulations of IBM quantum computers without needing physical access to a real device. It does this by using "snapshots" of actual quantum systems, which capture information like qubit connectivity and the types of errors that can occur [6].

Imagine you're building a new program for a quantum computer. Instead of testing your program directly on a real device (which can be expensive and hard to access), you can use fake providers to create a simulation. This simulation will mimic the behavior of a real quantum computer, including the common errors and inaccuracies found in these systems.

Why Use Fake Backends?

- Testing and Development: It lets you test and debug quantum algorithms before running them on a real device.
- Learning: It's an excellent tool for learning about quantum computing and understanding how errors affect quantum calculations.
- Optimization: It helps optimize quantum circuits before executing them on a real device.

Limitations

- Accuracy: Simulations might not be perfectly accurate, as the snapshots are from real systems that can change over time.
- Complexity: Simulating large-scale quantum systems can be computationally expensive.

While fake providers use snapshots of real quantum systems for its simulations, qiskit-aer offers a variety of simulators because it's a more general library. The fake providers system uses the most recent calibration results.

Results

We now show the results of the quantum simulation of Grover's algorithm for 4 qubits (Figure 1) for two cases of 1 and 2 marked elements, ω_1=0111 and ω_2 = 1101 (Figure 2). We will compare it with 3 fakes providers and finally present the fidelity of the results using the Hellinger metric:

$$h^2 = \frac{1}{2}\sum_x(\sqrt{p_x} - \sqrt{q_x})^2,$$

where p is the probability distribution of the q simulation and is the quantum computer.

Figure 3 presents Fake Osaka and Fake Auckland yield quite similar results. Notably, Fake LagosV2, despite having the lowest fidelity value, still provides good outcomes. This demonstrates

Figure 1. Grover's algorithm circuit for 4 qubits.

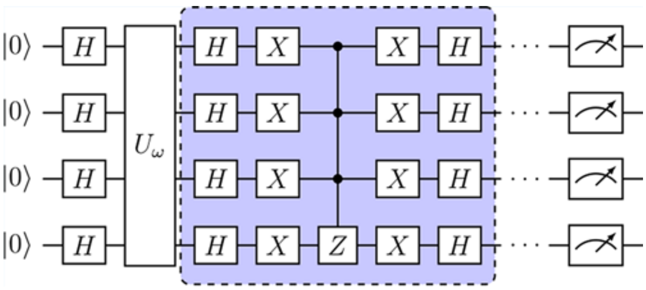

Figure 2. Circuits of the oracles of $\omega_1 = 0111$ and $\omega_2=1101$.

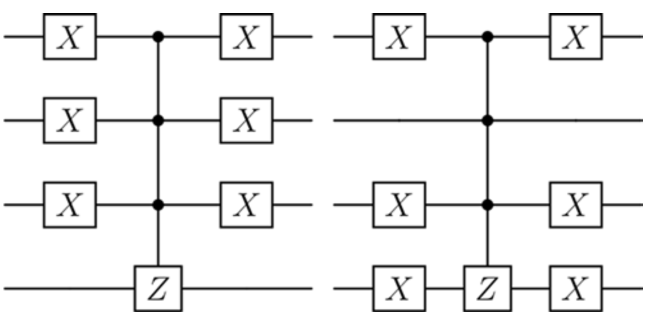

that Fake Providers exhibit behavior akin to real quantum computers. In Figure 4, we observe similar behavior, specifically for the case of two marked elements. Furthermore, Table 1 shows the fidelities of these providers when compared to the quantum simulator.

As mentioned, with these backends, it's possible to implement our quantum models and see how they behave. With these, we could observe, for example, quantum superiority in certain problems. Another useful feature would be that, since they already include the error of real quantum computers, we can use this as an exercise to reduce circuits through equivalences, improving our results and using this as a reference for future developments.

We also have to take into account the high cost of using real quantum computers today (with 10 minutes of free monthly use on IBM's QPUs), which limits research and development in this area.

Figure 3. Probability distribution of Grover's Algorithm with 4 qubits and one marked element

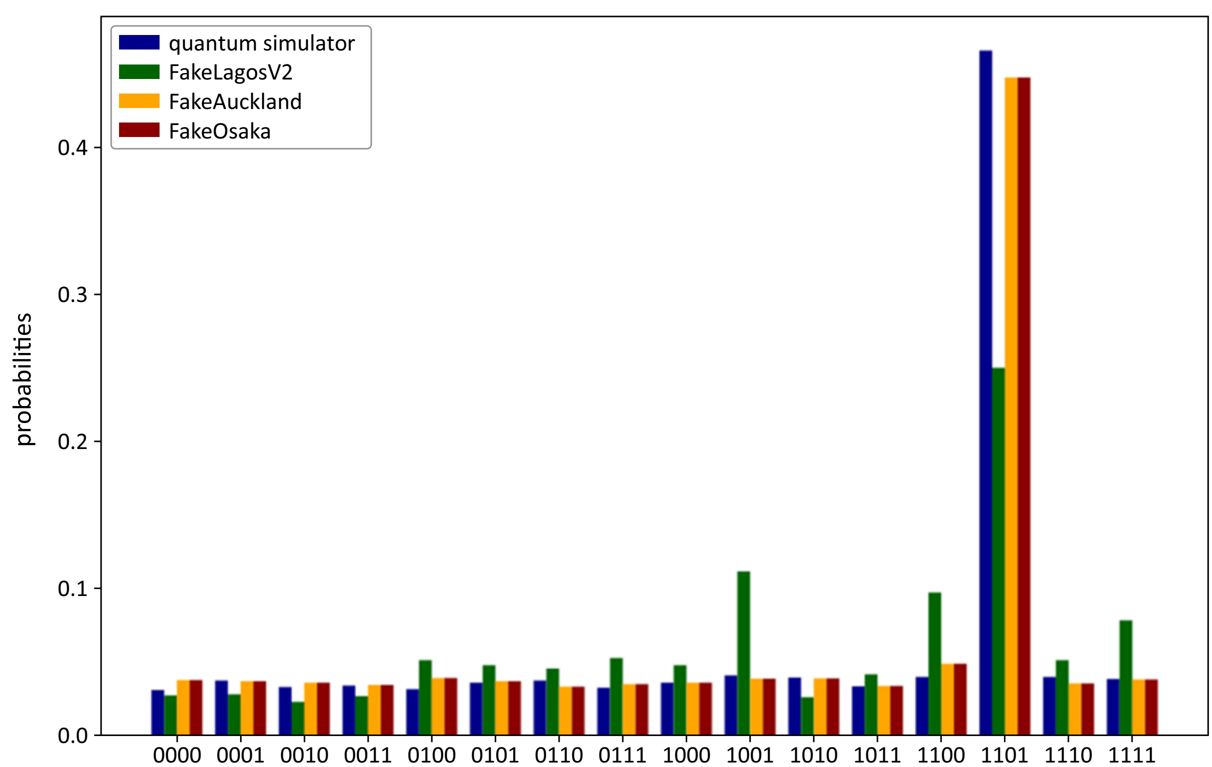

Figure 4. Probability distribution of Grover's Algorithm with 4 qubits and two marked elements.

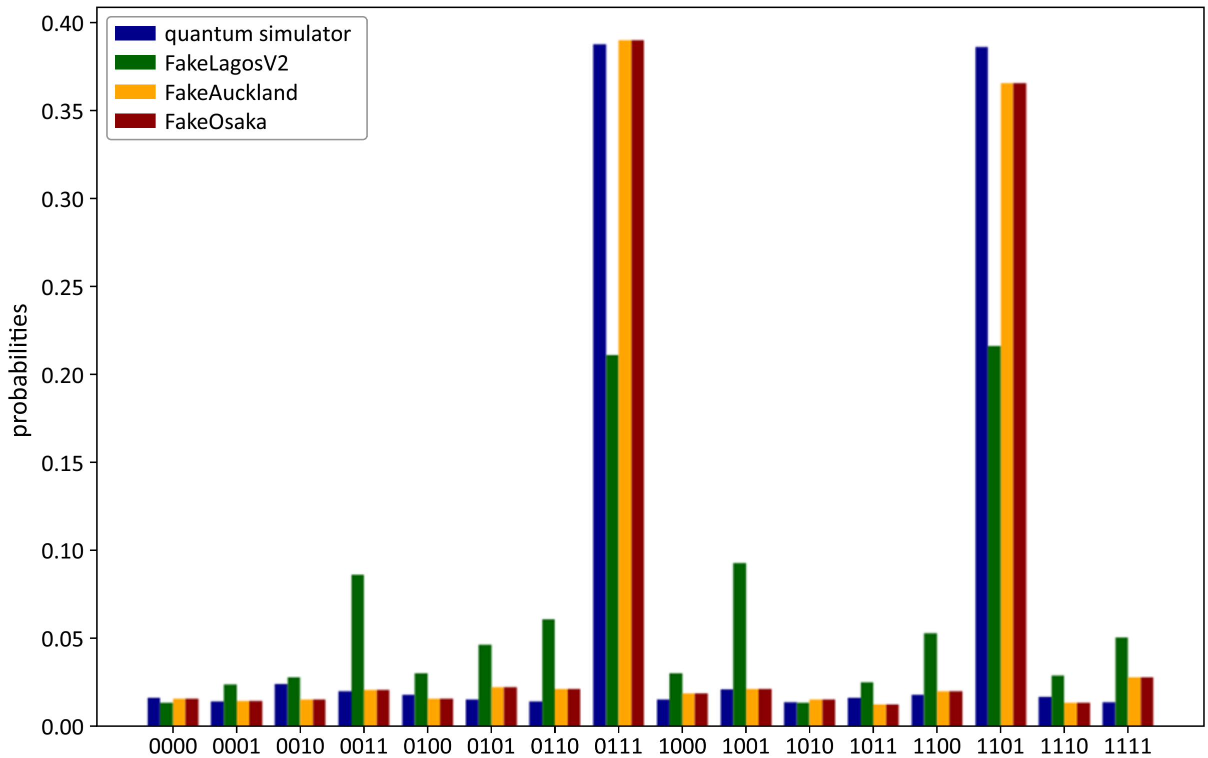

Table 1. Fidelity of Grover's algorithm with 4 qubits, using IBM's Fake Providers.

N° marked	Fake LagosV2	Fake Auckland	Fake Osaka
1	0.958	0.999	0.998
2	0.922	0.996	0.993

Conclusion

With these results, we can see that Fake providers are a tool for observing the behavior of quantum computers to determine if our algorithm implementations are performing as desired.

Although these are only snapshots of real quantum computers, most of which have already been retired, they show us how these computers have evolved over the years and that the error rate is decreasing, leading to the possibility of one day having a real, logical quantum computer.

Acknowledgement

This work was entirely funded by Project QIN-AFCCT-FC-CC-2024-6-11-1, supported by QuIIN-Quantum Industrial Innovation, the EMBRAPII CIMATEC Competence Center in Quantum Technologies. This funding was secured through MCTI Call number 053/2023, established with EMBRAPII.

References

1. Bennett CH. Logical reversibility of computation. IBM J Res Dev. 1973;17(6):525-532.
2. Toffoli T. Reversible computing. In: Proceedings of the 7th Colloquium on Automata, Languages and Programming; 1980. Berlin: Springer-Verlag; 1980. p. 632-644.
3. Shor PW. Polynomial-time algorithms for prime factorization and discrete logarithms on a quantum computer. SIAM Rev. 1999;41.
4. Chuang IL, Gershenfeld N, Kubinec M. Experimental implementation of fast quantum searching. Phys Rev Lett. 1998;80(15).

5. Grover LK. A fast quantum mechanical algorithm for database search. In: Proceedings of the 28th Annual ACM Symposium on Theory of Computing; 1996. New York: Association for Computing Machinery; 1996.

6. IBM Quantum. qiskit_ibm_runtime.fake_provider module [Internet]. IBM; [cited 2025 Jun 20]. Available from: https://docs.quantum.ibm.com/api/qiskit-ibm-runtime/fake_provider

Immersive Quantum Phenomena Laboratories: Principle of Light and Polarization

Rafael Bulcão[1,4], Henrique Sobrinho Ghizoni[1], Fernando Vieira Mascarenhas[1], Rafael Rodrigues Cezimbra[1], Yasmim Thasla[3,4], Anderson Correia Buarque[1,2], Ingrid Winkler[2,3,4]

[1]QuIIN - Quantum Industrial Innovation, EMBRAPII CIMATEC Competence Center in Quantum Technologies, SENAI CIMATEC University; [2]Department of Computational Modeling and Industrial Technology, SENAI CIMATEC University; [3]Institute for Science, Innovation and Technology in Industry 4.0/ INCITE INDUSTRIA 4.0; [4]Department of Industrial Management and Technology, SENAI CIMATEC University; Salvador, Bahia, Brazil

Teaching quantum physics concepts and phenomena can be facilitated through experimental practices. However, these practices are often costly and require dedicated space, making them unfeasible for low-resource educational institutions. Given these limitations, the use of virtual and augmented reality technology has emerged as an intermediary mechanism and teaching resource for quantum physics teaching. This study presents the preliminary development of the designed artifact and the applicability of an immersive laboratory to demonstrate the phenomena of polarization and the principle of light. This research follows the design science research (DSR) approach, proposing the initial development of the artifact and indicating its applicability as a quantum physics teaching tool, specifically for quantum optics phenomena. The proof-of-concept was developed within the UNITY engine and tested with the Meta Quest 3 and 3s headsets. As a result, an immersive, interactive, and functional environment was created for testing, evaluation, and use as a teaching tool. This work contributes to the development of a mobile and reusable teaching laboratory, proposing innovation in the educational path of quantum technologies.

Keywords: Quantum Immersive. Virtual Reality. Optical Physics. Polarization. Superposition. Light Principles.

Understanding quantum physics phenomena remains a challenging task. Keeping students engaged and reducing difficulties in assimilating abstract ideas, both in the classroom and in laboratory learning contexts, remains a challenge [1]. Gaps in information transmission, coupled with the limited content that stimulates abstract thinking in beginners, contribute to low active and meaningful student participation in experimental space activities [2]. Due to the limited equipment available, its high cost, and its sensitive handling, many students remain observers, while only a few actively participate [1,3].

Learning quantum technologies is a challenging task [4], as it requires mastering foundational concepts that underpin more advanced phenomena. Topics such as wave–particle duality, the quantization of light into discrete photons, and the control of their polarization [5] are central to quantum physics and often present significant conceptual barriers to newcomers [6,7]. These phenomena unfold at the nanometric scale, far beyond the reach of the naked eye, and often defy everyday intuition: photons, for instance, can exhibit both particle-like and wave-like behavior, a duality that challenges our classical understanding of nature [7]. Because they are abstract and not directly observable, such concepts require a high level of abstraction, making their teaching challenging, especially at introductory levels [4,5].

In the context, the use of virtual reality (VR) to represent abstract concepts through virtual simulations can potentially replace physical experiments, which would be costly, complex, or imperceptible to the naked eye [5,8]. Furthermore, it also enables remote access and interaction with content. Thus, building a laboratory that fosters the ability to think at multiple levels of abstraction can help students develop their skills [9,10].

A large-scale study found that learning outcomes after completing tasks in remote labs were as high as or superior to those in inperson labs [11]. This illustrates the potential of implementing VR technologies as a tool to overcome obstacles [12,13]

Received on 10 April 2026; revised 25 June 2026.

Address for correspondence: Rafael Bulcão. Av. Orlando Gomes, 1845 - Piatã, Salvador – BA – Brazil, Zipcode: 41650-010. E-mail: rafael.bulcao@fbter.org.br.

J Bioeng. Tech. Health 2026;9(7):735-740

Corresponding author:

and help expand experiences beyond the classroom, as the use of these resources potentially increases the chance of a positive impact on students and reinforces their use of this tool [14].

This study presents the preliminary development of the designed artifact and the applicability of an immersive laboratory to demonstrate the phenomena of polarization and the principle of light.

Materials and Methods

Design Science Research (DSR) [15] was adopted to combine applicable solutions and the generation of scientific knowledge, highlighting the particular relevance of research in the areas of quantum technologies, immersive technologies, and education, which are relevant domains for the project, through the proposed methodological approach and real-world applications related to the research problems and opportunities. The specific objectives of the study are: (1) develop a functional virtual laboratory focused on teaching quantum technologies; (2) visually design, in a VR environment, the properties of light; (3) implement interactive visualization of the polarization phenomenon in VR; and (4) present an initial digital model of the components that make up the immersive laboratory. To achieve the proposed objectives, the method followed the six DSR stages: (1) problem identification; (2) defining the solution's objectives; (3) model design and development; (4) demonstration of the developed model; (5) model evaluation; and (6) communication of the results to the scientific community and the manufacturing sector. In the first and second stages of the DSR, the problem was identified and the solution's objectives were defined based on an analysis of the research context and the limitations of traditional quantum technologies teaching approaches [6,16].

An exploratory review was conducted to obtain an overview of current knowledge on the development of VR laboratories for quantum technologies. We searched Google Scholar, CAPES, and Scielo databases for works published since 2015 using the keywords: ("Virtual Reality" AND "educational VR laboratory" AND "VR learning" AND "abstract VR learning" AND "quantum light principle" AND "quantum polarization phenomenon"). Of the articles found, we analyzed eight systematic reviews, the results of which will be discussed later.

In the phase that involves the development of the artifact and design applications, we conducted an exploratory focus group with our interdisciplinary team of senior researchers, experts, and students in quantum technologies and immersive technologies

We identified functional and non-functional requirements and success criteria for representing the quantum light and polarization principles in VR [17].

This study combines design strategies and digital tools, such as Blender v4.1, for 3D modeling and importing into Unity Engine for the development of a responsive application.

The proof of concept in a simulated educational environment is part of the phase four of the DSR, where participants explored and interacted with the immersive laboratory of the principles of light and polarization. The phase five of the DSR focused on artifact validation by collecting qualitative and quantitative data through user feedback. The Presence Questionnaire (PQ) was used to assess usability, sense of presence, and user immersion within the immersive environment [18].

The Likert scale also be used as an evaluation method to administer objective questionnaires to assess the proposed learning before and after the immersion. Feedback from interactions with the immersive environments provided by participants be collected and used to improve the development of the laboratory and the quantum technologies teaching process. The sixth stage of the DSR method involved the communication of results obtained from the work.

Results and Discussion

Appropriate, usercentered design requires identifying all considerations and limitations for more assertive guidance and aligning expectations

[19]. In this sense, for the initial development of the artifact, the goal is for the immersive experiment to operate with clear functional execution, a lower-cost proposal that does not negate the role of the physical laboratory, but rather offers a complementary option [20]. One of the objectives outlined for this study is the pursuit of cost reduction compared to a physical laboratory. The costs of acquiring and maintaining traditional experimental equipment are significantly high [20]. In the following sections, we present our findings, as well as the proposed guidelines related to scenarios, equipment, experimental design, and initial construction of the proposed immersive laboratory.

Choice of Technologies

The Unity Engine was chosen for its intuitive extensions that support the development of VR environments [21]. Additionally, applications can be tested directly on headsets or using head-mounted displays (HMDs). It significantly contributes to its robust documentation, simple and fast C# programming, and reduced build size. Compared to other free engines, such as Unreal Engine, Unity Engine is lighter, allowing applications to achieve higher frame rates, which is essential to avoid discomfort when using HMDs in this early prototyping phase [22]. The Meta Quest 3 and 3s headsets stand out as the most affordable available on the market, meeting the demand for a cost-effective solution [23]. Both options support immersive experiences with good performance, positioning themselves as a viable alternative for educational environments, virtual labs, and applications that prioritize cost-effectiveness. Both feature external cameras that allow for real-world environment scanning and the definition of safe zones, allowing users to move freely without the need for resetting when changing locations [24].

Virtual Scenario Planning

The scenario planning stage sought to identify likely interactions between the user and the immersive laboratory so that the simulation would stimulate learning. Digital tools designed for teaching quantum physics Physics Education Technology (PhET) and Quantum Flytrap were tested, analyzed and observations were made about them. PhET is a simulation that allows users to visualize the phenomenon and interact with the experiment in a 2D visual format, aimed at young people who already have prior exposure to quantum physics. Its interface contains a wealth of specific information; there are no step-by-step instructions or a small gamified system for an introductory educational tool [25]. Quantum Flytrap, which also uses 2D visualization, is aimed at younger audiences and researchers. To simplify simulations, the platform uses imaginative symbols to represent optical devices, creating recognizability and a welcoming introduction to quantum physics [26].

The adoption of storyboarding tools serves as a means of narrative illustrations that help sketch out ideas that aim to generate empathy with users in the face of the challenges posed, indicating necessary details even before 3D development [27].

Figure 1 demonstrates the division of three frames into beginning, middle, and end. This results in a structure in which the user begins the experience in the immersive laboratory, its operation and interaction with the environment, and how to end the experience.

Development of the Immersive Environment

The development of the immersive environment for visualizing quantum phenomena was based on the experiment kit used in traditional laboratories for simulation of the BB84 protocol [28]. In the BB84 protocol, laser is fired through a small photon gun, passing through half wave plate (HWP) and then directed at a translucent cube called a polarized beam splitter (PBS), thus directing the light particles toward the photon receivers according to the polarization of photons. In the preliminary environment developed for the proof of concept, photons are represented by red spheres, with eight arrows above them to indicate

Figure 1. Three-act storytelling draft for developing interaction on how to begin and end the experiment.

01 - Home screen to start the experiment

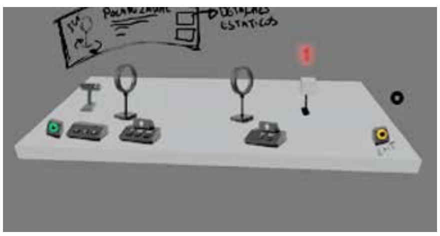

02 - Main area of the polarization experiment

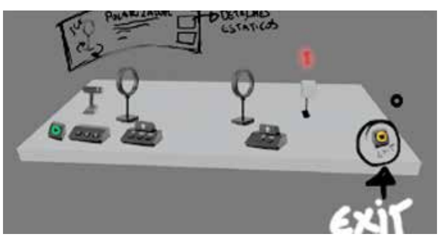

03 - How to end the experiment to return to the home screen

the polarization vectors. A single arrow represents polarization in only one direction, and two arrows represent polarization in two different directions simultaneously. Figure 2 shows the construction of a virtual demonstration. Each component of the experiment is represented in a simplified 3D format to facilitate user interaction and understanding. The emission of a light particle is represented as a sphere moving at a reduced speed compared to a real photon, to facilitate visualization and understanding of its trajectory and quantum behavior.

Also within the VR environment are two HWP's, displayed as circular lenses, which alter the photon's polarization, described by arrows. At the end of the experiment, the polarized light particle passes through the PBS, represented by a transparent cube, thus directing the particle to the quantum gate, indicated as sensors 0

Figure 2. Demonstration of the immersive laboratory with the emission of photons passing through the polarized lenses and directed to port 1 or 0.

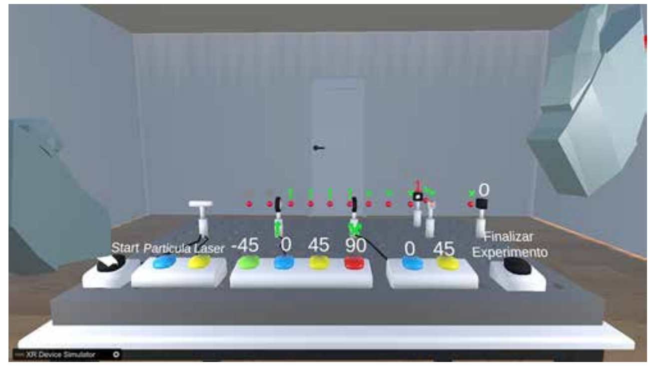

or 1 at the end of the experiment. Positioned on the left, a gray object symbolizes the laser source responsible for emitting a light particle, represented as a sphere.

The buttons on the experiment table serve as different actions for the pieces positioned on the table. The button to launch the laser or particle is labeled START, and the button to pause the experiment and end it is labeled STOP. To select the angle of the polarizing lens, buttons are linked to their respective polarization degrees. The preliminary lab results indicate clear advantages over traditional laboratory setups, revealing a scenario in which sensitive and costly equipment can be preserved from damage due to improper handling, thereby reducing maintenance expenses. By enabling remote interaction with experiments, the platform also offers a scalable model capable of reaching a global audience and broadening access to advanced scientific training. Such accessibility is particularly important in fields like quantum physics, where many foundational concepts are challenging. Quantum phenomena often defy everyday intuition; photons, electrons and other particles can behave both as discrete particles and as waves, a duality famously demonstrated in the double-slit experiment. Incorporating these counterintuitive principles into an interactive, remotely accessible environment not only fosters deeper understanding but also accelerates the dissemination of cuttingedge scientific knowledge.

Conclusion

This work sought to present preliminary results of the proof of concept and the applicability of a laboratory with immersive technologies as an educational tool for demonstrating the quantum phenomena of polarization and the principle of light.

Given the identified frameworks and the findings obtained, it is recommended that questionnaires be administered to professionals for visual and didactic validation of quantum teaching. It will also be necessary to administer the questionnaires to students, with and without prior knowledge of quantum phenomena, aiming to improve and refine the developments.

Research in this area could enhance and expand the use of immersive laboratories for educational purposes and as a complement to traditional laboratories.

Acknowlegement

This work has been fully funded by the project "iNOVATeQ Lato Senso Especialização em Comunicação Quântica - Pesquisador - QIN-FCRH-2024-1-2-1" in supported by QuIIN - Quantum Industrial Innovation, EMBRAPII CIMATEC Competence Center in Quantum Technologies, with financial resources from the PPI IoT/Manufatura 4.0 of the MCTI grant number 053/2023, signed with EMBRAPII. The authors also thank the Bahia State Research Support Foundation (FAPESB) and the National Council for Scientific and Technological Development (CNPQ); IW is a DT-1D productivity grant fellow (308783/2020-4).

References

1. Pirker J, Lesjak I, Guetl C. Maroon VR: a room-scale physics laboratory experience. In: Proceedings of the IEEE Virtual Reality Conference; 2017. p. 482-484.
2. Fox MFJ, Zwickl BM, Lewandowski HJ. Preparing for the quantum revolution: what is the role of higher education? Phys Rev Phys Educ Res. 2020;16:020131.
3. Pirker J, Kopf A, Kainz A, Dengel A, Buchbauer B. The potential of virtual reality for computer science education: engaging students through immersive visualizations. In: IEEE Conference on Virtual Reality and 3D User Interfaces Abstracts and Workshops; 2018.
4. Seskir ZC, Chiofalo M, Case N, Davis N, Decaroli C, Ercan I, et al. Quantum games and interactive tools for quantum technologies outreach and education. Opt Eng. 2022;61:38.
5. Ferreira PHD, Ghiglieno F, Tribuzi V. Atividades experimentais no ensino de óptica: uma nova revisão. Rev Bras Ensino Fís. 2024;46:e2024xxxx.
6. Ribeiro RLO, Figueiredo PS, Winkler I, Miranda MAS. Digital innovation and transformation conceptual model. Rev Ciênc Empres UNIPAR. 2024;24:138-161.
7. Frare VLF, Araujo IS, Veit EA. Uma revisão sistemática da literatura sobre o ensino de computação quântica. Rev Bras Ensino Fís. 2024;46:e20240253.
8. [Reference not provided.]
9. Pirker J, Dengel A. The potential of 360-degree virtual reality videos and real VR for education: a literature review. IEEE Comput Graph Appl. 2021;41(4):76-89.
10. Hu-Au E. Learning abstract chemistry concepts with virtual reality: an experimental study using a VR chemistry lab and molecule simulation. [Internet]. Basel: MDPI.
11. Dori YJ, Belcher J. How does technology-enabled active learning affect undergraduate students' understanding of electromagnetism concepts? J Learn Sci. 2005;14(2):243-279.
12. Chamusca IL, Cai Y, Silva PMC, Ferreira CV, Murari TB, Apolinario AL, et al. Evaluating design guidelines for intuitive, therefore sustainable, virtual reality authoring tools. Sustainability. 2024;16(5):xxxx.
13. Wong JY, Cao Q, Huang L, Xie Y, Winkler I, Cai Y. Evaluations of virtual and augmented reality technology-enhanced learning for higher education. Sustainability [Internet]. Basel: MDPI.
14. Stickdorn M, Schneider J. This is service design thinking: fundamentals, tools, cases. Amsterdam: BIS Publishers; 2010.
15. Lacerda DP, Dresch A, Proença A, Antunes Júnior JAV. Design science research: a research method to production engineering. Gest Prod. 2013;20(4):741-761.
16. Colombo E, Jaén M. Polarização da luz: uma proposta de experiências simples. Cad Catar Ensino Fís.
17. Bailenson JN, Yee N, Blascovich J, Beall AC, Lundblad N, Jin M. The use of immersive virtual reality in the learning sciences: digital transformations of teachers, students, and social context. J Learn Sci. 2008;17(1):102-141.
18. Witmer BG, Singer MJ. Measuring presence in virtual environments: a presence questionnaire. Presence (Camb). 1998;7(3):225-240.

19. Norman DA. The design of everyday things. New York: Basic Books; 1988.
20. Ma J, Nickerson JV. Hands-on, simulated, and remote laboratories: a comparative literature review. ACM Comput Surv. 2006;38(3):7.
21. Linowes J. Unity virtual reality projects. Birmingham: Packt Publishing; 2015.
22. Suwandi G, Khotimah S, Haryanto F, Suprijadi S. Effect of virtual reality video frame rate on visually induced motion sickness through electroencephalography measurement. 2024.
23. Wainwright T. The fight to control the headset market will intensify. Economist. 2023.
24. Meta Platforms Technologies LLC. Meta Quest 3 safety and warranty guide [Internet]. Menlo Park (CA): Meta Platforms Technologies LLC; 2023.
25. Wieman CE, Adams WK, Perkins KK. PhET: simulations that enhance learning. Science. 2008;322(5902):682-683.
26. Migdał P, Jankiewicz K, Grabarz P, Decaroli C, Cochin P. Visualizing quantum mechanics in an interactive simulation: Virtual Lab by Quantum Flytrap. Opt Eng. 2022;61(8):081808.
27. Lupton E. Design is storytelling. New York: Cooper Hewitt, Smithsonian Design Museum; 2017.
28. Thorlabs. Quantum Cryptography Analogy Demonstration Kit [Internet]. Newton (NJ): Thorlabs Inc.

A Critical Review of the Trading of Surplus Renewable Energy in the Context of a Proposal for a Universalization System

Abdon Campos dos Santos[1,3]*, Toni Alex Reis Borges[3,4], Filipe Cardoso Brito[1,3], Hugo Saba[2,3], Aloísio Santos Nascimento Filho[1,3]

[1]SENAI CIMATEC University; [2]Department of Exact and Earth Sciences, State University of Bahia (UNEB); [3]Center for Applied Research and Innovation (NPAI) UNEB/SENAI CIMATEC; Salvador, Bahia; [4]Federal Institute of Bahia; Feira de Santana, Bahia, Brazil

The growing participation of prosumers in the energy matrix has challenged the traditional models of regulation of the Brazilian electricity sector. This article presents a critical review of the current legislation, especially Law 14,300/2022, which regulates distributed micro and minigeneration, allowing credit compensation for the surplus of energy generated, but without enabling its free commercialization in the market. The limitations of the current remuneration model and the legislative proposals under discussion in Brazil are explored, such as Bill 4530/2019 and the sectoral reform planned for 2025–2028. In this context, it is proposed the development of a System for the Universalization of the Commercialization of Renewable Energy Surpluses, which is intended to unify and streamline the management of distributed generation credits, with the possibility of fostering innovation and sustainability in the Brazilian electricity sector.
Keywords: Distributed Generation. Prosumers. Free Energy Market. Unified Renewable Energy System. Energy Regulation.

Electric Power Systems (SEP) are integrated networks that include power plants, substations, transmission lines and consumers, connected to generate, transmit and distribute electricity. Generation takes place in strategically positioned plants: hydroelectric plants take advantage of rivers and lakes, thermal plants are installed in places of easy control, wind power in windy areas, and solar power in regions with high solar radiation. Thus, SEP covers the entire process, from production to the supply of energy to end users [1].

SEP are systems designed to provide quality electricity at the required time, serving from large to small consumers. Its essential requirements include: continuity (uninterrupted supply), compliance (compliance with standards), flexibility (adaptation to change), safety (protection of users) and maintenance (rapid recovery from failures). Its structure is divided into three main stages: generation (conversion of energy into electricity), transmission/distribution (energy transport) and consumption (use in homes, industries, etc.) [1].

Figure 1 illustrates the typical topology of a SEP [2]. Clarifying that, TUST stands for Tariff for the Use of the Transmission System [2]; TUSD is the Tariff for the Use of the Distribution System [2]; Elevator trafo: its purpose is to increase the voltage of the electric energy, ideal for the transmission of electricity over long distances [2]; The step-down trafo has the function of lowering the voltage of the electric energy, making it suitable for general use [2].

As recipients of the production of electricity, there are basically free and captive consumers [3]. Free consumers must have a minimum contracted demand of 2,500 kW to purchase energy from any source, and as of January 2020, this requirement will be reduced to 2,000 kW, according to Ordinance 514/2018 of the Ministry of Mines and Energy [19].

The global trend in the electricity market is to promote competition by allowing consumers to choose their suppliers, while the use of technologies such as smart meters advances to replace data-limited management with real-time energy trading in a liberalized market [2,4].

Received on 20 April 2026; revised 30 June 2026.
Address for correspondence: Abdon Campos dos Santos. Av. Orlando Gomes, 1845, Piatã, Salvador, Bahia, Brazil. Zipcode: 41650-010. E-mail: abdoncampos@gmail.com.

J Bioeng. Tech. Health 2026;9(7):741-747

Figure 1. Typical topology of a SEP: generation, transmission, and distribution.

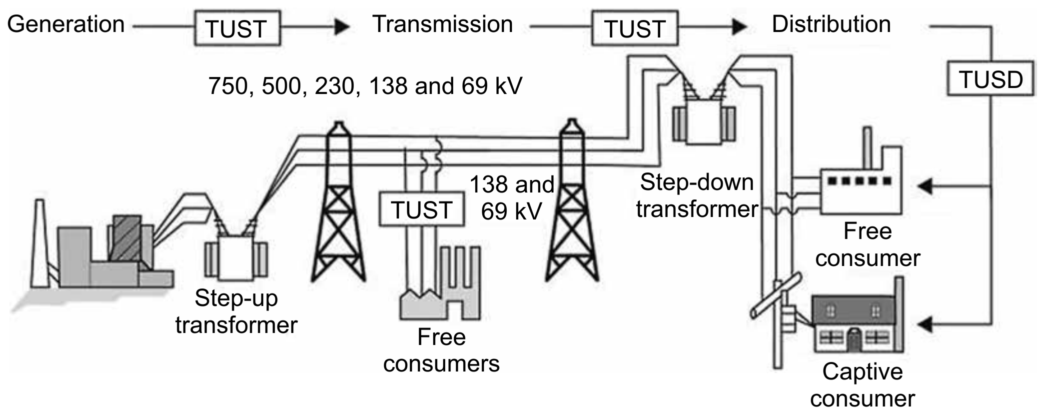

At the same time, the expansion of distributed generation (such as solar panels and wind turbines close to loads, driven by the need to reduce greenhouse gas emissions) is transforming energy flows, which were once unidirectional, into multidirectional, with many consumers starting to produce energy (prosumers, a combination of "producer" and "consumer"), called prosumers [2,4].

This shift replaces the traditional passive role of consumers with an active participation in the electricity system, while localized generation and microgrids open up new business opportunities in the sector [2,4].

The Brazilian legislation that authorizes prosumers to sell the surplus of their production to distributors is Law 14,300, of January 6, 2022, known as the Legal Framework for Distributed Generation [6]. This standard establishes the conditions for the electricity compensation system, allowing consumers who generate energy from renewable sources, such as solar photovoltaics, to inject the surplus into the electricity grid and be compensated for it, through credits or remuneration [5,6].

The legislation defines the criteria for microgenerators (up to 75 kW) and mini-generators (above 75 kW up to 5 MW), in addition to presenting transition rules for those who already operated under the old ANEEL regulation (Normative Resolution 482/2012) [11]. The new law aims to bring greater legal certainty and encourages the expansion of distributed generation in the country [6].

The "Sun Rate" was a popular term used to refer to the collection of the Tariff for the Use of the Distribution System (TUSD) [16] for consumers who have micro and mini-generation systems of electricity [17,18], not being a tax, but a tariff for the use of the infrastructure of the distribution network.

This tariff was instituted by Law 14,300/2022, which establishes the legal framework for distributed generation in Brazil, regulating the Electric Energy Compensation System (SCEE) and allowing renewable energy producers to inject the surplus into the grid and be compensated for it [17,18].

According to the Law, systems with a request for connection to the grid until January 6, 2023 maintain the exemption from charging TUSD Fio B until 2045, while for new installations (as of January 7, 2023), the charge is implemented progressively, starting at 15% in 2023 and reaching 100% from 2029 [18]; the Law also provides for exemptions for shared generation and for low-income consumers registered in social programs [18].

On the other hand, captive consumers can only buy energy in the Regulated Contracting Environment (ACR), being obliged to contract from the local distributor, with tariffs set by Aneel and without the possibility of negotiation, a group that includes all residential consumers, in addition to most commerce, small industries and rural properties [4].

Methodology Review

The methodology was divided into four phases. The first occurred with the bibliographic review of scientific literature in the two main bases for the dissemination of scientific productions (Figure 2). The second phase occurred with the verification of the legislation in force in Brazil, with the purpose of analyzing the current regulatory limits on the subject. The third phase occurred in the examination of the bills, in progress in the Brazilian legislative branch with the purpose of knowing which regulatory proposals orbit the proposed theme. The fourth and last phase consists of critical analysis and proposing an alternative to the problem pointed out.

Literature Review

Regarding the review of scientific productions on the subject, studies were searched in the Web of Science and Scopus databases, and the data were collected on June 5, 2025. Thus, in the query to the Scopus database, 358 records were located, while the Web of Science 103, both submitted to the search terms "energy transition, renewable energy, regulation", using the Boolean operator "and", for the terms contained in the fields "title" and "abstract"", without applying filters. In a total of 461 records, 126 were selected that address the theme proposed in this project, and, therefore, will be the object of further reading to extract relevant points for the research.

Gaps in Scientific Productions

The gap lies in the identification that none of the works directly addresses the design of a unified system, as will be the proposal for a system of universalization of the commercialization of renewable energy surpluses. In this opportunity, it is worth highlighting the identification of 05 (five) productions developed in Brazil (Table 1).

All research data in the scientific databases can be found at the link (https://drive.google.com/drive/folders/1E25l1qM0-FUEM28G1LUXk_s22dMMIJET?usp=sharing).

Figure 2. Flowchart of the bibliographic research.

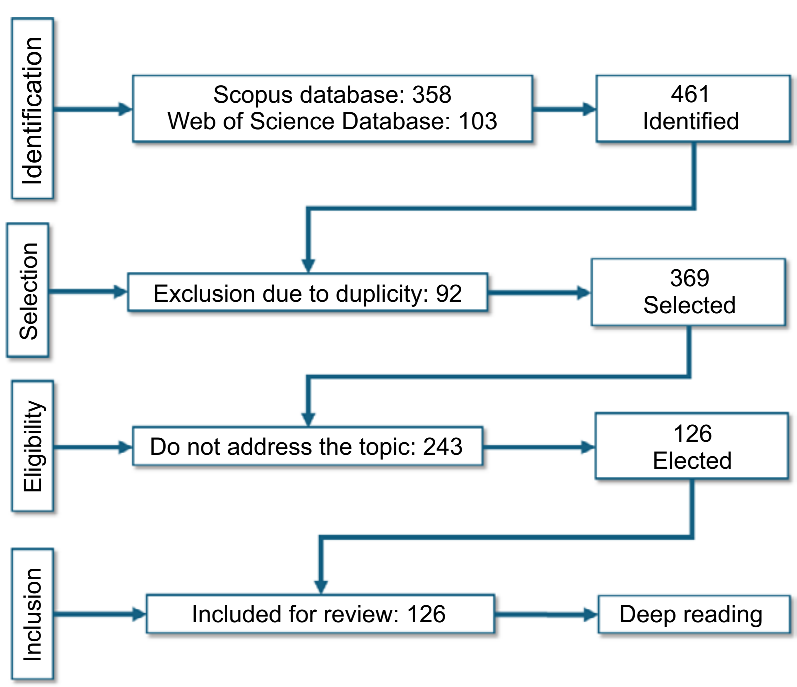

Table 1. Analysis of the approaches with the proposed theme.

Title	Approach Analysis
A Regime Complex and Technological Innovation in Energy System: A Brazilian Experience [11]	It examines the Brazilian experience in the energy transition, focusing on innovation and the evolution of the country's laws and regulations to promote carbon-free growth, which aligns with the context and objectives of a unified system in Brazil.
Amazon energy transition: The need to accelerate emission reduction by the extensive adoption of solar photovoltaics and storage in Brazil [12]	It analyzes the energy transition in Brazil, with a focus on the Amazon, and discusses energy policies and new regulations to promote the adoption of renewable technologies, which directly relates to the national scope of a unified system in Brazil.
Energy transition in Brazil: Is there a role for multilevel governance in a centralized energy regime? [13]	It examines the energy transition in Brazil, addressing multilevel governance in a centralized energy regime and the need to integrate local capacities in the formulation of policies and regulations to promote the transition, which is directly relevant to the context of a unified system.
Impact of the net-metering policies on solar photovoltaic investments for residential scale: A case study in Brazil [14]	It analyzes the impact of Brazilian net-metering rules on investments in residential photovoltaics, which is directly relevant to the Brazilian context of Law 14.300/2022 and the proposal for a unified system in Brazil.
The policy dimension of energy transition: The Brazilian case in promoting renewable energies (2000–2022) [15]	It examines the political dimension of the energy transition in Brazil, analyzing the design and implementation of public policies and the configuration of sectoral governance based on regulations, which is central to the context and objectives of a unified system in Brazil.

<u>Verification of the Legislation in Force in Brazil</u>

The Brazilian legislation in force through Law 14,300/2022 [6], does not allow prosumers (micro and mini-generators) to freely trade their surplus electricity in the market, being restricted to the compensation system with the distributor. However, there are several legislative proposals in progress that aim to expand this possibility, as we can see in Table 2.

<u>Gaps in Current Legislation and Proposals in Brazil</u>

Other proposals, such as PL 189/2021 [8], aim to encourage microgeneration through tax exemptions, but without directly dealing with commercialization in the free market. PL 1709/2022 [9] proposes adjustments to Law 14,300 to increase the collection of charges for new generators, while PL 624/2023 [10] seeks to reduce limitations imposed by distributors on energy injection, especially for the low-income population. In turn, PL 4530/2019 [7], deals with the bilateral commercialization of the surplus for micro and min energy generators, as well as the reform of the energy sector, proposed by Provisional Measure 1,300 of 2025 [20], address the Free Contracting Environment (ACL), but do not address the ideal of a unified system. Thus, a gradual legislative movement is observed that may make it possible, in the near future, for the full integration of prosumers into the free electricity market.

Conclusion

Law 14,300/2022, which establishes the legal framework for distributed microgeneration and minigeneration in Brazil, does not create a free energy market for prosumers in the traditional way. The current model allows participation in the electricity compensation system, in which the surplus generated can be injected into the distributor's network and converted into credits to reduce the consumption of active electricity in other consumer units of the same holder, including at

Table 2. Comparative legislative proposals.

Project	ACL	Target Audience	Other Effects
PL 4530/2019	Yes	Micro (≤ 75 kW) / Mini (≤ 5 MW)	Bilateral trading of surplus
Industry reform (2025–28)	Yes	All voltages (until 2028)	Full ACL opening for low voltage
PL 189/2021	No	Micro up to 100 kW	Exemption from network usage fees
PL 1709/2022	No	New microgenerators	Withdrawal of exemptions and increase of charges
PL 624/2023	No	Low-income consumers	Social stimulus, reduction of technical limitation

another address, or in shared generation systems, such as consortia and cooperatives. valid for up to 60 months.

However, the current model does not authorize the direct sale of the surplus to any entity, nor the use of credits in commercial or financial transactions or forums of the distributor's regulated environment, and participation in the ACL remains restricted to consumers with minimum contracted demand and registration with the Electric Energy Trading Chamber (CCEE).

With regard to the initiatives of bills, we have the highlights for Bill 4530/2019 [7] which proposes to allow generators of up to 5 MW to directly sell their surplus in the ACL, which represents an important advance towards the liberalization of the energy market for small producers. In addition, the reform of the electricity sector planned for 2025–2028, led by the federal government, proposes the opening of the free market to all consumers, including low voltage consumers, by March 2028, which would include homes and small businesses, however they do not provide for the unification of a single system, while the proposal for a unified system would emerge as an alternative to expand the possibilities of commercialization, and not be attached to the local generation distributor.

As normative alternatives, and possible advances, there are discussions about the transformation of energy assets over the surplus of renewable energy generation, and new trading models that could expand the use of credits or allow more flexible transactions, although still without legal support in the current model. Thus, the model provided for in Law 14,300 seeks to encourage distributed generation with regulatory certainty, but without configuring a free market environment for prosumers, as well as the legislative proposals do not make such a forecast, in the same way as scientific productions, especially in Brazil.

In this context of integration of prosumers into the free market of renewable electricity, the proposal of regulatory advances for the development of a unique environment is urgent and necessary. In this scenario, the ideal of the development of the universalization of the commercialization of renewable energy surpluses arises in order to unify the possible regulation of the free market for microgeneration and minigeneration of electricity from renewable sources. Thus, the use of public data, such as ANEEL (National Electric Energy Agency), EPE (Energy Research Company), and IBGE (Brazilian Institute of Geography and Statistics), seeks to model scenarios through modeling and planning technologies, such as MATLAB [21], to be used for modeling, simulation and analysis of renewable energy systems, and PLEXOS [22] to be applied in the optimization of the planning and operation of renewable energy markets. including the integration of renewable sources, with the purpose of demonstrating the thesis of the usefulness of a single model of commercialization of renewable energies.

References

1. Matias J, Leote LPN. Production, transmission and distribution of electricity. 1992.
2. Vasconcelos FM. Generation, transmission and distribution of electricity. Londrina: Editora e Distribuidora Educacional SA; 2017.
3. Brazilian Association of Energy Traders (ABRACEEL). Differences between free and captive consumers [Internet]. Brasília: ABRACEEL. Available from: https://abraceel.com.br/mercado-livre/diferencas-entre-consumidores-livres-e-cativos/
4. Leão R. Lecture notes: generation, transmission, distribution and electric energy. Ceará: Federal University of Ceará; 2009.
5. Cunha LMD, Barbosa Filho J. Comparative analysis of the economic feasibility of the installation of photovoltaic solar energy in family units [Internet]. Ponta Grossa: Atena Editora. Available from:https://atenaeditora.com.br/catalogo/post/analise-comparativa-da-viabilidade-economica-da-instalacao-de-energia-solar-fotovoltaica-em-unidades-familiares. doi:10.22533/at.ed.74119111117.
6. Brazil. Law No. 14,300, of January 6, 2022. Establishes the legal framework for distributed microgeneration and minigeneration, the electricity compensation system, and other provisions. Diário Oficial da União [Internet]. 2022 Jan 7;160(4-A Sect 1):1-6. Available from: https://www.in.gov.br/en/web/dou/-/lei-n-14.300-de-6-de-janeiro-de-2022-373438948
7. Brazil. Chamber of Deputies. Bill No. 4530, of 2019: provides for the commercialization of surplus electricity produced by micro- and minigenerators [Internet]. Brasília: Chamber of Deputies; 2019. Available from: https://www.camara.leg.br/propostas-legislativas/2219642
8. Brazil. Chamber of Deputies. Bill No. 189, of 2021: provides for incentives for microgeneration of electricity from renewable sources [Internet]. Brasília: Chamber of Deputies; 2021. Available from: https://www.camara.leg.br/propostas-legislativas/2260104
9. Brazil. Chamber of Deputies. Bill No. 1709, of 2022: amends Law No. 14,300/2022 to provide for charges applicable to microgeneration [Internet]. Brasília: Chamber of Deputies; 2022. Available from: https://www.camara.leg.br/propostas-legislativas/2304150
10. Brazil. Chamber of Deputies. Bill No. 624, of 2023: prohibits distributors from limiting energy injection from microgeneration systems [Internet]. Brasília: Chamber of Deputies; 2023. Available from: https://www.camara.leg.br/propostas-legislativas/2341094
11. Sharma P. A regime complex and technological innovation in energy systems: a Brazilian experience. In: Energy: crises, challenges and solutions. [Place unknown]: [publisher unknown]; [date unknown].
12. Pereira OS, Reis TM, Rüther R. Amazon energy transition: the need to accelerate emission reduction by the extensive adoption of solar photovoltaics and storage in Brazil. Energy Sustain Dev. 2024;80:101445. doi:10.1016/j.esd.2024.101445.
13. Lázaro LLB, Soares RS, Bermann C, et al. Energy transition in Brazil: is there a role for multilevel governance in a centralized energy regime? Energy Res Soc Sci. 2022;85:102404.Doi:10.1016/j.erss.2021.102404.
14. Leite NH, Guzman Lascano CP, Valente Morais HG, et al. Impact of net-metering policies on solar photovoltaic investments at residential scale: a case study in Brazil. Renew Energy. 2024;231:120788. doi:10.1016/j.renene.2024.120788.
15. Werner D, Lázaro LLB. The policy dimension of energy transition: the Brazilian case in promoting renewable energies, 2000-2022. Energy Policy. 2023;175:113480. doi:10.1016/j.enpol.2023.113480.
16. Brazil. Secretariat of Social Communication. “Sun tax” was instituted in the previous administration [Internet]. Brasília: Federal Government; 2023. Available from: https://www.gov.br/secom/pt-br/fatos/brasil-contra-fake/noticias/2023/08/201ctaxa-do-sol201d-foi-instituida-na-gestao-passada
17. Brazilian Electricity Regulatory Agency (ANEEL). Distributed micro- and minigeneration [Internet]. Brasília: ANEEL. Available from: https://www.gov.br/aneel/pt-br/acesso-a-informacao/perguntas-frequentes/micro-e-minigeracao-distribuida
18. Brazilian Electricity Regulatory Agency (ANEEL). Normative Resolution No. 1,000, of December 7, 2021: establishes the rules for the provision of the public electricity distribution service and repeals ANEEL Normative Resolutions No. 414/2010, No. 470/2011, and No. 901/2020 [Internet]. Brasília: ANEEL; 2021. Available from: https://www2.aneel.gov.br/cedoc/ren20211000.html
19. Brazil. Ministry of Mines and Energy. Ordinance No. 514, of December 27, 2018: regulates article 15, paragraph 3, of Law No. 9,074, of July 7, 1995, to reduce load limits for contracting electricity by consumers. Diário Oficial da União [Internet]. 2018 Dec 28 [Sect 1]. Available from: https://www.gov.br/mme/pt-br/acesso-a-informacao/legislacao/portarias/2018/portaria-n-514-2018.pdf/view
20. Brazil. Provisional Measure No. 1,300, of May 21, 2025: amends legislation concerning the electricity sector, including the Social Tariff, market opening, and cost sharing [Internet]. Brasília: National Congress; 2025. Available from: https://www.congressonacional.leg.br/materias/medidas-provisorias/-/mpv/168719

21. MathWorks. Modeling and simulation: MATLAB and Simulink [Internet]. Natick (MA): MathWorks; [date unknown]. Available from: https://www.mathworks.com/discovery/modeling-and-simulation.html

22. Energy Exemplar. PLEXOS energy modeling software [Internet]. [Place unknown]: Energy Exemplar; [date unknown]. Available from: https://www.energyexemplar.complexos

Production of Cellulose Nanofibrils from Agro-Industrial Residues: Systematic Review and Experimental Design via Glycerol Swelling and Extrusion

Marina R. de Andrade[1], Rodrigo D. O. Polkowski [2], Ana Paula B. Gonçalves[2], Joyce B. Azevedo[3], Rosana Fialho[1]*
[1]Federal University of Bahia, Polytechnic School; [2]TRL9 Lab Testing and Technical Analysis Ltd, Salvador, Bahia; [3]Federal University of Bahia, Institute of Science, Technology and Innovation; Camaçari, Bahia, Brazil

This study presents the systematic review and analysis of scientific articles on cellulose nanofibril (CNF) production from vegetable fibers, with a focus on environmentally friendly methods. The research followed the PRISMA protocol, selecting works that addressed complete extraction processes starting from vegetal fibers and reporting parameters such as length-to-diameter ratio (L/D), crystallinity, and yield of CNFs. Based on the bibliographic findings, a process flowchart and an experimental design were developed for CNF extraction from peach palm sheath, combining glycerol swelling, single-screw extrusion, and dilute acid hydrolysis (0.4–0.6% H_2SO_4). The choice of this route was based on its potential to promote controlled mechanical shear after glycerol plasticization, facilitating the opening of the cell wall and selective removal of amorphous regions while preserving crystallinity. The proposed methodology, supported by literature evidence, offers a technically feasible and sustainable approach for the valorization of agro-industrial residues, with potential for scaling up to pilot and industrial levels.
Keywords: Cellulose nanofibrils. Glycerol swelling. Single-screw extrusion. PRISMA protocol. Agro-industrial residues.

Nanotechnology has consolidated itself as a strategic field with applications in sectors such as healthcare, electronics, energy, composites, and packaging. In 2024, the global market was estimated at USD 14.56 billion, with projections to reach USD 227.54 billion by 2032, reflecting a compound annual growth rate (CAGR) of 41% [1]. This expansion is driven by the integration of advanced technologies into production processes and the development of innovative materials, although it still faces challenges such as high production costs, specific regulations, and communication barriers with the end consumer. In the nanocellulose segment, the global market reached USD 700 million in 2024 and is expected to reach USD 4.6 billion by 2034, with a CAGR of 20.6%, highlighting its potential as a sustainable, high-performance material applied in areas ranging from packaging to engineering composites. Europe maintains its leadership in production and R&D, while the Asia-Pacific region stands out for its rapid growth, favored by abundant raw materials and qualified labor [2].

Scientific progress follows this trend: in 2024, more than 256,000 articles on nanotechnology were indexed in the Web of Science, representing a 4% increase compared to 2023. In the field of patents, the European Patent Office received 199,264 applications in 2024, maintaining the previous year's level, with 2,934 of these related to nanotechnology, accounting for approximately 29% of the total. These indicators reinforce the relevance and competitiveness of the sector, as well as the need for technically efficient and economically viable production processes [3-5]. Among the most prominent materials, cellulose — an abundant polymer from renewable plant sources — offers great versatility. When processed at the nanoscale, it gives rise to cellulose nanofibrils (CNF), cellulose nanocrystals (NCC), or bacterial nanocellulose (BNC). CNF and NCC, of plant origin, can be obtained through chemical, mechanical, enzymatic, or combined routes, generally preceded by pretreatments to remove hemicellulose, lignin, and other constituents, thereby increasing fiber accessibility [6-7].

Received on 25 April 2026; revised 22 May 2026.
Address for correspondence: Felipe Pinto Oliveira. Federal University of Bahia; Rua Prof. Aristides Novis, 02, Federação. Salvador – BA – Brazil, Zipcode: 41650-010. E-mail: Rosana Fialho.

J Bioeng. Tech. Health 2025;9(7):748-754

Mechanical methods apply shear forces to delaminate the cell wall, while chemical methods promote surface modifications and selective removal of amorphous regions, releasing crystalline structures. The choice of the nanocellulose extraction method, associated with parameters such as time, temperature, concentration, and processing intensity, directly affects the yield, morphological properties, and cost of the nanomaterial [8-9]. In this context, the application of statistical tools is essential to quantify the effect of these variables and identify optimal combinations. Analyses such as ANOVA, Tukey's test, and response surface modeling (RSM) allow group comparisons, evaluation of interactions, and process optimization based on indicators such as yield, aspect ratio, crystallinity, and homogeneity.

This study will use the PRISMA method to select articles presenting quantitative data on yield and cellulose nanofibril quality, correlating them with total production time and cost. Based on this systematic approach and statistical data analysis, at least three extraction methods will be identified that stand out in mechanical strength, cost-effectiveness, and lower environmental impact, providing insights for future research and industrial applications.

Materials and Methods

The systematic review was conducted according to the PRISMA protocol (Preferred Reporting Items for Systematic Reviews and Meta-Analyses) [10], with the aim of identifying studies that described the process of obtaining cellulose nanofibrils from plant fibers, using chemical and/or mechanical methods, and that presented quantitative results related to the morphology, crystallinity, and yield of the nanomaterial.

The searches were carried out between 2021 and 2025 in four databases: Scopus, Web of Science, MDPI, and Engineering Village, restricted to articles published in English. Two distinct search strategies were employed, maintaining as common descriptors the terms "cellulose nanofibrils" and "methods," while varying the other parameters according to the research objective:

- Search 1 (Figure 1): "Cellulose nanofibrils AND Width AND Length AND Methods" — aimed at obtaining data on width, length, and aspect ratio.
- Search 2 (Figure2): "Cellulose nanofibrils AND Yield AND Methods"

— aimed at obtaining yield data.

In both strategies, after the initial identification, a screening stage was carried out, excluding review articles, duplicate articles, studies that did not address nanofibrils, and publications outside the scope or with insufficient information (classified as "others").

In the eligibility stage, the remaining articles were evaluated according to the following criteria: (i) effective production of nanofibrils, (ii) use of diluted acid hydrolysis, (iii) application of an environmentally friendly method, and (iv) use of plant fiber as raw material.

Finally, in the inclusion stage, only studies presenting at least one of the predefined results of interest for each search were considered:

- For Search 1: results for the L/D ratio of nanofibrils and crystallinity values.
- For Search 2: yield and crystallinity results.

This process resulted in the final inclusion of 11 articles for Search 1 (Figure 1) and 16 articles for Search 2 (Figure 2). These studies formed the analytical basis of the present research, serving as references for comparing and discussing the most efficient methods for obtaining cellulose nanofibrils.

Results and Discussion

The aspect ratio (length-to-diameter ratio) is an essential parameter for characterizing cellulose nanofibrils (CNF), as it directly influences their mechanical and viscous properties. High aspect ratios confer greater surface area and enable more

Figure 1. Methodological flowchart based on the PRISMA protocol considering "length" and "width" as keywords for the selection of articles that presented these data related to the developed nanofibrils.

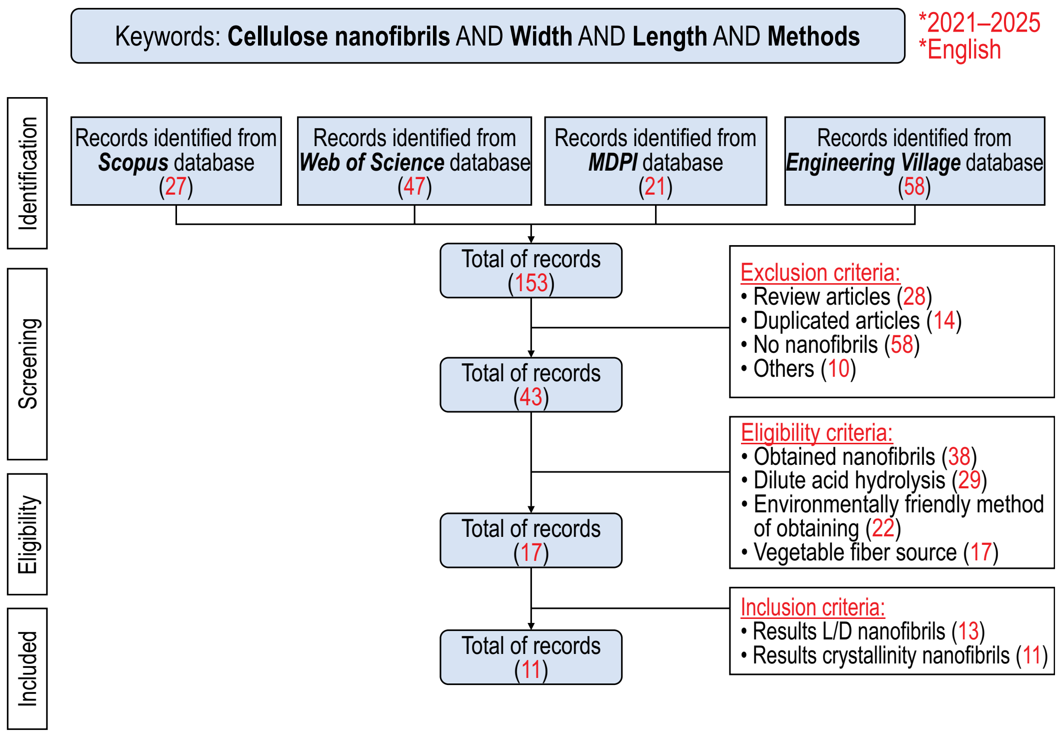

Figure 2. Methodological flowchart based on the PRISMA protocol considering "yield" as a keyword for the selection of articles that presented this data related to the developed nanofibrils.

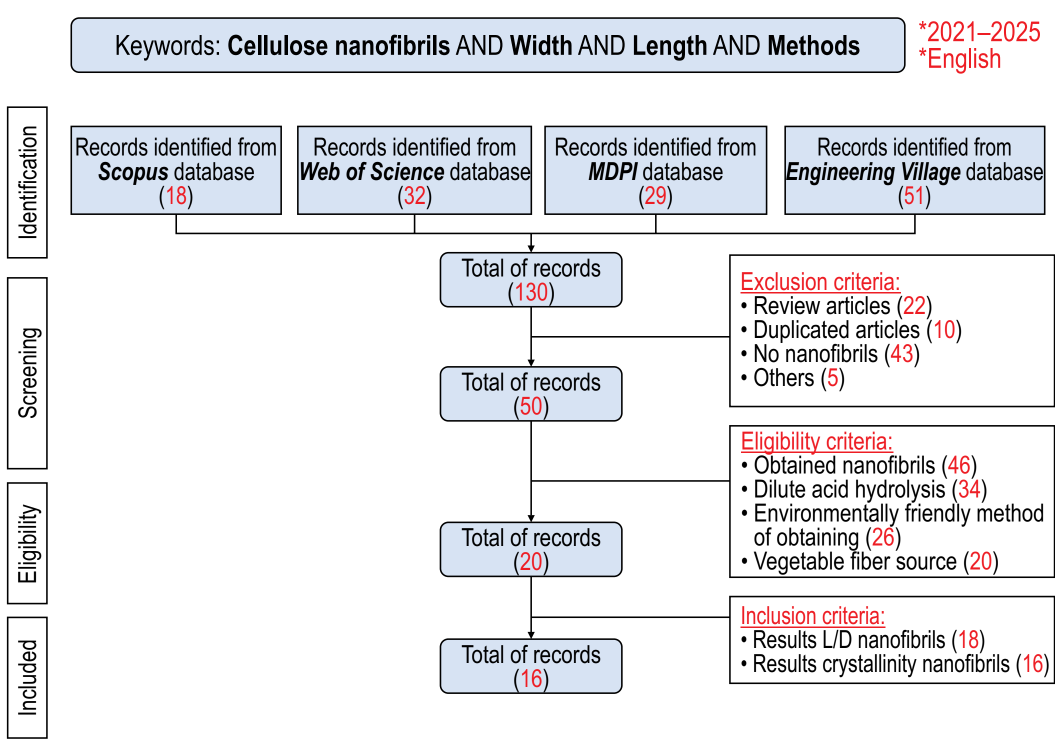

efficient load transfer in composite materials, while also promoting intermolecular interactions such as hydrogen bonding and Van der Waals forces, which are fundamental for rheological behavior and the formation of structured networks. Techniques such as AFM and TEM provide precise measurements of this ratio.

Well-established methods for obtaining CNFs include TEMPO-mediated oxidation, which introduces anionic carboxylate groups onto the fibril surface, resulting in highly stable and well-defined dispersions. Studies such as Lorevice and colleagues (2023) [11] demonstrated the production of nanofibrils with diameters between 1.2 and 2.0 nm in just three and a half hours, combining TEMPO oxidation with microfluidization—an efficient but chemically demanding method. Alternatively, deep eutectic solvents (DES), such as a mixture of choline chloride and lactic acid, have emerged as a sustainable route, offering excellent cellulose solubilization when coupled with mechanical fibrillation. Xu and colleagues (2023) [12] reported nanofibrils with an average thickness of 8.8 nm in about four hours, highlighting the potential of this approach for greener processing. However, what truly stands out in the context of the present investigation is the method combining single-screw extrusion with glycerol swelling followed by dilute acid hydrolysis. This protocol enables the production of nanofibrils in reduced time, without the need for expensive reagents or highly complex processes. As demonstrated by Lu and colleagues (2022) [13], glycerol acts as a pre-treatment agent by penetrating the cell walls and reducing interfibrillar cohesion, thereby facilitating physical delamination during extrusion. The subsequent hydrolysis, carried out with sulfuric acid at concentrations of 0.15–0.6%, selectively removes amorphous regions without significantly compromising crystallinity, resulting in nanofibrils with diameters between 20 and 60 nm and yields ranging from 62 to 75%, with total processing times of approximately 3.5–4 hours.

The work of Zhang and colleagues (2022) [14] further reinforces the applicability of this strategy by developing lignocellulosic nanofibril (LCNF) composites with polylactic acid (PLA) for use as 3D-printable filaments. In this study, single-screw extrusion not only promoted mechanical fibrillation after the prior glycerol swelling of fibers but also preserved part of the internal lignin, which contributed to improved interfacial compatibility with the polymeric matrix and enhanced mechanical performance of the composite. The presence of residual lignin provided additional strength, greater thermal stability, and rheological properties suitable for 3D printing, without compromising PLA processability. These results indicate that single-screw extrusion, when properly tuned for parameters such as L/D ratio, temperature, and screw speed, can simultaneously promote structural fiber opening and optimize integration with biodegradable polymers, adding value to the produced nanomaterial.

In comparison, methods such as TEMPO-mediated oxidation and DES processing offer advantages in terms of chemical functionalization and achieving highly stable dispersions but require specific reagents and additional purification steps. In contrast, extrusion with glycerol, particularly in bench-scale single-screw configurations (L/D $\approx$ 10.3), stands out as a simpler, lower-cost route, significantly reducing the use of aggressive chemicals while enabling the valorization of low-value lignocellulosic sources. This makes the process especially attractive for large-scale applications and the development of sustainable products, such as structural composites, barrier films, and filaments for 3D printing.

Justification and Structuring of the Experimental Process

The selection of the single-screw extrusion method as the central stage of the pre-treatment was based on its ability to promote controlled mechanical shear in fibers previously swollen in glycerol, facilitating the opening of the cellular structure and exposing the amorphous regions of the plant cell wall to the subsequent action of dilute acid hydrolysis. This process offers relevant advantages for lignocellulosic fibers with high structural rigidity, such as the outer sheaths of peach palm, as it combines operational simplicity, low cost, and reduced energy consumption compared to high-energy mechanical fibrillation methods such as high-pressure homogenization and disc milling. In addition, single-screw extrusion provides greater tolerance to raw material particle size variability, reducing the need for strict sieving and enhancing its applicability at pilot and industrial scales.

The methodological design was structured based on the studies by Zhang and colleagues (2022) and Lu and colleagues (2022), adapted to the available conditions and equipment, aiming at the production of cellulose nanofibrils from agro-industrial residues. The choice of glycerol swelling as a pre-treatment is grounded in its ability to penetrate cell walls, plasticize amorphous regions, and reduce the rigidity of the lignocellulosic matrix, thereby increasing internal accessibility to subsequent chemical attack. Combined with the moderate shear of single-screw extrusion (L/D ≈ 10.3), this process enhances the action of dilute acid hydrolysis (0.4–0.6% H_2SO_4), enabling the selective depolymerization of amorphous regions with minimal degradation of crystalline portions.

The methodology (Figure 3) was organized into sequential and integrated steps: selection and preparation of peach palm outer sheaths, discarding degraded samples; cutting into 3–5 cm fragments; drying and milling to the target particle size; glycerol swelling; single-screw extrusion according to parameters defined in the experimental plan; dilute acid hydrolysis under controlled conditions; neutralization; mechanical defibrillation using an Ultra-Turrax; centrifugation for phase separation; and freeze-drying to obtain the dry nanofibrils.

The experimental design was developed according to a 2^3 factorial arrangement, without replication at the central point, to evaluate the combined influence of critical parameters in three process stages: (i) swelling – variation of screw rotation speed (15–35 rpm) and number of passes (1–3), with assessment of swelling degree; (ii) acid hydrolysis – variation of temperature (80–100 °C), time (60–90 min), and acid concentration (0.4–0.6%), with crystallinity analysis by XRD; (iii) mechanical defibrillation – variation of speed (14,000–18,000 rpm) and residence time (10–20 min), with colloidal and structural characterization by zeta potential, DLS, TEM, XRD, TG, and DSC.

Figure 3. Simplified methodological flowchart of the nanofibril production process.

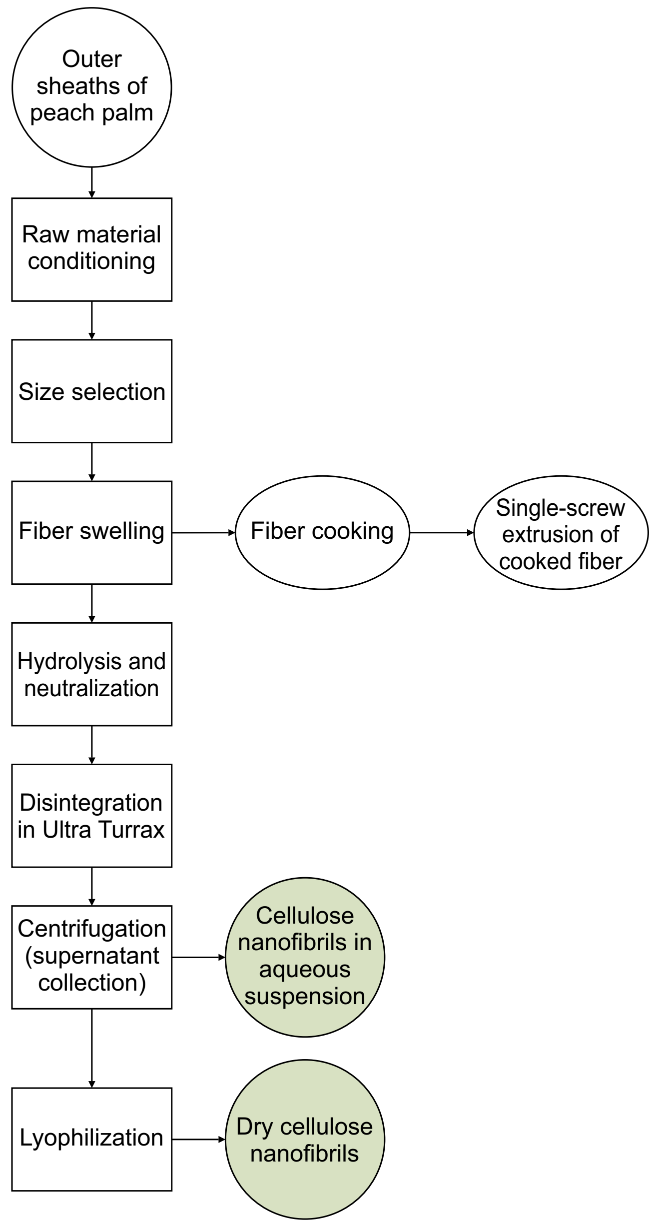

This approach, built from the literature and systematized in the experimental flowchart, does not yet aim to present results, but rather establishes a solid methodological basis for the future evaluation of the effect of operational conditions on the physicochemical and structural properties of nanofibrils. The proposed process remains aligned with sustainability principles, reducing the use of aggressive reagents, utilizing agro-industrial residues, and prioritizing low energy consumption, which favors its feasibility in industrial scale-up contexts.

Conclusion

From the application of the PRISMA protocol, articles were selected that provided the technical–scientific basis for defining the parameters and stages of the proposed method. The systematic screening allowed the identification of gaps and opportunities in the routes for obtaining cellulose nanofibrils, with emphasis on processes employing glycerol swelling, single-screw extrusion, and dilute acid hydrolysis as a combined strategy for physicochemical pretreatment and controlled delamination.

Based on a thorough analysis of the eligible studies, a process flowchart and an experimental design were developed to evaluate critical variables, covering steps from fiber preparation and granulometric selection to hydrolysis and final product recovery. The choice of single-screw extrusion, preceded by glycerol swelling, was supported not only by its operational simplicity and pilot-scale feasibility, but also by bibliographic evidence indicating its potential to plasticize the cell wall, increase the exposure of amorphous regions, and reduce the demand for energy and aggressive reagents.

The designed framework provides a solid basis for future trials, in which it will be possible to correlate operational conditions with crystallographic parameters obtained by XRD, enabling process optimization from a sustainable perspective and in line with the valorization of agro-industrial residues. The integration between the systematic review conducted under the PRISMA protocol and the experimental design ensures that the selected route is not only technically grounded but also supported by quantitative and qualitative evidence, reinforcing its scientific relevance and industrial applicability.

Acknowledgement

The authors thank the Federal University of Bahia (UFBA) for academic, institutional, and infrastructure support, and TRL9 LAB for providing the technical resources essential for carrying out this study.

References

1. Data Bridge Market Research. Global nanotechnology market size, share, and trends analysis report: industry overview and forecast to 2032 [Internet]. Pune: Data Bridge Market Research; 2024.
2. Market.US News. Nanocellulose market estimated CAGR of 20.6% through 2034 [Internet]. New York: Market.US; 2025 Jun 20.
3. StatNano. Top 10 countries by nanotechnology publications in 2024 [Internet]. Tehran: StatNano; 2025 Mar 16.
4. European Patent Office. Patent Index 2024 [Internet]. Munich: European Patent Office; 2025.
5. StatNano. Top 10 countries by EPO nanotechnology patents in 2024 [Internet]. Tehran: StatNano; 2025 Mar 16.
6. Phanthong P, Reubroycharoen P, Hao X, Xu G, Abudula A, Guan G. Nanocellulose: extraction and application. Carbon Resour Convers. 2018;1(1):32-43.
7. Rambaran T, Schirhagl R. Nanotechnology from lab to industry: a look at current trends. Nanoscale Adv. 2022;4(15):3238-3252.
8. Chirayil CJ, Mathew L, Thomas S. Review of recent research in nanocellulose preparation from different lignocellulosic fibers. Carbohydr Polym. 2014;112:337-349.
9. Czaikoski A. Estudo do comportamento reológico de nanofibras de celulose obtidas por diferentes métodos [dissertation]. Campinas: Universidade Estadual de Campinas; 2017.
10. Shamseer L, Moher D, Clarke M, Ghersi D, Liberati A, Petticrew M, et al. Preferred reporting items for systematic review and meta-analysis protocols (PRISMA-P) 2015: elaboration and explanation. BMJ. 2015;349:g7647.

11. Lorevice MV, Pinheiro IF, Silva E, Pereira FV, Barud HS. Designing 3D fractal morphology of eco-friendly nanocellulose-based composite aerogels for water remediation. Chem Eng J. 2023;462:142254.
12. Xu Y, Song X, Xie H, Yang G, Chen L, Huang L. Complete valorization of bamboo biomass into multifunctional nanomaterials by reactive deep eutectic solvent pretreatment: toward a waste-free biorefinery. Chem Eng J. 2023;462:142284.
13. Lu H, Hu Y, Yang X, Chen C, Zhao J, Chen W, et al. Screw extrusion pretreatment for high-yield lignocellulose nanofibrils (LCNF) production from wood biomass and non-wood biomass. Carbohydr Polym. 2022;277:118868.
14. Zhang Q, Wu X, Sun Y, Shi Z, Cheng Y. Lignocellulose nanofiber/polylactic acid (LCNF/PLA) composite with internal lignin for enhanced performance as a 3D-printable filament. Ind Crops Prod. 2022;178:114569.

Review of the Main Parameters for the Development of Antifouling Supports

Jamile de Melo Carvalho[1]*, Lilian Lefol Nani Guarieiro[2]
[1] SENAI CIMATEC University, Oil and Gas, Salvador, Bahia, Brazil
SENAI CIMATEC University; Salvador, Bahia, Brazil

Marine biofouling is the process by which organisms such as barnacles, mollusks, algae, and corals attach themselves to submerged surfaces, compromising the performance of structures such as ship hulls, sensors, and pipes. This accumulation increases hydrodynamic resistance, raises fuel consumption, and favors the spread of invasive species. To mitigate these effects, anti-fouling coatings began to be used, initially formulated with highly toxic biocides such as tributyltin (TBT) and triphenyltin (TPT). However, due to the prolonged environmental impacts of these compounds, their use was banned. Given this scenario, alternatives based on natural compounds, polymers, bio-inspired surfaces, and nanoparticles have emerged. This study aimed to conduct a systematic review of the literature to identify the main parameters involved in the development of anti-fouling coatings applied in marine environments. The search was conducted in the ScienceDirect, Scopus, Web of Science, PubMed, and SciELO databases, using the keyword "antifouling," with no time restriction. Approaches regarding material types, physicochemical properties, evaluation methods, and technical gaps were analyzed. VOSviewer software was used to map trends through keyword analysis. The results indicated a significant growth in publications from 2020 onwards, with contributions from China, the United States, and Brazil standing out. The review identified technological approaches, as well as testing standards that seek to ensure effectiveness, durability, and environmental safety. Despite advances, challenges such as field validation and the long-term durability of coatings remain significant obstacles.
Keywords: Marine Biofouling. Antifouling. Coating, Biocides.

Marine biofouling is a natural process in which organisms such as barnacles, mollusks, corals, mussels, and algae attach themselves to submerged surfaces, such as ship hulls, industrial structures, filtration membranes, and sensors, compromising their performance and integrity [1].

The accumulation of these organisms increases hydrodynamic resistance, raises fuel consumption, and intensifies carbon emissions, in addition to favoring the spread of invasive species [2]. In structures such as pipes and sensors, biofouling reduces efficiency, increases maintenance frequency, and shortens the useful life of surfaces [3]. Conventional anti-fouling coatings have made extensive use of highly toxic biocides, such as tributyltin (TBT), widely recognized as the most effective compound ever developed for this purpose. However, its serious environmental impacts, including toxicity to marine organisms, led to its total ban in 2008 by the International Maritime Organization (IMO] [4]. Considering the environmental damage associated with the use of toxic compounds in anti-fouling coatings, it is essential to develop solutions that are truly non-toxic and environmentally safe. To achieve this goal, it is essential to adopt multidisciplinary approaches that integrate knowledge of chemistry and physics, whose interactions contribute to the development of more effective anti-fouling strategies. The objective of this study was to conduct a systematic review of the literature focusing on the main parameters involved in the development of anti-fouling supports with low environmental impact applied to marine environments. The study sought to identify technological trends, characteristics of the materials used, and challenges faced, based on the analysis of scientific publications and keyword mapping performed with VOSviewer software.

Received on 17 April 2026; revised 15 May 2026.
Address for correspondence: Jamile de Melo Carvalho. Av. Orlando Gomes, 1845 - Piatã, Salvador – BA – Brazil, Zipcode: 41650-010. E-mail: jamile.carvalho@fbter.org.br.

J Bioeng. Tech. Health 2026;9(7):755-761

Materials and Methods

A systematic review of the literature was conducted to identify and analyze the main scientific advances in the development of antifouling coatings applicable to marine environments. Searches were performed on ScienceDirect, Scopus, Web of Science, PubMed, and SciELO platforms using the descriptor "antifouling" without time restrictions, with the aim of providing a comprehensive and up-to-date overview of the topic. Specific criteria were applied to refine the results: there was no language restriction, and only complete scientific articles with an experimental approach were considered. In addition, priority was given to studies available in open access and presenting technical data, such as type of material, physical-chemical and mechanical properties, exposure time, evaluation methods, and performance results under laboratory and/or field conditions. After the initial screening, 32 articles met the selection criteria and were included in the detailed analysis. The final choice was based on a qualitative analysis, considering the main technical highlights, such as the parameters evaluated and the experimental methods used. The evaluation of the data extracted from the articles was conducted with the support of Microsoft Excel, used for data organization and analysis, and VOSviewer, used for keyword mapping from the Web of Science database, which allowed conceptual connections between studies and the detection of recent advances related to the development of approaches that minimize environmental damage in the control of biofouling.

Results and Discussion

The analysis was qualitative in nature and resulted in the selection of 32 articles. Figure 1 shows the temporal evolution of publications on anti-fouling coatings, based on the analysis of the selected scientific articles. There was limited production between 2010 and 2020, with few papers published during this period, marked by initial approaches focused on natural extracts [5–7]. From 2021 onwards, there has been a steady stream of academic production, driven by the search for alternatives to conventional biocides and the advancement of analytical tools, such as X-ray fluorescence spectroscopy (XRF) [8] and computational modeling applied to coating performance [1]. Research has focused on superhydrophobic surfaces [9,10], bio-inspired coatings [11,12], with emphasis on the use of functional nanoparticles and the development of biocides with low environmental impact [13–16], in addition to previous studies focused on conventional systems with controlled release of metal ions, especially copper-based ones [8].

Figure 1. Annual distribution of scientific publications on antifouling coatings.

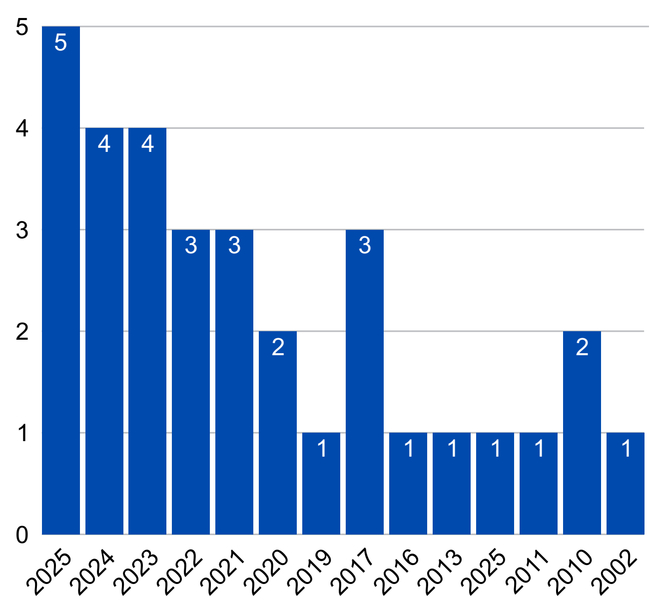

Currently, there is a continuous growth in the number of publications, reflecting the increase in interest and scientific production, with an emphasis on innovative biomaterials and nanotechnological approaches [17,18]. Recent trends point to the consolidation of technologies such as zwitterionic polymers [19,20] and multifunctional nanostructures [21], in addition to the growing demand for long-term studies and comprehensive ecological assessments of new anti-fouling materials.

The mapping of scientific production by country, shown in Figure 2, highlights China's leadership, especially in studies involving nanomaterials (such as cuprous oxide and silica) and surface modification techniques, such as controlled roughness [10,15,17]. Europe is represented by Italy, which stands out in the development of advanced polymers [22], while Sweden focuses its efforts on analytical methods and reducing environmental impacts [14]. Despite its vast marine biodiversity, Brazil still invests little in research aimed at developing non-toxic anti-fouling agents. This is still an innovative area in the country, with few research groups dedicated to the topic [5–7]. In terms of technological trends, Asian countries such as China, Korea, and Japan lead in the synthesis of new materials, while Europe and the United States prioritize practical applications, such as the use of sensors and field tests [12]. It is worth noting that in three articles, it was not possible to identify the country of origin of the research.

Figure 2. Countries with the highest scientific output on antifouling coatings.

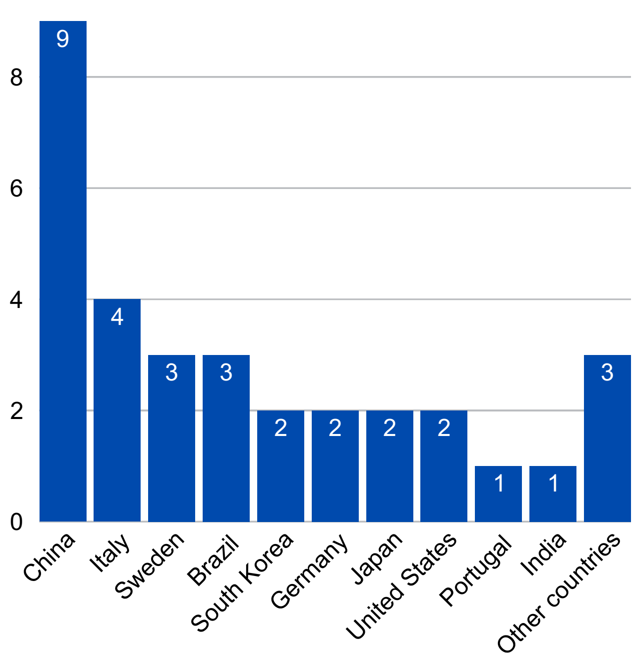

The analysis of the most frequent keywords in the articles, presented in Figure 3, reinforces the predominant focus on the terms “antifouling” and “biofouling,” which are the most frequent in research on antifouling coatings, reflecting the central focus of the area. Technological approaches such as nanoparticles [15,16], superhydrophobic surfaces [9,10], and controlled release [18] also stand out, indicating a trend toward effective solutions with low environmental impact. Terms such as “field tests” and “non-toxic biocides” [5,23,24,33], although less frequently cited, point to important gaps in practical validation and environmental safety. Figure 3 shows a transition from traditional methods to innovative and bio-inspired strategies.

The systematic review was expanded with the use of keyword mapping through VOSviewer, using 5,647 records from Web of Science with the word “antifouling” in the title.

In Figure 4, the graph shows four main clusters. The first, represented by the color green, focuses on studies related to coating technologies and the performance of materials applied to

Figure 3. Most frequent keywords in studies on antifouling coatings.

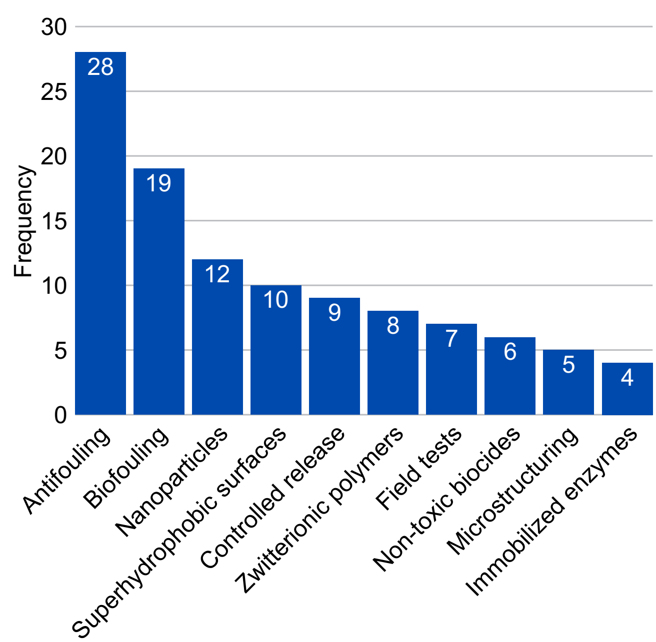

marine environments, highlighting terms such as "antifouling coating," "fouling release coatings," and "performance." The red cluster brings together research on colonization mechanisms and the challenges caused by biofouling, with an emphasis on keywords such as "biofouling," "adhesion," "settlement," and "toxicity." The blue cluster addresses investigations into interactions at the molecular level, including terms such as "surfaces," "protein adsorption," and "poly (ethylene glycol)." The yellow cluster integrates works that explore chemical composition, protein behavior, and material behavior in improving antifouling performance. The term "adhesion" stood out as the link between the biological and innovation areas in coatings, while "nanoparticles" presented more limited connections, indicating potential gaps to be explored. Overall, the results show that, although there have been significant advances in the practical effectiveness of antifouling agents, there is still a need for innovation to address biofouling.

Table 1 highlights the advancement and complexity of anti-fouling technologies, showing a critical balance between effectiveness and environmental responsibility. Biocidal coatings [8,14–16] remain effective but raise concerns about ecotoxicity. Alternatively, solutions based on natural bioactives [7,9,24,25] offer lower environmental impact but have reduced durability. Physical technologies, such as superhydrophobic [9,10,12] and micro/nanotextured [17,26,27] surfaces, stand out for their durability and absence of toxic compounds, making them particularly suitable for offshore structures that are difficult to maintain.

However, Table 1 also highlights the lack of standardization in validation criteria. The variation in testing methods, ranging from field tests [5,28] to projections based on laboratory data [26], makes it difficult to compare the results obtained between different technologies. In this context, hybrid systems [13,18,20] stand out for integrating different mechanisms (physical, chemical, biological), achieving synergy in

Figure 4. Keyword mapping in VOSviewer, highlighting four main clusters.

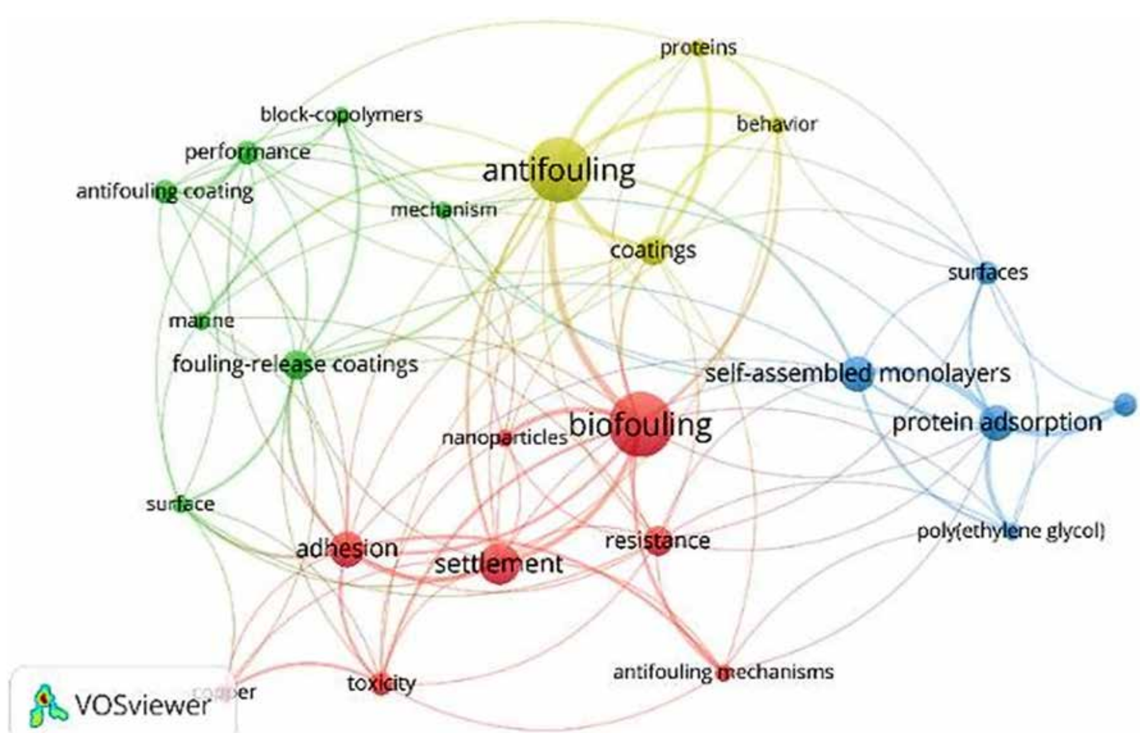

Table 1. Comparison of the main antifouling coatings in terms of mechanism of action, durability, removal, and applications.

Type	Mechanism of Action	Shelf Life	Removal	Applications	References
Biocides	Controlled release of toxic ions (Cu, Zn) or organic compounds (capsaicin).	1–5 years (depending on release rate) .	Natural degradation or mechanical cleaning.	Ship hulls, port structures	[8,13–16]
Physical (Micro/ Nanotextured)	Creation of rough/irregular surfaces to reduce larval adhesion.	2–10 years (high durability).	Abrasion resistant.	Marine sensors, pipes.	[17,26, 27,29]
Hydrophobic	Reduced wettability to hinder organism attachment.	1–3 years (limited by chemical degradation).	Cleaning with water jets or solvents.	Submerged equipment, aquaculture.	[9,10,21
Superhydrophobic	Combines extreme hydrophobicity and microstructures (contact angle >150°). and microstructures (contact angle >150°).	3–8 years (high resistance).	Self-cleaning (lotus effect).	Offshore wind energy, aquatic drones.	[9,10,12]
Polymers (Zwitterionic/ Hydrogels)	Neutral surface charge and hydration to repel biofilms.	6 months–2 years (renewable).	Degradation or recoating.	Membranes, medical implants.	[19–22,30]
Natural Bioactive Compounds	Release of extracts/ enzymes that inhibit larval settlement.	6 months–3 years (depending on stability).	Biodegradation.	Marine protected areas, sustainable aquaculture.	[5,7,22, 24,31]
Hybrids	Combines multiple mechanisms (e.g., biocide + texture).	2–7 years (synergy).	Varies depending on components.	Critical applications (petroleum, defense).	[13,18,20]

performance, durability, and functionality. The analysis reinforces that future developments should prioritize technologies with lower environmental impact, greater durability, and standardized validation, with hybrid systems emerging as a promising solution for critical environments, such as offshore platforms and oil industry structures.

Table 2 presents the main technical parameters of antifouling coatings, highlighting criteria such as thickness, adhesion, durability, environmental resistance, and effectiveness.Thin coatings, such as PDMS [27], are ideal for sensors, while thick coatings, such as thermoplastics [26], are suitable for robust structures. Hydrogels and zwitterionic polymers [19–21, 30] showed good adhesion, and durability ranged from 6 months to 10 years, with textured surfaces standing out [27]. In terms of environmental resistance, coatings with amorphous Fe [11] and PDMS [10] stood out, while materials such as capsaicin [18] showed lower stability. Antifouling efficacy was high on superhydrophobic surfaces [9], PDMS [10], chitosan [17], and enzymes [22]. Challenges remain, such as the lack of standardization of tests and the scarcity of long-term validations. Recommended solutions include combined methodologies, such as XRF with bioassays [14], as well as hybrid criteria.

Conclusion

Marine biofouling represents a significant technical and environmental challenge, especially

Table 2. Technical parameters and validation methods for anti-fouling coatings.

Parameter	Range/Description	Validation Methods	Representative Articles (No.)
Thickness	20–500 µm	Profilometry	[10,17,19,21, 26,27,30]
		Electron microscopy	
Adhesion	Zwitterionic polymers/ hydrog els: Excellent	Lab: ASTM D3359 (cross-cut), pull-off	[9,10,19–21, 26,30]
	Hydrophobic surfaces: Average	Field: Exposure to waves/currents	
Durability	6 months–10 years	Lab: Accelerated aging (UV saline)	[10,12,14, 26–28]
		Field: Monitoring (6–24 months)	
UV/Saltwater Resistance	High: PDMS, Amorphous Fe	Lab: UV/Saline Chambers (ASTM G154)	[10,11,13,19, 22,30]
	Medium/Low: Hydrogels, enzymes	Field: Exposure in coastal areas	
Antifouling efficacy	70–99% inhibition	Lab: Bioassays (larvae/biofilms)	[1,13,14,17, 22,24,28,32]
		Field: Natural colonization (6–12 months)	
Combined Methods	XRF + ecotoxicology	Example: XRF laboratory + field	[1,8,14,27]
	Microstructuring + bioassays		

in submerged structures, where it compromises functional performance, increases operating costs, and exacerbates ecological impacts. The systematic review carried out allowed us to map the main advances in the development of anti-fouling coatings with less environmental impact.

There has been a significant shift from the use of toxic biocides to bio-inspired solutions, driven by the negative impacts of conventional substances, such as toxicity to non-target organisms, bioaccumulation, and ecological imbalance in the marine environment. The analysis of the tables showed technological diversity, with emphasis on superhydrophobic surfaces, zwitterionic polymers, hydrogels, and hybrid systems, which have shown promise due to their high anti-fouling effectiveness. However, important challenges remain, such as the absence of standardized evaluation protocols, the scarcity of long-term studies, and the production limitations of some emerging technologies.

References

1. She W, Wang H, Linardi D, Chik SY, Lan Y, Chen F, et al. Mode of action of antifouling compound albofungin in inhibiting barnacle larval settlement. iScience. 2023;26(7):106981.
2. Morgan RN, Al Ali A, Alshahrani MY, Aboshanab KM. New insights on biological activities, chemical compositions, and classifications of marine actinomycetes antifouling agents. Microorganisms. 2023;11(10):2444.
3. Wang J, Li L, Wu Y, Liu Y. Design and application of antifouling bio-coatings. Polymers (Basel). 2025;17(6):793.
4. Cognetti G, Maltagliati F, Pretti C. Antifouling coatings and ecological control in marinas. Mar Pollut Bull. 2012;64(2):175-176.
5. Pereira RC, Carvalho AGV, Gama BAP, Coutinho R. Field experimental evaluation of secondary metabolites

from marine invertebrates as antifoulants. Braz J Biol. 2002;62(2):311-320.

6. Cuadrado-Silva CT, Castellanos-Hernández L, Osorno-Reyes OE, Ramos Rodríguez FA, Duque Beltrán C, Puyana-Hegedus M. Estudio químico y evaluación de la actividad antifouling del octocoral caribeño *Eunicea laciniata*. Quim Nova. 2010;33(3):656-661.
7. Ribeiro SM, Rogers R, Rubem AC, Muricy G, Pereira RC. Antifouling activity of twelve demosponges from Brazil. Braz J Biol. 2013;73(3):501-506.
8. Lagerström M, Ytreberg E. Quantification of Cu and Zn in antifouling paint films by XRF. Talanta. 2021;223:121820.
9. Bae S, Lee YJ, Kim MK, Kwak Y, Choi CH, Kim DG. Antifouling effects of superhydrophobic coating on sessile marine invertebrates. Int J Environ Res Public Health. 2022;19(13):7973.
10. He Z, Yang X, Mu L, Wang N, Lan X. A versatile "3M" methodology to obtain superhydrophobic PDMS-based materials for antifouling applications. Front Bioeng Biotechnol. 2022;10:998852.
11. Li Y, Zhang LY, Zhang C, Zhang ZR, Liu L. Bioinspired antifouling Fe-based amorphous coating via killing-resisting dual surface modifications. Sci Rep. 2022;12(1):1-10.
12. Doyle C, Ahmed M. Antifouling coatings inspired by biological templates. Macromol Rapid Commun. 2025;46(12):2400932.
13. Alfieri ML, Gonçalves C, Almeida JR, Correia-da-Silva M, Panzella L, Napolitano A. Sulfated phenolic polymers as non-toxic antifouling agents. Eur Polym J. 2024;208:112855.
14. Lagerström M, Butschle M, Larsson AI, Cachot J, Dam-Johansen K, Schackmann M, et al. Investigation of critical copper release rates for dose optimization of antifouling coatings. Prog Org Coat. 2025;198:108928.
15. Shi WZ, Liang YS, Lu B, Chen M, Li Y, Yang Z. Cuprous oxide nanoparticles: preparation and evaluation of antifouling activity. Quim Nova. 2019;42(6):638-641.
16. Tadros HRZ, Hamdona SK, El-Saharty AA, Moawad MN. Antifouling painting formulations containing green synthesized copper oxide nanoparticles using water extract of *Ulva fasciata*. Egypt J Aquat Res. 2023;49(1):17-22.
17. Yu D, Zhao X, Amores AP, Wang Y, Dutta J, Yang JL, et al. Chitosan coatings with modulated surface roughness for the inhibition of marine macrofouling. Int J Biol Macromol. 2025;316:144713.
18. Feng K, Li S, AlMasoud N, Li J, Ma Y, Yin C, et al. Nature-inspired silicone-polythiourethane coatings based on capsaicin analogue for marine biofouling control. Chem Eng J. 2025;518:164362.
19. Wu C, Zheng J, Hu J. Novel antifouling polysulfone matrix membrane modified with zwitterionic polymer. J Saudi Chem Soc. 2021;25(8):101281.
20. Murali S, Agirre A, Arrizabalaga J, Rafaniello I, Schäfer T, Tomovska R. Zwitterionic stabilized water-borne polymer colloids for antifouling coatings. React Funct Polym. 2024;196:105843.
21. Li G, Shang L, Li D, Huang Y, Long S, Li X. Construction of silane-modified polyampholyte hydrogel coatings for multi-scale antibiofouling. Polym Test. 2025;148:108844.
22. Zanoni M, Habimana O, Amadio J, Casey E. Antifouling activity of enzyme-functionalized silica nanobeads. Biotechnol Bioeng. 2016;113(3):501-512.
23. Magin CM, Cooper SP, Brennan AB. Non-toxic antifouling strategies. Mater Today. 2010;13(4):36-44.
24. Antifouling activity of marine bacterial extracts: a non-toxic alternative as biocide. Rev Biol Mar Oceanogr [Internet]. Available from: https://revistas.uv.cl/index.php/rbmo/article/view/4456
25. Almeida JR, Correia-da-Silva M, Sousa E, Antunes J, Pinto M, Vasconcelos V, et al. Antifouling potential of nature-inspired sulfated compounds. Sci Rep. 2017;7:42424.
26. Bus T, Dale ML, Reynolds KJ, Bastiaansen CWM. Thermoplastic, rubber-like marine antifouling coatings with micro-structures via mechanical embossing. Biofouling. 2020;36(2):138-145.
27. Cholkar A, McCann R, Perumal G, Chatterjee S, Swayne M, Kinahan D, et al. Advances in laser-based surface texturing for developing antifouling surfaces: a comprehensive review. Appl Surf Sci Adv. 2023;18:100513.
28. Bloecher N, Solvang T, Floerl O. Efficacy testing of novel antifouling systems for marine sensors. Ocean Eng. 2021;240:109983.
29. Richards C, Slaimi A, O'Connor NE, Barrett A, Kwiatkowska S, Regan F. Bio-inspired surface texture modification as a viable feature of future aquatic antifouling strategies: a review. Int J Mol Sci. 2020;21(14):5063.
30. Murosaki T, Ahmed N, Gong JP. Antifouling properties of hydrogels. Sci Technol Adv Mater. 2011;12(6):064706.
31. Soliman YAA, Brahim AM, Moustafa AH, Hamed MAF. Antifouling evaluation of extracts from Red Sea soft corals against primary biofilm and biofouling. Asian Pac J Trop Biomed. 2017;7(11):991-997.
32. Chen JD, Yi RZ, Sun CL, Feng DQ, Lin YM. Antifouling activity of simple synthetic diterpenoids against larvae of the barnacle *Balanus albicostatus* Pilsbry. Molecules. 2010;15(11):8072-8081.

Application of Machine Learning Techniques in the Optimization of Produced Water Treatment: A Literature Review

Diogo Souza Neiva Cardoso[1],*, Kleberson Ricardo de Oliveira Pereira[1], George Simonelli[1], Luiz Carlos Lobato dos Santos[1]

[1]*Oil, Gas, and Biofuels Research Group, Postgraduate Program of Chemical Engineering, Federal University of Bahia; Salvador, Bahia, Brazil*

The increasing complexity and variability of operational and physicochemical conditions in produced water treatment within the oil and gas industry require advanced computational solutions capable of managing multivariate data and modeling nonlinear behaviors. In this context, machine learning (ML) techniques have emerged as powerful tools for predicting critical parameters, optimizing treatment processes, and supporting decision-making. This study presents a critical review of publications from 2015 to 2025, focusing on the application of ML in the optimization of produced water treatment. The literature search was conducted in the Scopus database using specific descriptors and Boolean operators, and resulted in 81 selected studies. The number of publications has grown significantly since 2020, with the United States, China, Canada, and Brazil leading the research effort. The predominant techniques include artificial neural networks (ANNs), support vector machines (SVM), and ensemble models such as Random Forest and XGBoost, which showed high predictive accuracy ($R^2 > 0.90$ in most studies). Key input variables included operational parameters, ionic composition, and historical production data. Reported outcomes include improved removal efficiency, scale control, and operational cost reduction of up to 30%. Despite advances, limitations remain regarding overfitting risks, lack of long-term validation, and model interpretability. Overall, the findings suggest that ML techniques represent a promising approach to enhance produced water treatment, enabling more efficient, adaptable, and economically viable industrial applications.

Keywords: Process Optimization. Oil Industry. Artificial Neural Networks. Random Forest. XGBoost.

Produced water (PW) stands out as one of the major environmental and operational challenges faced by the oil industry, due to its large volumes and the variable composition of contaminants such as oils, greases, salts, suspended solids, and dissolved organic compounds [1-3]. This heterogeneous composition complicates the stable operation of treatment systems and undermines the predictability of key performance indicators, such as oil removal efficiency, chemical oxygen demand (COD), and turbidity [2,3].

Traditional modeling methods, based on empirical correlations, linear regressions, or classical statistical models, show significant limitations in handling multivariate processes and nonlinear behaviors, which are characteristic of real PW treatment systems. Although useful for understanding general trends, these approaches struggle to capture the complex interactions among variables that frequently occur in industrial operations subject to fluctuations in flow rate, composition, and operational conditions over time [3-5].

In this context, machine learning techniques have emerged as promising tools to overcome these limitations by enabling the modeling of complex nonlinear relationships, identifying the most influential variables, and optimizing operational parameters. Models such as artificial neural networks (ANNs), support vector machines (SVMs), decision trees, and ensemble methods, including Random Forest and XGBoost, have been applied to predict the removal efficiency of specific contaminants, adjust chemical dosing, and reduce energy consumption [3,6]. By offering

Received on 12 April 2026; revised 22 May 2026.
Address for correspondence: Diogo Souza Neiva Cardoso. Oil, Gas, and Biofuels Research Laboratory (PGBio), Postgraduate Program in Chemical Engineering (PPEQ), Federal University of Bahia (UFBA). Rua Prof. Aristides Novis, 2, Federação, Salvador, BA, Brazil. Zipcode: 40210-630. E-mail: dsncardoso.eq@gmail.com.

J Bioeng. Tech. Health 2026;9(7):762-769

higher predictive accuracy and adaptability to different operational scenarios, these techniques directly contribute to improving treatment system efficiency, ensuring compliance with environmental standards, and optimizing costs within the industrial context of produced water [1,5]. The adoption of such approaches has intensified in recent years, reflecting a global trend toward integrating computational intelligence into complex environmental processes.

Accordingly, this review study aims to critically assess the application of machine learning techniques in optimizing produced water treatment, highlighting the types of models employed, the most common input and output variables, the reported performance metrics, and the main limitations identified in the literature.

Materials and Methods

This literature review was conducted in a critical and interpretative manner, aiming to analyze the use of machine learning techniques in the modeling and optimization of produced water (PW) treatment processes. The search was carried out in the Scopus database using descriptors combined with Boolean operators: ("produced water" OR "oilfield produced water" OR "petroleum wastewater") AND ("machine learning" OR "artificial neural networks" OR "ANN" OR "support vector machine" OR "decision trees" OR "random forest" OR "XGBoost" OR "deep learning") AND ("treatment" OR "removal" OR "prediction" OR "optimization"). The bibliographic survey covered the period from January 2015 to July 2025, prioritizing articles published in indexed journals that presented practical applications or quantitative results related to PW treatment.

The choice of the Scopus database is justified by its status as one of the leading references for researchers worldwide, as well as its extensive collection of relevant studies on the topic. Scopus was also used to generate the bibliometric overview. From this database, indicators such as the annual volume of publications, geographic distribution by country/territory, and types of documents published during the selected period were collected and analyzed.

Studies applying various machine learning models, including artificial neural networks (ANNs), support vector machines (SVMs), and ensemble methods (Random Forest, XGBoost), were selected, focusing on predicting contaminant removal efficiency, optimizing operational parameters, or reducing costs and energy consumption. For each article, information was extracted regarding the type of model, input and output variables, performance metrics, such as the coefficient of determination (R^2), root mean square error (RMSE), and mean absolute percentage error (MAPE), as well as the main findings reported by the authors. The collected data were systematized in a spreadsheet and organized into a comparative table, enabling a descriptive and exploratory analysis of the most used algorithms, studied variables, and obtained results. Figure 1 illustrates the methodological procedure employed in this study.

Results and Discussion

Evolution and Profile of Publications

The evolution of publications related to the application of machine learning in produced water treatment is presented in Figure 2. Data extracted from the Scopus database totaled 81 publications.

A gradual increase is observed until 2022, followed by a more pronounced rise between 2023 and 2024, with the upward trend continuing into 2025, considering that the data were collected up to July of this year. This recent growth may be attributed to greater accessibility of ML tools, advancements in algorithms, and the growing interest in process automation and sustainability in treatment systems. Figure 3 shows the geographic distribution of the published studies.

The United States leads in the number of studies, reflecting its prominent role in adopting

Figure 1. Methodological procedure used to conduct this study.

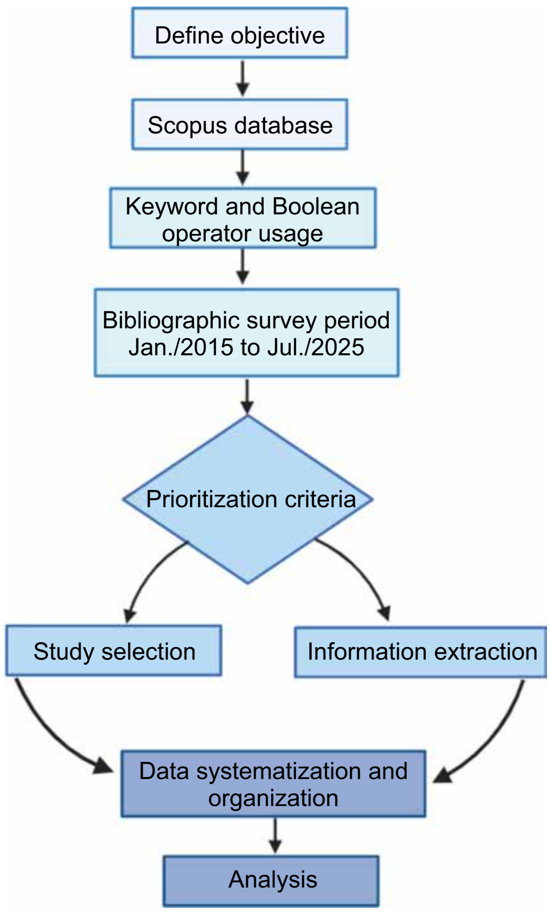

emerging technologies within the oil industry and environmental management. Following are Canada and China, as well as Middle Eastern countries (Saudi Arabia and Iran), where high volumes of produced water are generated due to oil exploration. Brazil holds an intermediate position with five publications, indicating growing interest in optimization solutions for produced water treatment. Other countries such as Egypt, India, Malaysia, and Nigeria show targeted initiatives that underscore the global reach of the topic and its potential application across diverse production contexts.

Regarding document types (Figure 4), journal articles predominate (60.5%), followed by conference papers (32.1%). This distribution reflects the consolidation of the topic within the scientific literature and the growing interest of the academic community in both applied studies and exploratory approaches.

Additionally, reviews, book chapters, and conference reviews appear in smaller proportions but play a strategic role in the systematization of knowledge, particularly in establishing conceptual frameworks, identifying research gaps, and proposing future research directions. The combination of these different types of

Figure 2. Publications per year.

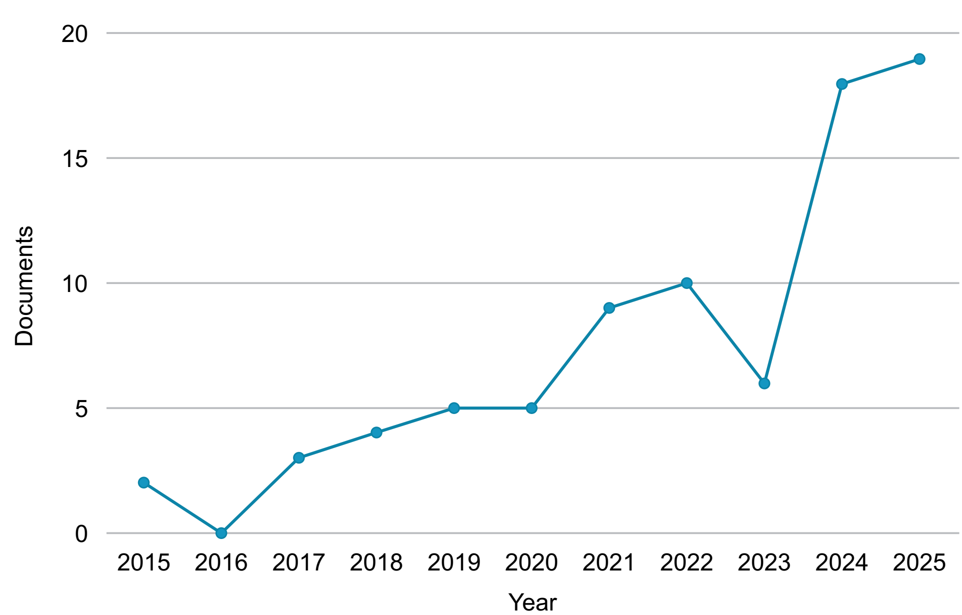

Figure 3. Publications by country/territory.

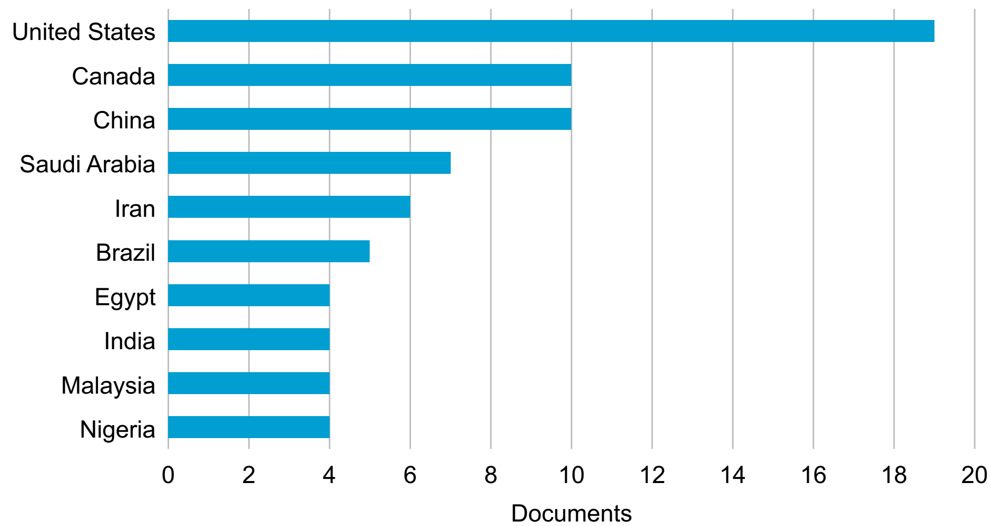

Figure 4. Types of published documents.

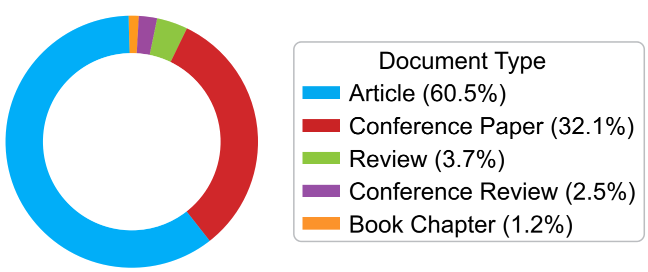

publications reflects an expanding field, marked by solid advances and, at the same time, openness to further investigation.

Machine Learning Techniques in the Optimization of Produced Water Treatment

Recently, machine learning techniques have gained prominence in the oil and energy sectors, particularly due to their ability to handle complex data and support the optimization of industrial processes [4,11]. In produced water (PW) treatment, this progress is reflected in a growing number of studies applying predictive models to enhance operational efficiency, reduce costs, and comply with increasingly stringent environmental regulations [6,13].

The choice of the most appropriate technique is closely linked to the nature of the problem, the availability and quality of the data, and the specific objectives of each application. This methodological diversity reflects the scientific community's effort to balance accuracy, interpretability, and industrial applicability [6,10,13]. When properly trained and validated, such models exhibit strong potential to anticipate critical behaviors and support decision-making, even under operational fluctuations and uncertainties [10,11].

Table 1 presents these studies, detailing the types of machine learning models employed, input and output variables, reported performance, and their respective reference.

The findings of this study highlight diverse applications of machine learning (ML) techniques in produced water treatment, encompassing artificial neural networks (ANNs), support vector machines (SVMs), ensemble algorithms (Random Forest, XGBoost), and classical statistical models such as ARIMA. The most common input variables included operational parameters (temperature, flow rate, pressure), ionic composition (Ca^{2+}, Mg^{2+}, Ba^{2+}, Sr^{2+}, Cl^{-}, SO_4^{2-}, etc.), physicochemical characteristics (salinity, oil content, suspended solids, COD), and, in some cases, geological data or historical production records. Some datasets were obtained from laboratory experiments or pilot plants, while other studies, such as Wang et al. [9] and Jiang and colleagues [12], utilized field time

Table 1. Studies employing machine learning in the optimization of produced water treatment.

Machine Learning	Main Objective	Input Variables	Output Variables	Performance (R^2 / MAPE)	Ref.
MLR, RF, XGBoost	Predict scale formation	Concentrations of Ca^{2+},Mg^{2+}, Ba^{2+}, Sr^{2+}, SO_4^{2-}, HCO_3^-, CO_3^{2-}, Cl^-, temperature, and pH	Scaling index	XGBoost: R^2=0.95	[7]
SVM, RF, XGBoost, etc. (8 models)	Predict desalination efficiency	Salt concentration, TDS, pH, temperature, pressure	Removal efficiency (%)	SVM: R^2=0.98	[8]
ANN	Predict oil growth rate	Daily processing capacity, oil content, polymer concentration, suspended solids	Oil growth rate	ANN: R^2≈0.83–0.91	[9]
ANN, XGBoost	Optimize membrane treatment	Temperature, flow rate, shear rate, pressure	Transmembrane pressure (TMP) and total resistance	ANN: R^2=0.95 XGBoost: R^2=0.97	[10]
Linear regression, KNN, ANN	Improve efficiency and reliability of filtration systems	Droplet radius, time, shear rate	Lift force, TMP, resistance	Lift force: R^2>0.99 TMP (KNN): R^2=0.90	[11]
RFR, ARIMA	Predict produced water volume and quality	Well age, production rate, location, geological data	Produced water volume	RFR: R^2>0.80; ARIMA: MAPE≈5.5%	[12]
ANN	Optimize treatment costs	Pressure, salt concentration, temperature, production rate	Cost, removal efficiency, coagulant dosage, etc.	Qualitative analysis	[13]
ANN, RSM	Optimize turbidity removal	Dosage, temperature, time	Removal efficiency (%)	ANN: R^2=0.99 RSM: R^2=0.99	[14]
ANN	Model biological polishing unit	Temperature, pH, COD, suspended solids	Effluent COD	ANN: R^2=0.84	[15]
ANN	Predict ion rejection in membranes	pH, pressure, flow rate	Ion rejection (%): Cl^-, Na^+, Mg^{2+}, Ca^{2+}	ANN: R^2>0.95	[16]

ANN (Artificial Neural Network); MLP (Multilayer Perceptron); SVM (Support Vector Machine); RF (Random Forest); XGBoost (Extreme Gradient Boosting); RFR (Random Forest Regression); ARIMA (AutoRegressive Integrated Moving Average); RSM (Response Surface Methodology) RMSE (Root Mean Square Error); MAPE (Mean Absolute Percentage Error)/ MLR (Multiple Linear Regression.

series data. Output variables primarily focused on predicting contaminant removal efficiency, ion rejection, oil growth rate, operational costs, and produced water volume. The ML models demonstrated robust performance, frequently achieving R^2 values above 0.90 with low error metrics (RMSE, MAPE).

Among the highlighted examples, different machine learning techniques were applied to specific and complex challenges in produced water treatment, always involving multiple correlated variables and nonlinear behavior. Tayyebi and colleagues [7] modeled scale formation based on ion concentrations (Ca^{2+}, Mg^{2+}, Ba^{2+}, Sr^{2+}, SO_4^{2-}, HCO_3^-, CO_3^{2-}, Cl^-), temperature, and pH, achieving an R^2 of 0.95 with XGBoost, which stood out for its ability to capture complex interactions among geochemical variables; however, the authors noted the need for constant calibration due to variations in water composition over time. Nallakukkala and colleagues [8] reached an R^2 of 0.98 using SVM to predict desalination efficiency via gas hydrates, highlighting the technique's capability to model nonlinear relationships between operational variables such as TDS, pH, temperature, and pressure; nevertheless, they acknowledged limitations related to the scarcity of experimental data at an industrial scale. Additionally, Wang et al. [9], predicting oil growth rate in settling tanks using ANN, reported R^2 values ranging from 0.83 to 0.91 but emphasized dependence on fragmented historical data and the risk of overfitting. Saddiqi et al. [10] demonstrated that ANNs and XGBoost achieved high R^2 values (0.95–0.97) when modeling transmembrane pressure and total resistance in membrane processes, while Saddiqi and colleagues [11] extended the modeling to hydrodynamic variables such as lift force, droplet radius, and shear rate, achieving $R^2 > 0.99$. These results reinforced the critical role of hydrodynamic variables in reducing fouling. Ezemagu and colleagues [14] showed that ANNs outperformed the response surface methodology (RSM) in predicting turbidity removal efficiency ($R^2 = 0.99$ versus 0.97), demonstrating a greater ability to model nonlinear relationships.

Nair and colleagues [16] combined ANNs with physicochemical models (Spiegler-Kedem and SHP) to predict ion rejection by nanofiltration, achieving R^2 values above 0.95; however, they cautioned about the need for long-term testing to assess fouling. Meanwhile, Aisyah and colleagues [15] applied ANN to model a biological polishing unit, obtaining an R^2 of 0.84. Although satisfactory, the study highlighted the model's sensitivity to variations in operational conditions and the difficulty of representing complex biological processes using traditional mathematical models.

Jiang and colleagues [12] explored different techniques: Random Forest Regression (RFR), an ensemble tree-based method, achieved an R^2 greater than 0.80, while the classical statistical model ARIMA reached a mean absolute percentage error (MAPE) of approximately 5.5% in forecasting time series of produced water volume and quality. This combination illustrates how different methods can be complementary, depending on the nature of the data. On the other hand, Taloba [13] presented a qualitative analysis indicating that ANNs can optimize energy consumption and reduce operational costs (up to 25% less energy and 30% lower costs). Although these gains are promising, the author emphasizes that industrial application requires broader experimental validation.

Thus, it is observed that multilayer perceptron (MLP) architectures of ANNs, combined with ensemble algorithms such as XGBoost and Random Forest Regression (RFR), predominate due to their ability to capture complex nonlinear relationships and handle multiple variables. Nonetheless, challenges remain: the risk of overfitting with limited datasets [2,11,17], the need for field validation, and improved model interpretability, which are fundamental aspects to enable large-scale applications.

Collectively, these studies demonstrate that by considering different types of variables and employing techniques suited to each case, the use of machine learning significantly enhances the ability to anticipate critical process behaviors, overcome the limitations of traditional models, and support operational decision-making in complex industrial scenarios. Therefore, the results suggest that applying machine learning to optimize produced water treatment offers gains in predictive accuracy, operational efficiency, and cost reduction provided it is supported by comprehensive datasets, long-term testing, and appropriate validation strategies.

Conclusion

This literature review addresses recent advances in the use of machine learning techniques to enhance produced water treatment processes. The following conclusions are drawn:

- There has been a marked increase in publications in recent years, indicating growing global interest in computational solutions applied to produced water management in the oil industry;
- Machine learning techniques overcome limitations of traditional statistical models by effectively modeling nonlinear and multivariate relationships typical of treatment processes;
- Artificial neural networks (ANNs), combined with ensemble algorithms such as XGBoost and Random Forest Regression (RFR), demonstrate higher predictive accuracy, with R^2 values exceeding 0.90 in most analyzed cases;
- The incorporation of operational, physicochemical, and historical production data enhances the ability to anticipate critical process behaviors and support decision-making in complex industrial scenarios;
- The reviewed studies demonstrate applications such as prediction of scale formation, estimation of contaminant removal efficiency, analysis of operational costs, and prediction of ion rejection in membranes, highlighting machine learning's role as a powerful tool for monitoring and optimizing produced water treatment.

Acknowledgment

The authors gratefully acknowledge the financial support from the Human Resources Program of the National Agency of Petroleum, Natural Gas and Biofuels (PRH/ANP – PRH36/UFBA), funded through investments by qualified oil companies under the R&D Clause of ANP Resolution No. 50/2015, as well as the National Council for Scientific and Technological Development (CNPq). In addition, this study was financed in part by the Coordenação de Aperfeiçoamento de Pessoal de Nível Superior - Brasil (CAPES) - Finance Code 001.

References

1. Abdelhamid C, Latrach A, Rabiei M, Venugopal K. Produced water treatment technologies: a review. Energies. 2025;18(1):63.
2. Al-Ajmi F, Al-Marri M, Almomani F, AlNouss A. A comprehensive review of advanced treatment technologies for the enhanced reuse of produced water. Water. 2024;16(22):3306.
3. Amakiri KT, Canon AR, Molinari M, Angelis-Dimakis A. Review of oilfield produced water treatment technologies. Chemosphere. 2022;298:134064.
4. Alardhi SM, Jabbar NM, Breig SJM, Hadi AA, Salman AD, Saedi LMA, et al. Artificial neural network and response surface methodology for modeling oil content in produced water from an Iraqi oil field. Water Pract Technol. 2024;19(8):3330-3349.
5. Chaal RE, Aboutafail MO. A comparative study of back-propagation algorithms: Levenberg-Marquardt and BFGS for the formation of multilayer neural networks for estimation of fluoride. Commun Math Biol Neurosci. 2022:1-17.
6. Ibrahim M, Haider A, Lim JW, Mainali B, Aslam M, Kumar M, et al. Artificial neural network modeling for the prediction, estimation, and treatment of diverse wastewaters: a comprehensive review and future perspective. Chemosphere. 2024;362:142860.
7. Tayyebi A, Alshami A, Tayyebi E, Owoade A, Talukder M, Ismail N, et al. Machine learning-based prediction of scale formation in produced water as a tool for environmental monitoring. Results Eng. 2025;26:105223.
8. Nallakukkala S, Tackie-Otoo BN, Aliyu R, Lal B, Nallakukkala JRD, Devi G. Application of machine learning algorithms to predict removal efficiency in treating produced water via gas hydrate-based desalination. Desalination. 2025;612:118961.
9. Wang Z, Wang C, Meng L, Qi X, Hong J. Prediction of sump oil growth rate towards gravitational settling of produced water in oilfield based on machine learning. Desalin Water Treat. 2024;317:100189.

10. Saddiqi HA, Javed Z, Ali QM, Ullah A. Optimization and predictive modeling of membrane-based produced water treatment using machine learning models. Chem Eng Res Des. 2024;207:65-76.
11. Saddiqi HA, Javed Z, Ali QM, Ullah A, Ahmad I. Modelling and predicting lift force and transmembrane pressure using linear, KNN, ANN and response surface models during the separation of oil drops from produced water. J Water Process Eng. 2024;66:106014.
12. Jiang W, Pokharel B, Lin L, Cao H, Carroll KC, Zhang Y, et al. Analysis and prediction of produced water quantity and quality in the Permian Basin using machine learning techniques. Sci Total Environ. 2021;801:149693.
13. Taloba AI. An artificial neural network mechanism for optimizing the water treatment process and desalination process. Alex Eng J. 2022;61(12):9287-9295.
14. Ezemagu IG, Ejimofor MI, Menkiti MC, Nwobi-Okoye CC. Modeling and optimization of turbidity removal from produced water using response surface methodology and artificial neural network. S Afr J Chem Eng. 2021;35:78-88.
15. Aisyah PY, Soehartanto T, Finazis RF, Afif K, Lokeswara R, Umamah F. Process dynamics modeling on polishing unit of artificial neural network-based produced water treatment system. In: Proceedings of the IEEE International Conference on Advanced Mechatronics, Intelligent Manufacture and Industrial Automation (ICAMIMIA); 2021. p. 23-27.
16. Nair RR, Protasova E, Strand S, Bilstad T. Effect of pH on produced water treatment using nanofiltration membranes: artificial neural network for performance assessment and steric hindrance pore model for flux variation evaluation. Desalin Water Treat. 2019;146:120-130.
17. Heydari B, Sharghi EA, Rafiee S, Mohtasebi SS. Use of artificial neural network and adaptive neuro-fuzzy inference system for prediction of biogas production from spearmint essential oil wastewater treatment in up-flow anaerobic sludge blanket reactor. Fuel. 2021;306:121734.

Mapping the Scientific Production on Artificial Intelligence Training for Workers in the Industrial Sector

Maine Maurícia Serra Dantas[1]*, Tatiana Loureiro da Silva[1], Thais Afonso Andrade[1], Camila de Sousa Pereira Guizzo[1], Claudio Fabiano Motta Toledo[2]

[1]SENAI CIMATEC University, GETEC, Salvador, Bahia; [2]USP- University of São Paulo; São Paulo, São Paulo, Brazil

The advent of Artificial Intelligence (AI), based technologies within the industrial sector has precipitated profound and disruptive transformations in operational routines and work dynamics, exerting a direct influence on the skill profile required of workers. These changes directly impact the set of skills required of professionals, who now need to transcend traditional technical expertise and develop new dimensions of knowledge. Given this context, the objective of this study is to map national and international scientific production about AI literacy for industrial workers. This is narrative research whose purpose is to identify, as evidenced in the literature, both the gaps and opportunities for improvement in professional training. The study revealed that, despite growing industry investments in intelligent systems, initiatives aimed at cultivating AI literacy among non-specialist professionals continue to be neglected. Furthermore, the available courses show a low alignment with industrial practice and fail to adequately consider the sociocultural profile of participants. Research indicates that AI training should go beyond the acquisition of technical knowledge, encompassing the development of reflective, adaptive, and interventional skills. Moreover, the literature highlights the importance of integrating inclusive strategies that address cultural, generational, and skills-level diversity in industrial environments, as these factors directly influence engagement, learning outcomes, and the equitable distribution of opportunities in an AI-driven economy. The expected results of this research are to identify the main challenges that can support more effective and sustainable educational strategies for professional qualification in the use of AI in the industrial sector.

Keywords: AI Training. AI Literacy. AI Literacy for Workers. AI Literacy in the Industrial Sector.

The integration of Artificial Intelligence (AI) within industrial contexts has precipitated profound transformations in the realm of work organization and the demand for novel professional competencies [1]. In addition to technical proficiency, it is essential to develop a critical, ethical, and practical understanding of the use of these technologies [2–3], considering not only mastery of the tools but also the ability to assess their impacts on the workplace, on society, and strategic decision-making.

AI by enhancing human capabilities, increases productivity, optimizes processes, and enables new business models, but also poses challenges related to professional responsibility and transparency in interactions with automated systems.

Received on 27 April 2026; revised 15 June 2026.
Address for correspondence: Maine Maurícia Serra Dantas. Av. Orlando Gomes, 1845 - Piatã, Salvador – BA – Brazil, Zipcode: 41650-010. E-mail: maine.dantas@aln.senaicimatec.edu.br.

J Bioeng. Tech. Health 2026;9(7):770-776

This ongoing advancement requires constant professional updating to ensure that skills remain relevant in the face of technological evolution and changing market demands [4]. The reviewed literature indicates that technological advances only translate into tangible benefits when accompanied by adequate, continuous, and context-specific training programs [5]. Such programs should integrate technical content with reflective and adaptive practices, enabling workers to operate effectively in dynamic, collaborative, and ethically responsible contexts, thus ensuring a more efficient, inclusive, and sustainable technological transition.

In this context, the present research aims to map national and international scientific production related to AI literacy aimed at industrial sector workers. The recent European regulation and the Brazilian Artificial Intelligence Plan 2024–2028 (PBIA) emphasize the urgency of large-scale training [6–7].

AI literacy is defined by the capacity to engage in critical reflection and ethical application, extending beyond mere technical mastery [2-8]. This approach broadens the understanding and responsible use of technology, preparing individuals to interpret, evaluate, and apply AI in a contextualized manner [9-10]. Such a perspective fosters the development of professionals capable of responding to emerging challenges and generating sustainable value in diverse contexts.

The worker moves from being a mere operator to becoming a critical agent of technology, [11] points out that mapping skills is essential to reducing the skills gap, and [12] highlights the need for workforce adaptation. Despite the economic advantages offered by AI, there are risks of job losses and increased inequality, as indicated by estimates of automation through 2030 and the potential social and economic disruptions that may follow [13–14].

Skilled workers can benefit more from AI, provided that adequate training is offered to them [11]. The absence of training exacerbates insecurities and resistance, making inclusive policies essential to ensure equity and reduce inequalities while fostering an environment of trust in technological adoption [15–16]. In this context, AI literacy can strengthen competitiveness and sustainable innovation [17].

It becomes urgent to investigate academic publications focused on AI literacy in industry, identifying trends, challenges, and gaps that can optimize worker training and enhance the positive impact of this technology while aligning these efforts with the evolving demands of the industrial sector.

It is therefore urgent to investigate academic publications focusing on AI literacy in industry to identify trends, challenges and gaps that could optimize worker training, enhance the positive impact of this technology and align these efforts with the evolving demands of the industrial sector.

Materials and Methods

This research was conducted through a narrative literature review. A narrative literature review describes or discusses a given topic based on the author's interpretation and critical analysis, drawing on a broad search of bibliographic or electronic information, without necessarily detailing the criteria adopted for the selection and evaluation of works [18]. This is a qualitative approach, chosen for its ability to integrate conceptual studies, institutional reports, and empirical evidence, enabling the discussion of different perspectives from authors on workers' literacy in the context of the growing adoption of Artificial Intelligence (AI) in the industrial sector.

The searches were carried out between May and July 2025 in the following databases: Scielo, Scopus, Web of Science, IEEE Xplore, and Google Scholar. Descriptors in English and Portuguese were used, including: "AI literacy for industrial workers," "industrial AI education," "artificial intelligence training," "AI in the industrial sector," "AI skills manufacturing," "alfabetização em inteligência artificial no setor industrial," and "letramento em IA."

Inclusion criteria: (i) studies published between 2000 and 2025; (ii) of a technical-scientific nature; and (iii) directly related to AI literacy, professional training, and impacts on work. Exclusion criteria: (i) duplicate works across databases; (ii) publications addressing exclusively technical aspects of AI without connection to training processes; and (iii) studies focused on non-industrial sectors, such as healthcare, basic education, commerce, and financial services.

As inclusion criteria, articles of any study design, book chapters, theses, dissertations, and institutional documents available online in full were considered, published between 2000 and 2025, in Portuguese, English, or Spanish, of a technical-scientific nature and directly related to AI literacy, professional training, and impacts on work. Excluded were duplicate works across databases, publications that addressed exclusively technical aspects of AI without connection to training processes, and studies focused on non-industrial sectors such as healthcare, basic education, and financial services.

Given the exploratory nature of the narrative review, the total number of documents identified in each database was not quantified. The selected texts were critically reviewed and organized into thematic axes: (1) definition of AI competencies for the industrial sector; (2) structural and cultural barriers to training; (3) reskilling and upskilling strategies; and (4) inclusion and ethics in AI literacy. The analysis sought to highlight consensus, divergences, and gaps, supporting a critical discussion on the topic.

Results and Discussion

Recognizing AI literacy in the industrial sector continues to face significant barriers. The reviewed literature highlights central gaps that hinder the broad, inclusive, and sustainable adoption of AI and reduce the effectiveness of training programs [1,6,11,21]. Most of the empirical evidence is concentrated in the manufacturing sector, which appears as the primary locus of analysis in the studies reviewed. These gaps manifest in the absence of evaluation metrics [1,3,21], the disconnection between training courses and industrial practices [1,11,22], workers' cultural resistance and insecurity [10,23], the neglect of ethical, social, and generational dimensions [6,7,10,22], and the weak articulation between workforce training and national reskilling policies [11,16,20].

The absence of reliable tools for diagnosing and measuring competencies is identified as one of the most recurrent obstacles [1,3,12,19,21,22]. The lack of reliable tools makes it difficult to monitor the development of competencies and limits the ability to continuously improve training programs. Evidence from the United States reinforces this problem, showing that the fragmentation of AI training initiatives makes it difficult to compare results and weakens integration with productive demands [26,28].

Another critical challenge lies in the disconnection between the training content offered and actual industrial practices. Programs that are overly generic or excessively technical tend to generate low engagement and limited results [1,11,22]. In manufacturing sectors in Pakistan, for instance, short-term training programs that were poorly aligned with shop floor activities resulted in low initial adherence. Conversely, when training was contextualized and integrated into operational routines, greater acceptance and organizational performance gains were observed [30]. International studies corroborate this finding, showing that training tailored to factory operations increases engagement and reduces resistance, particularly in emerging economies [25].

Cultural resistance and worker insecurity also represent recurring barriers. Research in manufacturing industries in Gujarat, India, revealed ambivalent perceptions: while some workers acknowledged efficiency gains, many associated AI with the risk of job displacement, which reduced their willingness to participate in training programs [23]. By contrast, experiences in factories in the Philippines showed that when training programs were adapted to local conditions and implemented gradually, workers demonstrated greater acceptance and incorporated AI into daily routines [31]. The cases analyzed show that the success of literacy programs depends on their adaptation to local cultural and organizational conditions.

Comparative analyses allow the observation of a trajectory of transformation: disjointed initiatives, characterized by low alignment with shop floor practices and worker insecurity, tend to generate rejection, whereas more contextualized programs promote greater integration of AI into industrial dynamics. The effectiveness of training is closely tied to how well educational content reflects the realities of industrial practice.

Another critical issue relates to the neglect of ethical, social, and generational dimensions. A significant portion of training programs continues to privilege technical content, while relegating to the background competencies associated with critical thinking, social responsibility, and adaptation to generational differences [6,7,10,22].

This limitation exacerbates inequalities and particularly affects non-specialist workers, who should be among the main beneficiaries of reskilling initiatives [11,21]. The literature converges in indicating that the most effective training programs are those that balance technical and human competencies, creating conditions for a more critical and responsible application of technologies.

Weaknesses are also evident in the sphere of public policies, where the absence of consistent national plans limits the effectiveness of AI literacy initiatives. In developing countries, large companies often advance with internal programs, while small and medium-sized industries remain on the margins of digital transformation [16,20].

In contrast, international experiences highlight possible solutions: in the United States, the creation of a federal coordination office and targeted funding for AI training have sought to reduce the fragmentation of initiatives, although regional inequalities in workforce preparation persist [26,28,29]; in Germany, long-term industrial policies associated with Industry 4.0 ensured that automation was accompanied by training programs, generating productivity gains and positive impacts in partner countries integrated into supply chains [27].

This heterogeneity reveals that the consolidation of AI literacy depends not only on technological diffusion but also on the ability to align public policies, business practices, and inclusive strategies.

In summary, the evidence indicates that the lack of adequate AI literacy undermines not only the qualification of workers but also the ability of industries to incorporate technologies strategically. Disjointed programs weaken innovation, intensify cultural resistance, and exacerbate inequalities, especially among small and medium-sized enterprises. On the other hand, experiences that integrate consistent evaluation, contextualized content, and long-term policies demonstrate that it is possible to align productivity gains with socioeconomic inclusion. The key challenge is to make AI literacy a structural axis of industrial development, combining competitiveness with the human dimension of work. Table 1 was created using data from the analyzed studies to present the research comprising this review more clearly.

Conclusion

This study showed that AI literacy in the industrial sector still faces barriers that limit its effectiveness, particularly the absence of evaluation metrics, the disconnection between training programs and shop floor practices, cultural resistance, the neglect of ethical and generational dimensions, and weaknesses in public policies.

For industrial managers, it is recommended to adopt validated diagnostic and competency identification tools for AI, capable of measuring existing skills and identifying gaps to be addressed, categorized by job profiles. In addition, training programs should be contextualized to shop floor routines, accessible to non-specialist workers, and designed to integrate both technical and human dimensions.

At the public policy level, clear and actionable measures are required. A first step is to establish validated tools to measure AI-related competencies, categorized by worker profiles, which can serve as a basis for targeted training. In parallel, governments should provide incentives for AI literacy programs tailored to small and medium-sized enterprises, since they are often excluded from large-scale initiatives. Finally, sustainable results depend on long-term national policies, aligned with industrial strategies and supported by partnerships with companies and educational institutions. For developing economies, these measures are particularly critical to reduce regional inequalities, strengthen SMEs, and ensure that industrial competitiveness advances together with socioeconomic inclusion.

At the educational level, universities and technical training centers should adapt their curricula to the real demands of industry, in collaboration with companies and policymakers.

Table 1. Study data.

Summary of the Used Studies				
	Author(s) and year of publication	**Country**	**Study Design**	**Objective**
1	Zahoor, Ahmed. (2025)	Pakistan	Quantitative	Investigate the influence of AI on business performance and HR management
3	Laupichler et al. (2023)	Germany	Quantitative	Validation of self-assessment tools for AI training courses
6	UNESCO, United Nations Educational, Scientific and Cultural Organization (2024)	France	Technical report	The UNESCO warns of the new digital divide caused by AI and proposes AI literacy as a universal and strategic right for global inclusion.
7	PBIA, Brazilian Artificial Intelligence Plan. 2024-2028 (2024)	Brazil	Technical report	The PBIA 2024–2028 sets guidelines for the ethical and strategic use of artificial intelligence in Brazil. The plan coordinates actions across infrastructure, education, the productive sector and government
10	Morandini et al. (2023)	Italy	Narrative review	Impact of AI on workers' skills and need for reskilling
11	OCDE, Organization for Economic Co-operation and Development and, SENAI, National Service for Industrial Training (2023)	Brazil	Technical report	The report highlights the urgency of aligning vocational training with technological demands through integrated strategies involving the productive sector, government, and education, fostering digital, cognitive, and socioemotional skills for the future of work.
12	Davenport & Ronanki (2018)	EUA	Descritive	Practical applications of AI in real-world organizations
16	Sidhu et al. (2024)	Bangladesh	Quantitative	Comparative analysis of skill gaps in emerging economies
19	Shen & Zhang (2024)	China	Quantitative empitical study	Analyzes the impact of AI on employment, highlighting that its adoption can promote job creation when accompanied by educational reforms that reduce regional and sectoral inequalities.
20	Barreto et al. (2023)	Brazil	Literature review	Impact of AI on labor productivity in Brazil
21	Mendoza et al., (2022)	Philippines	Quantitative	Systematic review of digital skilling for adults
22	Oluwaseyi et al. (2023)	Nigeria	Literature review	Future transformations of industries and society with AI
23	Patel & Patel (2024)	India (Gujarat)	Survey-based study	Worker perceptions of AI in Indian manufacturing
24	Salminen et al. (2024)	Europe	Qualitative	Alignment of industry needs and education in AI training
25	Gatabazi et al. (2025)	EUA	Literature review	Adoption of AI in global manufacturing industries
26	Oschinski, Crawford & Wu (2022)	EUA	Technical report	AI and the future of workforce training in the US
27	Krzywdzinski & Jürgens (2023)	Germany	Qualitative	Robotization and employment dynamics in German industries
28	CSET (2021)	EUA	Technical report	Policy recommendations for US AI workforce development
29	Alghamdi et al. (2023)	EUA	Quantitative	AI-enhanced education and workforce readiness in Nevada
30	Gulzar et al. (2024)	Pakistam	Survey-based study	AI training and high-performance work systems in Pakistan
31	Eusebio (2024)	Philippines	Survey-based study	Acceptance of AI in manufacturing industries in the Philippines

This integration helps align training content with productive practices, increasing the relevance of AI literacy programs and preparing workers for the critical and responsible use of AI.

References

1. Zahoor A. AI integration in workforce development: assessing training effectiveness in industrial settings. J Emerg Technol Ind Syst. 2025;3(1):13-28.
2. Long D, Magerko B. What is AI literacy? AI Mag [Internet]. 2020 [cited 2025 Jul 29];41(2):21-32. Available from: https://ojs.aaai.org/index.php/aimagazine/article/view/5318
3. Laupichler MC, Aster A, Perschewski J, Schleiss J. Evaluating AI courses: a valid and reliable instrument for assessing artificial-intelligence learning through comparative self-assessment. Educ Sci. 2023;13:978. doi:10.3390/educsci13100978
4. Sucipto H. The impact of artificial intelligence (AI) on human resource management practices. Management Studies and Business Journal . 2024;1(1):138-145. doi:10.62207/xey9mx18
5. Ng W, Leung J, Chu SKW, Qiao MS, et al. Conceptualizing AI literacy: an exploratory review. AI Soc. 2023. doi:10.1007/s00146-023-01682-2
6. UNESCO. AI literacy and the new digital divide: a global call for action [Internet]. Paris: UNESCO; 2024. Available from: https://www.unesco.org/en/articles/ai-literacy-and-new-digital-divide-global-call-action
7. Brasil. Ministério da Ciência, Tecnologia e Inovação. Plano Brasileiro de Inteligência Artificial (PBIA) 2024-2028. Brasília: MCTI; 2025. Available from: https://www.gov.br/lncc/pt-br/assuntos/noticias/ultimas-noticias-1/plano-brasileiro-de-inteligencia-artificial-pbia-2024-2028
8. Schardosim ML, Alves JR. Alfabetização, literacia e letramento: diferentes conceitos de um caminho comum. LínguaTec [Internet]. 2019;4(2):76-93. Available from: https://periodicos.ifrs.edu.br/index.php/LinguaTec/article/view/3665
9. Soares M. Letramento: um tema em três gêneros. Belo Horizonte: Autêntica; 2001.
10. Morandini S, Fraboni F, De Angelis M, Puzzo G, Giusino D, Pietrantoni L. The impact of artificial intelligence on workers' skills: upskilling and reskilling in organisations. Informing Sci. 2023;26:39-68. doi:10.28945/5078
11. Organisation for Economic Co-operation and Development, Serviço Nacional de Aprendizagem Industrial. Requalificação e atualização da força de trabalho preparada para o futuro da Indústria 4.0 e além. Brasília: SENAI; 2023. Available from: https://www.sp.senai.br
12. Davenport TH, Ronanki R. Artificial intelligence for the real world. Harv Bus Rev. 2018;96(1):108-116.
13. Manyika J, Chui M, Miremadi M, Bughin J, George K, Willmott P, et al. A future that works: automation, employment, and productivity. New York: McKinsey Global Institute; 2017.
14. Acemoglu D, Restrepo P. Artificial intelligence, automation and work [Internet]. Cambridge (MA): MIT Department of Economics; 2018. (Working Paper No. 18-01). Available from: https://ssrn.com/abstract=3098384
15. Shen Y, Zhang X. The impact of artificial intelligence on employment: the role of virtual agglomeration. Humanit Soc Sci Commun. 2024;11(1):1-14. doi:10.1057/s41599-024-02647-9
16. Sidhu GS, Sayem MA, Taslima N, Anwar AS, Chowdhury F, Rowshon M. AI and workforce development: a comparative analysis of skill gaps and training needs in emerging economies. Int J Bus Manag Sci. 2024;4(8):12-28. doi:10.55640/ijbms-04-08-03
17. Van Roy R, Zaman B. Unravelling the ambiguity of digital literacy: a systematic review of definitions. Comput Educ [Internet]. 2019;138:13-26. Available from: https://www.sciencedirect.com/science/article/pii/S0360131519300739
18. Rother ET. Revisão sistemática x revisão narrativa. Acta Paul Enferm. 2007;20(2):v-vi.
19. Holmes W, Bialik M, Fadel C. Artificial intelligence in education: promises and implications for teaching and learning. Boston: Center for Curriculum Redesign; 2019.
20. Barreto RC, Barros MRA, Carvalhaes F, Almeida R. O impacto da inteligência artificial na produtividade do trabalho. Rio de Janeiro: Instituto de Pesquisa Econômica Aplicada; 2023. Available from: https://www.ipea.gov.br/portal/images/stories/PDFs/TDs/td_2680.pdf
21. Mendoza-Chan J, Pee LG. Digital skilling of working adults: a systematic review. ComputEduc.2024;218:105076.doi:10.1016/j.compedu.2024.105076
22. Oluwaseyi JA. O futuro da inteligência artificial: transformando indústrias e a vida cotidiana. Rev Inov Tecnol Soc. 2024;6(1):15-29.
23. Patel M, Patel D. Employee perspectives on AI utilization in the manufacturing sector with special reference to Chhatral GIDC in Gujarat State: a survey-based study. 2024. doi:10.21276/ierj24993180695230
24. Salminen K, Hautamäki P, Jähi M. Aligning industry needs and education: unlocking the potential of AI via skills. In: Proceedings of PICMET 2024. 2024. doi:10.23919/PICMET64035.2024.10653328
25. Gatabazi E, Mijwil MM, Abotaleb M, Kapaya S. Global adoption of artificial intelligence in the manufacturing

industries. In: Advances in Artificial Intelligence Applications. 2025. doi:10.4018/979-8-3693-5231-1.ch015
26. Oschinski M, Crawford A, Wu M. AI and the future of workforce training [Internet]. Washington (DC): Center for Security and Emerging Technology; 2022. Available from: https://cset.georgetown.edu/publication/ai-and-the-future-of-workforce-training/
27. Krzywdzinski M, Jürgens U. Robotização e dinâmica de emprego nas cadeias de valor da indústria alemã. Berlin: WZB Berlin Social Science Center; 2023.
28. Center for Security and Emerging Technology. U.S. AI workforce policy recommendations [Internet]. Washington (DC): CSET; 2021. Available from: https://cset.georgetown.edu/publication/u-s-ai-workforce-policy-recommendations/
29. Alghamdi A, et al. AI-enhanced education in Nevada and its transformative impact on workforce readiness. Educ Technol Res Dev. 2023;71:125-140.
30. Gulzar M, Iqbal T, Ahmed S. Artificial intelligence, workforce training and high-performance work systems in the manufacturing sector of Pakistan. Artif Intell Rev. 2024;57:543-566. doi:10.1007/s10462-024-11013-9
31. Eusebio R. Acceptance of artificial intelligence in selected manufacturing industries in San Pablo City: an input on human resource. Int J Ind Manag. 2024;12(2):77-93.

Technological Overview: Analysis of Patents Related to the Use of Core-Shell Catalysts and ALD in Solid Oxide Fuel Cells

Iuri Dantas Passos da Mota[1]*, Marcos Makoto Toyama[1,2], Gerhard Ett[1,3], Lilian Lefol Nani Guarieiro[1]
[1]SENAI CIMATEC University; Salvador, Bahia; [2]Mauá Institute of Technology; São Caetano do Sul, São Paulo; [3]FEI University Center; São Bernardo do Campo, São Paulo, Brazil

This study analyzes patents registered between 2010 and 2025 involving solid oxide fuel cells (SOFC), atomic layer deposition (ALD), and core-shell structures. Data from Lens.org show that the combination of ALD and core-shell accounts for the largest number of registrations, reflecting broad industrial applicability. Combinations with SOFCs, on the other hand, have a low incidence, suggesting an area in the early stages of intellectual property protection. Only two registrations simultaneously associate SOFC, ALD, and core-shell, evidencing a little-explored technological frontier. Most filings occur in the US, Japan, South Korea, and the European Patent Office (EPO), with an emphasis on companies and research institutions. Brazil's presence is limited to one registration involving SOFC and core-shell, indicating the need for greater investment in applied research and intellectual property protection. The interface between these technologies represents an emerging niche with high innovative potential.
Keywords: SOFC. Core-shell. ALD. Sustainability. Solid Oxide Fuel Cells. Atomic Layer Deposition. Patent.

Fuel cells are efficient electrochemical devices that produce electricity through redox reactions, making them a clean energy alternative [1,2]. The development of SOFCs had milestones such as the discovery of solid electrolytes by Nernst (1892) and the first ceramic cell by Baur and Preis (1936) [3]. They stand out among high-temperature types, classified according to the electrolyte and operating range [4,5].

SOFCs, made with solid ceramic materials, operate between 800 and 1000 °C, favoring the kinetics of reactions with high efficiency and without noble metals [6,7]. This configuration allows flexibility in design and fuel choice [5]. Operation is based on fuel oxidation at the anode, oxidant reduction at the cathode, oxygen ion conduction through the electrolyte, and current generation in the external circuit.

Core-shell nanoparticles are composed of a core coated with one or more outer layers of another material [8,9]. The convention for naming them uses the symbol "@," reflecting the sequence of the layers that compose them [10]. According to Gawande and colleagues (2015) [11], the classification can also take into account the nature of the material, organic or inorganic, and the morphological characteristics of the shell, such as porosity, number of layers, or presence of cavities, factors that directly influence their properties and applications.

The ALD technique, developed in the 1970s and widespread after 2000, allows the deposition of ultra-thin films (<20 nm) with high uniformity, even on complex surfaces [12–15]. It is based on sequential and self-limiting chemical reactions, allowing precise thickness control. Its main variations are thermal ALD (ThALD) and plasma-enhanced ALD (PEALD), the latter enabling film growth at lower temperatures [12,16,17].

In this context, this study analyzes patents related to SOFCs, focusing on the application of core-shell catalysts and the ALD technique. The investigation continues a previous bibliometric analysis, expanding the scope to the field of intellectual property. Based on this approach, we seek to observe the transition from scientific knowledge to technological applications, identify innovation trends, main depositors, and areas with industrial potential. To this end, patents indexed in the Lens.org database are analyzed, using its

Received on 27 April 2026; revised 12 June 2026.
Address for correspondence: Iuri Dantas Passos da Mota. Av. Orlando Gomes, 1845 - Piatã, Salvador – BA – Brazil, Zipcode: 41650-010. E-mail: iuri.mota@fbter.org.br.

J Bioeng. Tech. Health 2026;9(7):777-784

analytical tools to map technological advances, identify gaps, and highlight innovations in the use of these technologies in solid oxide fuel cells.

Materials and Methods

The technological prospecting was carried out by collecting and analyzing patents available on the Lens.org database (https://www.lens.org), using the platform's own analytical tool. The main indicators are summarized in Table 1. The search was conducted in July 2025 and covered patents granted between 2010 and 2025. The year 2010 was adopted as the starting point in order to maintain consistency with a previous bibliometric investigation, conducted by the author, which addressed the same thematic area.

Four combinations of keywords were applied: “Solid Oxide Fuel Cell” AND “Atomic Layer Deposition”; “Solid Oxide Fuel Cell” AND “core-shell”; “Atomic Layer Deposition” AND “core-shell”; and the triple combination “Solid Oxide Fuel Cell” AND “Atomic Layer Deposition” AND “core-shell”, resulting in 17, 7, 39, and 2 records, respectively.

Although the triple combination resulted in only two records, this group should not be disregarded, as it includes patents with links to scientific literature through citations to non-patented sources (NPL) and presents relevant indicators of technological impact. This suggests that the integration of the three topics, still largely unexplored, represents an emerging field with strategic potential in the development of innovative solutions for SOFC.

Results and Discussion

Annual Patents Production

Figure 1 shows the annual evolution of patents published between 2010 and 2025 related to the terms “Solid Oxide Fuel Cell,” “core-shell,” and “Atomic Layer Deposition” in different combinations. The association between “Atomic Layer Deposition” and “core-shell” stands out, with the highest number of registrations in the period, peaking in 2024 with seven filings and remaining relatively stable since 2015. This pattern indicates technological consolidation in the use of core-shell structures of the ALD technique, with potential applications in various sectors, including SOFC.

In contrast, combinations with the term “Solid Oxide Fuel Cell” show a lower volume. The

Table 1. Patent data extracted from the Lens.org database with different thematic combinations.

Description	“SOFC” AND “ALD”	“SOFC” AND “Core-Shell”	“ALD” AND “Core-Shell”	“SOFC” AND “ALD” AND “Core-Shell”
Patent Registration	17	7	39	2
Simple Families	14	7	33	2
Extended Families	14	7	33	2
Patent Citations	17	4	36	2
Cited by Patents	7	2	19	2
Patent Citations	11	2	155	2
NPL Citations	10	3	28	2
NPL Citations	66	35	297	34
Resolved NPL Citations	27	12	211	11

Figure 1. Annual evolution of the number of patents published between 2010 and 2025, considering combinations of the terms "Solid Oxide Fuel Cell," "Atomic Layer Deposition," and "core-shell".

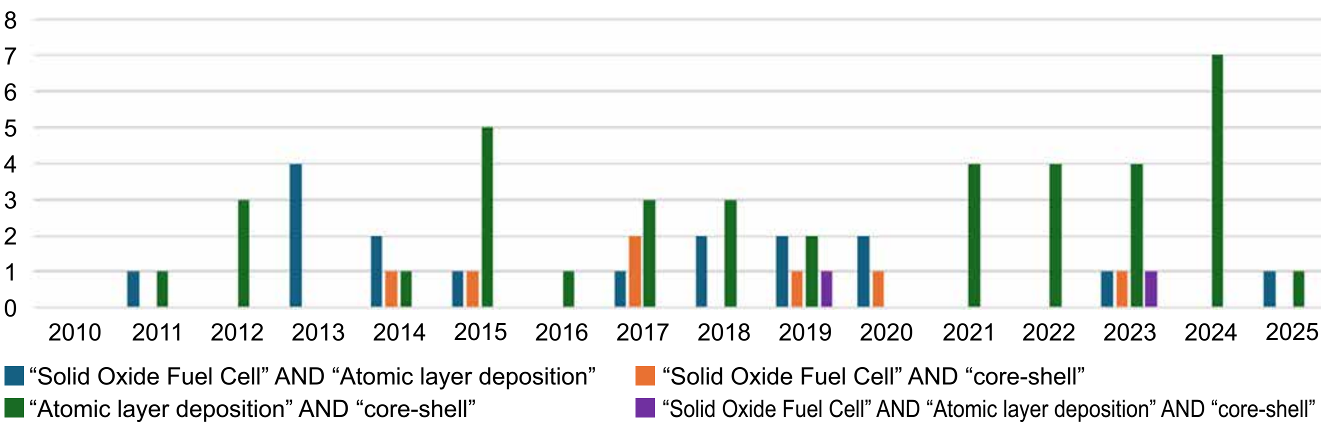

relationship with "Atomic Layer Deposition" peaked in 2013 but remained irregular. The combination with "core-shell" shows sporadic deposits, with no trend toward continuous growth. The more specific search, which combines the three terms, resulted in only two records, published in 2019 and 2023. The low occurrence indicates that this integration is still under-explored technologically, characterizing a specific niche, with limited interest and no signs of consolidation.

Main Patent Applicants

Table 2 lists the main patent filers for each combination of terms analyzed, highlighting the diversity of actors involved in the development of technologies related to SOFC, core-shell, and ALD, with variations according to the thematic focus.

In the combination "Solid Oxide Fuel Cell" and "Atomic Layer Deposition," Roeder Jeffrey F and Sonata Scient LLC stand out, with 5 registrations each, followed by Stanford University, with 4. The presence of academic institutions and individual researchers suggests strong involvement in applied research.

In turn, the combination of "Solid Oxide Fuel Cell" and "core-shell" presents a more dispersed panorama. The Korea Ceramic Technology Institute leads with 2 deposits, while the others appear with only 1 registration each. This pattern suggests a still incipient stage of development or a more specific interest on the part of the institutions involved.

In the combination of "Atomic Layer Deposition" and "core-shell," there is greater diversity of depositors, including companies and research centers. Sila Nanotechnologies INC and US Gov Sec Navy lead with four registrations, followed by Cellmobility INC, Nanosys INC, and Samsung with two. Other participants appear with isolated contributions. This distribution reinforces the technological potential of ALD application and core-shell structures, arousing significant interest, especially in the industrial sector.

In the more specific combination, with the three terms, all depositors appear with only one patent. Among them are Roeder Jeffrey F, Sonata Scient LLC, Van Buskirk Peter C, and Univ Colorado Regents. The absence of a dominant group or institution in this thematic combination indicates that the overlap of the three topics is still the subject of sporadic and scattered investigations.

Overall, the analysis shows a fragmented scenario, with few recurring applicants. This dispersion reflects both the variety of applications and the emerging nature of the integration between SOFC, ALD, and core-shell structures.

Table 2. Distribution of the main patent filers by combination of terms.

"SOFC" AND "ALD"		"SOFC" AND "core-shell"		"ALD" AND "core-shell"		"SOFC" AND "ALD" AND "core-shell"	
Dep	**Doc**	**Dep**	**Doc**	**Dep**	**Doc**	**Dep**	**Doc**
Roeder Jeffrey F	5	Korea Ceramic Technology Institute	2	Sila Nanotechnologies INC	4	Roeder Jeffrey F	1
Sonata Scient LLC	5	Coppe Ufrj	1	Us Gov Sec Navy	4		
Univ Leland Stanford Junior	4	Korea Inst Ceramic Eng & Tech	1	Cellmobility INC	2	Sonata Scient LLC	1
Van Buskirk Peter C	4	Nissan North America INC	1	Nanosys INC	2		
Honda Motor CO LTD	3	Roeder Jeffrey F	1	Samsung Electronics CO LTD	2	Univ Colorado Regents	1
Prinz Friedrich B	3	Sonata Scient LLC	1	Ajou Univ Industry—academic Cooperation Foundation	1		
Zeberoff Anthony F	3	Univ Colorado Regents	1	Avantama AG	1	Van Buskirk Peter C	1
Sumitomo Metal Mining CO	2	Van Buskirk Peter C	1	Becker Carsten	1		
Univ Colorado Regents	2	Zeberoff Anthony F	1	Benayad Anass	1	Zeberoff Anthony F	1

Dep, Depositors; Doc, Documents.

Geographical Distribution of Inventors

Table 3 shows the countries with the highest number of inventors linked to patents for different combinations of "Solid Oxide Fuel Cell," "Atomic Layer Deposition," and "core-shell." The United States and South Korea predominate, reflecting their leadership in research and innovation.

In the combination of "Atomic Layer Deposition" and "core-shell," the US leads with 23 inventors, followed by South Korea [10]. Other countries appear with occasional participation, such as Switzerland, China, Germany, France, Israel, the Netherlands, and Taiwan, highlighting a broad international scenario, with emphasis on the US, Asia, and Europe.

In the combination of "Solid Oxide Fuel Cell" and "Atomic Layer Deposition," the US also leads with 12 inventors, followed by Japan, Estonia, Finland, and South Korea, with smaller shares. In the association between "Solid Oxide Fuel Cell" and "core-shell," the US has three inventors, followed by South Korea and Brazil, with one inventor each. The Brazilian presence, although

Table 3. Geographic distribution of inventors by country, considering combinations of the terms “Solid Oxide Fuel Cell,” “Atomic Layer Deposition,” and “core-shell”.

<table>
<tr><th colspan="2">“SOFC” AND “ALD”</th><th colspan="2">“SOFC” AND “core-shell”</th><th colspan="2">“ALD” AND “core-shell”</th><th colspan="2">“SOFC” AND “ALD” AND “core-shell”</th></tr>
<tr><th>Country</th><th>Documents</th><th>Country</th><th>Documents</th><th>Country</th><th>Documents</th><th>Country</th><th>Documents</th></tr>
<tr><td>United States</td><td>12</td><td rowspan="3">United States</td><td rowspan="3">3</td><td>United States</td><td>23</td><td rowspan="9">United States</td><td rowspan="9">2</td></tr>
<tr><td>Japan</td><td>3</td><td>South Korea</td><td>10</td></tr>
<tr><td rowspan="3">Estonia</td><td rowspan="3">1</td><td>Switzerland</td><td>2</td></tr>
<tr><td rowspan="3">South Korea</td><td rowspan="3">1</td><td>China</td><td>1</td></tr>
<tr><td>Germany</td><td>1</td></tr>
<tr><td>Finland</td><td>1</td><td>France</td><td>1</td></tr>
<tr><td rowspan="3">South Korea</td><td rowspan="3">1</td><td rowspan="3">Brazil</td><td rowspan="3">1</td><td>Israel</td><td>1</td></tr>
<tr><td>Netherlands</td><td>1</td></tr>
<tr><td>Taiwan</td><td>1</td></tr>
</table>

isolated, suggests an opportunity for insertion in technological development related to this specific area. The most restricted combination, involving the three terms, has only two inventors, both from the US, confirming that this integration is still under-explored in patents.

Brazil appears only in the combination “Solid Oxide Fuel Cell” and “core-shell,” with no records in the others. This points to limited participation in the generation of intellectual property in these areas, but also to a strategic opportunity for action, such as a strategy to boost applied research, foster international collaborations, and expand Brazil's presence.

In general, the data reinforce the leading role of the US and South Korea in the advancement of these technologies, while other countries contribute in a sporadic manner, composing a global panorama of development.

Main CPC Classification Codes

Table 4 shows the most recurrent cooperative patent classification (CPC) codes in patents resulting from different combinations of “SOFC”, “ALD” and “core-shell”. These codes group patents by technological areas, allowing the identification of the main areas of development.

In the combination of “SOFC” and “ALD”, the codes Y02E60/50 (17 records), focused on technologies for reducing greenhouse gas emissions, and Y02P70/50 (11 records), related to sustainable industrial processes, stand out. Also noteworthy are classifications related to SOFC and zirconium oxide electrolytes (H01M2008/1293 and H01M8/1253), as well as codes for chemical vapor deposition (C23C16/405 and C23C16/45555).

In the combination “SOFC” and “core-shell,” the most frequent codes include Y02E60/50, H01M2008/1293, and H01M4/8657, the latter associated with layered electrodes, indicating a focus on sustainable electrochemical devices.

For “ALD” and “core-shell,” codes related to surface engineering and ultrathin coatings predominate, such as C23C16/45555, C23C16/403 (aluminum, magnesium, or beryllium coatings), and C23C16/4417

Table 4. Top ten CPC codes identified in the combinations of terms analyzed.

"SOFC" AND "ALD"		"SOFC" AND "core-shell"		"ALD" AND "core-shell"		"SOFC" AND "ALD" AND "core-shell"	
CPC	**Q**	**CPC**	**Q**	**CPC**	**Q**	**CPC**	**Q**
Y02E60/50	17	Y02E60/50	6	B82Y30/00	8	H01M2008/1293	2
Y02P70/50	11	H01M2008/1293	5	C23C16/45555	8	Y02E60/50	2
H01M2008/1293	10	H01M4/8657	4	C23C16/403	7	A61K6/818	1
H01M8/1253	7	H01M4/86	2	Y02E60/50	7	A61K6/822	1
C23C16/405	6	H01M4/8885	2	C23C16/4417	6	B33Y70/00	1
C23C16/45555	6	H01M8/12	2	C23C16/45525	6	C04B2235/3217	1
H01M4/8867	5	Y02P70/50	2	C04B2235/3217	5	C04B2235/3225	1
C23C16/40	4	A61K6/818	1	C04B35/62813	5	C04B2235/3229	1
H01M4/9058	4	A61K6/822	1	C04B35/62884	5	C04B2235/3232	1
H01M8/1246	4	B33Y70/00	1	C23C16/405	5	C04B2235/3246	1

Q, Qunatity.

(powder materials), in addition to B82Y30/00, focused on the application of nanotechnology in materials.

In the combination of the three terms, despite the small number of patents, codes H01M2008/1293 and Y02E60/50 stand out again, indicating a focus on electrochemical devices with a positive environmental impact.

In summary, the data point to a variety of technological areas, with an emphasis on clean energy, sustainable processes, electrochemistry, and nanotechnology, reflecting the interdisciplinary nature and high potential of the technologies analyzed.

Legal Status of Patent Documents

Table 5 shows the legal status of patents in different combinations of "SOFC," "ALD," and "core-shell," classifying them as active or inactive. The combination of "ALD" and "core-shell" has the highest number of active patents (33), indicating a growing field with significant technological potential.

In contrast, "SOFC" and "ALD" are dominated by inactive registrations (12), suggesting a previous phase of activity or a recent decline in interest. The combination of "SOFC" and "core-shell" is balanced, with 5 active and 2 inactive patents, pointing to possible recent consolidation.

In the combination of the three terms, there are only 2 documents: 1 active and 1 inactive, which reinforces the initial and little-explored nature of this integration in the field of patents.

These data help to assess the degree of maturity of the technologies analyzed, highlighting more consolidated areas and others that are still emerging, with room for new **innovations.**

Challenges and Opportunities

The integration of core-shell catalysts and the ALD technique in the development of SOFCs is a field that has yet to be fully explored, both in academia and in the technological arena. Patent analysis highlights this gap: only two records were identified that simultaneously address the

Table 5. Distribution of the legal status of the patent documents found.

"SOFC" AND "ALD"		"SOFC" AND "core-shell"		"ALD" AND "core-shell"		"SOFC" AND "ALD" AND "core-shell"	
Status	**Quantity**	**Status**	**Quantity**	**Status**	**Quantity**	**Status**	**Quantity**
Inactive	12	Inactive	2	Inactive	6	Inactive	1
Active	5	Active	5	Active	33	Active	1

three elements, one of which is active and the other inactive. This data reinforces the perception that this specific combination represents a technological frontier still in formation.

Despite the limited number, the most recurrent CPC codes (H01M2008/1293 and Y02E60/50) point to advanced electrochemical technologies and environmental mitigation, signaling the strategic potential of this combination. Individually, patents dealing with "ALD" and core-shell show greater frequency and predominance of active status, indicating continued interest in these areas.

These data, combined with a previous bibliometric study, help to paint a broader picture of the challenges and opportunities in this area. From a patent perspective, there is a notable scarcity of consolidated solutions that integrate the three technologies, hindering practical application. On the other hand, existing records demonstrate innovation and links to sustainability and energy efficiency. The growing interest in solutions applicable to the energy transition and the continuity of active filings reinforce the existence of room for innovation, especially with the joint engagement of academic and industrial efforts.

Thus, although still in its early stages, the combination of ALD, core-shell, and SOFCs shows promising fundamentals. Its advancement will depend on strategies to overcome technical barriers while taking advantage of the opportunities of an evolving technological landscape.

Conclusion

The analysis of patents involving "Solid Oxide Fuel Cell," "Atomic Layer Deposition," and "core-shell" revealed different levels of technological maturity. The combination of 'ALD' and "core-shell" has the highest number of registrations, distributed across several countries and sectors, reflecting broad applicability and prominence in the innovation landscape. Combinations with SOFC, on the other hand, are less frequent, especially those combining all three terms, with only two registrations between 2019 and 2023.

Despite the low occurrence, one of the two documents remains active, indicating recent interest in protecting the technology. The associated CPC codes point to a link with electrochemical devices and energy conversion technologies. Most filings occurred in jurisdictions such as the US, Japan, South Korea, and EPO, covering national and international applications, evidence of global protection strategies.

Among the main filers are companies such as General Electric and LG Chem, as well as universities and research centers, reinforcing open innovation and the academic role in generating patentable technologies. The significant number of active patents suggests continued interest in ALD- and core-shell-based solutions, although still incipient in the context of SOFCs.

In the Brazilian case, only one deposit related to the combination of "SOFC" and "core-shell" was identified, with no records involving "ALD." This low representation highlights a gap in the protection of advanced energy technologies and reinforces the need for policies that encourage applied research and its conversion into intellectual property assets.

In summary, the interface between ALD, core-shell, and SOFC represents an emerging niche, with low current density but high innovation potential. The existence of active documents and strategic technical classifications indicates promising opportunities for institutions and companies wishing to explore this technological frontier.

Acknowledgement

We thank Senai Cimatec University for its institutional support, Fundep for its research support, the Rota 2030 Project for promoting industrial innovation, and the Graduate Program in Industrial Management and Technology for the academic training it provides.

References

1. Grove WR. XXIV. On voltaic series and the combination of gases by platinum. Philos Mag J Sci. 1839;14:127-130. doi:10.1080/14786443908649684.
2. Nascimento AC, Mohallem NDS. Materiais usados na constituição dos principais componentes de células a combustível de óxido sólido. Cerâmica. 2009;55:46-52. doi:10.1590/S0366-69132009000100006.
3. Möbius HH. On the history of solid electrolyte fuel cells. J Solid State Electrochem. 1997;1:2-16. doi:10.1007/s100080050018.
4. Kirubakaran A, Jain S, Nema RK. A review on fuel cell technologies and power electronic interface. Renew Sustain Energy Rev. 2009;13:2430-2440. doi:10.1016/j.rser.2009.04.004.
5. Stambouli AB, Traversa E. Solid oxide fuel cells (SOFCs): a review of an environmentally clean and efficient source of energy. Renew Sustain Energy Rev. 2002;6:433-455. doi:10.1016/S1364-0321(02)00014-X.
6. Singhal SC, Kendall K. High-temperature solid oxide fuel cells: fundamentals, design and applications. Oxford: Elsevier; 2003. p. 1-18.
7. Minh NQ. Ceramic fuel cells. J Am Ceram Soc. 1993;76:563-588. doi:10.1111/j.1151-2916.1993.tb03645.x.
8. Ghosh Chaudhuri R, Paria S. Core/shell nanoparticles: classes, properties, synthesis mechanisms, characterization, and applications. Chem Rev. 2012;112(4):2373-2433. doi:10.1021/cr100449n.
9. Lu W, Guo X, Luo Y, Li Q, Zhu R, Pang H. Core-shell materials for advanced batteries. Chem Eng J. 2019;355:208-237. doi:10.1016/j.cej.2018.08.132.
10. Schileo G. Recent developments in ceramic multiferroic composites based on core/shell and other heterostructures obtained by sol-gel routes. Prog Solid State Chem. 2013;41(4):87-98. doi:10.1016/j.progsolidstchem.2013.09.001.
11. Gawande MB, Goswami A, Asefa T, Guo H, Biradar AV, Peng DL, et al. Core-shell nanoparticles: synthesis and applications in catalysis and electrocatalysis. Chem Soc Rev. 2015;44(21):7540-7590. doi:10.1039/C5CS00343A.
12. George SM. Atomic layer deposition: an overview. Chem Rev. 2010;110(1):111-131. doi:10.1021/cr900056b.
13. Knoops HCM, Potts SE, Bol AA, Kessels WMM. Atomic layer deposition. In: Hurle DTJ, editor. Handbook of crystal growth. Amsterdam: North-Holland; 2015. p. 1101-1134. doi:10.1016/B978-0-444-63304-0.00027-5.
14. Hashmi MSJ, editor. Comprehensive materials processing. Amsterdam: Newnes; 2014.
15. ShahMohammadi M, Mukherjee R, Sukotjo C, Diwekar UM, Takoudis CG. Recent advances in theoretical development of thermal atomic layer deposition: a review. Nanomaterials (Basel). 2022;12(5):831. doi:10.3390/nano12050831.
16. Kim H, Oh IK. Review of plasma-enhanced atomic layer deposition: technical enabler of nanoscale device fabrication. Jpn J Appl Phys. 2014;53(3S2):03DA01. doi:10.7567/JJAP.53.03DA01.
17. Mallick BC, Hsieh CT, Yin KM, Gandomi YA, Huang KT. On atomic layer deposition: current progress and future challenges. ECS J Solid State Sci Technol. 2019;8(4):N55-N61. doi:10.1149/2.0201903jss.

Instructions for Authors

The Authors must indicate in a cover letter the address, telephone number and e-mail of the corresponding author. The corresponding author will be asked to make a statement confirming that the content of the manuscript represents the views of the co-authors, that neither the corresponding author nor the co-authors have submitted duplicate or overlapping manuscripts elsewhere, and that the items indicated as personal communications in the text are supported by the referenced person. Also, the protocol letter with the number should be included in the submission article, as well as the name of sponsors (if applicable).

Manuscripts may be submitted within designated categories of communication, including:

- Original basic or clinical investigation (original articles on topics of broad interest in the field of bioengineering and biotechnology applied to health). We particularly welcome papers that discuss epidemiological aspects of international health, clinical reports, clinical trials and reports of laboratory investigations.
- Case presentation and discussion (case reports must be carefully documented and must be of importance because they illustrate or describe unusual features or have important practice implications).
- Brief reports of new methods or observations (short communications brief reports of unusual or preliminary findings).
- State-of-the-art presentations (reviews on protocols of importance to readers in diverse geographic areas. These should be comprehensive and fully referenced).
- Review articles (reviews on topics of importance with a new approach in the discussion). However, review articles only will be accepted after an invitation of the Editors.
- Letters to the editor or editorials concerning previous publications (correspondence relating to papers recently published in the Journal, or containing brief reports of unusual or preliminary findings).
- Editor's corner, containing ideas, hypotheses and comments (papers that advance a hypothesis or represent an opinion relating to a topic of current interest).
- Innovative medical products (description of new biotechnology and innovative products applied to health).
- Health innovation initiatives articles (innovative articles of technological production in Brazil and worldwide, national policies and directives related to technology applied to health in our country and abroad).

The authors should checklist comparing the text with the template of the Journal.

Supplements to the JBTH include articles under a unifying theme, such as those summarizing presentations of symposia or focusing on a specific subject. These will be added to the regular publication of the Journal as appropriate, and will be peer reviewed in the same manner as submitted manuscripts.

Statement of Editorial Policy

The editors of the Journal reserve the right to edit manuscripts for clarity, grammar and style. Authors will have an opportunity to review these changes prior to creation of galley proofs. Changes in content after galley proofs will be sent for reviewing and could be required charges to the author. The JBTH does not accept articles which duplicate or overlap publications elsewhere.

Peer-Review Process

All manuscripts are assigned to an Associate Editor by the Editor-in-Chief and Deputy Editor, and sent to outside experts for peer review. The Associate Editor, aided by the reviewers' comments, makes a recommendation to the Editor-in-Chief regarding the merits of the manuscript. The Editor-in-Chief makes a final decision to accept, reject, or request revision of the manuscript. A request for revision does not guarantee ultimate acceptance of the revised manuscript.

Manuscripts may also be sent out for statistical review ou *ad hoc* reviewers. The average time from submission to first decision is three weeks.

Revisions

Manuscripts that are sent back to authors for revision must be returned to the editorial office by 15 days after the date of the revision request. Unless the decision letter specifically indicates otherwise, it is important not to increase the text length of the manuscript in responding to the comments. The cover letter must include a point-by-point response to the reviewers and Editors comments, and should indicate any additional changes made. Any alteration in authorship, including a change in order of authors, must be agreed upon by all authors, and a statement signed by all authors must be submitted to the editorial office.

Style

Manuscripts may be submitted only in electronic form by www.jbth.com.br. Each manuscript will be assigned a registration number, and the author notified that the manuscript is complete and appropriate to begin the review process. The submission file is in OpenOffice, Microsoft Word, or RTF document file format for texts and JPG (300dpi) for figures.

Authors must indicate in a cover letter the address, telephone number, fax number, and e-mail of the corresponding author. The corresponding author will be asked to make a statement confirming that the content of the manuscript represents the views of the co-authors, that neither the corresponding author nor the co-authors have submitted duplicate or overlapping manuscripts elsewhere, and that the items indicated as personal communications in the text are supported by the referenced person.

Manuscripts are to be typed as indicated in Guide for Authors, as well as text, tables, references, legends. All pages are to be numbered with the order of presentation as follows: title page, abstract, text, acknowledgements, references, tables, figure legends and figures. A running title of not more than 40 characters should be at the top of each page. References should be listed consecutively in the text and recorded as follows in the reference list, and must follow the format of the National Library of Medicine as in Index Medicus and "Uniform Requirements for Manuscripts Submitted to Biomedical Journals" or in "Vancouver Citation Style". Titles of journals not listed in Index Medicus should be spelled out in full.

Manuscript style will follow accepted standards. Please refer to the JBTH for guidance. The final style will be determined by the Editor-in-Chief as reviewed and accepted by the manuscript's corresponding author.

Approval of the Ethics Committee

The JBTH will only accept articles that are approved by the ethics committees of the respective institutions (protocol number and/or approval certification should be sent after the references). The protocol number should be included in the end of the Introduction section of the article.

Publication Ethics

Authors should observe high standards with respect to publication ethics as set out by the International Committee of Medical Journal Editors (ICMJE). Falsification or fabrication of data, plagiarism, including duplicate publication of the authors' own work without proper citation, and misappropriation of the work are all unacceptable practices. Any cases of ethical misconduct are treated very seriously and will be dealt with in accordance with the JBTH guidelines.

Conflicts of Interest

At the point of submission, each author should reveal any financial interests or connections, direct or indirect, or other situations that might raise the question of bias in the work reported or the conclusions, implications, or opinions stated - including pertinent commercial or other sources of funding for the individual author(s) or for the associated department(s) or organizations(s), and personal relationships. There is a potential conflict of interest when anyone involved in the publication process has a financial or other beneficial interest in the products or concepts mentioned in a submitted manuscript or in competing products that might bias his or her judgment.

Material Disclaimer

The opinions expressed in JBTH are those of the authors and contributors, and do not necessarily reflect those of the SENAI CIMATEC, the editors, the editorial board, or the organization with which the authors are affiliated.

Privacy Statement

The names and email addresses entered in this Journal site will be used exclusively for the stated purposes of this journal and will not be made available for any other purpose or to any other party.

Brief Policies of Style

Manuscript	Original	Review	Birief Comunication	Case Report	Editorial ; Letter to the Editor; Editor' s Corner	Innovative Medical Products	State-of-the-Art	Health Innovation Initiatives
Font Type	Times or Arial	Times or Arial	Times or Arial	Times or Arial	Times or Arial	Times or Arial	Times or Arial	Times or Arial
Number of Words – Title	120	90	95	85	70	60	120	90
Font Size/Space-Title	12; double space	12; double space	12; double space	12; double space	12; double space	12; double space	12; double space	12; double space
Font Size/Space-Abstracts/Key Words and Abbreviations	10; single space	10; single space	10; single space	10; single space	-	-	10; single space	10; single space
Number of Words – Abstracts/Key Words	300/5	300/5	200/5	250/5	-	-	300/5	300/5
Font Size/Space-Text	12; Double space	12; Double space	12; Double space	12; Double space	12; Double space	12; Double space	12; Double space	12; Double space
Number of Words – Text	5,000 including spaces	5,500 including spaces	2,500 including spaces	1,000 including spaces	1,000 including spaces	550 including spaces	5,000 including spaces	5,500 including spaces
Number of Figures	8 (title font size 12, double space)	3 (title font size 12, double space)	2 (title font size 12, double space)	2 (title font size 12, double space)	-	2 (title font size 12, double space)	8 (title font size 12, double space)	8 (title font size 12, double space)
Number of Tables/Graphic	7 title font size 12, double space	2 title font size 12, double space	2(title font size 12, double space)	1(title font size 12, double space)	-	-	7 title font size 12, double space	4 title font size 12, double space
Number of Authors and Co-authors*	15	10	5	10	3	3	15	10
References	20 (font size 10,single space	30(font size 10,single space	15 (font size 10,single space)	10 (font size 10,single space)	10 (font size 10,single space	5(font size 10,single space	20 (font size 10,single space	20

*First and last name with a sequencing overwritten number. Corresponding author(s) should be identified with an asterisk; Type 10, Times or Arial, single space. Running title of not more than 40 characters should be at the top of each page. References should be listed consecutively in the text. References must be cited on (not above) the line of text and in brackets instead of parentheses, e.g., [7,8]. References must be numbered in the order in which they appear in the text. References not cited in the text cannot appear in the reference section. References only or first cited in a table or figures are numbered according to where the table or figure is cited in the text. For instance, if a table is placed after reference 8, a new reference cited in table 1 would be reference 9.1 would be reference 9.

,

,

Checklist for Submitted Manuscripts

❑1. Please provide a cover letter with your submission specifying the corresponding author as well as an address, telephone number and e-mail.

❑2. Submit your paper using our website www.jbth.com.br. Use Word Perfect/Word for Windows, each with a complete set of original illustrations.

❑3. The entire manuscript (including tables and references) must be typed according to the guidelines instructions.

❑4. The order of appearance of material in all manuscripts should be as follows: title page, abstract, text, acknowledgements, references, tables, figures/graphics/diagrams with the respective legends.

❑5. The title page must include a title of not more than three printed lines (please check the guidelines of each specific manuscript), authors (no titles or degrees), institutional affiliations, a running headline of not more than 40 letters with spaces.

❑6. Acknowledgements of persons who assisted the authors should be included on the page preceding the references.

❑7. References must begin on a separate page.

❑8. References must be cited on (not above) the line of text and in brackets instead of parentheses, e.g., [7,8].

❑9. References must be numbered in the order in which they appear in the text. References not cited in the text cannot appear in the reference section. References only or first cited in a table or figures are numbered according to where the table or figure is cited in the text. For instance, if a table is placed after reference 8, a new reference cited in table 1 would be reference 9.

❑10. Reference citations must follow the format established by the "Uniform Requirements for Manuscripts Submitted to Biomedical Journals" or in "Vancouver Citation Style".

❑11. If you reference your own unpublished work (i.e., an "in press" article) in the manuscript that you are submitting, you must attach a file of the "in press" article and an acceptance letter from the journal.

❑12. If you cite unpublished data that are not your own, you must provide a letter of permission from the author of that publication.

❑13. Please provide each figure in high quality (minimum 300 dpi: JPG or TIF). Figure must be on a separate file.

❑14. If the study received a financial support, the name of the sponsors must be included in the cover letter and in the text, after the author's affiliations.

❑15. Provide the number of the Ethics Committees (please check the guidelines for authors).